Mathematical and Experimental Investigation of Yeast Colony Development –
A Model System for the Growth of Filamentous Fungi in Heterogeneous Environments

Der Fakultät Maschinenwesen

der

Technischen Universität Dresden

zur

Erlangung des akademischen Grades

Doktoringenieur (Dr.-Ing.)

vorgelegte Dissertation

Dipl.-Ing. Thomas Walther

geboren am 22.07.1973 in Meerane

Tag der Einreichung: 19.03.2004

OUTLINE

1.   LIST OF SYMBOLS

(Please note that the symbols listed in this section do not refer to notations used in the literature review.)

A	area covered by one sampling point in the OD measurements [μm^2]
c_N	nutrient concentration [$g \cdot L^{-1}$]
c_M	messenger concentration [$g \cdot L^{-1}$]
$c_{M,crit}$	critical messenger concentration [$g \cdot L^{-1}$]
D	diffusion constant [$m^2 \cdot s^{-1}$]
D_0	diffusion constant in water [$m^2 \cdot s^{-1}$]
D_{agar}	diffusion constant in agar [$m^2 \cdot s^{-1}$]
DW	dry weight fraction of wet biomass
d_C	cell diameter [μm]
g	correction summand for the intensity of transmitted light
h	height of the growth field [μm]
I_B	intensity of transmitted light in the blank
$I_{B,max}$	maximum intensity of transmitted light in the blank
I_S	intensity of transmitted light in the sample
$I_{S,n}$	normalized intensity of transmitted light in the sample
i	index of a lattice node
K	calibration factor for the calculation of cell density from OD [μm^{-2}]
l	length of the growth field [μm]
l_C	length of a cell [μm]
$m_{A,average}$	average mass of a growth field [g]
$m_{A,sample}$	mass of a growth field [g]
m_C	mass of a cell [g]
m_G	mass of glucose in a standard growth field [g]
$m_{G,vial}$	mass of glucose in vial [g]
n	number of lattice nodes
$n_{C,p}$	number of proliferating unit cells
$n_{C,s}$	number of stationary unit cells
OD	optical density
OD_{sample}	optical density of the sample
$OD_{standard}$	optical density of the standard with known glucose concentration
$r_{N,con}$	total nutrient consumption rate [$g \cdot L^{-1} \cdot h^{-1}$]
$r_{N,main}$	nutrient uptake rate per cell due to maintenance [$g \cdot h^{-1}$]
$r_{N,prol}$	nutrient uptake rate per cell due to proliferation [$g \cdot h^{-1}$]
$r_{N,rep}$	nutrient replenishment rate [$g \cdot L^{-1} \cdot h^{-1}$]
$r_{M,spec}$	specific messenger emission rate [$g^{-1} \cdot h^{-1}$]
R	specific nutrient uptake rate due to maintenance [$g \cdot g^{-1} \cdot h^{-1}$]
s	state of a lattice node
s_C	state of a cell

T_C	time constant for cell decay [h]	
T_M	time constant for messenger decay [h]	
Δt	time step for the discretization of the continuous time scale [h]	
Δt_p	replication interval (generation time) [h]	
V	volume of the standard growth field [cm^3]	
V_C	volume of a cell [μm^3]	
V_i	volume assigned to one lattice node [L]	
w	standard width of the growth field [μm]	
Y	biomass yield on the nutrient [$g \cdot g^{-1}$]	
ρ_C	density of wet biomass [$g \cdot cm^{-3}$]	
ω	agar concentration [% (w/v)]	

2. INTRODUCTION

Fungi are important members of many ecosystems. They are responsible for the decomposition of organic matter and undergo a large number of interactions with members of different genera (Ritz, 1993). The natural environment of fungi is characterized by fluctuations in nutrient availability and spatially distributed nutrient resources. During evolution, fungi developed several adaptation mechanisms to cope with these environmental changes: Fungal colonies are able to time the outgrowth from a local nutrient source with regard to the spatial distribution of adjacent nutrient sources (Boddy & Abdalla, 1998; Donnelly & Boddy, 1997). The translocation of nutrients within the mycelium enables fungi to grow through areas that are completely depleted of nutrient, respectively, to compensate the lack of nutrients in a part of the mycelial network (Hughes & Boddy, 1994; Olsson & Gray, 1998). Furthermore, fungal colonies adapt their cell density to a given nutrient concentration, i.e., with decreasing nutrient availability the density of the mycelium declines allowing for the search of new nutrient resources at minimum expense of biomass and energy (Ritz, 1995; Ritz *et al.*, 1996). This, certainly, incomplete list of possible interactions of fungal communities with their environment is meant to illustrate the difficulty to describe and to predict the response of such communities to environmental changes.

In search for a conclusive theory that comprises the impact of all environmental factors on the response of a fungal community, the aspect of adaptation of population density to a given nutrient concentration was studied extensively. In particular, agar plate experiments were carried out wherein fungal colonies were inoculated in the center of the plate and the growth pattern of the colony was analyzed with respect to nutrient availability. Due to the dynamic interplay of the growing mycelium, nutrient uptake and non-stationary nutrient concentration within the growth substrate, spatio-temporal mathematical models are necessary to fully understand the response of this system. In a series of papers, reaction-diffusion models were developed that qualitatively predict the growth pattern of fungal colonies in a heterogeneous environment (Davidson, 1998; Davidson & Park, 1998; Davidson *et al.*, 1996a; Davidson *et al.*, 1996b; Davidson *et al.*, 1997). These models describe colony growth based on uptake and transformation of nutrient into biomass, nutrient depletion and diffusion, and transport of nutrient within the mycelium. Simulations show the evolution of colony patterns with a constant cell density and the establishment of local gradients in the nutrient concentration. However, due to the strong abstraction of the biological process, the results are hard to interpret and model parameters were not assigned to biological parameters or functions. In a very recent set of papers, quantitative models for the mycelial development of *Rhizoctonia solani* were presented (Boswell *et al.*, 2002; Boswell *et al.*, 2003). In addition to the above described processes, these models incorporate the microscopic behavior of fungal hyphae, i.e., the generation of new cells by branching of hyphal tips and the loss of tips by anastomosis. Furthermore, they account for the operation of different nutrient-translocation mechanisms (Boswell *et al.*, 2002). Although the authors claim to reproduce experimental results quantitatively by their simulations, the structure as well as some aspects in the parameterization of these models are highly questionable. In particular, the mathematical

description of nutrient uptake and intracellular nutrient translocation is contra-intuitive and contradicts a number of experimental findings (see Section 3.3.1).

Assessing the basis of experimental data and the state of mathematical modeling of fungal growth, regulatory phenomena that control the development of mycelia on the population scale are far from being understood. This lack of understanding is mainly owed to the shear number and complex interplay of environmental and biological factors which directly points to the necessity for a further simplification of the model system. In this context, yeasts which can be regarded as "simple" fungi can serve as a valuable tool to study mycelial growth on a level of much lower complexity: Dimorphic yeast species are able to form colony patterns that are similar to patterns created by higher fungi (Boschke & Bley, 1998). In contrast to the mycelium of higher fungi, which consists of long, tube-like hyphae, colonies of many yeast species are built up of well separated - pseudo-hyphal - cells. As a consequence, translocation of nutrients and information within the mycelium is negligible, which represents a significant simplification when compared to higher fungi. However, as will be shown in the following sections this approximation does not hold for all cultivation conditions and requires a careful microscopic verification.

Since yeast colonies can be viewed as a population of individual cells, striking similarities to the growth of bacterial colonies arise. Immobile bacteria are also known to form filamentous colony patterns with a declining cell density at small nutrient concentrations. The evolution of bacterial colony patterns was explained based on the assumptions of diffusion-limited growth (DLG) (Kawasaki *et al.*, 1997; Matsushita *et al.*, 1998) *or* a quorum-sensing-based self-organization process (Ben-Jacob *et al.*, 1994) – a hypothesis that is currently favored by most biologists. According to the DLG theory, the growing edge of the colony takes up all the nutrient that diffuses towards the colony causing the establishment of a nutrient gradient and truncation of growth in the colony center due to nutrient depletion. According to the model developed by Ben-Jacob and co-workers (Ben-Jacob *et al.*, 1994, Cohen *et al.*, 1996), the formation of characteristic patterns is the result of an interplay between the directed movement along nutrient gradients, the stop of proliferation in the absence of food, and the chemotactic effect of long-range chemorepellents as well as short-range chemoattractants. Since messenger concentration is related to cell number, here, colony development is controlled by a quorum-sensing (QS) mechanism. Biologically, the basic assumptions of both theories are quite different. However, patterns generated in simulations according to both models are nearly identical. Thus, *qualitative* similarities between simulated and experimental colony patterns solely show that these patterns can be generated based on the proposed mechanisms, but do not prove that these mechanisms are of any relevance in the actual biological system. This unsatisfactory situation is similar to theoretical studies on fungal development and can only be overcome by the setup of *quantitative* models and the comparison of predicted results with experimental data. However, the elaboration of measures that are characteristic for colony development on one hand, as well as the support of experimental results by a broad and reliable data basis on the other, are highly demanding problems.

In the present study, the model yeasts *Candida boidinii* and *Yarrowia lipolytica* were cultivated in petri dishes on solid agar substrates. A new method for the quantification of

local cell density within the mycelium was developed. Using this non-invasive technique, not only the cell-density profile for a given point in time, but also the dynamics of profile evolution within a single colony can be conveniently monitored. Growth of the colonies was investigated for different nutrient resources under various degrees of limitation. In particular, colony extension rates, final colony diameters, cell-density profiles, and total biomass accumulation within the colonies were found to vary strongly depending on yeast species and cultivation conditions.

As outlined above, various potential regulatory mechanisms may influence yeast colony development. In order to test, whether a particular mechanism is present or not, models were developed that simulate the spatio-temporal development of yeast colonies based on different assumptions. These models are of hybrid cellular automaton type and describe discrete cells and continuously distributed nutrients and messengers. In contrast to most of the above mentioned approaches, these models are scaled. Environmental as well as biological parameters have clearly assigned functions and lie in the physiologically relevant range. As will be shown, results of the simulations can be easily compared to experimental results and may thus serve as a tool to verify model assumptions or to derive further questions that need to be answered experimentally.

3. LITERATURE REVIEW

3.1. Growth of Yeasts under Stringent Conditions

In laboratory cultivations microorganisms such as yeasts are commonly grown under optimum environmental conditions. These favorable growth conditions – among others – comprise sufficient nutrient supply, appropriate osmolarity of the growth medium, and optimum temperature. Large deviations from these ideal conditions usually coincide with a drop of specific growth rates and are, therefore, considered as stringent or stressful. In the present study, the focus lies on the response of yeasts populations to nutritional stress, i.e., to the starvation for carbon or nitrogen sources. The behavior of yeast colonies is determined by both, physiological and morphological changes on the microscopic single-cell level, as well as regulatory phenomena on the macroscopic population level. Therefore, the knowledge about both stages of regulation is reviewed in the following sections.

3.1.1. Entry into Non-proliferating States

When yeasts become limited for fermentable energy-rich carbon sources (e.g., hexose sugars) in the presence of ample nitrogen, they gradually arrest in the cell cycle and reprogram their metabolic regulation. After the switch to the utilization of alternative carbon sources such as ethanol or acetate, slow vegetative growth is continued until metabolizable carbon sources are depleted from the medium. This biphasic growth is commonly described as diauxy and mirrors the preferential use of energy-rich carbon sources by the microorganisms. In the absence of utilizable carbon sources, yeasts exit the cell cycle and become quiescent, i.e., they stop proliferation but are still viable (see Werner-Washburne *et al.* (1993) for a detailed review). This off-shot from the mitotic cell cycle is commonly referred to as stationary phase. Metabolism slows down and the rate of protein synthesis drops to approximately 10% when compared to exponentially growing cells. Upon diauxic shift, but much stronger during entry into the stationary phase, the cell wall is thickened and a number of stress response genes are expressed that provide the cell with a higher resistance to changing environmental conditions (Werner-Washburne *et al.*, 1993). Furthermore, the storage carbohydrates glycogen and trehalose are accumulated as an energy resource to meet maintenance requirements during long-term survival of the cells (Parrou *et al.*, 1999). Stationary *Saccharomyces cerevisiae* cells maintain nearly 100% viability up to 100 days when suspended in distilled water (Granot & Snyder, 1993).

When yeasts are severely starved for nitrogen in the presence of high carbon source concentrations they also enter stationary phase. The physiological and transcriptional response of the cells under these conditions is not as deeply investigated as for carbon limitation. However, characteristics of stationary cells under both conditions appear to be nearly identical except for the significantly higher storage-carbohydrate content of nitrogen-limited cells (Parrou *et al.*, 1999).

The transition into stationary phase is reversible. The reentry into the mitotic cell cycle is triggered by carbon-source availability (Granot & Snyder, 1993): When quiescent cells were

suspended in media containing high concentrations of various carbon sources but no other essential nutrients, cells lost viability within 20 days. Furthermore, the time span to bud emergence was essentially shortened when the cells were exposed to high carbon source concentrations for a short time prior to the incubation in rich medium. These findings were interpreted as an induction of early cell cycle events by the presence of carbon sources independent of their assimilation. Interestingly, nitrogen-starved cells were also activated by carbon source availability whereas supplementation of ammonium in the absence of carbon sources had no effects on viability.

While the transition to the stationary phase is a strategy to overcome moderate periods of nutrient limitation, the formation of dormant bodies is observed when yeast become nutrient limited for extended time spans or in response to particular combinations of lacking nutrients. In the absence of fermentable carbon sources and moderate nitrogen starvation, diploid *S. cerevisiae* cells undergo meiosis to form haploid spores. Spores possess an extremely high tolerance to environmental conditions and maintain the ability to germinate up to several years (Schlegel, 1992).

3.1.2. Dimorphism

Yeasts are simple fungi and categorized in the class of ascomycetes (Schlegel, 1992). In their simplest form they exclusively exist as almost round single-cell organisms. However, a large number of yeasts has the ability to switch their morphology from the round-shaped (yeast-like) form to an elongated hyphal or pseudohyphal growth form (Barnett, 1990). The change in cell morphology is called dimorphism and is the prerequisite to develop mycelial colony patterns. Additionally, differentiation phenomena appear to be related to the virulence of pathogenic yeasts (Ernst, 2000). Most knowledge about the regulation of dimorphism on the molecular level originates from the study of this phenomenon in the yeasts *S. cerevisiae* and *Candida albicans*. However, environmental factors that trigger the dimorphic switch vary strongly depending on the yeast species (compare e.g. Ernst (2000) and Mösch (2000)). These differences arise from different challenges that the microorganisms have to master in their particular ecological niche. Therefore, an extension of regulatory processes found in *C. albicans* and *S. cerevisiae* to other yeasts is not straightforward. However, from the analysis of pseudohyphal development in these model yeasts general characteristics were elaborated which describe fundamental principles in the formation of filamentous structures in yeast colonies.

Phenotype

Under appropriate cultivation conditions, *S. cerevisiae* cells can switch from the yeast-like morphology, (length: 4.2 µm, diameter: 3.0 µm) to the elongated pseudohyphal growth form (length: 6.7 µm, diameter: 1.9 µm) (Gimeno *et al.*, 1992). Pseudohyphal cells show a distal budding pattern, i.e., newly formed buds are located opposite to the mother cell's birth end. In contrast to yeast-like cells, pseudohyphal cells remain attached to each other. Repeated polarized budding results in the formation of filamentous structures that are built up of chains of separated single cells. These filaments exhibit invasive growth, i.e., they penetrate the

surface of solid substrates searching for new nutrient resources (Gimeno *et al.*, 1992). Whether or not this ability to grow invasively arises from the excretion of proteolytic enzymes or solely from the exertion of mechanical force is still under debate (Mösch, 2000).

In contrast to *S. cerevisiae*, *C. albicans* is able to form pseudohyphae as well as true hyphae. Both morphologies are considered as distinct cell types since different mechanisms appear to regulate the development of these growth forms (Ernst, 2000). When growing in the hyphal cell morphology, *C. albicans* secretes proteases and adhesins enabling invasive growth. Since differentiation and invasiveness of *C. albicans* cells were found to be important factors for the virulence of this yeast, regulatory mechanisms that control the yeast-hyphae transition were investigated in detail.

Effectors of Morphogenesis

In *S. cerevisiae* the dimorphic switch is induced upon nitrogen limitation while carbon limitation results in growth arrest, i.e., the entry into the stationary phase (Kron *et al.*, 1994; Palecek *et al.*, 2002). However, the presence of the amino acids proline and histidine at comparatively high concentrations induces the dimorphic switch while mixtures of them or other amino acids inhibit yeast-hyphae transitions (Mösch, 2000). The differentiation to elongated cell morphologies and polarized growth enables the yeast to grow away from an environment that is depleted from nitrogen or to penetrate solid substrates in search for new nitrogen resources – a situation that *S. cerevisiae* probably often has to face when growing on ripening fruits.

In diploid cells, the presence of ethanol causes hyperfilamentation even in the presence of high nitrogen concentrations (Lorenz *et al.*, 2000). Fusel alcohols, such as isoamyl alcohol and 1-butanol, induce differentiation in haploid cells in emers and submers cultivations. While ethanol is the major metabolic by-product during growth of *S. cerevisiae* on glucose, fusel alcohols are formed in the amino acid metabolism under nitrogen-limited conditions. Three major hypothesis were discussed that explain the dimorphic switch in response to elevated concentrations of these alcohols (Lorenz *et al.*, 2000): Firstly, the yeast may simply try to escape an environment poisoned by its own metabolites. As a second hypothesis, the yeast may have the ability to determine nutrient availability by the detection of the formed by-products. Accordingly, high by-product concentrations indicate nutrient limitation and, consequently, the population grows away from its current location. Furthermore, a quorum-sensing mechanism similar to bacteria was suggested that prevents the accumulation of high cell densities based on the emission and detection of metabolites that induce accelerated growth away from high cell densities. Interestingly, pseudohyphal cells of *S. cerevisiae* induced by nitrogen limitation were only observed on solid agar substrates and not in liquid culture (Gimeno *et al.*, 1992). Concerning the above described effect of volatile metabolic by-products on morphogenesis it is tempting to speculate, that the dimorphic switch is absent in liquid culture because small amounts of metabolites that serve as inducers are readily diluted or stripped out via the exhaust gas stream. In contrast they may accumulate and affect growth when comparatively high local cell densities are built up during growth on solid substrates. As the only exception, Miled *et al.* (2001) reported the induction of the pseudohyphal phenotype in submers chemostat cultivations. However, details about the gas

flow through the fermenter, as well as the biomass, nutrient and metabolite concentrations in the chemostat were not provided by the paper. Therefore, the experimental results are hard to interpret with respect to the above described hypothesis.

C. albicans undergoes the dimorphic transition in response to high temperatures and the presence of serum in the cultivation medium which reflects the behavior of the pathogenic yeast upon host invasion. Hyphae are absent at pH lower than 6, and at high glucose or ammonium concentrations. Similar to *S. cerevisiae,* proline induces hyphal development. The supplementation of cultivation media with N-acetylglucosamine, the monomer of the cell wall component chitin, also stimulates the formation of filaments (Ernst, 2000). Furthermore, Hornby *et al.* (2001) found that *C. albicans* emits farnesol which inhibits the dimorphic transition in response to several inducers, while it does not affect the growth rate of the microorganism even at comparatively high concentrations. Farnesol is secreted at a constant rate irrespective of the environmental conditions. It was argued that this compound serves as a quorum-sensing molecule and is responsible for the inoculum size effect, i.e., the repressed formation of filaments at high cell concentrations (Hornby *et al.*, 2001). Due to the medical relevance of *C. albicans* the dimorphic switch of this yeast was mainly studied in response to factors crucial for host invasion rather than upon nutrient limitation. However, from the outlined variety of effectors in the yeast-hyphae transition of both yeasts, the adaptation to different environmental challenges is obvious.

Molecular-biological Regulation of Dimorphism

Although factors that induce differentiation vary strongly between yeasts, the signal transduction pathways that process environmental signals appear to be similarly structured. In *S. cerevisiae* and *C. albicans* filamentous growth is induced by the activation of the mitogen-activated protein kinase (MAPKinase) pathway and the cAmp-activated protein kinase A (PKA) pathway. Both signal transduction pathways function in parallel and are activated by a receptor-associated (RAS) protein that mediates receptor signals to the intracellular response (Fig. 3.1) (Ernst, 2000; Mösch, 2000).

Despite an extensive experimental investigation of signal-transduction pathways that control differentiation, the knowledge about their regulation is still incomplete. The receptor proteins identified so far do not account for all environmental signals that are known to induce filamentation. Thus, in some instances it remains unclear whether differentiation in response to different effectors is regulated by different genes (or gene families), or the signal-transduction pathways share a metabolic intermediate (Palecek *et al.*, 2002). (E.g. in *S. cerevisiae*: Differentiation induced by alcohols vs. differentiation induced by nitrogen starvation. Inducing alcohols are produced as metabolic by-products under nitrogen-limited conditions.) Furthermore, a quantitative description of regulatory phenomena is still missing, e.g., the question at which concentrations (or which ratio) of glucose and ammonium, respectively, filamentation is induced cannot be answered.

The induction of the pseudohyphal development coincides with changes in cell-cycle regulation (e.g. the delay of bud emergence), and a tight regulation of apical and isotropic cell growth to eventually form an elongated cell. Although a number of genes was identified

to participate in the regulation of pseudohyphal growth, the "fine tuning" of these processes is still poorly understood (Palecek *et al.*, 2002).
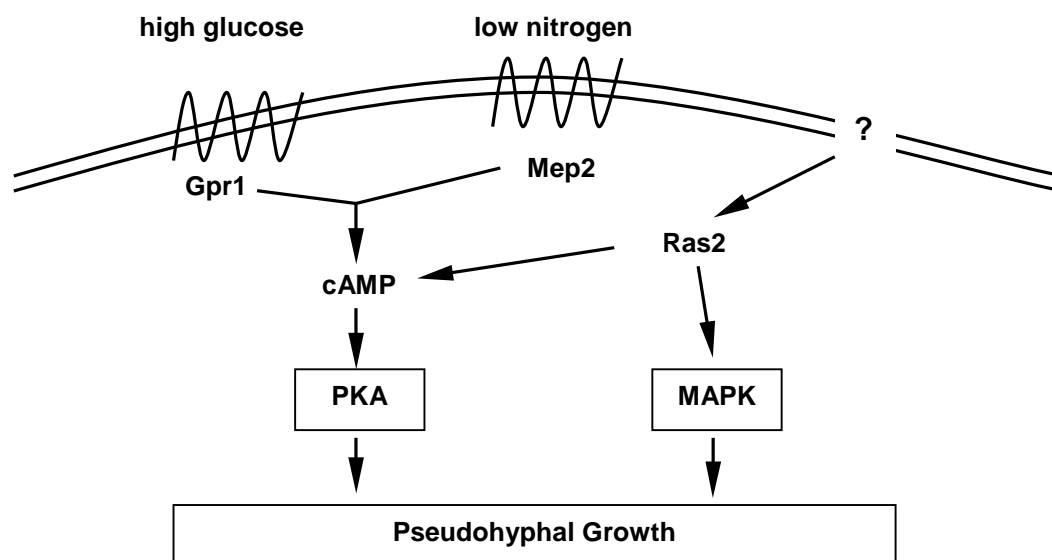
Figure 3.1: Schematic view of signal-transduction cascades for the regulation of filamentous growth in *S. cerevisiae*. Low nitrogen and high glucose concentrations, respectively, are detected by the receptors Mep2 and Gpr1. Via intermediate steps (not shown here) the receptor signals result in elevated levels of cAMP which stimulates filamentous growth via activation of the protein kinase (PKA) pathway. Ras2 also plays a crucial role in filamentous growth. It is activated by an unknown signal and induces differentiation via activation of cAMP or through the MAPK pathway, respectively (The figure is adopted from Palecek *et al.* (2002)).

3.1.3. Ammonia-mediated Guidance of Yeast Colonies

While a considerable body of experimental data about the behavior of individual yeast cells under changing environmental conditions was accumulated, comparatively little is known about the coordination of growth on the population level. Recently, volatile ammonia was identified as an important messenger in yeast colony development (Palkova *et al.*, 1997). Colonies of nine different genera were shown to emit ammonia when they utilized a mixture of amino acids as a carbon source. No ammonia was detected when the colonies were grown in presence of an energy-rich carbon source like glucose (Palkova *et al.*, 1997). Since yeast colonies were found to grow away from regions of high ammonia concentrations, ammonia emission is interpreted as a long-distance starvation signal between adjacently growing yeast populations.

Single yeast colonies exhibit sustained emission of ammonia. In contrast, when two yeast colonies grow in close neighborhood to each other, ammonia is emitted earlier and in a pulse-wise manner (Palkova & Forstova, 2000). Periods of alkalization are interrupted by

acidification of the medium. In case of *Candida mogii*, the time span between two ammonia pulses was estimated with 80-100 hours (Palkova *et al.*, 1997). Furthermore, adjacent colonies synchronize ammonia pulses irrespective of their developmental stage (Palkova & Forstova, 2000). This behavior is also induced when the second yeast colony is substituted by a chemical source of ammonia, but is not present when solutions containing either NaOH or NH_4^+ are supplemented to the medium (Palkova *et al.*, 1997). Considering the comparatively high concentrations of 5 $g \cdot L^{-1}$ ammonium sulfate in the cultivation medium, this result is partially surprising. The addition of NaOH to the medium should cause an upshift in pH that, according to the law of mass action (Equ. 3.1 and 3.2, (Mortimer, 1987)), coincides with higher ammonia concentrations in the medium.

$$NH_3 + H_2O \Leftrightarrow NH_4^+ + OH^- \qquad\qquad (3.1)$$

$$K_B = \frac{[NH_4^+][OH^-]}{[NH_3]} = 1.8 \cdot 10^{-5} \qquad\qquad (3.2)$$

The absence of any effect upon NaOH supplementation, however, was not discussed. Furthermore, periods of alkalization and acidification were found to correspond to changes in the colony morphology. During the acidic phase, colonies of *C. mogii* appear relatively smooth and are mainly built up of pseudohyphal cells. Upon transition to the alkaline phase, colony morphology changes to a rough 'spaghetti-like' structure. On the microscopic scale, the decomposition of pseudohyphal cells into non-dividing yeast-like cells is observed. Since colony areas that face the neighboring colony are longer exposed to alkaline conditions, the repeated change in single cell morphology, accompanied by the growth arrest of cells exposed to an alkaline environment, appears to cause the asymmetric growth of adjacent yeast populations (Palkova & Forstova, 2000). Furthermore, it was shown that the acid-to-alkali transition is accompanied by pronounced changes in the transcriptome of the engaged cells indicating a high degree of coordination of these processes (Palkova *et al.*, 2002).

However, at the present stage of investigation, it is not clear whether the upshift of pH in the substrate around the colony is caused by an active emission of ammonia by the cells. Alternatively, the alkalization may be the consequence of nutrient uptake by active proton-symport systems which means that the release of volatile ammonia from the substrate only represents a secondary effect (described by Equ. 3.1) (Palkova *et al.*, 2002). According to this hypothesis, ammonia can be regarded as a long-range mediator of pH. Whatever is the primary factor that facilitates the outlined effects, the high degree of coordination and the specific transcriptional response to these signals indicate, that ammonia or pH serve as important messengers or signals, respectively, to guide colony development on the population level.

Ammonia is only detected in colonies that utilize amino acids as a carbon source (Palkova *et al.*, 1997). Since colony development does not appear to be less coordinated in the absence of this particular nutrient, it is more than likely that several other compounds have a similar potential to serve as messengers during yeast colony growth.

3.2. Characterization of the Model Organisms

In the present study, the yeasts *Yarrowia lipolytica* and *Candida boidinii* were employed as model organisms. Both species have the ability to switch from the yeast-like growth form to a filamentous cell morphology (Barnett, 1990) and may, therefore, serve to study the mycelial colony development.

In contrast to a large number of dimorphic yeast species, *C. boidinii* and *Y. lipolytica* are considered as apathogenic yeasts which is an indispensable requirement for their cultivation and manipulation in standard microbiology laboratories. On the other hand, both yeasts are regarded as 'non-conventional' yeasts, which means that – at present – only little is known about the molecular biology of these organisms when compared to *S. cerevisiae* or *C. albicans*.

3.2.1. Phylogenetical Characterization

Y. lipolytica was formerly classified as *Candida lipolytica* since for a long time no sexual state had been described for this yeast. After the identification of a sexual life cycle in the sixties of the last century, the perfect form was finally reclassified as *Y. lipolytica* (Barth & Gaillardin, 1997). The yeast differs considerably from other ascomycetes. Phylogenetic trees derived from sequence comparison of well conserved genes exhibit a branch for *Y. lipolytica* that is clearly separated from *Schizosaccharomyces pombe* and the vast majority of other ascomycotous yeasts. Homologous genes from *Y. lipolytica* show low similarity to sequences from *S. cerevisiae* or *C. albicans* which hampers the identification and characterization of genes based on Southern hybridization and heterologous expression in conventional hosts (Barth & Gaillardin, 1997). Therefore, comparatively little is known about the metabolical and morphological regulatory mechanisms in *Y. lipolytica* on the level of gene transcription.

The yeast *C. boidinii,* as a member of the genus *Candida,* does not possess a sexual life cycle. It is phylogenetically distant from *Candida tropicalis* (the type species of the genus Candida) (Suzuki & Nakase, 2002) and delimits a clade of phylogenetically closely related methanol-assimilating yeasts (Kurtzman & Robnett, 1998; Middelhoven & Kurtzman, 2003). Due to the choice of two phylogenetically distinct yeast species it is possible to study regulatory phenomena in colony development on a rather diverse genetic background.

3.2.2. Physiological Characterization

Besides standard carbon sources that are commonly applied in microbial cultivations, *Y. lipolytica* is able to utilize n-alkanes, 1-alkenes and fatty acids (Barth & Gaillardin, 1997). Because of the ability to assimilate these non-conventional substrates, *Y. lipolytica* was tried to be applied in the degradation of dispersed or concentrated fat from industrial plants in food industry. However, until today no process was presented that meets economic requirements. Furthermore, *Y. lipolytica* was studied for its ability to transform various carbon sources into organic acids, such as citric, isocitric, 2-ketoglutaric, and 2-hydroxyglutaric acid, respectively (Barth & Gaillardin, 1997). Because of its high economic relevance, the production of citric

acid was studied in particular. Upon nitrogen limitation, *Y. lipolytica* was shown to excrete high levels of citric and isocitric acid. The total yield of organic acids and the ratio of citric to isocitric acid strongly depends on the carbon source and the used strain (Barth & Gaillardin, 1997).

C. boidinii has the economically relevant ability to assimilate methanol. Besides earlier attempts to use this methylotrophic yeast in the production of single-cell protein it now becomes more and more attractive as a host for heterologous protein production (Gellissen, 2000; Komeda *et al.*, 2002). Since key enzymes of the methanol degradation pathway can constitute up to 30 % of the total intracellular protein, their respective promoters can be used for a strong and tightly controlled protein expression (Gellissen, 2000). The effective secretion of produced proteins and the absence of strong hyperglycosylation are further advantages to conventional hosts such as *S. cerevisiae* or *E. coli* (Gellissen, 2000).

3.2.3.   Regulation of Dimorphism

In comparison to the well studied yeasts *C. albicans* and *S. cerevisiae* only little is known about the regulation of the dimorphic transition in the here applied species. A database search for literature focusing on the regulation of dimorphism in *C. boidinii* yields no results. Therefore, data reviewed in this section exclusively refer to the yeast *Y. lipolytica*. Information about the genetic basis of the dimorphic switch in *Y. lipolytica* is also rare. The regulation of this process appears to be rather different from *S. cerevisiae* or *C. albicans* (Dominguez *et al.*, 2000). Furthermore, difficulties in the heterologous expression of *Y. lipolytica* genes in *S. cerevisiae* and *vice versa* hamper the search for key regulatory genes. Therefore, investigations of dimorphism in this yeast are mainly restricted to the analysis of cell morphology in response to various external effectors. Details about signal-transduction cascades that trigger the yeast-hyphae transition with respect to environmental factors are widely missing.

Influence of Carbon and Nitrogen Sources

The yeast-hyphae transition of *Y. lipolytica* was mainly studied in liquid culture since, in contrast to *S. cerevisiae*, no major differences to the growth on solid substrates appear to exist. Dominguez *et al.* (2000) found that in cultivations of the yeast in complex media (media containing peptone) filamentous and yeast-like cells coexist. In minimal media cells remain in the yeast form while the supplementation with serum or N-acetylglucosamine induces the dimorphic transition (Dominguez *et al.*, 2000). This stands in contrast to results of Ruiz-Herrera & Sentandreu (2002) who detected the coexistence of both cell types in minimal medium with glucose as the carbon source and the absence of mycelial cells when glycerol served as the only carbon source. Furthermore, high concentrations of ammonium sulfate in the medium were found to support the formation of mycelial morphologies (Ruiz-Herrera & Sentandreu, 2002; Szabo, 1999). In a study by Ruiz-Herrera & Sentandreu (2002), the substitution of ammonium by glutamate or glutamine inhibited the formation of mycelial cells under any tested conditions. Furthermore, Dominguez *et al.* (2000) claim that the induction of hyphal cells upon nitrogen starvation, as found for *S. cerevisiae*, is absent in *Y. lipolytica*.

Influence of pH

The pH of the medium was found to be another crucial parameter for the yeast-hyphae transition of *Y. lipolytica*. At low pH values of about 3, no cells with a filamentous morphology are formed. At pH 7, the transition to hyphal cells is strongly induced and yeast cells are absent (Ruiz-Herrera & Sentandreu, 2002). Szabo & Stofanikova (2002) found that the presence of high amounts of organic nitrogen sources is critical for the pH-dependent morphogenic switch. It was argued that at high pH values the active uptake of nitrogen sources via proton-symport systems is hampered and, as a consequence, the yeast becomes unable to form filaments. These results are contradictory to results of Ruiz-Herrera & Sentandreu (2002), who found a complete suppression of mycelial cell morphologies at pH 7 when glutamine or glutamate served as the nitrogen sources.

Influence of Citrate

Citrate, as a major metabolic by-product in cultivations of *Y. lipolytica*, is an important positive effector for the yeast-hyphae transition of this yeast. As described by Ruiz-Herrera & Sentandreu (2002), the application of citrate buffers considerably increased the percentage of mycelial cells under any condition when compared to the usage of phosphate-buffer systems. These results are consistent with findings of Dominguez *et al.* (2000) who also reported a better dimorphic transition when this acid was present in the medium.

Data about the dimorphic switch of *Y. lipolytica* in response to environmental factors are rare and partially contradictory. Inconsistent observations may arise from the inadequate characterization of the cultivation conditions. In several cases the exertion of nitrogen or carbon limitation is poorly defined. E.g., Szabo & Stofanikova (2002) claimed that a supplement of 5 % (w/v) bacto peptone to a minimal medium containing 2 % glucose only serves as a nitrogen source. They, however, overlooked the ability of *Y. lipolytica* to utilize amino acids as a carbon source. Experimental data about the time course of glucose and amino acid concentrations that preclude this point of criticism were not presented. Furthermore, Dominguez *et al.* (2000) consider a minimal medium containing 1 % glucose and 0.5 % ammonium sulfate as being nitrogen-limited - a view that is highly questionable considering a C/N ratio of at least 4:1 in growing yeast and a yield of about 0.4 gram biomass per gram glucose and about 7 gram biomass per gram ammonium sulfate (see Table 5.1 in this study). In addition, despite the obvious relevance of pH and citrate concentration in the medium, most morphological studies do not provide these data as a reference. Therefore, observations that were assigned to a particular medium compound cannot be distinguished from the secondary effect of a pH shift or the presence of citric acid, respectively. In some aspects the interpretation of experimental data is also questionable. Szabo & Stofanikova (2002) speculated that because of the higher cell volume the formation of filaments requires more energy and input of building blocks than the growth in the yeast form. According to this hypothesis, hyphal cells are only formed at high nutrient concentrations and cells remain in the yeast form at severe nutrient limitation. Considering the large body of experimental data that suggest the formation of mycelial morphologies as a strategy of fungal communities to escape areas that are limited for nutrients, this hypothesis appears to be dubious.

Furthermore, a higher mass-specific energy demand for the formation of hyphal cells is not evident since – despite a considerably higher chitin content in the cell walls of hyphal cells (Gow et al., 1994) – the cellular compositions of both cell types are nearly identical.

Summarizing the critical review of the regulation of dimorphism in *Y. lipolytica* one has to note that due to the high complexity of this process a reliable basis of information is still widely missing.

3.3. Mathematical Models for the Growth of Microbial Communities

3.3.1. Reaction-diffusion Models for the Growth of Fungal Mycelia

In a series of papers, a Scottish group which is certainly leading in the mathematical analysis of mycelial growth, developed reaction-diffusion models that describe fungal growth at different levels of abstraction (Boswell *et al.*, 2002; Boswell *et al.*, 2003; Davidson, 1998; Davidson & Park, 1998; Davidson *et al.*, 1996a; Davidson *et al.*, 1996b; Davidson *et al.*, 1997). In a first crude approach, hyphae were assumed to be generated by an activator which was considered to be a key enzyme for the conversion of nutrient into biomass (Davidson *et al.*, 1996a; Davidson *et al.*, 1996b). Colony extension was represented by the diffusion of the activator which was assumed to be autocatalytically produced from a growth limiting nutrient. Among other aspects, colony extension and mutual repulsion of adjacently growing colonies were investigated by simulations. In a next step, mycelial growth was described by the autocatalytic generation of active hyphae from a growth limiting nutrient (Davidson, 1998). In this model the distinction between internal and external nutrient reservoirs (i.e., nutrients present in the agar and nutrients held by the fungus) was introduced which allows for the description of nutrient redistribution inside the mycelium. The model served to simulate mycelial development in systems with heterogeneously distributed nutrients. The above mentioned mathematical models of fungal colony development are qualitative, i.e., models are not scaled in space and time. Furthermore, model parameters do not refer to recognized biochemical and physical parameters. Thus, predictions of these models cannot be quantitatively compared to experimental results which is the vital requirement for the verification of model assumptions and the assessment of simulated results. Because of these obvious shortcomings, these qualitative approaches are not described in the literature-review section. However, since these models nicely illustrate the line along which progress in the mathematical description of mycelial growth was made, they are discussed in detail in Appendix A.

In a series of recently developed models, mycelial development of *Rhizoctonia solani* is claimed to be quantitatively described (Boswell *et al.*, 2002; Boswell *et al.*, 2003). In Boswell *et al.* (2002), the authors mainly focus on fungal growth in an agar-plate system with an initially homogeneous distribution of nutrients. The development of biomass-density profiles during the outgrowth of the mycelium from a small disc-like inoculum is described by a one-dimensional model. Simulations are quantitatively compared to experimental results. In a second paper (Boswell *et al.*, 2003), the model is extended to the two-dimensional

description of mycelial development in a heterogeneous system which consists of isolated agar patches containing different amounts of nutrients. Furthermore, the influence of fungal growth on the pH of the medium is modeled. In both papers, the authors focus on the role of different translocation mechanisms in the capture of new nutrient resources. In particular, simulations mean to explain characteristics which were elaborated in the experimental investigation of nutrient translocation inside fungal mycelia, where radioactively labeled compounds were used to map internal nutrient concentrations.

Model Structure

The development of fungal mycelia is mathematically described by the linkage of macroscopic system properties to microscopic aspects of hyphal growth (Boswell *et al.*, 2002; Boswell *et al.*, 2003): The mycelium is assumed to consist of three components which are active hyphae, inactive hyphae and hyphal tips. Active hyphae are tube-like elements which are involved in the translocation of intracellular nutrients. Inactive hyphae are vacuolated elements of the mycelium not involved in nutrient transport. Hyphal tips represent the ends of active hyphae. The presence of hyphal boundaries is neglected and the mycelium is modeled as being a continuous distribution of biomass. In order to incorporate the microscopic characteristics of mycelial development, biomass growth is restricted to the ends of the hyphae, i.e., as a tip moves it generates new (active) hyphal elements. In order to incorporate the consequences of nutrient redistribution, the model distinguishes between external and internal nutrients, respectively. The fungal colony grows and takes up external nutrients. Internal nutrient is used to fuel the generation of hyphae, i.e. the migration of tips. The internal nutrient is redistributed inside the mycelium according to the local demand. This redistribution is facilitated by two distinct mechanisms, i.e. active and passive translocation, respectively.

Mycelium and growth medium (the agar) are considered as being two-dimensional, i.e., no concentration gradient is assumed to establish over the depth of the agar. However, in Boswell *et al.* (2002) mycelial development is described in only one dimension. Thus, the model consists of the components: active hyphal density, $m(x, t)$; inactive hyphal density $m'(x, t)$; tip density, $p(x, t)$; external nutrient concentration, $s_e(x, t)$; and internal nutrient concentration, $s_i(x, t)$. Model components are balanced according to Equations (3.3) – (3.7)

$$\frac{\partial m}{\partial t} = f_m(m, m', p, s_i, s_e) \tag{3.3}$$

$$\frac{\partial m'}{\partial t} = f_{m'}(m, m', p, s_i, s_e) \tag{3.4}$$

$$\frac{\partial p}{\partial t} = -\frac{\partial}{\partial x} J_p(m, m', p, s_i, s_e) + f_p(m, m', p, s_i, s_e) \tag{3.5}$$

$$\frac{\partial s_i}{\partial t} = -\frac{\partial}{\partial x}(J_i^{pas}(m, m', p, s_i, s_e) + J_i^{act}(m, m', p, s_i, s_e)) + f_i(m, m', p, s_i, s_e) \tag{3.6}$$

$$\frac{\partial s_e}{\partial t} = -\frac{\partial}{\partial x} J_e(m, m', p, s_i, s_e) + f_e(m, m', p, s_i, s_e) \tag{3.7}$$

wherein (J) represent flux (migration), and (f) denote reaction terms, respectively. Active hyphae (m) are generated by the migration of hyphal tips (p) and fade to the inactive state (m') with time constant (d).

$$f_m = \left| J_p(m, m', p, s_i, s_e) \right| - d \cdot m \tag{3.8}$$

Interestingly, the rate for the transition of active hyphal elements to the inactive form (d·m), was defined to be independent from the nutrient concentration. This assumption of spontaneous state transition (strong vacuole formation), however, is certainly contra-intuitive and stands in contrast to other investigations of fungal growth, where this state transition is commonly defined to occur upon nutrient deficiency (Nielsen 1993; Paul & Thomas, 1996). Consistently with Equ. 3.8, inactive hyphae are produced by the decay of (m). The degradation is assumed to be exponential with time constant (r). However, in the simulations degradation of inactive hyphae is neglected, i.e. r = 0.

$$f_{m'} = d \cdot m - r \cdot m' \tag{3.9}$$

The migration of hyphal tips (p) (referring to the extension of hyphae) is described by flux (J_p)

$$J_p = v \cdot s_i \cdot p \tag{3.10}$$

where the velocity of the tips is assumed to be proportional to internal nutrient concentration (s_i). ((v) simply represents a positive constant.) In Davidson (1998), mycelial extension was modeled by a diffusion process which clearly did not correctly describe the growth of immobile fungal cells. Here, the extension of hyphae is modeled by a convective flux (migration) of tips leaving behind a trail of immobile hyphal elements, i.e. biomass. Thus, the incorporation of microscopic features of fungal growth represents a significant improvement of the mathematical description of hyphal growth.

New tips are produced by subapical branching of hyphae. The rate of branch formation is assumed to be proportional to internal nutrient concentration and a positive constant (b) (Equ. 3.11, 1st term). Tips are lost by the fusion of tips with hyphal elements. Thus, the rate of tip loss is assumed to be proportional to the local concentration of hyphal elements (m) and tips (p), as well as to a positive constant (z) (Equ. 3.11, 2nd term).

$$f_p = b \cdot s_i \cdot m - z \cdot m \cdot p \tag{3.11}$$

The redistribution of nutrient (s_i) inside the mycelium is modeled by two distinct processes, namely active and passive nutrient translocation. Nutrient flux due to passive (J_i^{pas}) and

active (J_i^{act}) translocation, respectively, are assumed to increase with higher density of hyphal elements (m).

$$J_i^{pas} = -D_i \cdot m \cdot \frac{\partial s_i}{\partial x} \qquad (3.12)$$

$$J_i^{act} = D_a \cdot m \cdot s_i \cdot \frac{\partial p}{\partial x} \qquad (3.13)$$

(D_i) and (D_a) represent the effective diffusion constants through a mycelium of fractal structure. The authors, furthermore, assume that active nutrient translocation is a "tip-driven process", i.e., internal nutrient is actively translocated towards regions of higher tip density (Equ. 3.13). Internal nutrient is assumed to be acquired by the uptake of external nutrient (Equ. 3.14, 1st term). It is transformed into hyphal elements with efficiency (c_2) (Equ. 3.14, 2nd term). The cost of active translocation is described by the 3rd term in Equ. 3.14, wherein (c_4) is a positive constant.

$$f_i = c_1 \cdot s_i \cdot m \cdot s_e - c_2 \cdot \left| J_p(m,m',s_i,s_e) \right| - c_4 \left| J_i^{act}(m,m',s_i,s_e) \right| \qquad (3.14)$$

Internal nutrient is assumed to be acquired by an autocatalytic reaction, i.e., the more internal nutrient is present the higher the uptake rate of external nutrient (Equ. 3.14, 1st term). This assumption, however, is contradictory to experimental studies on the regulation of carbon assimilation in yeast. It is well recognized that a number of metabolites or intermediate products which accumulate in a cell repress reaction steps that are upstream in the metabolic pathway (Rizzi et al., 1997). In particular, elevated levels of intracellular glucose or close derivates inhibit the uptake of external glucose by the microorganisms (Rizzi et al., 1997; Teusnik et al., 1998). Although these studies were focusing on single-cell organisms that cannot redistribute nutrients inside extended mycelia, it appears questionable that nutrient uptake in excess of local needs can be described by the proposed process. Furthermore, the chosen definition of nutrient uptake (which in fact allows uptake rates to become infinitely high in the absence of biomass growth) neglects experimental characterizations of sugar-uptake systems in microorganisms where maximum glucose-uptake rates in the range of 2 mmol·g^{-1}·h^{-1} were determined for different yeasts (Lucas & van Uden, 1986; Nobre et al., 1999). Thus, the postulation of an autocatalytic nutrient uptake is highly questionable. If this postulation, however, is an essential requirement for the desired behavior of the model, the definition of nutrient uptake should be carefully discussed and results of the simulations should be interpreted with extreme care. Both was neglected in the papers.

The external nutrient (s_e) is depleted from the agar with f_e

$$f_e = -c_3 \cdot s_i \cdot m \cdot s_e , \qquad (3.15)$$

and diffuses according to Fick's law

$$J_e = -D_e \cdot \frac{\partial s_e}{\partial x}.$$

(3.16)

Here, (c_3) is a positive constant smaller than (c_1) to account for the cost of active nutrient uptake, and (D_e) represents the diffusion constant of the nutrient in agar. Since the extra cellular volume (i.e. the volume of the agar) is much higher than the volume enclosed by the mycelium, the concentrations of external and internal nutrient, respectively, have to be balanced for two separate reservoirs. As correctly stated in (Davidson, 1998), the transition of a defined number of molecules from the large external volume to the comparatively small cellular volume causes a significant change of the internal concentration while external concentration remains relatively constant. This effect, however, is neither considered nor discussed in the Boswell models $((c_1)$ and (c_3) are constants of similar value.).

In Boswell *et al.* (2003), the course of pH in the medium is simulated in addition to the above mentioned model components. The authors define the generation of H^+ ions to be proportional to the concentration of internal nutrient (glucose) without any experimental evidence for this crude approximation. Furthermore, they neglect any reaction that these ions may undergo once they are emitted into the medium (equations not shown). This simplification, however, yields an inadequate calculation of pH since a number of pH-active substances (ammonium, phosphate, and potentially organic acids secreted by the fungus) are present in the medium at comparatively high concentrations. Due to the presence of these substances, released H^+ ions are bound and pH can be expected to remain constant for very high amounts of added hydrogen ions. Thus, the estimation of pH by the proposed model, will certainly fail to yield adequate results.

Model Parameterization and Comparison of Model Predictions to Experimental Results
Despite the questionable structure of the model, simulations for the mycelial development of *R. solani* in agar-plate systems were compared to biomass distributions estimated in growth experiments (Boswell *et al.*, 2002). Experiments were carried out by inoculating a small disc of mycelium in the center of an agar plate. The agar contained an initially homogeneously distributed nutrient reservoir with glucose being the growth-limiting nutrient. At daily intervals, samples of the mycelium were cut out from the agar at different distances from the inoculation site. Samples were dried to estimate the distribution of dry biomass along the colony radius.

Corresponding simulations predicted the development of a monotonically declining biomass-density profile along the colony radius. The monotonic descent of the biomass-density profile was in good qualitative agreement with the experimental findings. Since in the simulations a density of hyphal elements was calculated (elements of unit length per cm), results of the simulations had to be rescaled for the quantitative comparison with experimental data which were represented by densities of dry biomass (mg dry biomass per cm^2). The best fit was obtained using a scaling factor of $K_H = 10^{-3}$ mg $\cdot$ L^{-1} (with L = 1 cm representing the unit length of one hyphal element). Since the hyphal diameter of $d_C = 10$ μm for *R. solani* was

reported (Boswell *et al.,* 2002), a corresponding biomass density of $\rho = 1.27$ $g \cdot cm^{-3}$ can be calculated according to

$$\rho = \frac{m_H}{V_H} = \frac{K_H \cdot L}{0.25 \cdot \pi \cdot d_H^2 \cdot L} \ . \tag{3.17}$$

This value is in good agreement with *wet* biomass densities of fungi ($\rho_{wet} = 1.1$ $g \cdot cm^{-3}$) estimated in bioseparation studies (Datar & Rosen, 1993). However, since the described comparison of experimental and simulated results refers to the distribution of *dry* biomass, this value is unrealistic and the calibration factor (K_H) should be corrected using relation

$$K_H = \frac{\rho_{wet} \cdot V_H \cdot DW}{L} \ , \tag{3.18}$$

wherein (DW) denotes the dry weight fraction of wet biomass. For DW = 0.3 (a value that corresponds to exponentially growing cells) Equ. 3.18 yields $K_H = 0.259 \cdot 10^{-3}$ $mg \cdot cm^{-1}$. Thus, the model underestimates the experimentally determined biomass production approximately by factor 4. This obvious lack of fit was not discussed by the authors.

Generally, when searching for the origin of differences between model predictions and experimental data, the comparison of model parameters with independent experimental studies may provide valuable information about potential sources of error. In particular, it was tried to recalculate the biomass yield on the external nutrient glucose. In the model, glucose (s_e) is taken up by the hyphae and converted into an internal growth limiting substance (s_i) which is not further described. Since balance equations refer to *molar* concentrations of the nutrients and no molar mass of the internal nutrient is provided, the mass-specific biomass yield on glucose cannot be recalculated. The incorrect parameterization comprises almost all model terms. Since units of individual terms in the balances are inconsistent, any parameter evaluation is impossible. Furthermore, 8 out of 13 model parameters refer to the internal nutrient concentration (s_i), i.e., the rate of 8 processes depends on this variable. Considering that (s_i) was not measured in *any* of the described experiments and no reference for the origin of the parameter estimations was provided, the reliability of parameter estimations cannot be assessed.

Considering the obviously inadequate parameterization of the model, the presented simulations are far from providing a *quantitative* understanding of mycelial growth. Since the model structure also comprises several dubious terms, even the correct *qualitative* description of fungal growth has to be questioned. Because of these intolerable shortcomings, the extension of simulations to patchy model environments and conclusions drawn from the calculations shall not be discussed here.

The correct design of models which describe fungal growth on the basis of nutrient translocation inside the mycelium requires reliable data about the chemical structure of the nutrients held by the fungus (or this pool of substances), as well as detailed knowledge about uptake, reaction, and transport kinetics of these compounds. Furthermore, the development of analytical techniques that facilitate the quantitative monitoring of internal nutrient

concentrations are necessary to validate model predictions. Obviously, the experimental elaboration of the required information is an extremely demanding and time-consuming process. Thus, alternative approaches have to be developed in order to describe fundamental aspects of fungal growth. In this context, the investigation of yeast colony development may provide valuable information about the regulation of cell growth in the absence of nutrient translocation inside the mycelium. Since yeast mycelia that are built up of pseudohyphal cells can be considered as populations of individual cells, striking similarities to bacterial colonies arise. In order to illustrate the state-of-the art in the modeling of pattern formation in bacterial populations, the following section reviews mathematical approaches in the description of bacterial colony development.

3.3.2. Models for Growth of Bacterial Colonies

Bacteria are able to form a variety of complex colony patterns with respect to different environmental conditions. In particular, populations of the motile bacterium *Bacillus subtilis* were investigated for their response to variations in nutrient concentration and agar softness, a parameter that corresponds to the resistance which the growth substrate exerts to the motion of the bacteria. Observed patterns can be summarized in a morphology chart similar to phase plots (Fig. 3.2) (Matsushita *et al.*, 1998). On hard and dry surfaces, corresponding to high agar concentrations, colony patterns change from dense and compact morphologies (region B) to sparsely branched diffusion-limited aggregation (DLA) like patterns (region A). With decreasing agar concentration concentric ring structures (region C) as well as compact disc patterns are observed (region D) when nutrient concentration is fixed at high levels. At intermediate agar concentrations and very low nutrient concentrations the colony morphology switches to densely branched patterns (region E), a morphology that according to (Ben-Jacob *et al.*, 1994) also occurs at higher agar concentrations. This difference, however, may arise from small deviations in experimental details and do not appear to be of crucial significance.
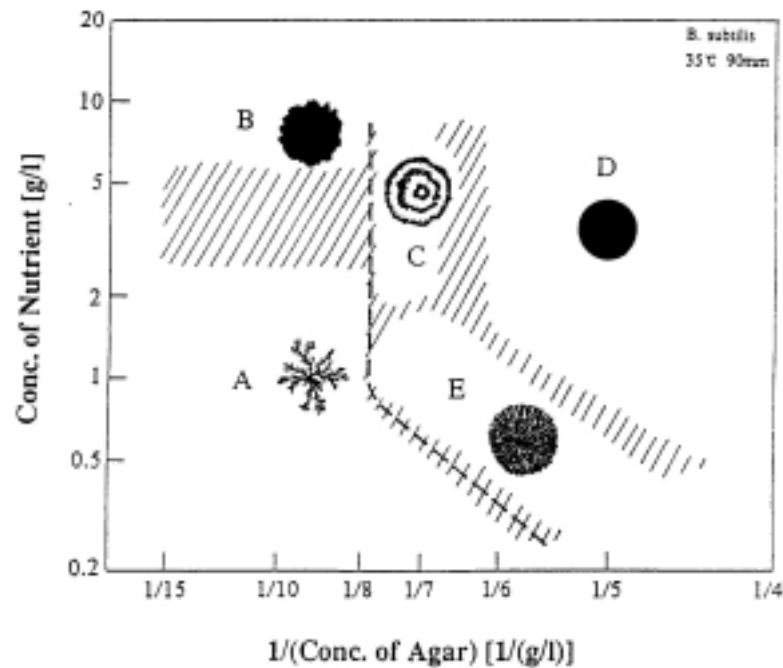
Figure 3.2: Morphological phase diagram of experimentally derived colony morphologies of *B. subtilis* which were obtained when the concentration of agar or nutrient, respectively, were varied (Matsushita *et al.*, 1998).

In search for regulatory mechanisms that trigger the response of a bacterial population to environmental changes, several authors developed mathematical models that are based on rather different biological assumptions. However, as will be discussed simulations that are based on different fundamental assumptions yield patterns that exhibit striking similarities to experimentally derived colony morphologies.

Models Describing Nutrient and Motility-dependent Pattern Formation

A Japanese group developed various models that describe the transition between distinct colony morphologies in different regions of the phase plot (Fujikawa, 1994; Kawasaki *et al.*, 1997; Matsushita *et al.*, 1998). In its most recent and generalized form, Matsushita *et al.*, (1998) presented a reaction-diffusion model that reproduces changes in colony morphology over the whole parameter range. This model is meant to explain all observed changes based on the variation of the initial nutrient concentration in the agar, and the agar concentration, respectively. Here, different agar concentrations correspond to changes in the diffusion constant of the bacteria.

The model describes actively moving bacteria that may undergo a transition to an inactive state. New bacteria are generated by the autocatalytic transformation of the growth limiting nutrient. The total population density is represented by the sum of active bacteria (b(r, t)) and inactive bacteria (s(r, t)). The density of active and inactive bacteria is balanced using the equations (Matsushita *et al.*, 1998)

$$\frac{\partial b}{\partial t} = \nabla(d(b,n) \cdot \nabla b) + \varepsilon \cdot n \cdot b - a(b,n) \cdot b \qquad (3.19)$$

and

$$\frac{\partial s}{\partial t} = a(b,n) \cdot b \; . \qquad (3.20)$$

Nutrient concentration (n(r, t)) is balanced applying relation

$$\frac{\partial n}{\partial t} = \nabla^2 n - n \cdot b \; . \qquad (3.21)$$

The coefficient (a(b, n)) describes the transition from the active to the inactive state. It is assumed to decrease for high nutrient and bacteria concentrations, respectively. The authors waived to provide the exact definition of this coefficient. The normalized diffusion constant (d), represents the ratio of the diffusion constants of bacteria and nutrient, respectively. (d) was assumed to depend on the local density of active bacteria (b) and the nutrient concentration (n). In most presented simulations, however, (d) was fixed for a given agar concentration. Only for the generation of "Eden-like" (Matsushita *et al.*, 1998) colony patterns (region A) the diffusion constant varied with the bacterial density (b). It was, however, not explicitly defined how (d) changes with the nutrient concentration (n) and bacterial density (b), respectively. The efficiency of the conversion of the nutrient into bacteria is denoted by the parameter (ε). Again no exact value for this parameter was provided.

The spatio-temporal evolution of bacterial colonies was simulated solving the system of coupled reaction-diffusion equations (3.19-3.21)(Matsushita *et al.*, 1998). According to the simulations, the switch from compact solid colony patterns to filamentous structures (region B -> region A,) is the result of diffusion-limited growth (DLG) of the colony (fixed (d), decreased (n_0)). The growing edge of the population takes up all the nutrient that diffuses towards the colony and growth in the colony interior stops as a consequence of nutrient depletion. In contrast, transitions from the DLG-like patterns to densely branched morphologies (region A -> region E) was assigned to a higher diffusion constant (d), i.e. a higher motility of the microorganisms, at a fixed initial nutrient concentration (n_0). Disc-like colony patterns (region D) were obtained at high diffusion constants and high initial nutrient concentrations. Accordingly, the authors claim to describe changes in colony morphology only by effects exerted by nutrient availability and/or motility of the bacteria.

However, the model has to be strongly criticized: The cell-density-dependent transition of active bacteria to an inactive state (see a(n,b)) obviously incorporates cell-cell interactions that are not clearly discussed and contradicts the attempt to describe solely nutrient and motility-dependent processes. It is notable, that these non-specific cell-cell interactions yield similar results, irrespective whether they are incorporated into the diffusion term (d) (Kawasaki *et al.*, 1997) or into the state transition rate (a) (Matsushita *et al.*, 1998). This, however, is a very important question when considering the actual biological system.

Furthermore, the cell-density-dependent definition of (a) or (d), represents an *observation* but does not explain its *origin*. Thus, the model structure is inaccurate with respect to the assumptions that were meant to be investigated and should be carefully discussed when interpreting the results of simulations. It is also not discussed why the diffusion constant (d) only in region B was defined to be a function of the bacterial density while it was assumed to exclusively depend of the agar concentration in the other regions of the phase plot. Furthermore, the presented simulations are only qualitative. Model parameters were not compared to experimentally determined estimates and simulated colony patterns were not scaled to real spatial dimensions. Considering that (i) the model structure is inaccurate (with respect to the assumptions explicitly discussed by the authors), (ii) the definition of important coefficients is incomplete, (iii) parameters do not refer to recognized literature data, and (iiii) the reader is unable to compare simulated results with experiments, this model is inadequate for the description of pattern formation in bacterial colonies.

Communicating-walkers Model

In contrast to Matsushita *et al.* (1998) and Kawasaki *et al.* (1997), theoretical studies by the Israelian group of Ben-Jacob and co-workers explicitly model messenger mediated cell-cell interactions and investigate the influence of these processes on colony development of *B. subtilis* (Ben-Jacob *et al.*, 1994; Cohen *et al.*, 1996). Since the model structure is highly complex, only the fundamental ideas shall be reviewed in the following section. For details of the full implementation of all processes the reader is referred to Cohen *et al.* (1996).

The model describes discrete walkers (representing a quantity of several thousand bacteria) that actively move and proliferate. Upon depletion of internal energy, active walkers undergo a transition to an inactive state. Inactive walkers are immobile and do not proliferate. They correspond to sporulated bacteria. The internal energy (E_i) of a walker (i) is depleted by maintenance requirements and the cost of active movement. It is replenished by the uptake and conversion of nutrient ($C(r, t)$). Proliferation is assumed to occur when the amount of internal energy reaches a critical concentration. Internal energy of a walker and nutrient concentration in the agar are balanced according to equations

$$\frac{dE_i}{dt} = \kappa \cdot C_{consumed} - \frac{E_m}{\tau_R} \tag{3.22}$$

and

$$\frac{\partial C}{\partial t} = D_C \nabla^2 C - \sigma_a \cdot C_{consumed} , \tag{3.23}$$

where (D_C) represents the diffusion constant of the nutrient in the agar, and ($\sigma_a(r, t)$) denotes the density of active walkers. (κ) describes the energy yield on the nutrient, E_m is the cost of all processes (movement, maintenance, excluding proliferation) and (τ_R) is the minimal time for reproduction.

The active movement of bacteria is modeled by assuming that active walkers perform an off-lattice random walk similar to Brownian motion. A walker advances to the adjacent on the lattice when the boundary between the lattice nodes was hit (N) times. The increasing resistance to the movement of bacteria which is exerted when the agar concentration is high (i.e., the agar surface is dry) is implemented assuming that the number of hits necessary for a position change of a walker (N) increases with higher agar concentrations.

In addition, the model accounts for chemotaxis, i.e., long range mutual repulsion of bacterial cells due to the emission of repellents, short range chemoattraction, as well as directed movement of bacterial cells towards higher nutrient concentrations. The introduction of chemotactic terms was motivated by experimental findings that suggested a quorum-sensing mechanism to coordinate sporulation of *B. subtilis* and identified a chemotactic response of bacterial cells to gradients in nutrient concentration (Cohen *et al.*, 1996). In order to incorporate the messenger-mediated quorum sensing in bacterial populations, a diffusible chemorepellent (R(r, t)) was introduced which was assumed to be emitted by sporulated cells and to be taken up by active walkers. Furthermore, an exponential decay rate of the compound was defined. The concentration of the repellent was balanced according to equation

$$\frac{\partial R}{\partial t} = D_R \cdot \nabla^2 R + \sigma_a \cdot \Gamma_R - \sigma_a \cdot \Omega_R \cdot R - T_R \cdot R , \qquad (3.24)$$

wherein (D_R) denotes the diffusion constant of the messenger, and (σ_s(r, t)) is the density of sporulated bacteria. (Ω_R), (Γ_R), and (T_R) are positive constants. The directionality of bacterial movement along gradients of nutrient or messenger concentration, respectively, was incorporated by giving the pure random walk of the cells a bias towards regions of high nutrient or low messenger concentrations, respectively. (The exact implementation of chemotaxis shall not be discussed here. Please refer to Cohen *et al.* (1996) for further notice.)

With this set of model assumptions it is possible to mimic the development of bacterial colonies with respect to variations in nutrient supply and motility of the bacteria (determined by the agar concentration). In contrast to the above described reaction-diffusion approaches, the model not only predicts colony morphologies similar to experimental patterns, but also reproduces measured variations in the colony extension rate at different levels of nutrient concentration. Furthermore, the authors avoided the introduction of model terms that do not correspond to the underlying model assumptions. The model was parameterized using quantitative measures which refer to clearly defined biochemical functions. However, details about the parameter estimation provided in the paper are certainly insufficient to assess the quality of the approximations. In particular, it is not clear whether the simulations quantitatively compare to experimental results. However, due to the clearly defined model structure, even a solely qualitative interpretation of the simulations provides considerable evidence for the adequacy of the model and contributes to the understanding of the actual biological processes.

As discussed by Cohen *et al.* (1996), the mechanisms that drive transitions between growth scenarios, i.e., growth conditions where either nutrient chemotaxis or quorum sensing are dominant, still remain under question. Therefore, different ranges of nutrient concentration require different sets of model parameters and no theory could be established so far, that yields consistent results in the whole experimental range. However, the open discussion of weaknesses of the model allows experimentalists as well as modelers to design experiments or theories that provide additional information to incorporate all mentioned effects into a conclusive description of bacterial colony development. This interpretation of computational biology clearly has to be preferred over approaches that mean to describe a whole set of experimental phenomena on the cost of an inconsistent model structure or a questionable parameterization of the equations.

3.3.3. Conclusions

The description of the development of microbial communities, obviously, is a demanding experimental and mathematical problem. The macroscopic behavior of a population is determined by interactions of individual cells with their dynamically changing microscopic environment. Since state variables, such as biomass, nutrient, and messenger concentration, respectively, are hard to quantify with such a high spatial resolution, these interactions cannot be monitored up to present. As a consequence, high uncertainties about regulatory phenomena during population development exist. Mathematical models may help to characterize these regulatory phenomena by compensating the lack of experimental data by simulations. The comparison of calculated macroscopic patterns with experimentally assessable measures may then serve to evaluate hypotheses about potential regulatory mechanisms.

As outlined above, a considerable number of theoretical studies is focused on the coordination of colony development in fungal and bacterial colonies. Due to the high complexity of these models, small changes in the model structure and/or parameterization, respectively, cause significant changes in the predicted growth patterns. However, most of the described models contain terms that, clearly, do not refer to the postulated assumptions (e.g., the cell-density-dependent rate of cell-state transition in Matsushita *et al.* (1998)), or which are not supported by experimental results (e.g., the autocatalytic acquirement of internal nutrient in Boswell *et al.* (2002)). Since the authors waived for a discussion of these terms, model predictions are highly questionable and inadequate to support experimental investigations. From these shortcomings, the request for a clearly defined model structure has to be derived. In particular, the model should be free from bias arising from not explicitly considered interactions. If, eventually, a process was identified to be vital for the desired behavior of a model (as the autocatalytic generation of internal nutrient in Boswell *et al.* (2002; 2003) might be), this finding should be carefully discussed since it might inspire experiments that serve to prove or to reject this hypothesis.

As shown by the comparison of models for the development of bacterial colonies, a merely qualitative comparison of simulated and experimentally derived growth patterns is insufficient to prove a model assumption to be right or wrong. Thus, only the application of models that are *scaled* for space and time can effectively support the experimental investigation of

regulatory processes in these systems. Since interactions between model components are often non-linear, the choice of correct values for the model parameters is crucial for a correct simulation of colony development. Ideally, parameters should be estimated in independent experiments or adopted from approved literature data. The parameterization of a quantitative model by 8 parameters that were obviously not determined by measurements is intolerable (see Boswell *et al.* (2002; 2003)). Furthermore, parameters should refer to recognized and commonly used measures for the description of microbial growth. This will enable the reader to evaluate model predictions by a comparison of model parameters with the large body of quantitative experimental data available the biochemical literature.

The here described requests may appear trivial to the reader since they represent established practice in the quantitative description of microbial growth in biochemical engineering. However, in the context of theoretical investigations of fungal (and bacterial) colony development it appears to be necessary to particularly stress the importance of a realistic model parameterization and a discussion of numerical results based on quantitative data. Only when the simulations are carried out on the basis of a clearly defined model structure, fundamental assumptions can be actually evaluated, thereby directing experimental research to alternative mechanisms in case of inadequate fit. As will be shown, the renunciation of "parameter (model) tuning" can provide valuable information even when simulations do not reproduce experimental results.

4. MATERIALS AND METHODS

4.1. Microorganisms and Media

Yarrowia lipolytica H222 was kindly provided by Prof. Gerold Barth from the Institute of General Microbiology, TU Dresden, Germany. *Candida boidinii* DSM70034 was acquired from the DSMZ. *Saccharomyces cerevisiae* ∑1278 was provided from Prof. Fink, Massachusetts Institute of Technology, USA. Microorganisms were kept on YGC (Merk) agar plates at 4 °C and were subcultured every 4 weeks.

Growth media were derived from a standard minimal medium (Atlas, 1996) containing $20\,g \cdot L^{-1}$ glucose (Merck) as the only carbon source, $5\,g \cdot L^{-1}$ $(NH_4)_2SO_4$ (Merck) as the only nitrogen source, and $1.7\,g \cdot L^{-1}$ YNB (Sigma) as a defined vitamin and trace-element base. For the preparation of solid growth substrates 2 % (w/v) bacto agar (Merck) was supplemented to the media. In order to impose various degrees of carbon or nitrogen limitation, the concentration of glucose or $(NH_4)_2SO_4$ in the medium was decreased while the content of all other medium components was kept constant. Furthermore, **c**asamino **a**cids (**CA**, acid hydrolyzate of casein, Merck) were used to substitute the standard carbon and nitrogen sources, i.e. glucose and ammonium sulfate. In Table 4.1 compositions of all growth substrates applied in this study are summarized.

Table 4.1: Compositions of media applied in this study. Concentration of YNB was $1.7\,g \cdot L^{-1}$ in all experiments. In solid substrates the agar content was $20\,g \cdot L^{-1}$.

Notation	Limitation	Carbon source	Nitrogen source
C-G-20	Carbon	$20\ g \cdot L^{-1}$ glucose	$5\ g \cdot L^{-1}$ $(NH_4)_2SO_4$
C-G-4	Carbon	$4\ g \cdot L^{-1}$ glucose	$5\ g \cdot L^{-1}$ $(NH_4)_2SO_4$
C-G-2	Carbon	$2\ g \cdot L^{-1}$ glucose	$5\ g \cdot L^{-1}$ $(NH_4)_2SO_4$
C-G-0.2	Carbon	$0.2\ g \cdot L^{-1}$ glucose	$5\ g \cdot L^{-1}$ $(NH_4)_2SO_4$
C-G-0.02	Carbon	$0.02\ g \cdot L^{-1}$ glucose	$5\ g \cdot L^{-1}$ $(NH_4)_2SO_4$
C-CA-20	Carbon	$20\ g \cdot L^{-1}$ casamino acids	$5\ g \cdot L^{-1}$ $(NH_4)_2SO_4$
C-CA-10	Carbon	$10\ g \cdot L^{-1}$ casamino acids	$5\ g \cdot L^{-1}$ $(NH_4)_2SO_4$
C-CA-2	Carbon	$2\ g \cdot L^{-1}$ casamino acids	$5\ g \cdot L^{-1}$ $(NH_4)_2SO_4$
C-CA-0.2	Carbon	$0.2\ g \cdot L^{-1}$ casamino acids	$5\ g \cdot L^{-1}$ $(NH_4)_2SO_4$
C-CA-0.02	Carbon	$0.02\ g \cdot L^{-1}$ casamino acids	$5\ g \cdot L^{-1}$ $(NH_4)_2SO_4$
N-A-0.5	Nitrogen	$20\ g \cdot L^{-1}$ glucose	$0.5\ g \cdot L^{-1}$ $(NH_4)_2SO_4$
N-A-0.1	Nitrogen	$20\ g \cdot L^{-1}$ glucose	$0.1\ g \cdot L^{-1}$ $(NH_4)_2SO_4$
N-A-0.05	Nitrogen	$20\ g \cdot L^{-1}$ glucose	$0.05\ g \cdot L^{-1}$ $(NH_4)_2SO_4$
N-A-0.005	Nitrogen	$20\ g \cdot L^{-1}$ glucose	$0.005\ g \cdot L^{-1}$ $(NH_4)_2SO_4$
N-CA-20	Carbon	$20\ g \cdot L^{-1}$ glucose	$20\ g \cdot L^{-1}$ casamino acids
N-CA-2	Nitrogen	$20\ g \cdot L^{-1}$ glucose	$2\ g \cdot L^{-1}$ casamino acids
N-CA-0.2	Nitrogen	$20\ g \cdot L^{-1}$ glucose	$0.2\ g \cdot L^{-1}$ casamino acids
N-CA-0.02	Nitrogen	$20\ g \cdot L^{-1}$ glucose	$0.02\ g \cdot L^{-1}$ casamino acids

Media were autoclaved for 20 minutes at 120 °C. For the investigation of colony development described in Section 5.2, pH in the growth substrate was not controlled. In the investigations of pH-dependent colony growth (Section 5.4.2), initial pH of the media was adjusted to values between 4 and 8 prior to sterilization using NaOH (1 mol·L^{-1}) and HCl (1 mol·L^{-1}).

4.2.   Cultivation Conditions in the Growth Experiments

4.2.1.   Enforcement of One-dimensional Colony Development

The one-dimensional development of *Y. lipolytica* and *C. boidinii* mycelia, respectively, was investigated on various combinations of carbon and nitrogen sources at two different degrees of limitation (applied media: C-G-4 and C-G-2, C-CA-20 and C-CA-10, N-A-0.1 and N-A-0.05, N-CA-20 and N-CA-2). Thin layers of solid growth substrate were created by pipetting 2 mL of autoclaved medium into standard plastic petri dishes (outer diameter: 60 mm, inner diameter: 52 mm). After solidification of the substrate, growth fields of 10 mm width were cut out from the agar using a sterile scalpel. Yeasts precultured on C-G-20 agar substrate (see Table 4.1) were transferred to the growth fields with a sterile tooth pick. In order to impose one-dimensional mycelial growth, colonies were inoculated as a thin line in the center of the growth field. Petri dishes were sealed using parafilm to prevent drying and incubated at 25°C in a climate chamber (Friocell, MMM). Details of the experimental setup are summarized in Fig. 4.1.
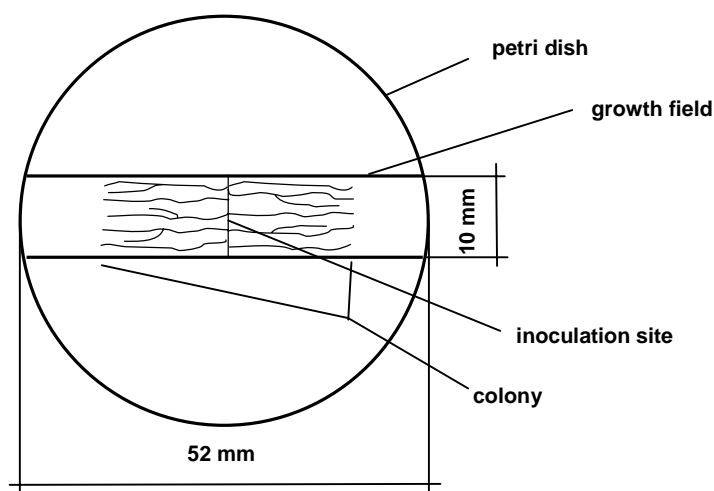
Figure 4.1:   Schematic view of the experimental setup for the investigation of one-dimensional colony development. The figure shows the bottom of a petri dish and the dimensions of the rectangular growth field which was cut out from the agar.

### 4.2.2. Investigation of Nutrient Replenishment due to Cell Decay

In order to investigate whether the development of *Y. lipolytica* and *C. boidinii* colonies is influenced by nutrient replenishment due to cell decay, colonies of the model yeasts were precultured for 14 days on rectangular growth fields as described above. After this period, the interior of the colonies was cut out from the agar using a sterile scalpel. The stripe of the colony boundary which remained on the growth field (width approximately 1 mm) was further cultivated. The progression of the colony radius as well as the cell-density profile which was measured after 35 days were compared to undisturbed growing control colonies. The role of nutrient replenishment was investigated for carbon limitation on C-G-2 medium and for nitrogen limitation on N-A-0.05 medium (see Table 4.1). For each treatment ("cut-out colonies" and controls), at least five replicate runs were started at a time. Cell-density profiles were estimated from the average of 3 individual colonies using the method described in Section 4.3.

4.2.3. Investigation of the Influence of Volatile Compounds on Colony Development

Cultivations of Colonies in the Headspace of a Yeast Population

In order to investigate the influence of volatile metabolic by-products on yeast colony development, small freshly inoculated populations were cultivated in the headspace of a giant colony. After six days of incubation, microscopic images of the small colonies were taken (motorized Microscope Axioscope 2 FS mot, Carl-Zeiss, magnification 12.5x) and their morphology was compared to colonies growing in the absence of a giant colony but under otherwise identical conditions. Furthermore, pH in the growth substrate of both, small and giant colonies was determined. For each cultivation condition, two replicate runs were analyzed.

Fig. 4.4 shows the details of the experimental setup. The bottom parts of two petri dishes were attached to each other, one containing the small colony and the other holding the giant colony. Dishes were filled with 2 mL agar substrate containing different nutrient reservoirs. Both, small and giant colonies were cultivated under limitation of the same nutrient but at different initial concentrations (Table 4.2). Small colonies were inoculated as a dot in the center of the rectangular growth fields (dimensions: 20 mm x 20 mm) using a sterile toothpick. Giant colonies were created by plating a yeast suspension onto the agar substrate. The inoculum for giant colonies was obtained from an overnight culture, cultivated in 100 mL Erlenmeyer flasks containing 30 mL C-G-20 minimal medium (Table 4.1). Flasks were incubated at room temperature on a rotary shaker at 300 rpm. 2 mL of the preculture were transferred to 2 mL plastic tubes. Cells were harvested by centrifugation at 12195 x g for 5 min. Clear supernatant was discarded and the cell pellet was resuspended in 1 mL sterile distilled water. 100 µL of this suspension were plated onto the growth field using a sterile spatula. The yeast populations were incubated at room temperature (approximately 25 °C).
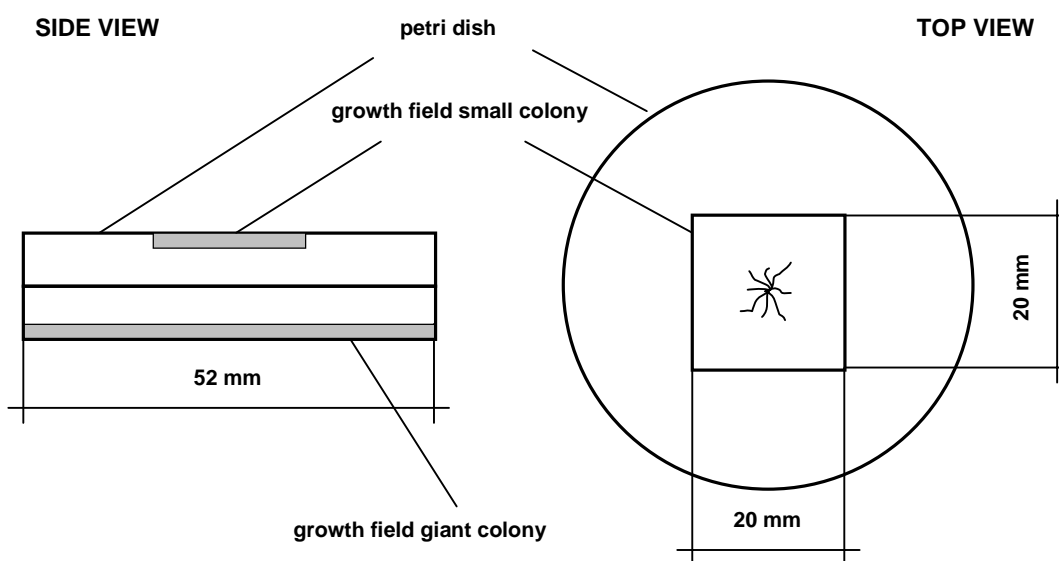
Figure 4.2: Schematic view of the experimental setup to investigate the influence of volatile compounds on yeast colony morphology. For details see text.

Table 4.2: Compositions of media applied in the combined cultivation of giant and small colonies.

Nutrient conc. small colony	Notation*	Nutrient conc. giant colony	Notation*
carbon limitation			
0.02 g·L^{-1} glucose	C-G-0.02	2 g·L^{-1} glucose	C-G-2
0.2 g·L^{-1} casamino acids	C-CA-0.2	0.2 g·L^{-1} casamino acids	C-CA-0.2
nitrogen limitation			
0.05 g·L^{-1} $(NH_4)_2SO_4$	N-A-0.05	0.5 g·L^{-1} $(NH_4)_2SO_4$	N-A-0.5
0.2 g·L^{-1} casamino acids	N-CA-0.2	2 g·L^{-1} casamino acids	N-CA-2

*Notations refer to complete medium compositions provided Table 4.1.

Cultivations of Colonies under an Ammonia Atmosphere

The effect of volatile ammonia on the development of small colonies was investigated by exposing small colonies to different concentrations of the volatile alkali. In these experiments the setup shown in Fig. 4.2 was slightly modified. The growth field of the giant colony was substituted by a solid agar (2 % (w/v)) medium containing 50 g·L^{-1} ammonium sulfate. Ammonia atmospheres of different stringency were created by supplementing various amounts of NaOH (2 mol·L^{-1}) to the ammonium sulfate medium. Small colonies were incubated under these ammonia atmospheres and analysed as described above.

4.3. Analytical Methods

4.3.1. Monitoring of Cell-density-profile Development

For every combination of medium composition and yeast, 5 replicate runs were started at a time. Colony diameters were measured at least weekly to monitor the progression of the growing perimeter. Colony-density profiles of the colonies were estimated at different intervals according to the following protocol: Microscopic images were taken along the longitudinal axis of the colonies (microscope: Axioscope 2 FS mot, Zeiss; camera: Hamamatsu C5810; magnification: 12.5x; transmitted light mode (lamp voltage: 1.6 V)) and assembled to obtain a single photograph. Since growth of the colonies is symmetrical, these photographs comprised only one moiety of the colony, i.e., the area between inoculation site and outer edge of the population. Local intensity of the transmitted light ($I_S(x)$) was estimated using the line morphology routine of the OPTIMAS 6.1 image-analysis-software package running in the luminescence mode. (The coordinate (x) denotes the position on the longitudinal colony axis.) The distance between the sampling points was 69 µm. ($I_S(x)$) was corrected for background shading by the addition of a correction summand ($g(x)$) yielding the normalized intensity of the transmitted light ($I_{S,n}$).

$$I_{S,n}(x) = I_S(x) + g(x) \tag{4.1}$$

The correction summand ($g(x)$) was calculated from the difference between the global maximum intensity of transmitted light ($I_{B,max}$) and the local intensity of transmitted light ($I_B(x)$) estimated from microscopic images of blank growth fields.

$$g(x) = I_{B,max} - I_B(x) \tag{4.2}$$

The optical density (OD) profile of the colonies was estimated according to equation

$$OD(x) = -\log \frac{I_{S,n}(x)}{I_{0,n}} \tag{4.3}$$

wherein ($I_{0,n}$) represents the normalized intensity of transmitted light measured in the absence of cells.

For every colony six OD profiles were estimated and averaged. The distance between these profiles was 0.45 mm. OD measurements of at least two different colonies were averaged to yield the final profile ready for analysis.

4.3.2. Calibration of OD for Local Cell Density

In order to calibrate the OD of carbon-limited colonies for local cell density, OD profiles (average of 10 individual profiles, distance between profiles: 0.85 mm, distance between

sampling points: 36 µm) of glucose-limited *Y. lipolytica* and *C. boidinii* colonies incubated on C-G-2 medium were estimated at different times within the first 36 h of cultivation (Fig. 4.3).
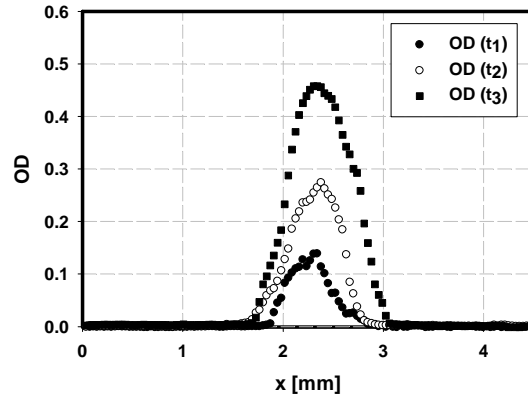
Figure 4.3: Example of OD measurements on glucose-limited *Y. lipolytica* colonies (C-G-2 medium) for the calibration of OD for local cell density. Individual plots represent the average of 10 profiles measured across the colonies. Profiles were estimated at 3 different times (t_1, t_2, t_3) within the first 36 h of cultivation.

Immediately after the OD measurements, colonies were cut out from the agar, transferred to 1.5 mL plastic tubes (Eppendorf), and incubated at 50 °C for 15 min in 250 µL gel solubilization buffer (Gibco). After the agar gel was completely dissolved, samples were centrifuged at 15244 x g for 10 min. The supernatant was discharged and the cell pellet was resuspended in 0.5 % TWEEN 20 to obtain well separated single cells. Samples were diluted to allow for a convenient quantification of cells using an Abbe-Zeiss cell counting chamber.

Since growth fields (Fig. 4.1) were cut out by hand, small deviations in the width of the agar tiles occurred. In order to increase accuracy of the calibration, cell number (n_S) estimated on a growth field of width (r) was normalized for the standard width (w = 10 mm) according to relation

$$n_{S,n} = \frac{n_S \cdot w}{r},$$

(4.4)

yielding the number of cells ($n_{S,n}$) on a standard growth field.

Furthermore, the dimensions of suspended cells (obtained as described above) and pseudohyphal cells in colonies that were incubated for up to 28 days were estimated using the line morphology routine of the OPTIMAS 6.1 image analysis software package. In yeast colonies round-shaped cells and pseudohyphal cells coexist throughout the whole cultivation. Since colony morphology and extension rate of the colony diameter mainly depend on the behavior of pseudohyphal cells, all cell-density estimations were normalized to the average size of the filamentous cell type. Thus, the total cell number of cells in the calibration experiments ($n_{S,n}$) was corrected for the total number of unit cells (n_C), i.e. pseudohyphal cells, using relation

$$n_C = \frac{V_{C,s} \cdot n_{S,n}}{V_C} \, .$$

(4.5)

Here, (V_C) denotes the volume of the unit cells (see Section 6.5) and ($V_{C,s}$) represents the average volume of suspended cells.

The number of unit cells in a colony equals the integral of local cell density ($c_C(x) = [\mu m^{-2}]$) over the area covered by the OD measurements (A).

$$n_C = \int_A c_C(x) \cdot dA$$

(4.6)

Since the calibration factor (K) relates OD to local cell density according to Equ.

$$c_C(x) = K \cdot OD(x),$$

(4.7)

the combination of equations 4.6 and 4.7 yields

$$n_C = K \cdot \int_A OD(x) \cdot dA \, .$$

(4.8)

The distance between the sampling points (u) was very small (u = 36 μm). Therefore, the integral in Equ. 4.8 could be conveniently discretized obtaining

$$n_C = K \cdot \sum_{i=1}^{N} \left[OD(i) \cdot \Delta A \right]$$

(4.9)

with (N) being the number of sampling points

$$N = \frac{A}{\Delta A}$$

(4.10)

and (ΔA) representing the area between adjacent sampling points.

$$\Delta A = w \cdot u$$

(4.11)

(K) was estimated after a linear regression from the ascent of the cell density ($n_C \cdot \Delta A^{-1}$) vs. sum of colony OD plot (Equ. 4.12, Fig. 4.4). In the following Sections, the sum of colony OD is referred to as "total OD".

$$\frac{n_C}{\Delta A} = K \cdot \sum_{i=1}^{N} OD(i)$$

(4.12)
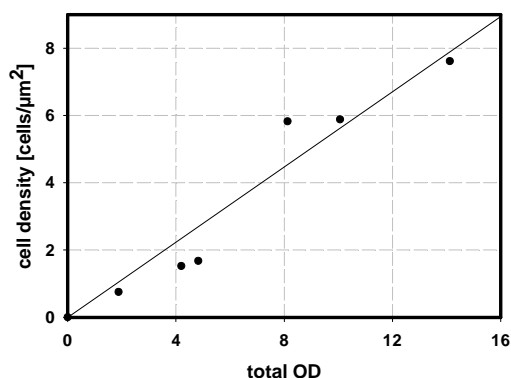
Figure 4.4: Cell density vs. "total OD" plot for the determination of the calibration factor (K) of carbon-limited *Y. lipolytica* colonies. Cells were cultivated on C-G-2 medium. The "total OD" of young colonies was estimated at different points of time within the first 36 h of cultivation. See text for details.

The calibration curve for carbon-limited *C. boidinii* colonies is provided in Appendix B.

For the carbon-limited growth on casamino acids, the calibration factor (K) determined under glucose limitation was corrected for different cell sizes using Equ.

$$K_2 \cdot V_{C2} = K_1 \cdot V_{C1}, \tag{4.13}$$

where (K_1) is the known calibration factor measured for cells with a volume (V_{C1}) and (K_2) is the new calibration factor for cells with a volume of (V_{C2}).

Under severe nitrogen limitation, old cells strongly incorporate storage carbohydrates which causes a drastic increase of their OD. In order to account for this phenomenon, a slightly different protocol for the calibration of OD for cell density was used: OD profiles of nitrogen-limited colonies growing on N-A-0.05 agar medium were estimated after 21 days of cultivation. After the OD measurements, several parts of different size and location were cut out from the colonies and processed as described above to estimate the total cell number in the removed colony areas. Applying equations 4.4 and 4.5, cell number was corrected for the standard width of the growth fields and the average size of the pseudohyphae. According to Equ. 4.12, the corrected cell number was divided by the area between adjacent sampling points and plotted vs. the total OD of the cut-out colony areas. The calibration factor (K) was estimated from the ascent of the regression line. The calibration curves for nitrogen-limited *Y. lipolytica* and *C. boidinii* colonies are provided in Appendix B. For the nitrogen-limited growth of the yeasts on casamino acids, (K) was corrected for different cell sizes using Equ. 4.13.

4.3.3. Estimation of Glucose Concentration in the Growth Field

Growth fields were scratched out from the petri dish and transferred to 1.5 mL plastic tubes. To dissolve the agar matrix, 30 µL gel solubilization buffer (Gibco) per 10 mg of gel were added and incubated for 20 min at 50 °C. Samples were centrifuged at 15244 x g for 5 min to separate the cells. The glucose content of the clear supernatant was estimated using the

Megazyme^{TM} Glucose Test Kit. The amount of glucose per vial ($m_{G,vial}$) was calculated according to Equ. 4.14, wherein (OD_{sample}) represents the optical density of the sample, and (OD_{stand}) denotes the optical density estimated for the standard solution (glucose concentration c_{stand} = 1 mg·mL^{-1}) provided with the test kit. From the sample OD the basal value of 0.020 was subtracted to account for the influence of the solubilization buffer. (V_{agar}) and (V_{buffer}) represent the volumina of the growth field and the volume of the gel solubilization buffer, respectively. (Here, a density of the agar gel of 1 mg·mL^{-1} was assumed.)

$$m_{G,vial} = \frac{OD_{sample}}{OD_{stand}} \cdot (V_{agar} + V_{buffer}) \cdot c_{stand} \qquad (4.14)$$

In order to account for variations in the dimensions of the growth fields, the amount of glucose per vial ($m_{G,vial}$) was normalized for the average mass ($m_{A,average}$) of all analyzed growth fields yielding the normalized mass of glucose ($m_{G,norm}$) in an average growth field.

$$m_{G,norm} = \frac{m_{G,vial} \cdot m_{A,average}}{m_{A,sample}} \qquad (4.15)$$

Since the average mass of the analyzed growth fields may differ from the mass of the standard growth field (standard dimensions: 1 cm x 5.2 cm x 0.09 cm) used in the simulations, the glucose content in the standard growth field (m_G) was calculated according to

$$m_G = m_{G,norm} \cdot S. \qquad (4.16)$$

Here, (S) represents the ratio of the *measured* glucose content in standard agar stripes ($m_{G0,measured}$) that were not used in the cultivations but stored and analyzed under the same conditions, and the mass of glucose in these agar stripes (m_{G0}) *calculated* from the initial glucose concentration and the volume of the standard growth field.

$$S = \frac{m_{G0,measured}}{m_{G0}} \qquad (4.17)$$

4.3.4.   Estimation of pH in the Growth Field

In the experiments described in Section 5.4.2, the pH of the growth field of the colonies was determined using test papers with a resolution of 0.3 pH units (Merck, measurement range pH 4.9-7.9) and 1 pH unit (Merck, measurement range pH 1-10), respectively. Agar tiles (dimensions: 5 mm x 10 mm) were cut out from the growth fields and placed on small stripes of the test paper. The color reaction was compared to a pH scale. For each colony, the pH of five tiles was analyzed and averaged. (Although the tiles were taken from different locations within the growth substrate, under most conditions no considerable differences between the sampling points were detected which is mainly owed to the crude estimation method.) pH was estimated weakly. For each sampling time, pH was measured in two colonies.

In the investigations of the influence of volatile compounds on colony development (Section 5.4.1), pH in the growth fields of the giant and small colonies was measured using a pH meter (pH-Level 2, InoLab, WTW) equipped with a plane pH electrode (SenTix 41, diameter 10 mm, WTW).

4.4. Estimation of Biomass-yield Coefficients

Biomass yields of both yeasts on different nutrients was determined in shake flask experiments. 250 mL Erlenmeyer flask were filled with 100 mL medium and incubated at room temperature on a rotary shaker at 300 rpm.

In order to ensure the limitation of a particular nutrient, its concentration was strongly decreased when compared to the standard minimal medium (C-G-20 in Table 4.1). Media for the determination of biomass-yield coefficients are listed in Table 4.3.

Table 4.3: Compositions of media for the determination of biomass yields on different nutrients

Nutrient	Medium
Carbon limitation	
glucose	C-G-2
casamino acids	C-CA-10
Nitrogen limitation	
$(NH_4)_2SO_4$	N-A-0.5
casamino acids	N-CA-1.5

For each combination of nutrient and yeast, two replicate runs were started at a time. Flasks were inoculated with 0.5 mL of a washed yeast suspension obtained from an overnight culture grown on C-G-20 medium (Table 4.1) under otherwise identical cultivation conditions. Biomass growth was followed by OD measurements at 570 nm using a spectrophotometer (Genesis 10UV, Thermospectronic Rochester). Cultivations were aborted when OD remained constant for two days. 2 mL of the yeast suspension were transferred to 2 mL plastic tubes of known weight.

Cells were separated from the cultivation medium by centrifugation at 15244 x g for 10 min and washed once with distilled water. The plastic tubes containing the cell pellets were dried in a climate chamber at 80 °C until weight consistency. Dry biomass content of the tubes was calculated from the weight difference with and without the cell pellet. For each flask six tubes were filled and dried. The biomass-yield coefficients (Y) (listed in Table 5.1) were calculated from the dry biomass content of the flasks at the end of the cultivation and the initial content of limiting nutrient. The inoculum of the flasks was negligibly small.

4.5. Program Development and Simulations

The simulation routines were implemented using the KDevelop-software package together with the Qt C++ libraries from Trolltech[TM]. Simulations were carried out on a LINUX platform (SUSE 8.1) using a single-user PC.

# 5. EXPERIMENTAL INVESTIGATION OF YEAST COLONY DEVELOPMENT

5.1. Growth Strategies of Yeast Colonies at Different Nutrient Concentrations

### 5.1.1. Induction of Mycelial Colony Morphologies

In order to investigate growth strategies of yeast colonies at different degrees of nutrient limitation, the model organisms *Candida boidinii* and *Yarrowia lipolytica* were cultivated in petri dishes on solid agar (2 g·L^{-1}) substrates containing a defined reservoir of food resources. The composition of the growth medium was derived from a minimal medium containing 20 g·L^{-1} glucose, serving as the only carbon source, 5 g·L^{-1} ammonium sulfate, representing the only nitrogen source, and 1.7 g·L^{-1} yeast nitrogen base (YNB), containing all essential vitamins and trace elements (Atlas, 1996). Various degrees of nutrient limitation were imposed by the selective dilution of one essential nutrient (carbon or nitrogen source) in the medium. Furthermore, glucose or ammonium sulfate were substituted by casamino acids to study the influence of different carbon and nitrogen sources on colony development. A medium was considered to impose carbon limitation when (according to the estimated biomass yields on the applied carbon and nitrogen sources (Table 5.1)) after the complete depletion of the carbon source ample nitrogen could be expected to be present in the medium. Nitrogen-limited conditions were defined analogously.

Since the yeasts were cultivated on a comparatively large number of different media, a short-notation was introduced to provide an easy reference to the medium composition. The first letter in the notation refers to the limiting nutrient resource (**C**arbon or **N**itrogen). The second part denotes the particular nutrient which served as the carbon or nitrogen source (**G**lucose, **A**mmonium sulfate, **C**asamino **A**cids). The number provides the concentration of the limiting nutrient in grams per liter. E.g., the notation C-CA-0.2 denotes a medium which imposes carbon limitation with 0.2 g·L^{-1} casamino acids serving as the only carbon source. The concentrations of the other medium components (in the above described example nitrogen source (ammonium sulfate), trace element base (YNB), and agar) remain constant when compared to the standard minimal medium. The complete medium composition for each notation is provided in Table 4.1.

In contrast to the yeast *S. cerevisiae*, which only forms filamentous colony patterns under severe nitrogen limitation, both model yeasts develop mycelial morphologies irrespective of the limiting nutrient. Images of *Y. lipolytica* and *C. boidinii* colonies cultivated on different food resources at various degrees of limitation are provided in Figs. 5.1-5.4. Images were taken after 21 days of incubation. Please note that the presented colony patterns do not show the final state of the cultivations but rather correspond to intermediate stages in colony development.

C-G-20

C-G-2

N-A-0.5

C-G-0.2
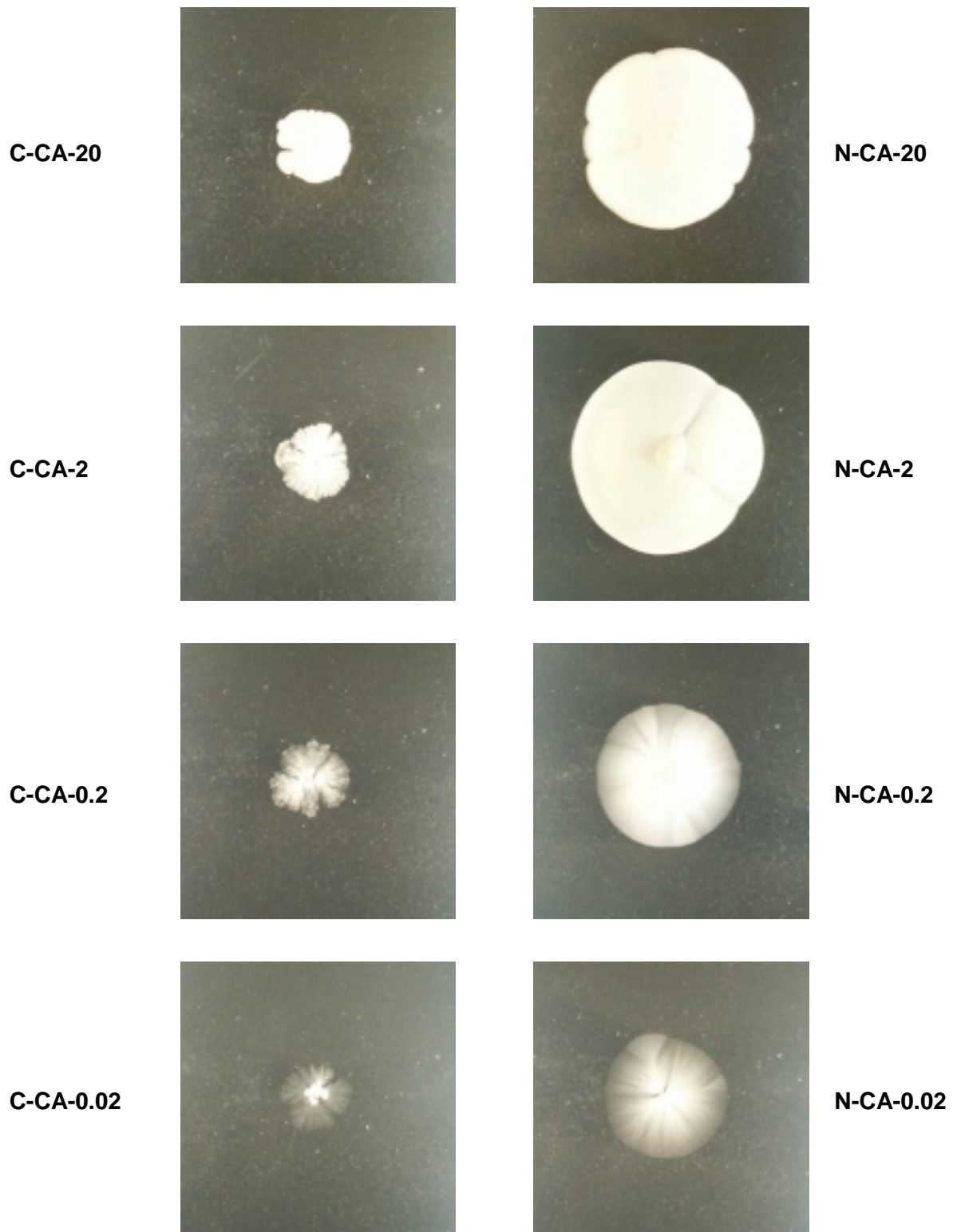
N-A-0.05

C-G-0.02

N-A-0.005
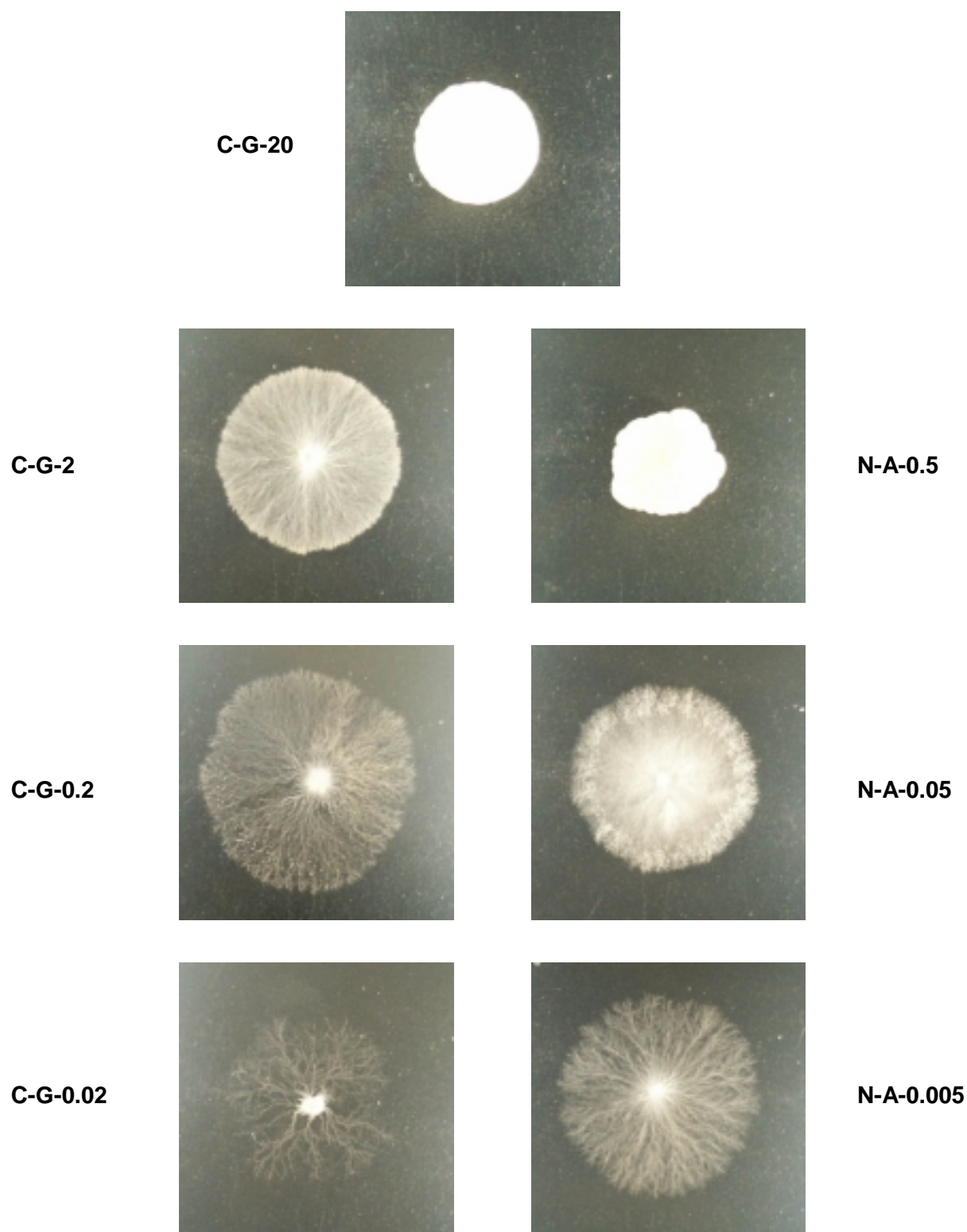
Figure 5.1: Morphology of *Y. lipolytica* colonies growing under various degrees of nutrient limitation. The growth media were derived from the minimal medium described in Section 4.1 by the selective dilution of either nitrogen or carbon source. **Left column**: Carbon-limited colonies growing on glucose as the only carbon source. **Right column**: Nitrogen-limited colonies growing on ammonium sulfate as the only nitrogen source. Short notations referring to medium compositions are provided next to the images (see Table 4.1 for details). Cultivation time was 21 days. Width of the images represents 2.8 cm.
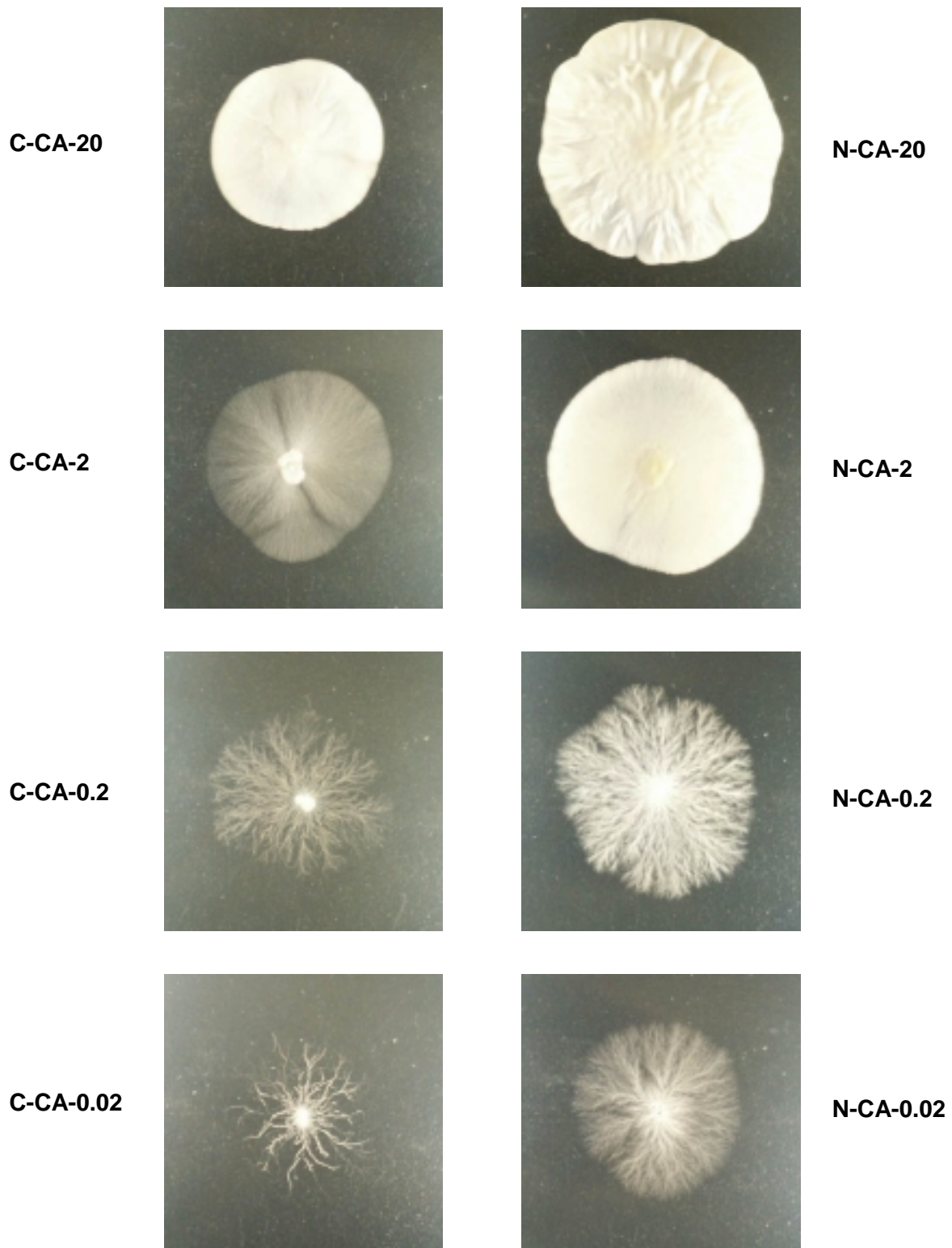
Figure 5.2: Morphology of *Y. lipolytica* colonies growing under various degrees of nutrient limitation. The growth media were derived from the minimal medium described in Section 4.1 by the selective dilution of either nitrogen or carbon source. **Left column**: Carbon-limited colonies growing on casamino acids as the only carbon source. **Right column**: Nitrogen-limited colonies growing on casamino acids as the only nitrogen source. Short notations referring to medium compositions are provided next to the images (see Table 4.1 for details). Cultivation time was 21 days. Width of the images represents 2.8 cm.
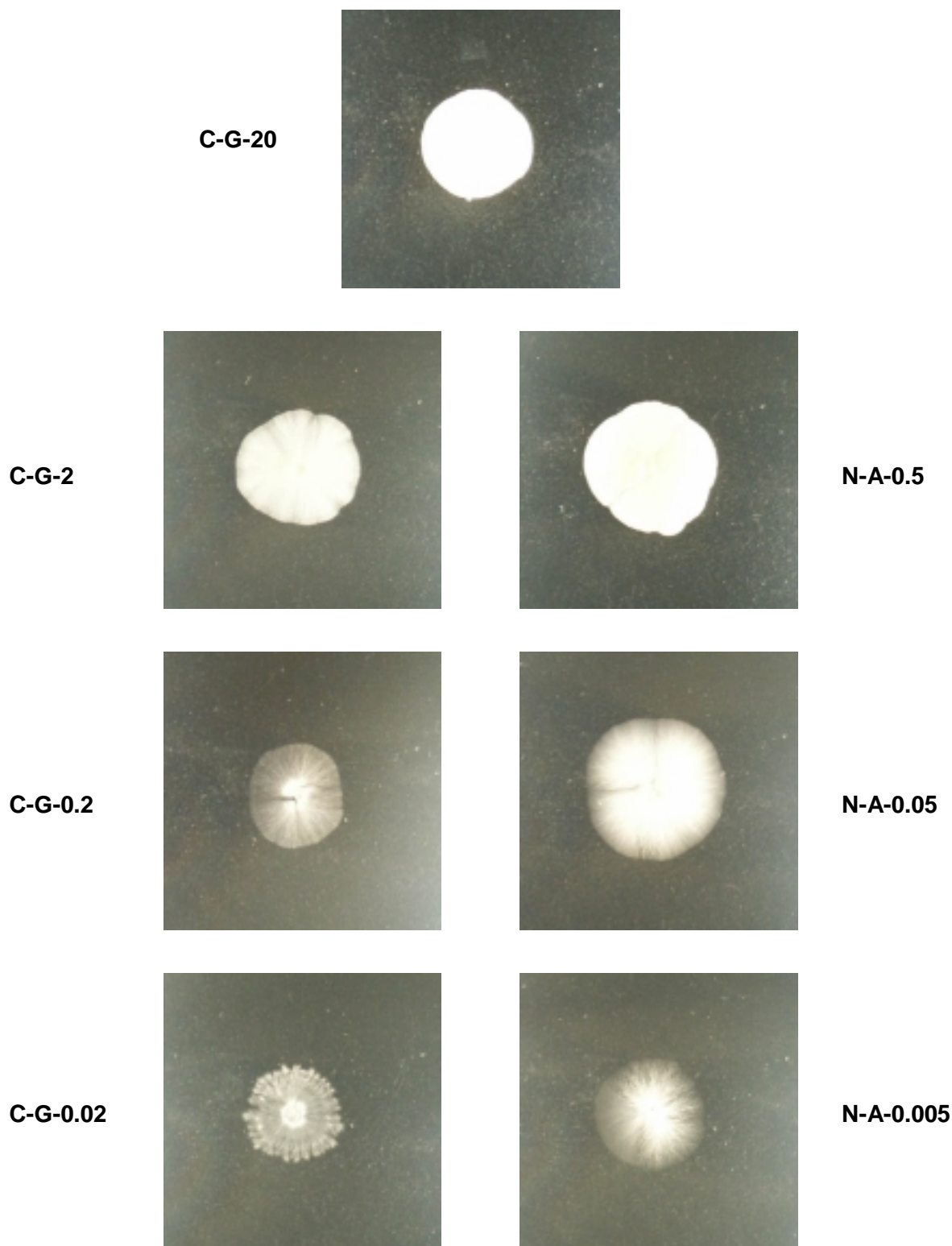
Figure 5.3: Morphology of *C. boidinii* colonies growing under various degrees of nutrient limitation. The growth media were derived from the minimal medium described in Section 4.1 by the selective dilution of either nitrogen or carbon source. **Left column**: Carbon-limited colonies growing on glucose as the only carbon source. **Right column**: Nitrogen-limited colonies growing on ammonium sulfate as the only nitrogen source. Short notations referring to medium compositions are provided next to the images (see Table 4.1 for details). Cultivation time was 21 days. Width of the images represents 2.8 cm.

Figure 5.4: Morphology of *C. boidinii* colonies growing under various degrees of nutrient limitation. The growth media were derived from the minimal medium described in Section 4.1 by the selective dilution of either nitrogen or carbon source. **Left column**: Carbon-limited colonies growing on casamino acids as the only carbon source. **Right column**: Nitrogen-limited colonies growing on casamino acids as the only nitrogen source. Short notations referring to medium compositions are provided next to the images (see Table 4.1 for details). Cultivation time was 21 days. Width of the images represents 2.8 cm.

In general, at high nutrient concentrations colony morphologies of both model yeasts are solid and exhibit a smooth boundary. Under strong nutrient limitation, mycelial colony patterns are formed and the colony boundaries become frayed. In particular, *Y. lipolytica* colonies are highly similar to fungal mycelia. The cell density within the colony declines with increasing degree of nutrient limitation. However, even under severe nutrient limitation, colony patterns of *C. boidinii* are rather dense (Figs. 5.3 and 5.4). Only carbon-limited *Y. lipolytica* colonies exhibit sparsely branched filamentous structures at very low nutrient concentrations (Figs. 5.1 and 5.2). Furthermore, under most conditions no significant drop in the size of the colonies can be observed although the concentration of limiting nutrient decreases in an order of three magnitudes. In case of *Y. lipolytica* growing under glucose or ammonium sulfate limitation, the transition to mycelial morphologies even coincides with a pronounced enlargement of the colony diameter (Fig. 5.1).

The transition to mycelial colony patterns is caused by the microscopic differentiation from almost round (yeast-like) cells to elongated (pseudohyphal) cells. In *Y. lipolytica* and *C. boidinii* colonies the differentiation of cells is only prevented at high nutrient concentrations (see solid colonies on the medium C-G-20 in Figs. 5.1 and 5.3). Due to the accumulation of high cell densities on these media, individual cells cannot be captured by transmitted-light photography. Therefore, differentiation of the yeast cells at the microscopic level is shown by comparing the morphology of *S. cerevisiae* cells that grow round-shaped under carbon limitation and switch to the pseudohyphal growth form when severely starved for nitrogen (Fig. 5.5). As outlined in Section 3.1.2, this change in morphology facilitates directed growth of individual cells away from the inoculation site and is the prerequisite for the formation of mycelial colony patterns.
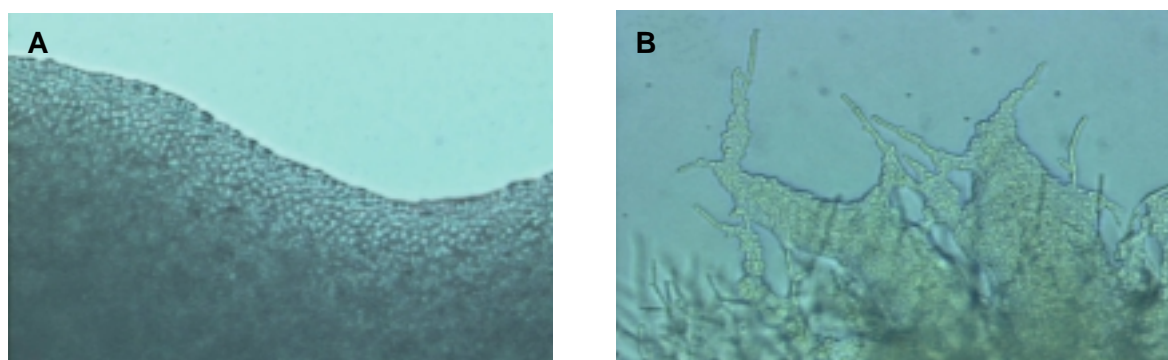
Figure 5.5: Microscopic images of the colony boundaries of (A) carbon-limited (medium C-G-0.2) and (B) nitrogen-limited (medium N-A-0.005) *S. cerevisiae* colonies at early stages of the cultivation. Width of the images represents 150 µm.

5.1.2. Adaptation of Mycelial Colonies to Different Nutrient Concentrations

To study the adaptation of mycelial yeast colonies to nutrient availability, the model organisms were cultivated on various carbon (glucose, casamino acids) and nitrogen (ammonium sulfate, casamino acids) sources at two different degrees of nutrient limitation. Since the results of the experimental characterization of colony development were meant to

be compared to one-dimensional models, colonies were cultivated on rectangular growth fields and inoculated as a line (Fig. 5.6, see Section 4.2 for further details). The cell-density profile of the colonies was estimated by taking microscopic images along the longitudinal axis of the colony, measuring the OD profile from the intensity of the transmitted light, and calibrating OD for local cell number (see Section 4.3).

Figure 5.6:   Rectangular *Y. lipolytica* colony growing on 10 g/L tryptone as the only nitrogen source. Cultivation time was 28 days. Width of the image represents 10.4 cm.

The extension of the colonies was followed using a ruler. Although colonies grew in a rectangular shape, the extension of the mycelia along the longitudual axis of the growth field is referred to as colony diameter in the following sections. The time course of the colony diameter and colony extension rates provided in Fig. 5.7 and Table 5.1 represent the average of at least four replicate runs. Under glucose-limiting conditions, final colony diameters of *C. boidinii* colonies varied strongly between different batches of experiments (maximum 14 mm, minimum 8 mm). The origin of these deviations was not definitely identified. However, to increase reliability of the data, colony extension rates and final diameter of glucose-limited *C. boidinii* colonies were estimated from the average of 5 independent batches of experiments (each batch comprising at least 4 replicates).

Under most imposed conditions, colony diameters grow linearly until the edge of the growth field is reached (Fig. 5.7, Table 5.1). As the only exceptions, carbon-limited *C. boidinii* colonies, as well as colonies of the same yeast cultivated on 20 $g \cdot L^{-1}$ casamino acids as the only nitrogen source, stop growth at a final colony diameter which is significantly smaller than the extensions of the growth field (Fig. 5.7, Table 5.1).
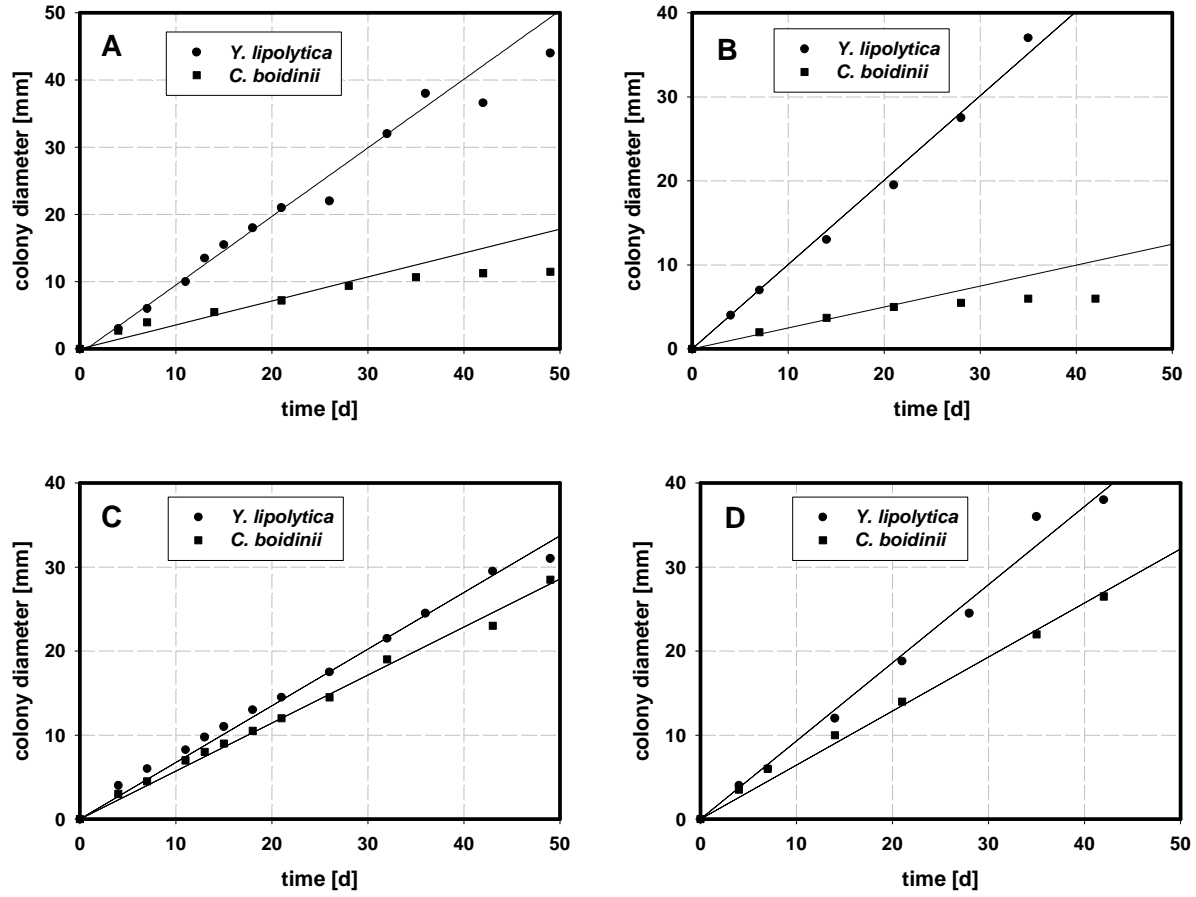
Figure 5.7: Colony diameters of *Y. lipolytica* and *C. boidinii* colonies vs. time. (A) Carbon-limited colonies growing on glucose (C-G-2). (B) Carbon-limited colonies growing on casamino acids (C-CA-10). (C) Nitrogen-limited colonies growing on ammonium sulfate (N-A-0.05). (D) Nitrogen-limited colonies growing on casamino acids (N-CA-2).

Interestingly, the extension rate of mycelial yeast colonies was found to be independent from the initial nutrient concentration (Table 5.1), a result which is consistent with findings for the growth of higher fungi (see Gow (1994) and references therein). Carbon-limited *Y. lipolytica* colonies extend with a rate of approximately 1 mm·d^{-1}. Under nitrogen limitation, growth of the yeast is faster on casamino acids (1 mm·d^{-1}) when compared to cultivations on ammonium sulfate (0.7 mm·d^{-1}). Under all cultivation conditions, growth of *C. boidinii* colonies was found to be somewhat slower with extension rates of 0.5-0.7 mm·d^{-1}. According to equation

$$\Delta t_p = \frac{2 \cdot l_C}{v}$$

(5.1)

the replication interval (Δt_p), necessary to form a new cell, was calculated from the average length of pseudohyphal cells (l_C) and the growth rate of the colony diameter (v). (l_C) was estimated at different cultivation times and various locations within the colony using the image analysis software package OPTIMAS.

47

Table 5.1: Summary of growth parameters for *C. boidinii* and *Y. lipolytica* colonies cultivated on different carbon and nitrogen sources under two different degrees of nutrient limitation.

Medium	Extension rate (v) [mm·d^{-1}]	Cell length (l_C) [µm]	Cell diameter (d_C) [µm]	Replicat. time (Δt_p) [h]	Final colony diameter [mm]	Biomass yield (Y) [g·g^{-1}]
Y. lipolytica						
C-G-4 (C-G-2)*	0.9 (1.0)*	30	2.3	1.7 (1.4)*	52*	0.33
C-CA-20 (C-CA-10)*	1.0	27	3.0	1.3 (1.4)*	52*	0.14
N-A-0.1 (N-A-0.05)*	0.7	27	3.0	1.83	52*	7.2
N-CA-20 (N-CA-2)*	1.0 (0.9)*	21	3.0	1.0	52*	2.5
C. boidinii						
C-G-4 (C-G-2)*	0.5	19	2.7	1.7	10 ±2	0.42
C-CA-20 (C-CA-10)*	0.2	14	2.1	3.3	6 ±1	0.04
N-A-0.1 (N-A-0.05)*	0.6 (0.5)*	24	2.7	2.3 (2.1)*	52**	5.2
N-CA-20 (N-CA-2)*	0.5 (0.7)*	21	2.7	2.1 (1.6)*	20 ±2 (52**)*	2.3

* Numbers in parentheses refer to the second nutrient concentration (see left column in parentheses) when the results for the two concentrations were different.

**A maximum colony diameter of 52 mm indicates that the outer edge of the growth field was reached by the colony boundary.

In contrast to the extension rates of the colony diameters, cell-density profiles vary significantly with nutrient availability (Figs. 5.8 and 5.9). (Since colonies are symmetrical in shape, figures only show the cell density profiles in one half of the colony with the coordinate x = 0 representing the inoculation site.) With increasing nutrient limitation, the total cell number within the mycelium declines. In case of carbon limitation, the drop in total cell number is roughly proportional to the decrease in nutrient availability (Fig. 5.8). Under nitrogen-limiting conditions, however, a deprivation of the limiting nutrient source does not directly correspond to the observed decrease in total cell number (Fig. 5.9).

The morphology of the cell-density profiles depends on both, the applied yeast species as well as the particular cultivation conditions. Carbon-limited *C. boidinii* colonies are characterized by a rapidly declining cell density and a small final colony diameter when compared to the size of the growth field. (Please note that colony-density profiles of *C. boidinii* in Fig. 5.8 (B, D) show the final stage in colony development. For all other cultivation conditions, the presented cell-density profiles only represent intermediate states, since colony growth continues for up to several weeks.) In contrast, *Y. lipolytica* colonies limited for carbon sources exhibit large areas of slowly declining or constant cell density, respectively (Fig. 5.8 A, C). Close to the inoculation site, however, regions of rather high cell density can be observed. In particular, when glucose serves as the carbon source a sharp transition between these two sections is evident (Fig. 5.8 A). Although not explicitly investigated, the

peak in cell number at the inoculation site appears to correspond to the presence of undifferentiated yeast-like cells.
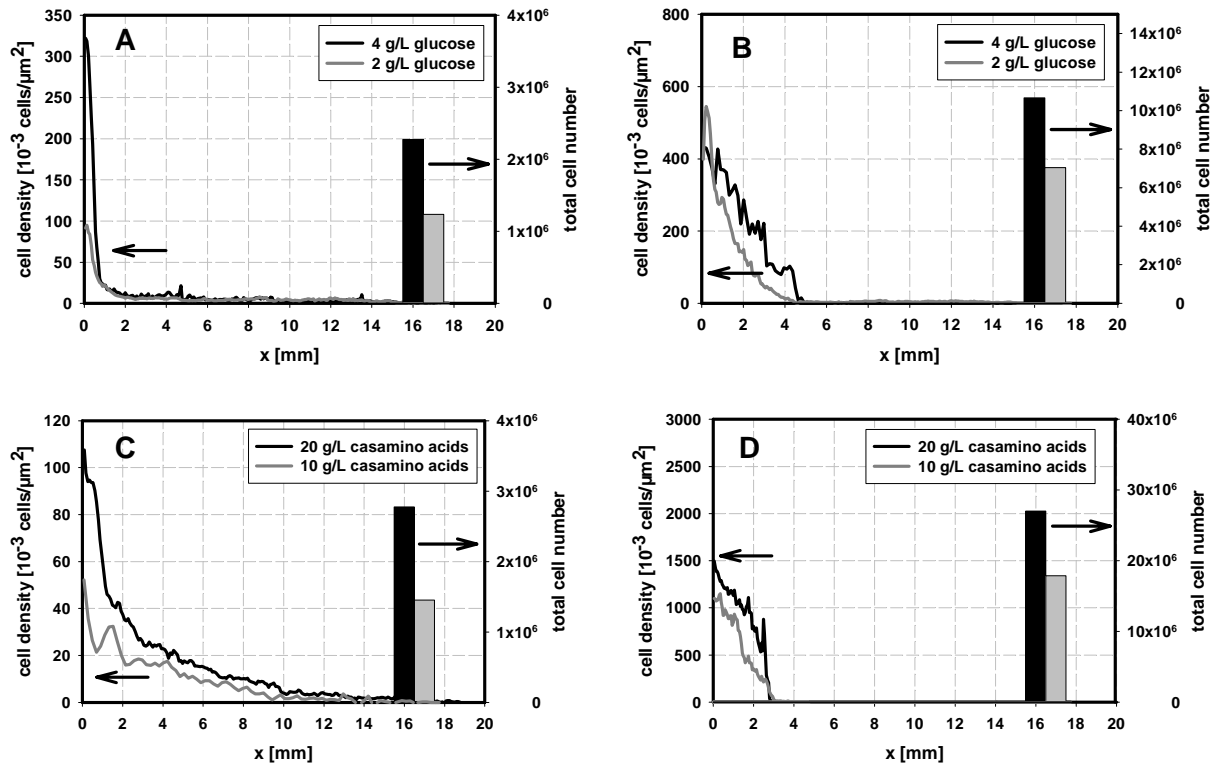
Figure 5.8: Cell-density profiles and total cell numbers of *Y. lipolytica* and *C. boidinii* colonies growing under carbon limitation. Profiles were estimated after 35 days of cultivation. (A) *Y. lipolytica* growing on glucose as the limiting carbon source (media C-G-4 and C-G-2). (B) *C. boidinii* growing on glucose as the limiting carbon source (media C-G-4 and C-G-2). (C) *Y. lipolytica* growing on casamino acids as the limiting carbon source (media C-CA-20 and C-CA-10). (D) *C. boidinii* growing on casamino acids as the limiting carbon source (media C-CA-20 and C-CA-10).

Under severe nitrogen limitation, both yeasts form colonies that finally cover the whole growth field (Table 5.1). In *Y. lipolytica* colonies, the formation of regions with slowly descending cell-density profiles becomes already evident after 35 days of cultivation (Fig. 5.9 A, C). Since growth of *C. boidinii* is somewhat slower, colonies do not yet exhibit areas of constant cell density (Fig. 5.9 B, C). However, since colony development continues for several weeks the formation of cell-density plateaus can also be expected also for this yeast.
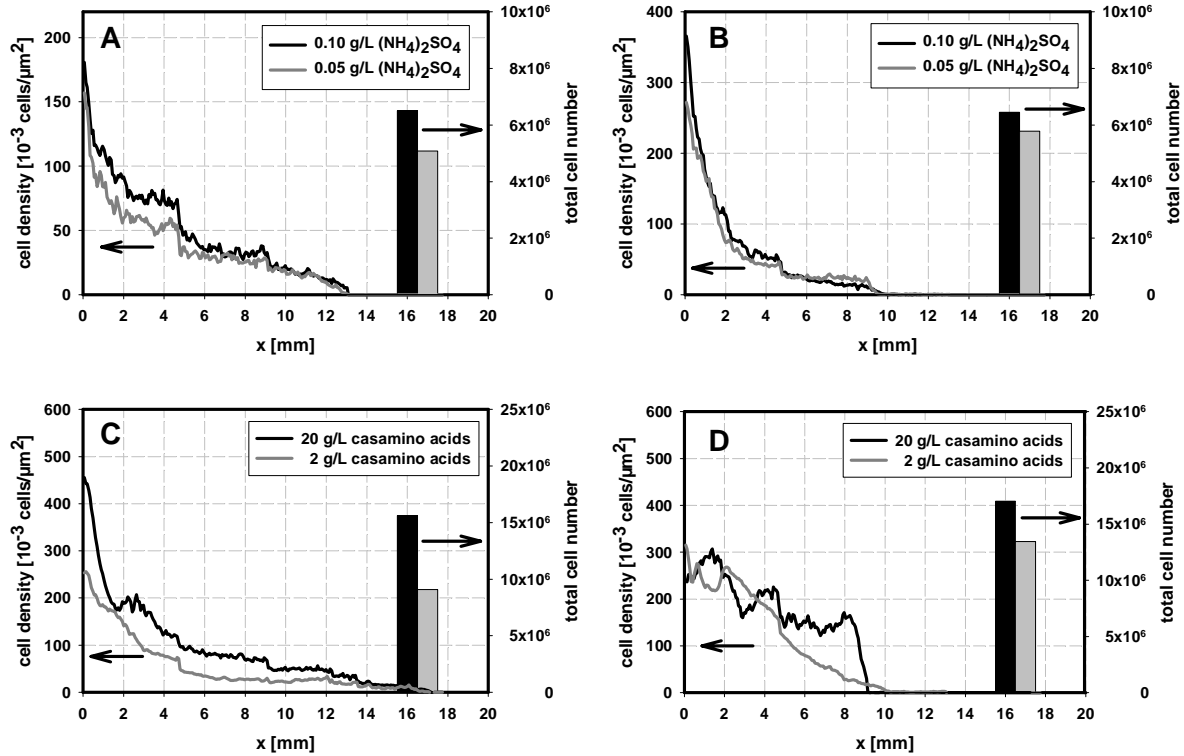
Figure 5.9: Cell-density profiles and total cell numbers of *Y. lipolytica* and *C. boidinii* colonies growing under nitrogen limitation. Profiles were estimated after 35 days of cultivation. (A) *Y. lipolytica* growing on $(NH_4)_2SO_4$ as the limiting nitrogen source (media N-A-0.1 and N-A-0.05). (B) *C. boidinii* growing on $(NH_4)_2SO_4$ as the limiting nitrogen source (media N-A-0.1 and N-A-0.05). (C) *Y. lipolytica* growing on casamino acids as the limiting nitrogen source (media N-CA-20 and N-CA-2). (B) *C. boidinii* growing on casamino acids as the limiting nitrogen source (media N-CA-20 and N-CA-2).

5.2.   Spatio-temporal Development of Mycelial Colonies

In order to analyze the spatio-temporal evolution of mycelial yeast colonies, the development of cell-density profiles was monitored over a time span of up to 35 days. At longer cultivation times, growth of the colonies becomes highly heterogeneous causing an inadequately high experimental effort to obtain reproducible results. The model yeasts were cultivated on the carbon and nitrogen sources described above. In contrast to Section 5.1, the development of the colonies was only investigated for one concentration of a particular nutrient. The development of *C. boidinii* colonies on casamino acids as the only carbon source was extremely poor and heterogeneous. Therefore, growth of the yeast under these conditions was not further analyzed.

5.2.1.   Development of Carbon-limited Colonies

Colony Development on Glucose as the only Carbon Source

The cell-density profiles were estimated using the protocol described in Section 4.3. Furthermore, the total cell numbers within the colonies were calculated from the integral of

the cell density over the colony area. Please note that cell densities and total cell numbers presented in the charts refer to the dimensions of unit cells. These dimensions vary strongly depending on yeast species and cultivation conditions (Table 5.1). Therefore, the *cell* density may differ significantly between different treatments although the *biomass* density is nearly identical. To provide the reader with a reference for the comparison of biomass densities and the accumulation of total biomass under different cultivation conditions, in all charts the corresponding OD values are provided at the secondary ordinate axis. Here, "total OD" refers to the sum of the OD values of all sampling points (see Section 4.3).

In Fig. 5.10 the development of cell-density profiles and total cell numbers in carbon-limited *C. boidinii* and *Y. lipolytica* colonies growing on 2 g·L^{-1} glucose as the only carbon source (medium C-G-2) is depicted. Under these conditions, strong differences in the growth strategies of the two model organisms are evident. At the beginning of the cultivation, rapid cell growth in *C. boidinii* colonies results in the accumulation of high cell numbers close to the inoculation site (Fig. 5.10). The (net)formation of new cells is restricted to the colony boundary since no increase in local cell density can be observed behind the growth front of the colony (Fig. 5.10 A). In the course of the cultivation, the edge of *C. boidinii* colonies propagates at a constant rate (Fig. 5.7) whereas the number of new cells formed per time declines (Fig. 5.10 A, B).
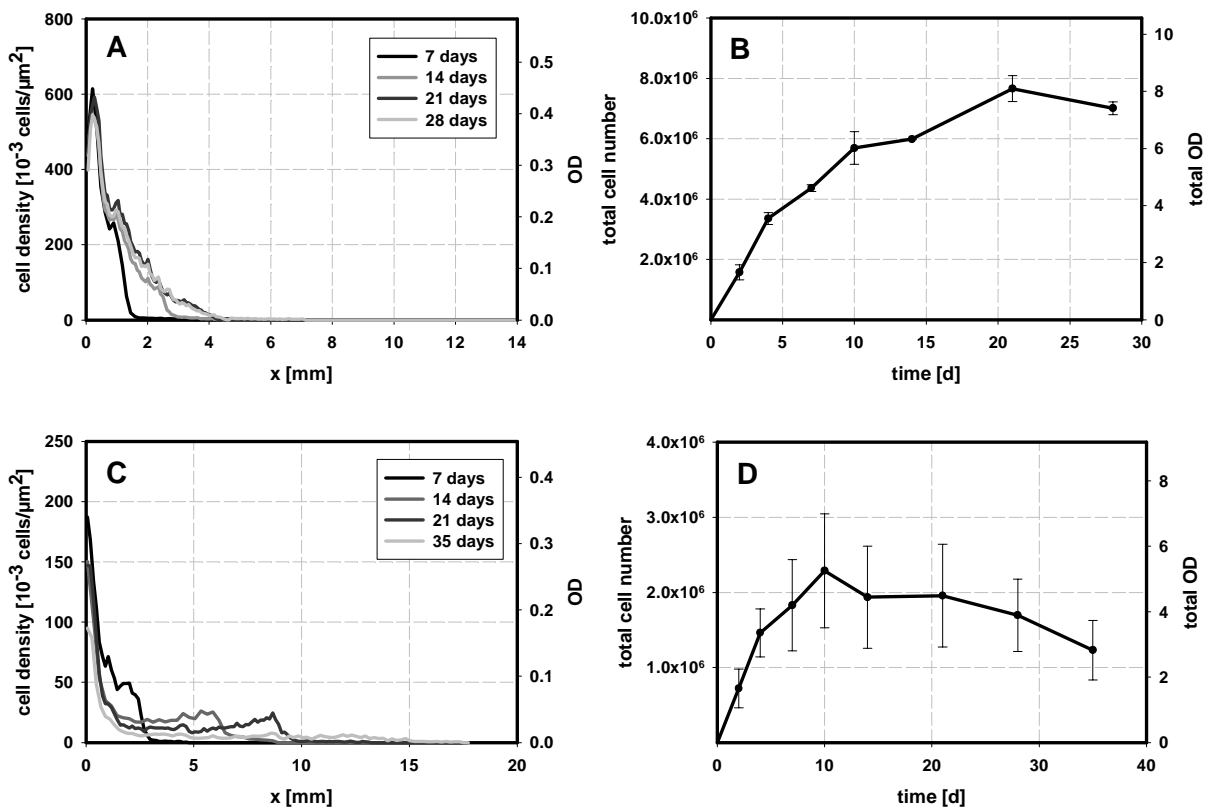
Figure 5.10: Development of carbon-limited (A, B) *C. boidinii* and (C, D) *Y. lipolytica* colonies growing on glucose as the only carbon source (medium C-G-2). (A, C) Spatio-temporal development of the cell-density profile in one colony moiety. (B, D) Development of the total cell number in one colony moiety.

This behavior causes a strong decrease of local cell density at higher colony diameters, and a saturation of the total cell number vs. time curve at cell numbers of approximately $8 \cdot 10^6$ cells (Fig. 5.10 A, B). After a cultivation time of 28 days, the development of glucose-limited *C. boidinii* colonies reaches its final stage. The colony-density profiles after 21 and 28 days of cultivation as well as the total cell numbers are nearly identical and the populations stop to expand (Fig. 5.10 A, B).

At early stages of the cultivation, the development of glucose-limited *Y. lipolytica* colonies is similar to the behavior found for *C. boidinii*. High cell numbers accumulate during the first days of colony development and the cell-density profile exhibits a steep descent (Fig 5.10 C). In the course of the cultivation, the mycelia expand and new cells are formed at the colony boundary, while OD measurements of the colony density suggest that local cell density in the colony interior declines. After 10-14 days of cultivation, the rate of cell decay surpasses the gain by newborn cells and the total cell number within the colonies declines continuously (Fig. 5.10 D). After 35 days of cultivation, the total cell number in glucose-limited *Y. lipolytica* colonies drops to a value of approximately 60 % when compared to the maximum at 10 days. Thus, the formation of constant cell-density profiles in carbon-limited *Y. lipolytica* colonies appears to be the result of a continuous cell decay in the colony interior coinciding with the formation of new cells at the colony boundary. However, at the current stage of the investigation it is not clear, whether the drop in local OD is the result of a complete cell decay. Alternatively, it may be caused by the emission of parts of the cell interior into the growth substrate, i.e., the result of a strong vacuolization of the cells. Thus, the drop of OD in the inner colony sections corresponds to a declining local biomass density rather than to a change in cell number.

In order to test whether the depletion of the limiting carbon source is responsible for the stop of colony extension in *C. boidinii* colonies, the glucose content of the growth fields was estimated by an enzyme assay according to the method described in Section 4.3.3. The measurements show a rapid consumption of the nutrient in cultivations of both yeasts (Fig. 5.11).
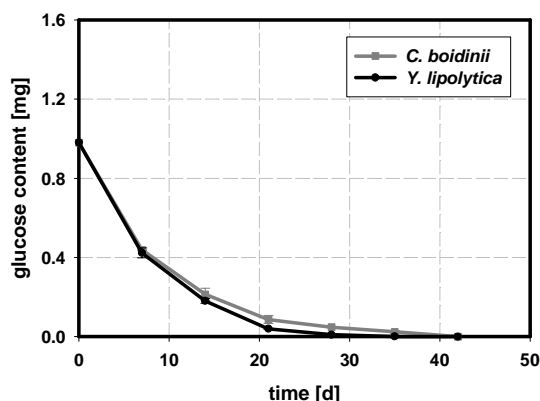
Figure 5.11: Estimated glucose content in the growth field of *Y. lipolytica* and *C. boidinii* colonies growing on glucose as the only carbon source (medium C-G-2). Data points represent double estimates.

After 28 days the concentration of the limiting nutrient resource is extremely low and after 35 days it cannot be detected in the substrate. The complete depletion of glucose coincides with the stop of colony development of *C. boidinii* colonies. Thus, the presence of this nutrient resource is essential for the colony extension of this yeast (compare Figs. 5.7 A, 5.10 A and 5.11).

In contrast to these findings, colonies of *Y. lipolytica* continue to extend after glucose is depleted. From measurements of the glucose content and the local cell density, the hypothesis can be derived that carbon-limited *Y. lipolytica* colonies can expand even in the absence of the primary nutrient using the decay products of potentially dying cells in the colony interior as a food resource (compare Figs. 5.7 A, 5.10 C, and 5.11). In order to test this hypothesis, the inner parts of glucose-limited *Y. lipolytica* and *C. boidinii* colonies were removed after 14 days of cultivation by cutting out the agar substrate with a sterile scalpel. Only a small stripe of cells (width approximately 1mm) remained on the growth field and was further cultivated for (in total) 56 days. If the hypothesis of cannibalizing growth as described above is true, the removal of cells in the colony interior is equivalent with the reduction of a nutrient resource. Thus, "cut-out" *Y. lipolytica* colonies can be expected to develop smaller cell densities.
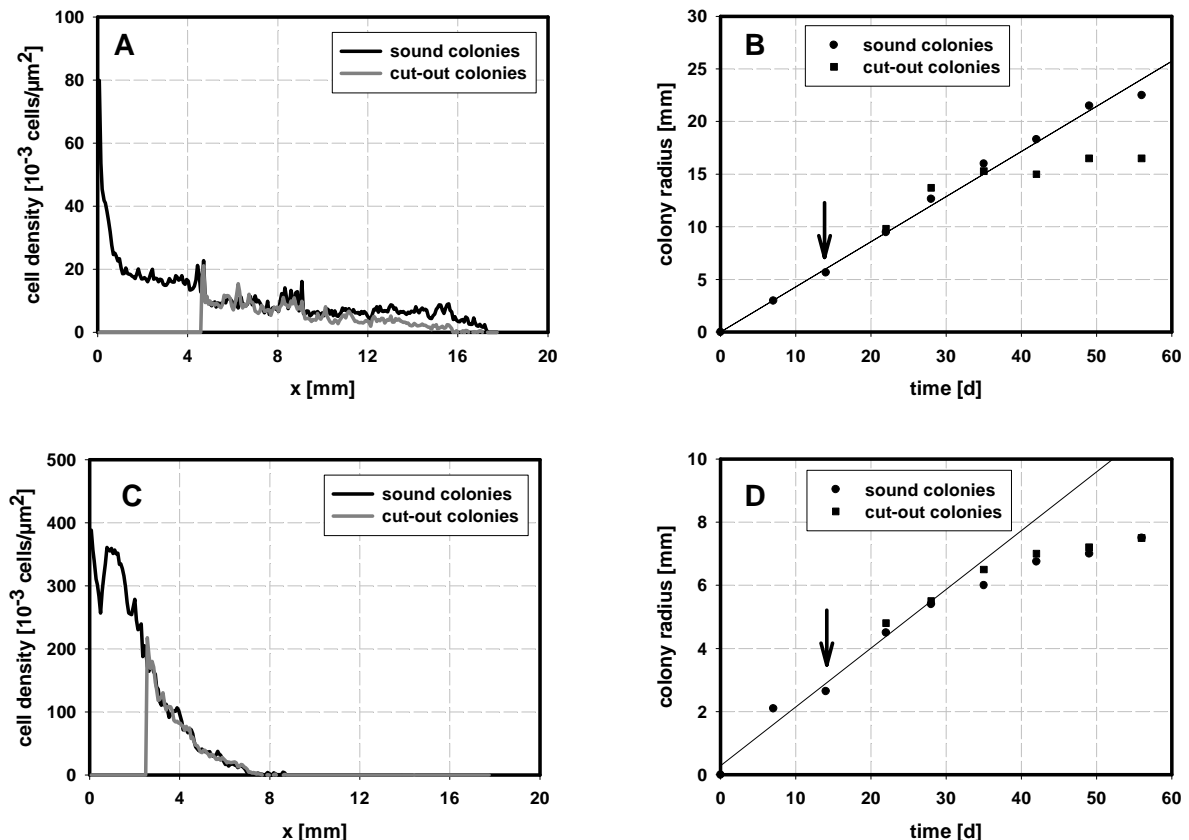
Figure 5.12: Development of glucose-limited (A, B) *Y. lipolytica* and (C, D) *C. boidinii* colonies that grow undisturbed vs. colonies with a removed colony interior. (A, C) Cell-density profiles in one colony moiety after 35 days of incubation. (B, D) Colony radius vs. time. The time of removal of the colony interior is indicated by an arrow (B, D). Colonies were cultivated on C-G-2 medium.

Accordingly, the development of sound colonies was compared to "cut-out" colonies with respect to changes of the cell-density profiles and in the extension of the colonies, respectively (Fig. 5.12).

As expected, *Y. lipolytica* colonies with a removed interior exhibit smaller cell densities after 35 days of cultivation when compared to the undisturbed mycelia (Fig. 5.12 A). Furthermore, the colony diameter of "cut-out" colonies stops to extend after 35 days, while undamaged colonies grow linearly further until the edge of the growth field is reached (Fig. 5.12 B). When these findings are combined with measurements of the glucose content and cell density, the results clearly prove the hypothesis of cannibalizing growth in glucose-limited *Y. lipolytica* colonies. At late stages of the cultivation, proliferating cells in the colony boundary utilize cell-decay products in the absence of glucose as a secondary nutrient resource. In contrast to *Y. lipolytica*, "cut-out" *C. boidinii* colonies do not exhibit any differences when compared to their undisturbed counterparts (Fig. 5.12 C, D). The colony diameter reached in this batch of experiments is somewhat higher than the average size of colonies estimated from 5 different batches (compare Fig. 5.7 A and Fig. 5.12 D). However, these deviations are subject to the variations in colony extension of glucose-limited *C. boidinii* populations described above. Since the depletion of glucose after 35 days of cultivation coincides with the stop of colony extension, a significant utilization of alternative carbon sources can be precluded under these conditions.

In order to estimate the rate of local cell decay in glucose-limited *Y. lipolytica* colonies, the OD of the colonies was measured at different distances from the inoculation site over a period of 35 days. Fig. 5.13 shows the logarithmic plot of OD versus time at distances of 1 mm and 2 mm from the colony center. Time constants for cell decay (T_C) were calculated from the slope of the regression lines and summarized in Table 5.2.
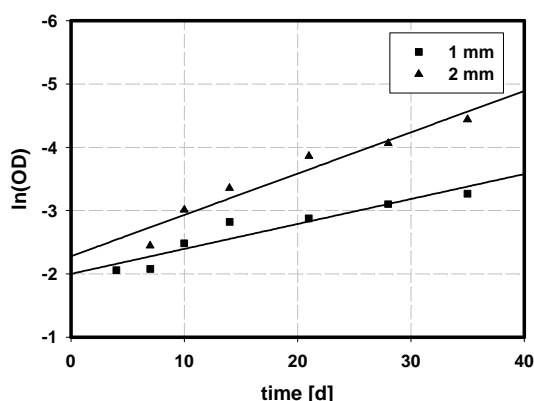
Figure 5.13: Logarithmic plot of local OD (as a measure for local cell density) in carbon-limited *Y. lipolytica* colonies at distances of 1 mm and 2 mm from the inoculation site vs. time. Colonies were cultivated on C-G-2 medium.

Close to the inoculation site, cells decay significantly slower. With larger distances from the colony center, time constants for cell decay appear to decrease gradually. A possible reason for this behavior was not identified. However, the significantly smaller cell decay close to the inoculation site appears to correspond to the presence of undifferentiated yeast-like cells.

Table 5.2: Time constants of cell decay (T_C) at various distances from the inoculation site.

Distance from inoc. site [mm]	T_C [h]
1	615
2	369
3	358
4	375
5	300
6	307

Colony Development on Casamino Acids as the only Carbon Source

The development of carbon-limited *Y. lipolytica* populations growing on casamino acids as the only carbon source is very similar to glucose-limited conditions. During the cultivation, the cell density inside the colony declines (Fig. 5.14 A) while the colony expands continuously until the edge of the growth field is reached (Fig. 5.7, Table 5.1).
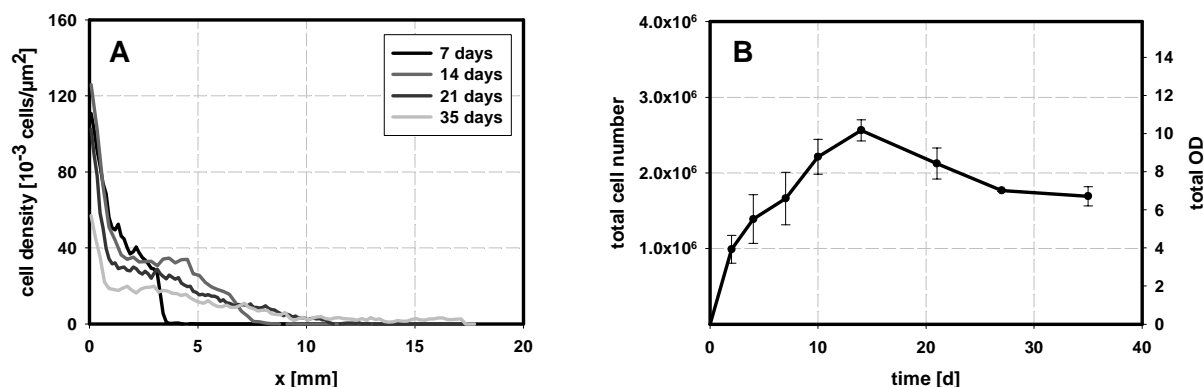
Figure 5.14: Development of carbon-limited *Y. lipolytica* colonies growing on 10 g·L^{-1} casamino acids as the only carbon source (medium C-CA-10). (A) Spatio-temporal development of the cell-density profile in one colony moiety. (B) Development of the total cell number in one colony moiety.

As observed for the glucose-limited growth, cell number passes through a maximum at an early stage in colony development (Fig. 5.14 B). Thus, the same mechanism comprising the utilization of cell decay products in the absence of the primary nutrient appears to be present. However, since neither the concentration of the amino acids was determined, nor the behavior of colonies with a removed interior was analyzed, this hypothesis is not supported by additional experimental data.

5.2.2.   Development of Nitrogen-limited Colonies

Colony Development on Ammonium Sulfate as the only Nitrogen Source

While growth patterns of the model yeasts are clearly distinct when growing under carbon-limiting conditions, colony development under nitrogen limitation with ammonium sulfate

(0.05 g·L⁻¹, medium N-A-0.05) as the only nitrogen source appears to be nearly identical. In the beginning of cultivation, high cell densities are accumulated and growth is restricted to the colony boundary (Fig 5.15 A, C). In the course of colony development, the number of newborn cells formed per time interval declines causing a descending cell-density profile along the colony diameter. The total cell number increases continuously and appears to reach a maximum value at a cultivation time of approximately 28-55 days (Fig. 5.15 B, D). Once established, local cell density (biomass concentration) remains constant. Thus, no significant drop of total cell number is observed during 35 days of cultivation.
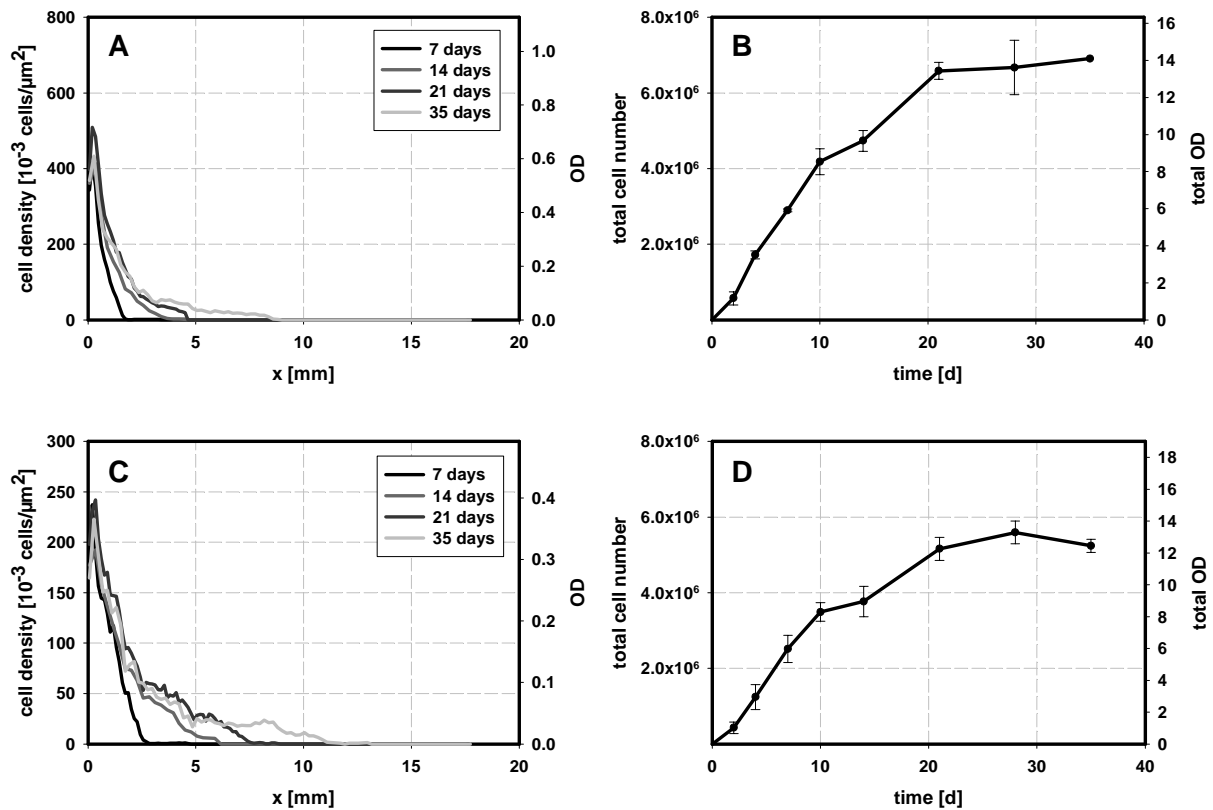
Figure 5.15: Development of nitrogen-limited (A, B) *C. boidinii* and (C, D) *Y. lipolytica* colonies growing on ammonium sulfate (0.05 g·L⁻¹) as the only nitrogen source (medium N-A-0.5). (A, C) Spatio-temporal development of the cell-density profile in one colony moiety. (B, D) Development of the total cell number in one colony moiety.

When the model yeasts are grown on ammonium sulfate as the only nitrogen source, no drop in cell density in the inner colony sections is observed during a cultivation time of 35 days. Thus, during this period of the cultivation cell decay and cannibalizing growth – as in the development of carbon-limited *Y. lipolytica* colonies - appears to play only a minor role (if any). Nevertheless it was tested, whether a removal of the colony interior affects the development of the populations. The colony interior was removed after 14 days of incubation and the development of "cut-out" and undisturbed colonies was followed for a total cultivation time of 49 days. As becomes obvious in Fig. 5.16, no significant differences between the differently treated colonies occur. Neither the extension rate nor the cell-density profiles of

"cut-out" colonies deviates from sound mycelia. These findings are in good agreement with the absence of cell decay during the observed time span (Fig. 5.15). However, since the total cell number appears to reach a maximum value at cultivation times of 28–35 days, this mode of colony extension may become relevant at later stages of colony development.
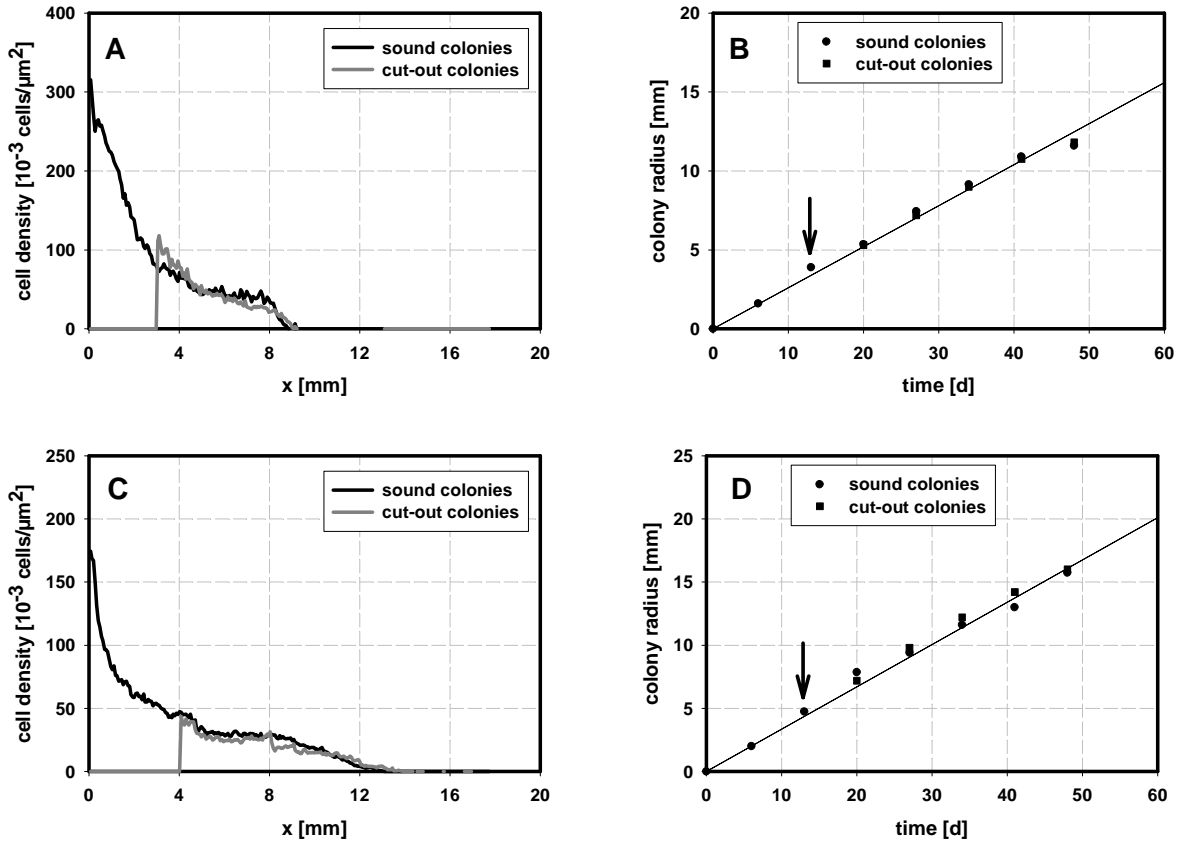
Figure 5.16: Development of nitrogen-limited (A, B) *C. boidinii* and (C, D) *Y. lipolytica* colonies that grow undisturbed vs. colonies with a removed colony interior. (A, C) Cell-density profiles after 35 days of incubation. (B, D) Colony radius vs. time. The time of removal of colony interior is indicated by an arrow (B, D). Colonies were cultivated on N-A-0.05 medium.

Colony Development on Casamino Acids as the only Nitrogen Source

For the nitrogen-limited growth on casamino acids as the only nitrogen source (2 g·L^{-1}, medium N-CA-2), significant differences between the model organisms are evident. Growth of *C. boidinii* on casamino acids is similar to the development on ammonium sulfate. The cell density behind the growing colony boundary remains constant and total cell number increases continuously throughout the experimentally observed time span (Fig. 5.17 A, C). In contrast, growth of *Y. lipolytica* exhibits strong similarities to the growth of the yeast under carbon-limiting conditions. Colony extension coincides with a drop of cell density in the inner colony sections, and the total cell number (biomass) shows a maximum at a cultivation time of 14 days (Fig. 5.17 C, D).
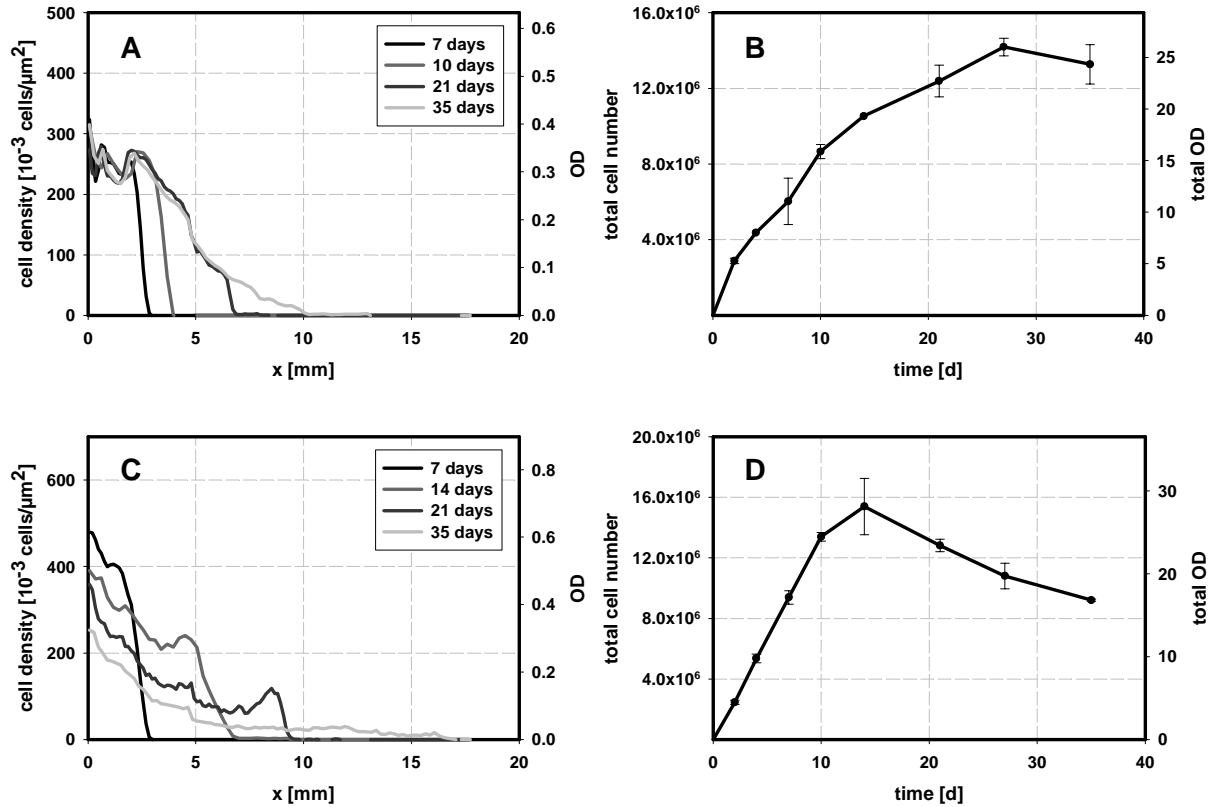
Figure 5.17: Development of nitrogen-limited (A, B) *C. boidinii* and (C, D) *Y. lipolytica* colonies growing on casamino acids as the only nitrogen source (medium N-CA-2). (A, C) Spatio-temporal development of the cell-density profile in one colony moiety. (B, D) Development of the total cell number in one colony moiety.

5.3. Biomass Balances and Limits for the Estimation of Cell Densities by OD Measurements

As outlined in Section 3.3.3, mycelial development can only be quantitatively compared to simulations if cell-density measurements provide a reliable and accurate data basis. Thus, the limits and plausibility of quantitative biomass estimations had to be tested. To do so, the theoretical *dry* biomass content of a colony was compared to the amount of *wet* biomass which was determined by OD measurements. The theoretical amount of dry biomass (BM_{dry}) was calculated from the volume of the growth field (V), the initial nutrient concentration ($c_{N,ini}$) and the biomass yield (Y) on the limiting food resource (Table 5.3).

$$BW_{dry} = c_{N,ini} \cdot V \cdot Y \qquad (5.2)$$

Wet biomass was calculated from the total cell number ($n_{C,tot}$) estimated by OD measurements, the volume of a single cell (V_C) (Equ. 6.27) and its *wet* density (ρ_C=1.1 g·cm^{-3} (Datar & Rosen, 1993)).

$$BM_{wet} = n_{C,tot} \cdot V_C \cdot \rho_C \qquad (5.3)$$

From these two estimates, the apparent dry weight fraction (DW_{app}) of the cells was calculated.

$$DW_{app} = \frac{BM_{dry}}{BM_{wet}} \qquad\qquad (5.4)$$

For exponentially growing yeast cells, the dry weight fraction (DW) lies in the range of 0.3. Considerably smaller values indicate an overestimation of wet biomass by the OD measurements or a strong vacuolization of the cells. Higher values of (DW_{app}) point to an underestimation of the wet biomass content or a strong incorporation of storage material. Thus, the calculation of (DW_{app}) in combination with the microscopic assessment of the cells within the mycelium provide an estimate for the plausibility of the quantitative biomass measurements.

Evaluation of OD Measurements on Carbon-limited Populations

In Table 5.3 biomass balances and the calculated dry weight fraction (DW_{app}) of *Y. lipolytica* and *C. boidinii* cells cultivated under carbon limitation are provided. For the calculations the maximum cell number reached in the experiments was applied. (E.g., in case of glucose-limited colony development of *Y. lipolytica,* wet biomass was estimated from the cell number determined after 10 days of cultivation (Fig. 5.10 D).)

Table 5.3: Biomass balances of carbon-limited *C. boidinii* and *Y. lipolytica* colonies growing on glucose or casamino acids as the only carbon source. Comparison of the expected biomass calculated from the yield on the nutrient resource, and the maximum accumulated biomass estimated from OD measurements.

| Nutrient	*Y. lipolytica*		*C. boidinii*
	Glucose	**Casamino acids**	**Glucose**
Concentration [$g \cdot L^{-1}$]	2	10	2
Vol. growth field [mL]	0.234	0.234	0.234
Mass nutrient [mg]	0.468	2.34	0.468
Yield [$g \cdot g^{-1}$]*	0.33	0.14	0.42
dry Biomass, predicted (BM_{dry}) [mg]	**0.15**	**0.33**	**0.20**
Total OD (maximum)**	5.2	10.1	8.1
Calibration factor [μm^{-2}]	0.55	0.365	1.37
Total cell number	$2.0 \cdot 10^6$	$2.5 \cdot 10^6$	$7.7 \cdot 10^6$
wet Biomass, estimated (BM_{wet}) [mg]	**0.27**	**0.53**	**0.92**
Dry weight (DW_{app})	**0.57**	**0.61**	**0.21**

* Biomass yield (Y) was estimated in shake flask experiments as described in Section 4.4.

** For the calculations, the maximum OD determined during colony development was used.

For cultivations of *Y. lipolytica* under carbon limitation, comparatively high (DW_{app}) values were calculated (Table 5.3), i.e., OD measurements appear to underestimate the biomass content of these colonies. However, in glucose-limited *Y. lipolytica* colonies, the maximum biomass content is reached prior to the complete depletion of glucose from the medium (compare Figs. 5.10 C and 5.11). In addition, cell decay is observed before the total cell number peaks at 10 days of the cultivation (Fig. 5.10 C, D). Thus, the maximum biomass concentration in colony development has to be smaller than the theoretical value which is calculated under the assumptions of i) complete conversion of limiting nutrient and ii) absence of cell decay. Therefore, under glucose limitation, biomass estimations by OD measurements are in good agreement with other experimental observations and provide reliable quantitative data. As will be explicitly shown in Section 6.3.3, nutrient and biomass balances are in good agreement when DW = 0.27 for proliferating cells is assumed. Since carbon-limited *Y. lipolytica* colonies growing on casamino acids show the same qualitative behavior as under glucose limitation, biomass estimations also appear to be plausible for these conditions.

For glucose-limited colony development of *C. boidinii*, a DW of 0.21 was calculated to fit experimentally determined biomass concentrations to the theoretical yield (Table 5.4). This value corresponds to slightly vacuolated cells which are likely to be present at longer cultivation times (Nielsen, 1993). However, even if the biomass content is somewhat underestimated, the accuracy of the presented method is still comparable or higher than alternative techniques for biomass estimation in fungal mycelia (compare Boswell *et al.* (2002) and see discussion in Section 7.1.1). Thus, under carbon limitation, OD measurements of the colonies provide reliable and adequate estimates of the biomass accumulation in populations of both yeasts.

Evaluation of OD Measurements on Nitrogen-limited Populations

When ammonium sulfate serves as the sole nitrogen source, biomass estimates in *Y. lipolytica* and *C. boidinii* colonies can only be fitted to the theoretical values if a very small (DW_{app}) is assumed (Table 5.4). These values correspond to a strong vacuolization of the cells, i.e., an extremely low nitrogen content. Comparing the morphology of individual cells in carbon or nitrogen-limited colonies, respectively, it becomes obvious that pseudohyphae starved for nitrogen vacuolize right behind the apical cell. In contrast, vacuolization in carbon-limited populations is only observed in the inner parts of the colony (Figs. 5.18 and 5.19).

Furthermore, vacuolized nitrogen-limited cells incorporate high amounts of storage carbohydrates which most likely causes a strong increase of their OD (Please note the granules in nitrogen-limited cells in the inner colony regions shown in Figs. 5.18 B and 5.19 B.). Thus, in contrast to carbon-limited cells, where vacuolization results in a decreasing OD of the cells, the absence of cytoplasm in nitrogen-limited cells growing on ammonium sulfate cannot be detected by OD measurements. In addition, it is not clear whether the amount of accumulated storage carbohydrates corresponds to the nitrogen content of the cells. Therefore, OD measurements do not provide reliable quantitative data about the biomass distribution and composition, respectively, in colonies of *Y. lipolytica* and *C. boidinii* that are severely starved for ammonium sulfate as the only nitrogen source.

Table 5.4: Biomass balances of nitrogen-limited *C. boidinii* and *Y. lipolytica* colonies growing on ammonium sulfate or casamino acids as the only nitrogen source. Comparison of the expected biomass calculated from the yield on the nutrient resource, and the maximum accumulated biomass estimated from OD measurements.

Nutrient	*Y. lipolytica*		*C. boidinii*	
	Ammonium sulfate	Casamino acids	Ammonium sulfate	Casamino acids
Concentration [g·L^{-1}]	0.05	2	0.05	2
Vol. growth field [mL]	0.234	0.234	0.234	0.234
Mass nutrient [mg]	0.012	0.468	0.012	0.468
Yield [g·g^{-1}]*	7.2	2.5	5.2	2.3
dry Biomass, predicted (BM$_{dry}$) [mg]	**0.08**	**1.17**	**0.06**	**1.08**
Total OD (maximum)**	13.3	28.1	14.1	26.2
Calibration factor [µm^{-2}]	0.61	0.78	0.71	0.79
Total cell number	5.6·10^6	15·10^6	6.9·10^6	14·10^6
wet Biomass, estimated (BM$_{wet}$) [mg]	**1.17**	**2.47**	**0.63**	**1.89**
Dry weight (DW$_{app}$)	**0.07**	**0.47**	**0.10**	**0.57**

* Biomass yield Y was estimated in shake flask experiments as described in Section 4.4.

** For the calculations the maximum OD determined during colony development was used.
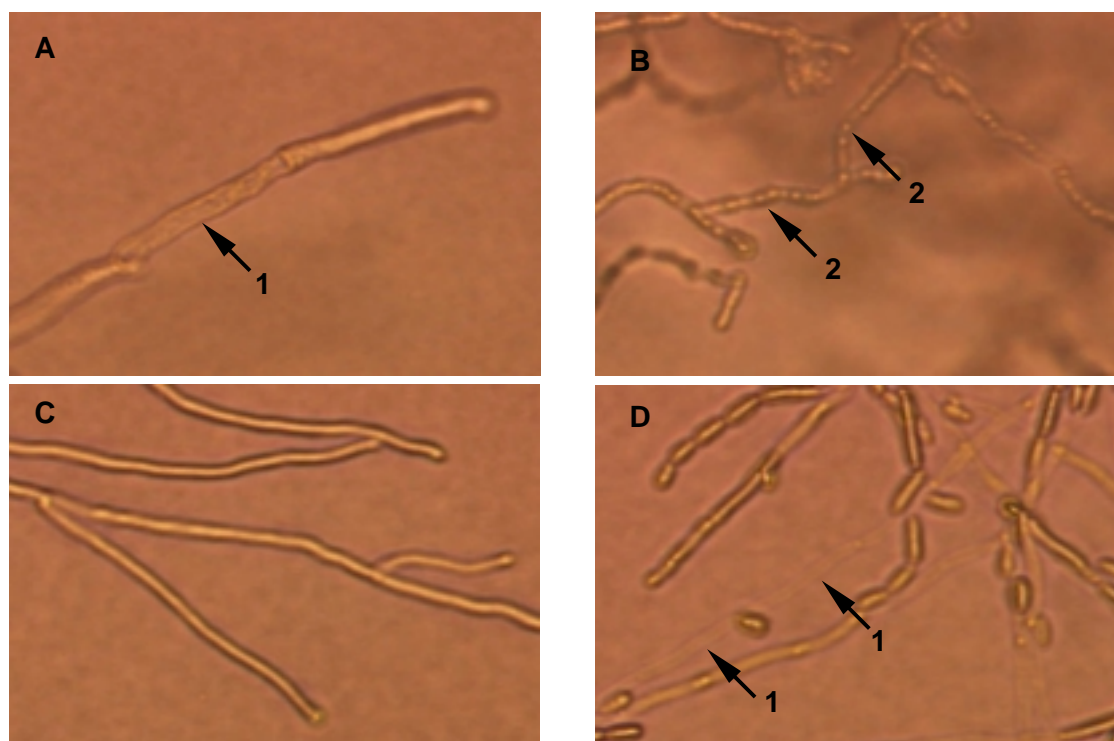
Figure 5.18: Comparison of the microscopic morphology of *Y. lipolytica* cells growing in (A, B) nitrogen-limited (medium N-A-0.05) or (C, D) glucose-limited (medium C-G-2) colonies. (A, C) Cells in the colony boundary. (B, D) cells in the colony interior. Cultivation time was 28 days. The arrows indicate 1) vacuolized cells and 2) inclusion bodies. Width of the images represents 90 µm.

Furthermore, strong uncertainties about the interpretation of the cell-density estimates arise when casamino acids serve as the nitrogen source. Here, OD measurements appear to underestimate the biomass content of the colonies, since a high (DW_{app}) was calculated to fit the measured biomass content to the theoretical value (Table 5.4). This finding is apparently contradictory to the results obtained for nitrogen-limited cells utilizing ammonium sulfate. However, the deviations possibly arise from the different degree of nitrogen limitation in the media. Since the medium with casamino acids as the limiting nutrient resource (N-CA-2) contains higher amounts of nitrogen when compared to the ammonium sulfate medium (N-A-0.05), more cells may be formed with a smaller specific content of storage carbohydrates.

Whatever the reason, OD measurements on nitrogen-limited colonies of the model organisms can neither be applied to quantitatively monitor cell (biomass) densities in the populations, nor to estimate the nitrogen content of the cells, respectively. The development of colonies growing under nitrogen limitation can only be assessed qualitatively by OD measurements. Quantitative estimates provided in charts which show cell-density profiles or total cell numbers of nitrogen-limited colonies (see Sections 5.1 and 5.2) should be interpreted with extreme care.
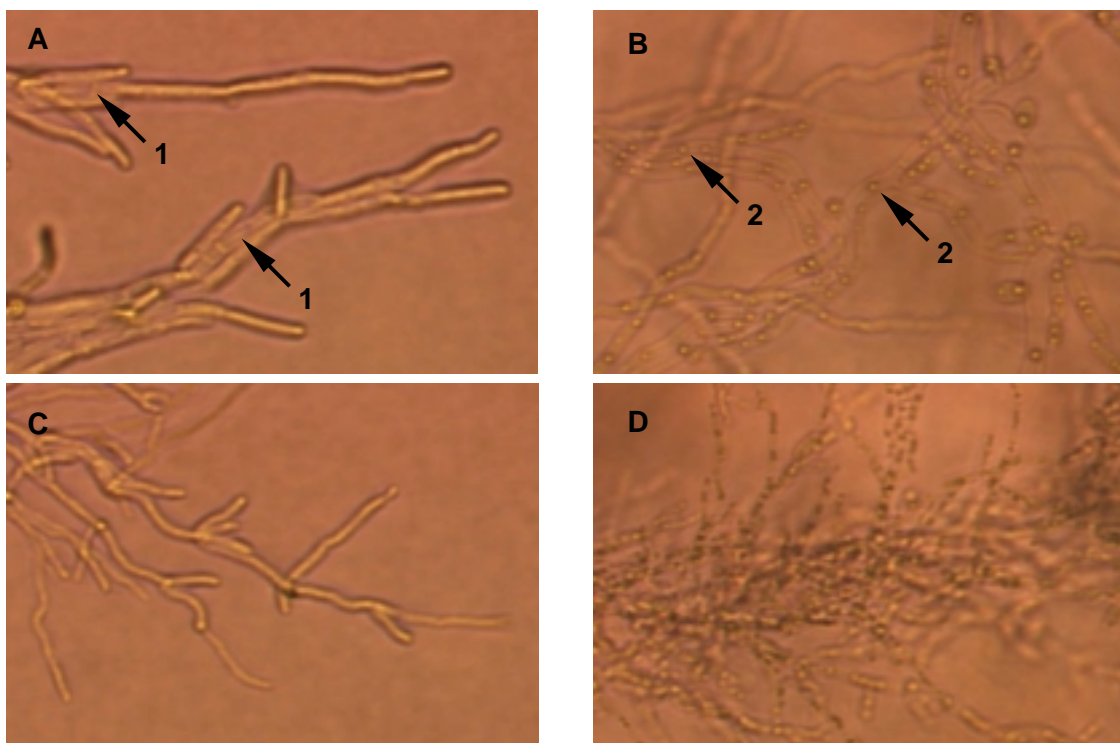
Figure 5.19: Comparison of the microscopic morphology of *C. boidinii* cells growing in (A, B) nitrogen-limited (medium N-A-0.05) or (C, D) glucose-limited (medium C-G-2) colonies. (A, C) Cells in the colony boundary. (B, D) cells in the colony interior. Cultivation time was 28 days. The arrows indicate 1) vacuolized cells and 2) inclusion bodies. Width of the images represents 90 µm.

5.4. Influence of Environmental Factors on Yeast Colony Development

5.4.1. Influence of Volatile Compounds on Colony Morphology

Yeasts and fungi emit a large number of volatile metabolic by-products. To study the influence of these compounds on the development of yeast populations, freshly inoculated colonies were exposed to the headspace of giant colonies of the same species. The bottom parts of two substrate-filled petri dishes were attached to each other containing the small colony on one side and the giant colony on the other. Small colonies were inoculated on rectangular growth fields (dimensions: 2 cm x 2 cm) using a toothpick. Giant colonies were created by plating a yeast suspension onto the agar substrate. Both colonies were cultivated under limitation of the same nutrient but at different initial nutrient concentrations (Tab. 5.5, for details see Section 4.2.3).

After six days of incubation, photographs of the small colonies were taken and their morphology was *qualitatively* compared to undisturbed colonies growing under otherwise identical conditions. Furthermore, the pH was estimated in both, the growth substrates of the small as well as of the giant colonies, respectively.

Qualitative Effects of Volatile Compounds on Colony Development

In general, colony development of the model yeast is affected by volatile compounds that are emitted by a giant colony. In particular, carbon-limited colonies exhibit a strong decrease of the cell density within the mycelium when cultivated in the headspace of a giant colony (Figs. 5.20 and 5.21). This effect can also be observed in nitrogen-limited populations. Under these conditions, however, the response is less pronounced and in case of *C. boidinii* extremely weak.

The drop of cell density in carbon-limited colonies is mainly caused by the absence of round cells. In case of undisturbed growth, yeast-like cells densely cover the scaffold formed by pseudohyphal cells. The volatile compounds emitted by the giant colonies induce the differentiation into the filamentous cell form. In Fig. 5.22 the morphology of individual cells in exposed and undisturbed carbon-limited *Y. lipolytica* colonies growing on casamino acids is compared. It is evident, that yeast-like cells are almost completely absent in populations that are cultivated in the headspace of giant colonies.
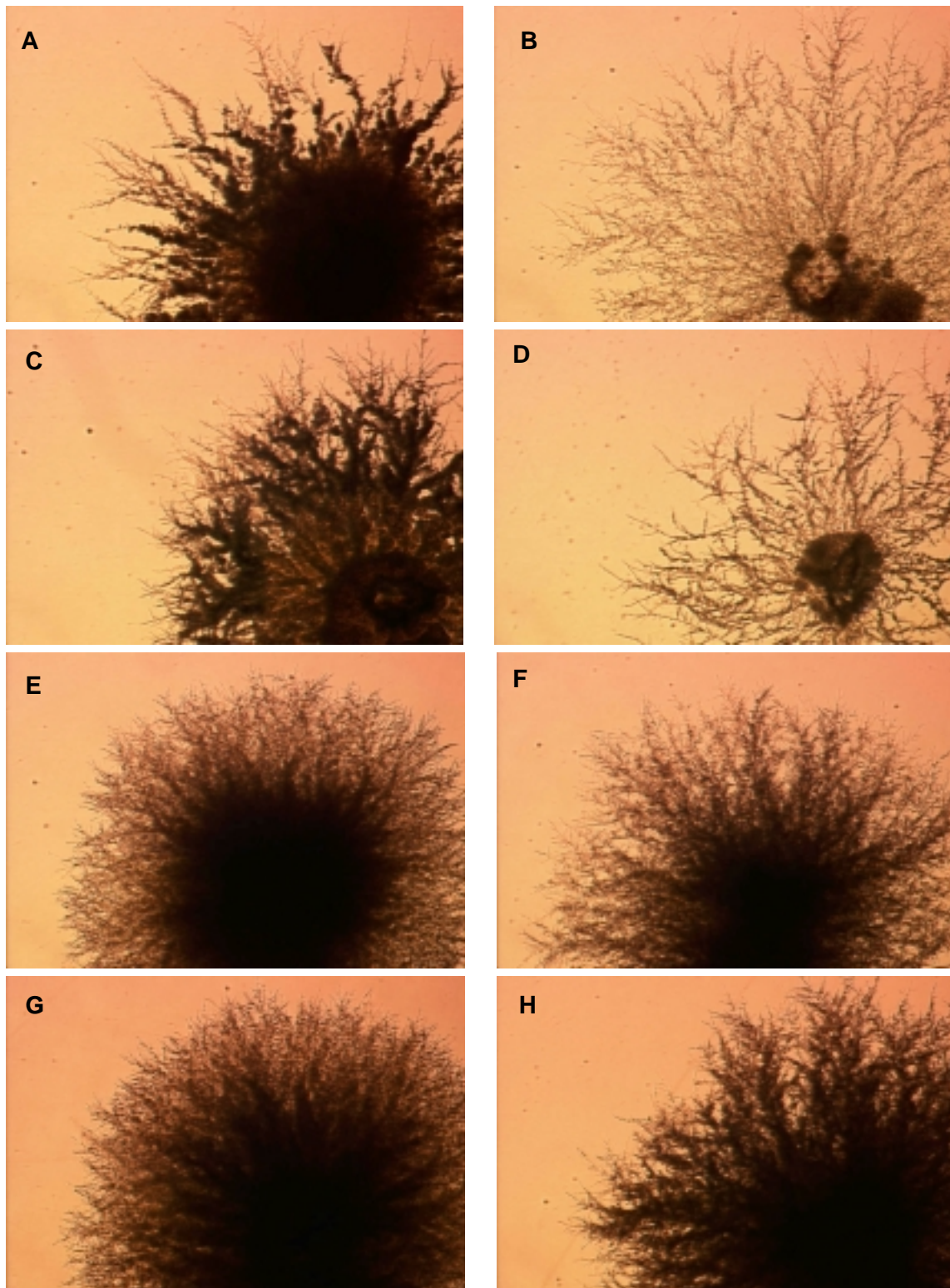
Figure 5.20: Morphology of *Y. lipolytica* colonies that grew undisturbed (left column) vs. colonies that were exposed to the headspace of a giant colony (right column). (A, B) Carbon-limited colonies growing on casamino acids (medium C-CA-0.2). (C, D) Carbon-limited colonies growing on glucose (medium C-G-0.2). (E, F) Nitrogen-limited colonies growing on ammonium sulfate (medium N-A-0.05). (G, H) Nitrogen-limited colonies growing on casamino acids (medium N-CA-0.02). Cultivation time was 6 days. Width of the images represents 4.6 cm.
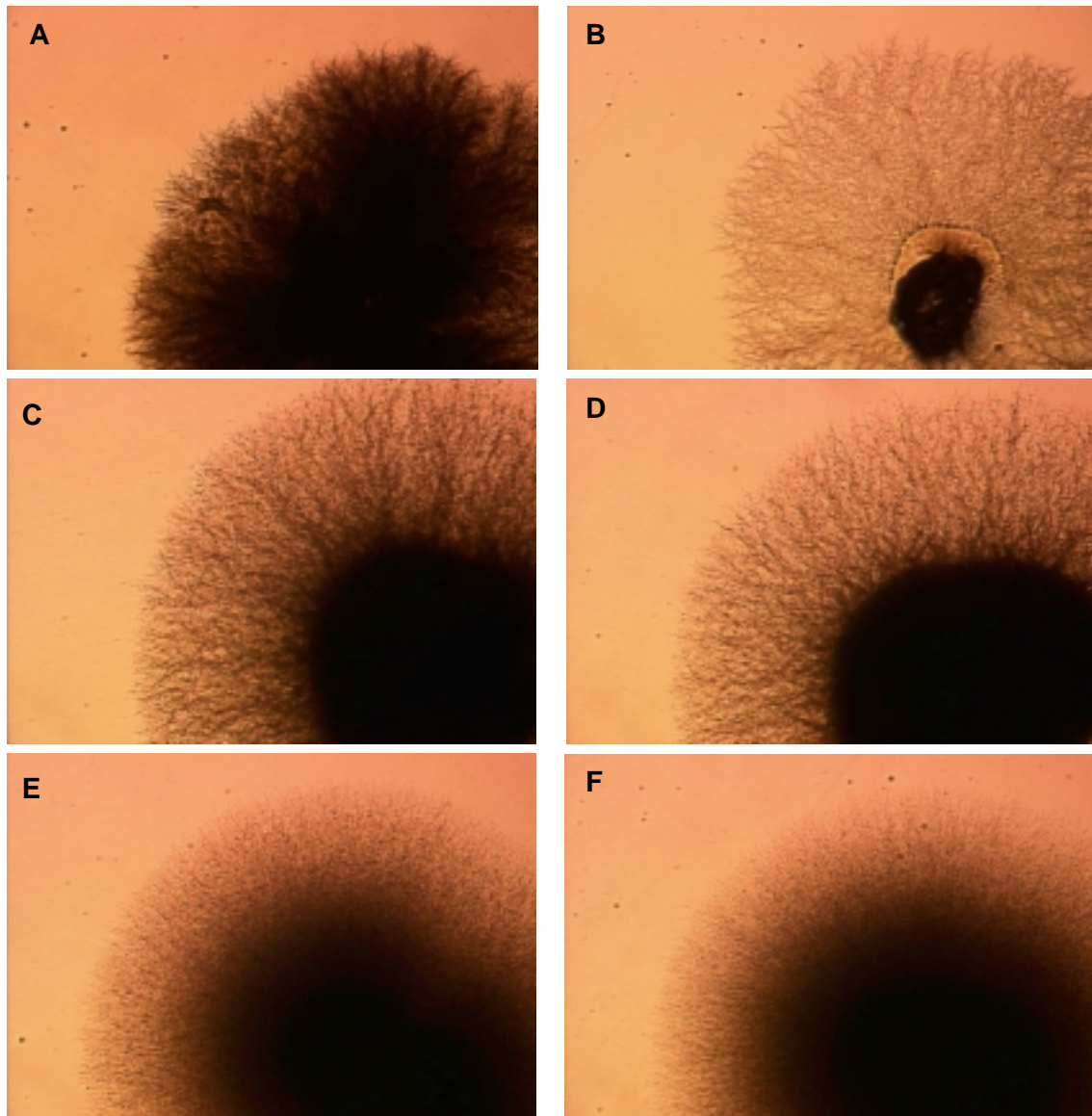
Figure 5.21: Morphology of *C. boidinii* colonies that grew undisturbed (left column) vs. colonies that were exposed to the headspace of a giant colony (right column). (A, B) Carbon-limited colonies growing on glucose (medium C-G-2). (C, D) Nitrogen-limited colonies growing on ammonium sulfate (medium N-A-0.5). (E, F) Nitrogen-limited colonies growing on casamino acids (medium N-CA-0.02). Cultivation time was 6 days. Width of the images represents 4.6 cm.
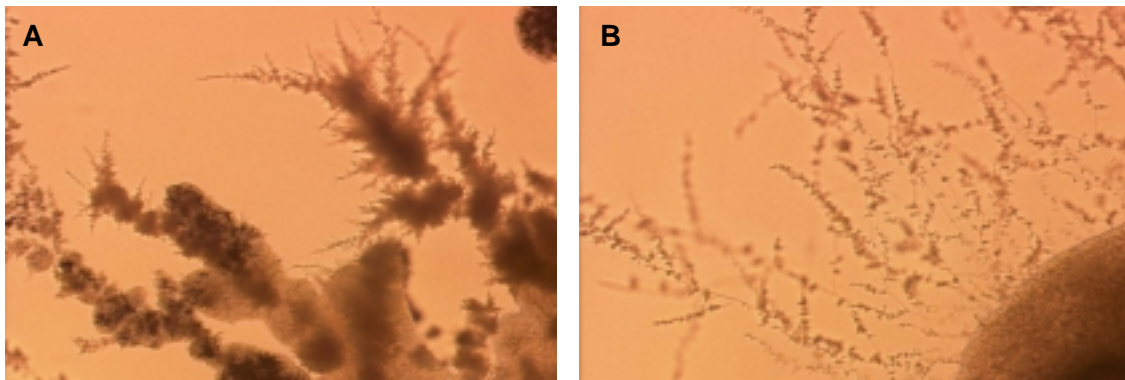
Figure 5.22: Comparison of microscopic growth patterns of *Y. lipolytica* colonies growing on 0.2 g·L^{-1} casamino acids as the only carbon source (medium C-CA-0.2). (A) Undisturbed colony. (B) Colony cultivated in the headspace of a giant colony. Width of the images represents 600 μm. Cultivation time was 6 days.

From the observed changes in the morphology of exposed colonies the question can be derived, whether colony development is controlled by nutrient availability or mediated by metabolic by-products (messengers) that are emitted by the cells. To investigate this question, small colonies were exposed to identical concentrations of volatile compounds (emitted by one giant colony which was inoculated with the same cell number and incubated at identical nutrient concentrations), but cultivated at different nutrient concentrations. In Fig. 5.23 the morphology of glucose-limited *C. boidinii* colonies is compared with respect to changes induced by the cultivation on different nutrient concentrations and changes arising from the exposure to a giant colony. Populations that are cultivated in the headspace of a giant colony accumulate smaller cell numbers. Comparing the morphology of exposed colonies it can be seen, that this effect is significantly less pronounced at higher nutrient concentrations. In cultivations of *C. boidinii* and *Y. lipolytica* on different nutrient resources the same tendencies can be observed (data not shown). Therefore, it can be concluded that colony development is not controlled by a single factor. In particular, the differentiation of cells appears to be controlled by both, nutrient supply and the concentration of metabolic by-products.
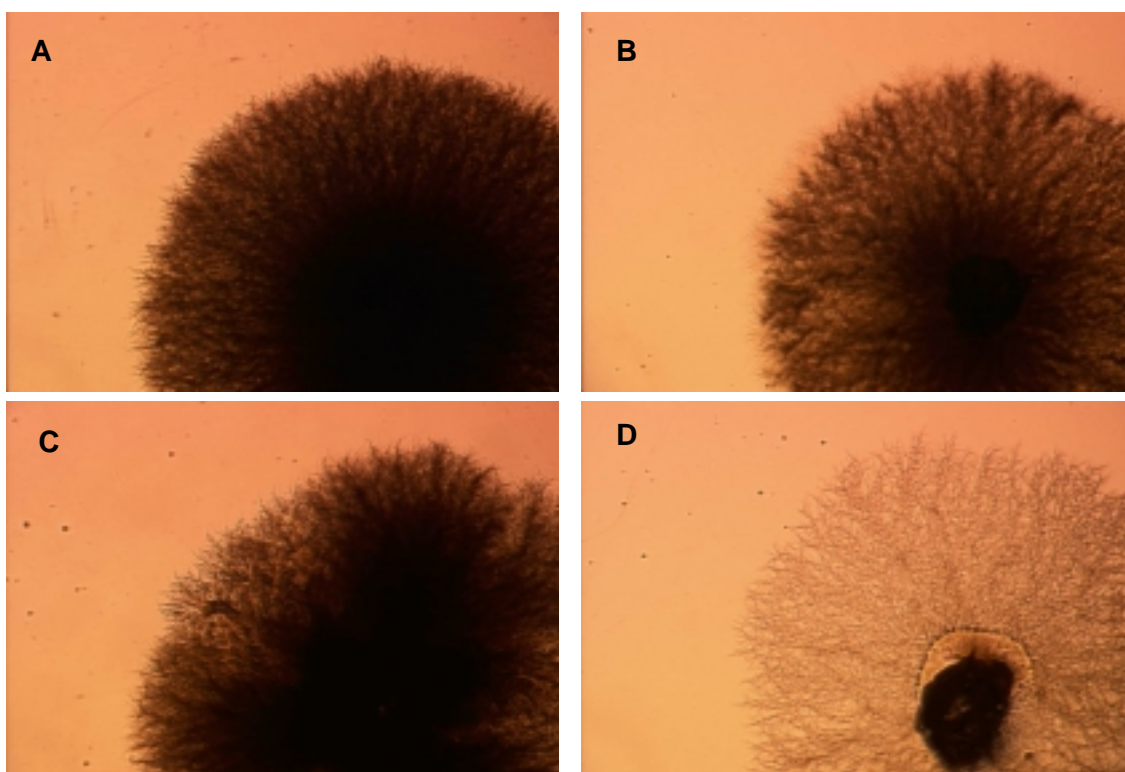
Figure 5.23: Influence of volatiles emitted by a giant colony on the colony morphology of glucose-limited *C. boidinii* colonies at different glucose concentrations. (A, C) undisturbed colonies. (C, D) colonies that were cultivated in the headspace of a giant colony. The initial glucose concentration in the growth field of the small colonies was (A, B) 0.02 g·L^{-1} (medium C-G-0.02) and (C, D) 0.002 g·L^{-1} (medium C-G-0.002). Giant colonies were cultivated on C-G-0.02 medium. Cultivation time was 6 days. Width of the images represents 4.6 mm.

Determination of pH Changes During Headspace Cultivations

In experimental studies, several volatile compounds were identified that not only have a morphogenic effect, but also influence pH in the medium (see Section 3.2 and 3.3). In particular, citric acid and ammonia are pH-active substances. Therefore, pH measurements in the growth substrate may help to identify growth conditions where these compounds are released or may prove the absence of these substances.

pH in giant colonies (Table 5.5)

Under all tested conditions, significant changes in the pH of the substrates are detected. When the model yeasts are grown under carbon limitation with casamino acids as the sole carbon source, the medium pH is strongly increased. Under all other cultivation conditions, giant colonies acidify their growth substrate during the observed cultivation time of 6 days. The smallest pH with 2.6-2.7 can be observed when ammonium sulfate serves as the limiting nitrogen source.

pH in small colonies (exposed vs. undisturbed, Table 5.5)

When *Y. lipolytica* colonies utilize casamino acids as the only carbon source, the increase of pH in the giant colony coincides with a higher pH in the exposed colonies. Furthermore, the acidification of glucose-limited giant colonies of both yeasts appears to induce a somewhat stronger decrease of pH in exposed colonies than in their undisturbed counterparts. Thus, under these conditions the pH in exposed colonies is shifted towards values present in the giant colonies. Contrary to this behavior, the pH in nitrogen-limited populations growing in the headspace of a giant colony is significantly higher than in undisturbed populations, although a strong acidification in the giant colonies is observed.

Table 5.5: Summary of pH values in the growth substrate of colonies that were exposed to the headspace of a giant colony (2) vs. colonies that grew undisturbed (1). Cultivation time was 6 days. The presented pH values represent the average of two replicate experiments.

No. of colonies	medium small colony	medium giant colony	initial pH	pH small colony	pH giant colony
Y. lipolytica					
carbon limitation					
1	C-G-0.2	-	5.5	4.8	-
2	C-G-0.2	C-G-2	5.5	4.4	3.7
1	C-CA-0.2	-	5.5	5.1	-
2	C-CA-0.2	C-CA-0.2	5.5	6.6	6.6
nitrogen limitation					
1	N-A-0.05	-	5.3	3.4	-
2	N-A-0.05	N-A-0.5	5.3	4.1	2.6
1	N-CA-0.2	-	5.7	3.4	-
2	N-CA-0.2	N-CA-2	5.7	4.6	3.8
C. boidinii					
carbon limitation					
1	C-G-0.2	-	5.5	4.8	-
2	C-G-0.2	C-G-2	5.5	4.3	3.3
nitrogen limitation					
1	N-A-0.05	-	5.3	4.0	-
2	N-A-0.05	N-A-0.5	5.3	4.1	2.7
1	N-CA-0.2	-	5.7	4.2	-
2	N-CA-0.2	N-CA-2	5.7	4.2	3.8

Influence of Volatile Ammonia on Colony Development

During the cultivation of *Y. lipolytica* on casamino acids as the only carbon source, the increase of pH in the giant colony coincides with a significant alkalization of the substrate of the exposed small colony. According to experimental investigations of Palkova & Forstova (2000) and Palkova *et al.* (1997), this upshift in pH is most likely caused by the transition of volatile ammonia. To test whether the observed changes in colony morphology are induced by the presence of this alkaline compound, carbon-limited colonies were cultivated under an

ammonia atmosphere. Experiments were carried out in the above described experimental setup. Instead of the giant colony, an agar medium containing 5 % (w/v) ammonium sulfate supplemented by various amounts of NaOH (2 mol·L^{-1}) served as the ammonia source (for details see Section 4.2.3). After 6 days of cultivation, growth of the colonies was visually assessed and the pH of the growth substrate was estimated. As can be seen in Table 5.6, the pH in the substrate (which corresponds to the ammonia concentration, Equ. 3.2) increases with higher amounts of NaOH that are supplemented to the ammonium sulfate medium.

Table 5.6: Summary of pH values in the growth substrate of colonies that were exposed to the volatile ammonia emitted from an agar substrate containing 5% (w/v) $(NH_4)_2SO_4$ and various amounts of NaOH. Cultivation time was 6 days. The presented pH-values represent the average of two replicate experiments.

medium	volume NaOH [μL]	initial pH	pH growth substrate	pH $(NH_4)_2SO_4$ medium	growth
Y. lipolytica					
C-G-0.2	0	5.5	3.8	4.5	+
C-G-0.2	2	5.5	5.6	5.6	+
C-G-0.2	4	5.5	6.3	5.9	+
C-G-0.2	8	5.5	6.9	6.4	+
C-G-0.2	**12**	**5.5**	**7.4**	**7.0**	**-**
C-CA-0.2	0	5.5	4.9	4.9	+
C-CA-0.2	2	5.5	5.9	5.6	+
C-CA-0.2	4	5.5	6.5	6.0	+
C-CA-0.2	8	5.5	7.2	6.5	+
C-CA-0.2	**12**	**5.5**	**7.5**	**7.0**	**-**
C. boidinii					
C-G-0.2	0	5.5	4.3	4.4	+
C-G-0.2	2	5.5	5.8	5.3	+
C-G-0.2	4	5.5	5.9	5.6	+
C-G-0.2	8	5.5	6.7	6.3	+
C-G-0.2	**12**	**5.5**	**7.5**	**7.0**	**-**

Ammonia strongly influences the development of carbon-limited *Y. lipolytica* colonies (Fig. 5.24). In all colonies growth is truncated at a pH of approximately 7.0-7.5 (12 μL NaOH). Exposed colonies exhibit smaller cell densities and differentiation appears to be induced at earlier stages of colony development (Fig. 5.24). Although ammonia is not formed under glucose-limitation, it has qualitatively similar effects under these conditions as during growth on casamino acids. Contrary to these observations, the transition to filamentous patterns in glucose-limited *C. boidinii* colonies is inhibited by the presence of ammonia (Fig. 5.25).

The pH in the presented undisturbed *Y. lipolytica* colonies was estimated with 3.8 (glucose) and 4.9 (casamino acids). When exposed to the ammonia atmosphere, pH increases to 6.9–7.2, which is slightly higher than during the described cultivations in the headspace of giant colonies.
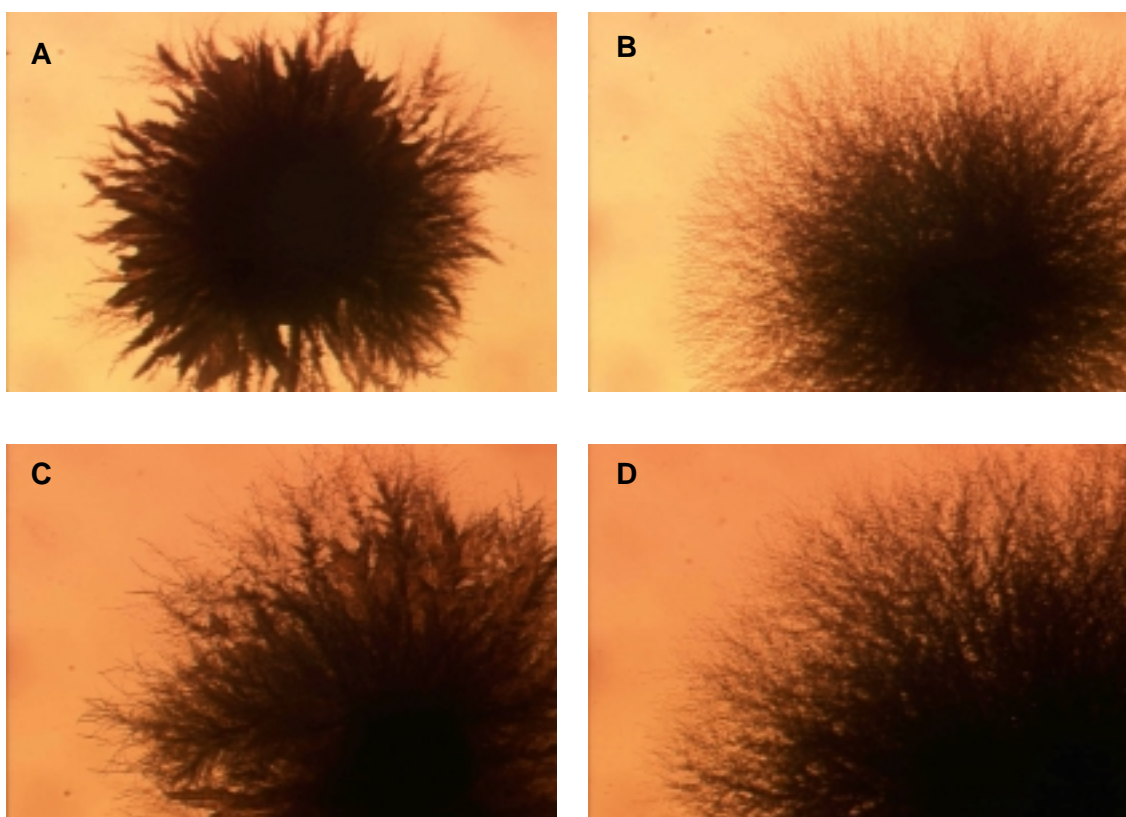
Figure 5.24: Influence of the exposure to volatile ammonia on the colony morphology of carbon-limited *Y. lipolytica* colonies. Colonies were cultivated on (A, B) casamino acids (medium C-CA-0.2), or on (B, D) glucose as the only carbon source (medium C-G-0.2). (A, C) Undisturbed colonies. (B, D) Colonies incubated under an ammonia atmosphere. The ammonia atmosphere was created by placing the bottom part of a petri dish containing a medium which was supplemented with 5 % (w/v) $(NH_4)_2SO_4$ and 8 µL NaOH opposite to the growth field of the shown colonies (for details see Section 4.2.3). Cultivation time was 6 days. Width of the images represents 4.6 mm.
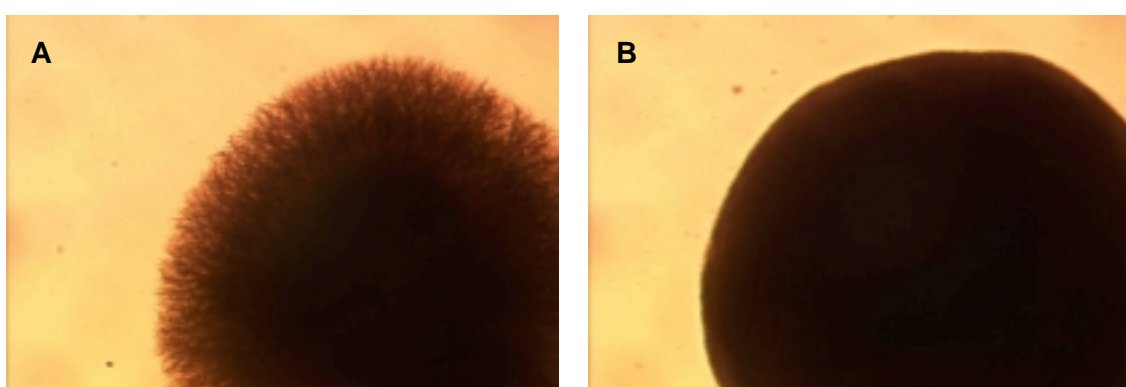
Figure 5.25: Influence of the exposure to volatile ammonia on the colony morphology of carbon-limited *C. boidinii* colonies growing on glucose as the only carbon source (medium C-G-0.2). (A) Undisturbed colony. (B) Colony incubated under an ammonia atmosphere. The ammonia atmosphere was created by placing the bottom part of a petri dish containing a medium which was supplemented with 5 % (w/v) $(NH_4)_2SO_4$ and 8 µL NaOH opposite to the growth field of the shown colonies (for details see Section 4.2.3). Cultivation time was 6 days. Width of the images represents 4.6 mm.

However, morphologies of *Y. lipolytica* colonies incubated under an ammonia atmosphere are significantly different from colonies that were exposed to the headspace of giant colonies (compare Figs. 5.21 and 5.24), indicating that ammonia only partially accounts for the observed changes.

5.4.2. Influence of pH on Yeast Colony Development

During the investigation of the influence of volatile compounds on colony development strong changes in the medium pH were detected. Ruiz-Herrera & Sentandreu (2002) found that pH is a strong effector of cell morphology. Hence, the question arises how changes in pH affect yeast colony development. Therefore, carbon-limited yeast colonies were cultivated at various initial pH-values of the substrate and colony development was analyzed as described in Section 5.2.

Influence of pH on the Biomass Yield on Glucose

The influence of the medium pH on the biomass yield on glucose was investigated in shake flask experiments (medium C-G-2, for details see Section 4.4). The initial pH was varied between 3 and 8. The pH of the medium was not controlled during the experiments.

The biomass yield of *Y. lipolytica* on glucose strongly depends on pH. The maximum yield with 0.33 (grams biomass per gram glucose) is obtained at pH 5. Under acidic conditions, the yield decreases only slightly, whereas a significant drop to approximately one-third of the maximum value can be observed for increasing pH values (Fig. 5.26 A). In contrast to this behavior, the biomass yield of *C. boidinii* does not vary strongly with the medium pH. The yield coefficient was estimated with approximately 0.4 $g \cdot g^{-1}$ (Fig. 5.26 B).
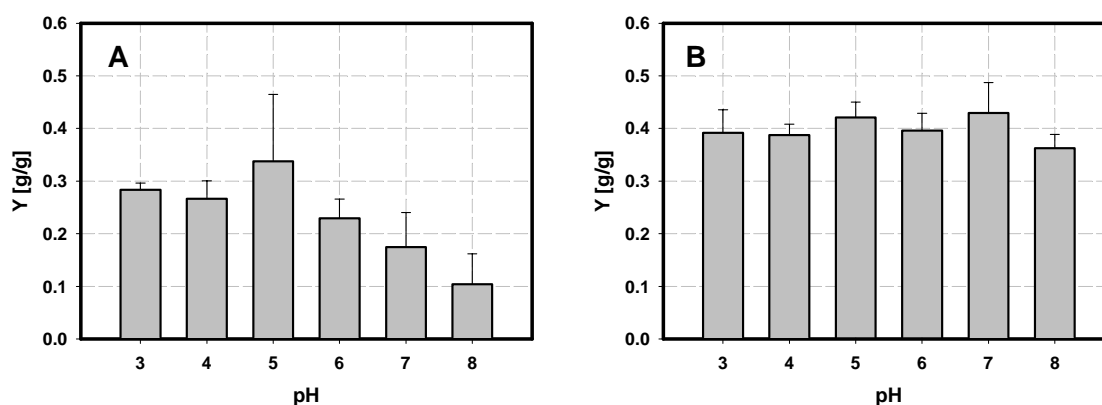
Figure 5.26: Biomass yield of *Y. lipolytica* (A) and *C. boidinii* (B) in liquid culture on glucose at different initial pH of the medium.

Influence of pH on Carbon-limited *Y. lipolytica* Colonies Growing on Glucose

The development of glucose-limited colonies (medium C-G-2) was only investigated for pH-values between 4 and 8, because the agar substrate does not solidify below pH 4. The analysis of the spatio-temporal development of glucose-limited *Y. lipolytica* colonies shows a significant influence of the substrate pH (Figs. 5.27 and 5.28). Under comparatively strong acidic conditions (pH 4), the highest local cell densities are accumulated. With increasing pH local cell densities in the mycelia gradually decline (Fig. 5.27). This behavior becomes also

evident in the time course of the total cell number of the colonies. At the smallest pH the highest cell numbers are accumulated, while for the other growth conditions a decreased biomass accumulation is observed (Fig. 5.28 B). These findings do not correspond to the dependency of biomass yield on medium pH in submers cultivations (see above). Furthermore, the decay rate of total biomass is somewhat smaller at pH 4 when compared to cultivations at higher pH. At pH 4 and pH 5, a smaller growth rate of the colony diameter can be observed (Fig. 5.28 A).
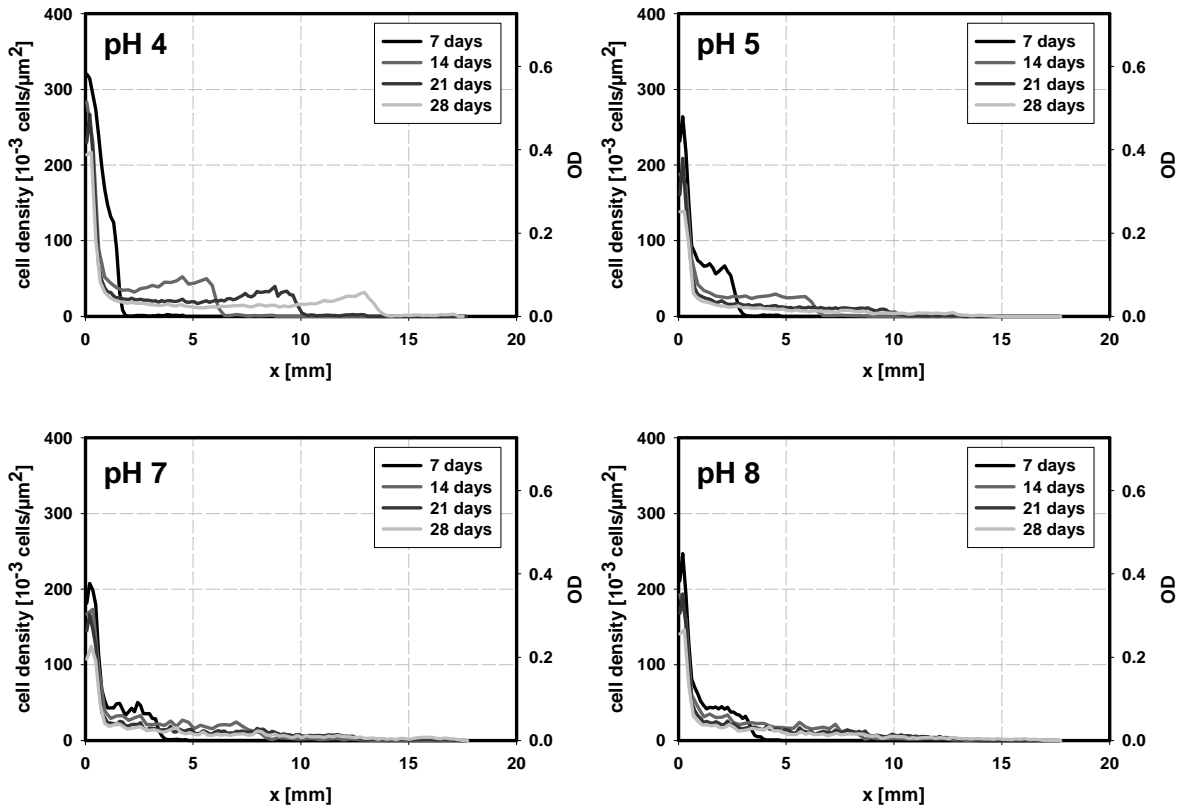
Figure 5.27: Spatio-temporal development of the colony-density profiles of carbon-limited *Y. lipolytica* colonies growing on glucose as the sole carbon source (medium C-G-2). Influence of the initial pH in the growth substrate.
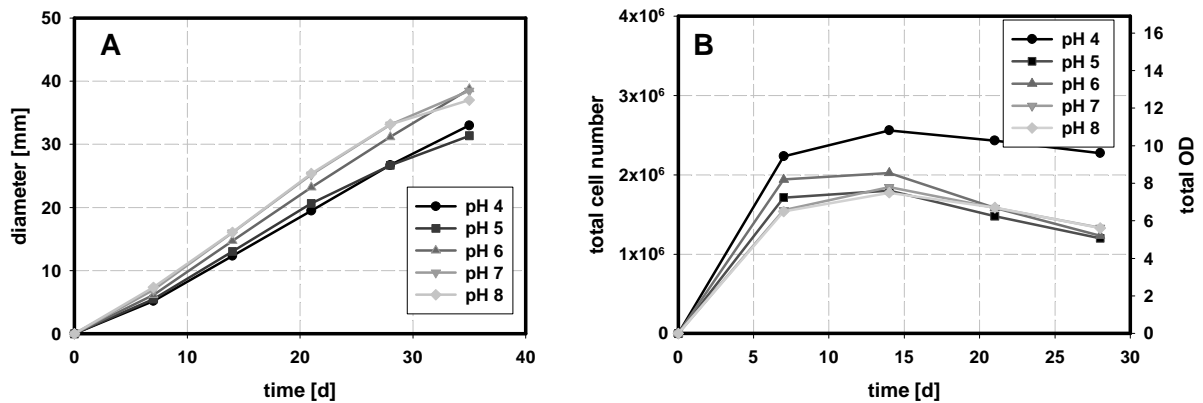
Figure 5.28: Extension of the colony diameters (A) and development of total cell numbers (B) of carbon-limited *Y. lipolytica* colonies growing on glucose as the sole carbon source (medium C-G-2). Influence of the initial pH in the growth substrate.

In Fig. 5.29 the temporal development of the average pH in the substrate is shown. Measurements were carried out using indicator paper with a resolution of 0.3 pH units. The estimations represent the average of 5 sampling points along the longitudinal axis of the colony. During cultivations with the initial pH 4, the acidity of the substrate dropped below the measurement range of the test paper. Therefore, this experiment was not further analyzed.
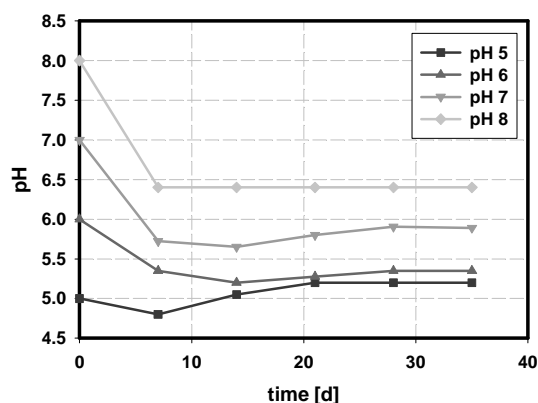
Figure 5.29: Changes of the average pH in the growth substrate during colony development of carbon-limited *Y. lipolytica* colonies growing on glucose as the only carbon source (medium C-G-2). pH was estimated from the average of 5 sampling points along the longitudinal axis of the colonies.

Under all tested conditions, the substrate pH initially decreases. The strength of the acidification declines with smaller initial pH. While at pH 8 a downshift of 1.5 units is observed during the first 7 days of cultivation, at pH 5 only a very small drop is detected (Fig. 5.29). In the further course of the cultivation, pH slightly increases. Only in experiments with the initial pH 8, it remains constant after the acidification.

Influence of pH on Carbon-limited *C. boidinii* Colonies Growing on Glucose

Colony growth of *C. boidinii* is strongly affected by the substrate pH. Similar to *Y. lipolytica* highest local cell densities as well as the strongest accumulation of total biomass are observed at pH 4. With increasing pH, colonies gradually form mycelia with smaller local cell densities which contain less biomass (Figs. 5.30 and 5.31 B). In contrast to the behavior found for *Y. lipolytica*, colony extension rates are nearly constant for small initial pH values and significantly drop at the initial pH 8 (Fig. 5.31 A).
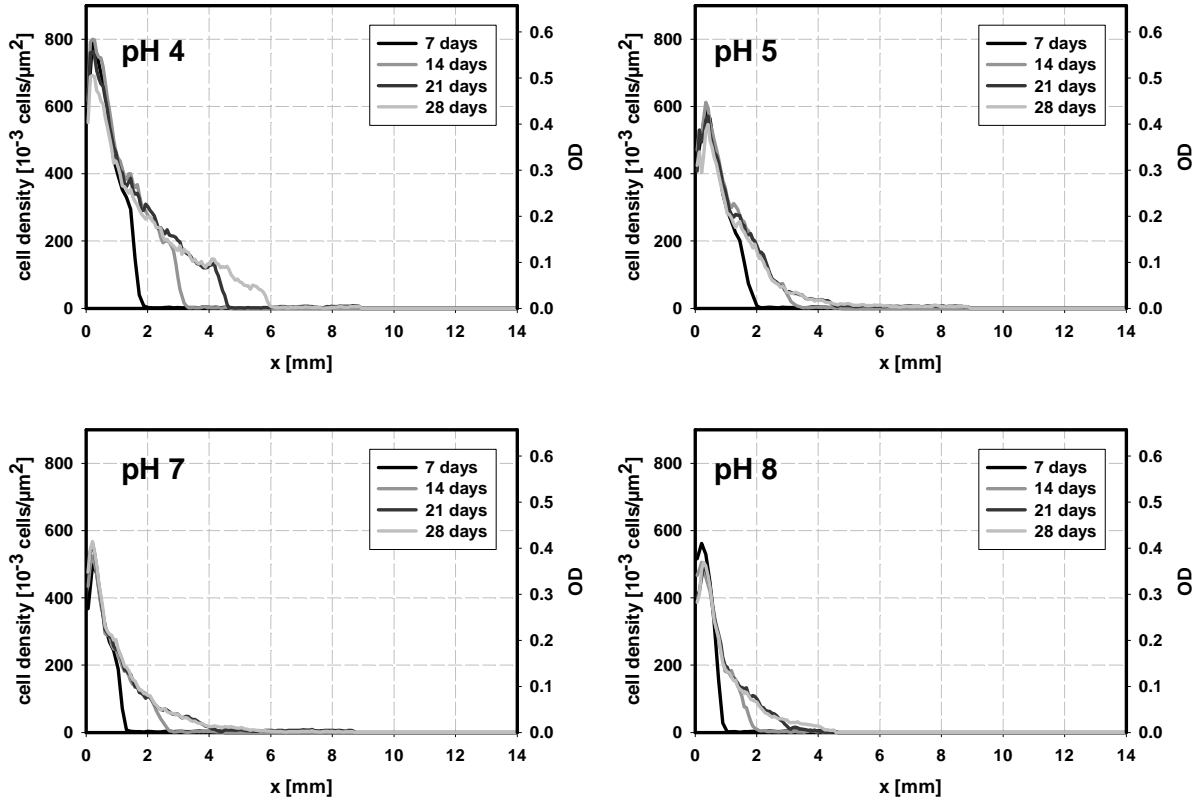
Figure 5.30: Spatio-temporal development of the colony-density profiles of carbon-limited *C. boidinii* colonies growing on glucose as the sole carbon source (medium C-G-2). Influence of the initial pH in the growth substrate.
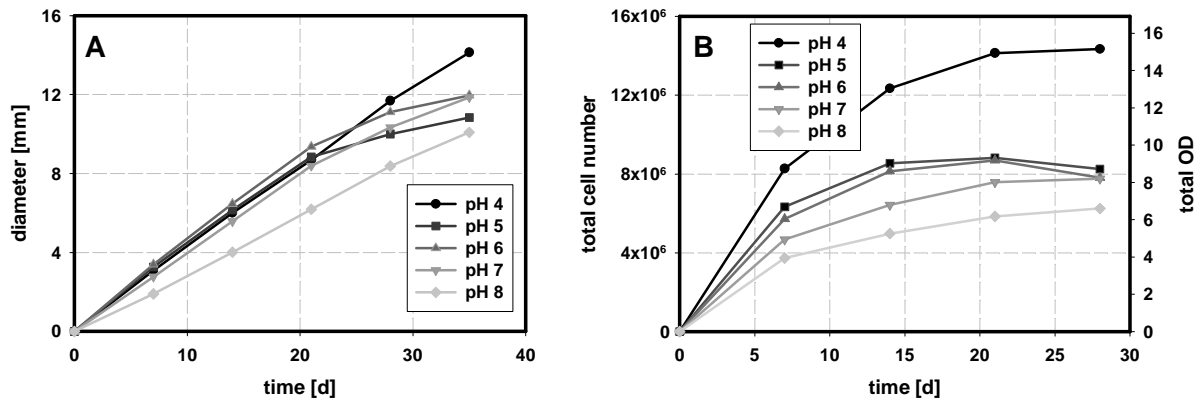
Figure 5.31: Extension of the colony diameters (A) and development of total cell numbers (B) of carbon-limited *C. boidinii* colonies growing on glucose as the sole carbon source (medium C-G-2). Influence of the initial pH in the growth substrate.

Strong differences between the model yeasts are also evident when the course of the substrate pH is compared. In cultivations of *C. boidinii* the pH initially declines but exhibits no increase at later stages of the cultivation.
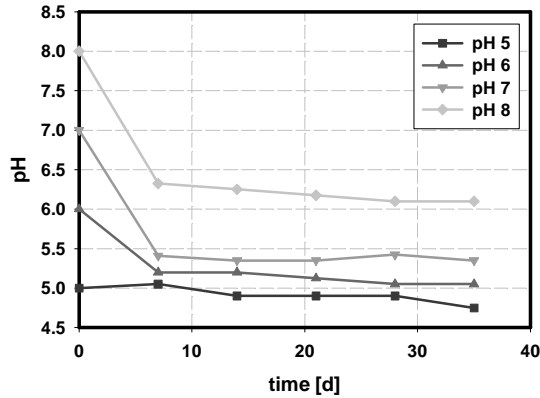
Figure 5.32: Changes of the average pH in the growth substrate during colony development of carbon-limited *C. boidinii* colonies growing on glucose as the only carbon source (medium C-G-2). pH was estimated from the average of 5 sampling points along the longitudinal axis of the colonies.

Interestingly, the final pH estimated in submers cultivations (for details see Section 4.4) differs significantly from the pH reached during colony development. Although in both sets of experiments the yeasts were cultivated on identical nutrient concentrations (C-G-2 medium), the microorganisms acidify the growth medium much stronger when grown in liquid culture (Table 5.7). As the only exception, a higher final pH in submers cultivations is reached when *Y. lipolytica* is cultivated at the initial pH 8.

Table 5.7: Comparison of the final pH in submers cultivations and agar plate experiments in cultivations of *C. boidinii* and *Y. lipolytica* on glucose as the limiting carbon source. Cultivation medium C-G-2. Submers cultivations were carried out in shake flasks under the conditions described in Section 4.4. pH was measured when OD stopped to increase at the end of the cultivation. pH in emers cultivations refers to the average pH in the agar substrate of the yeast colonies estimated after 35 days of colony development.

initial pH	final pH			
	C. boidinii		*Y. lipolytica*	
	submers	emers	submers	emers
3	2.6	-*	2.7	-*
4	2.8	-**	3.0	-**
5	2.8	4.8	3.0	5.2
6	2.9	5.0	3.0	5.4
7	3.2	5.4	5.3	5.9
8	3.7	6.1	6.7	6.1

* Final pH values are missing because the yeasts were not cultivated under these conditions. ** Final pH values are missing because the pH was outside the measurement range of the test paper.

Influence of pH on Carbon-limited *Y. lipolytica* Colonies Growing on Casamino Acids

The influence of substrate pH on the colony development of *Y. lipolytica* on casamino acids as the sole carbon source (medium C-CA-10) was investigated in a range between pH 5 and pH 8. An investigation at smaller pH is impossible since the agar does not solidify under these conditions.

The development of *Y. lipolytica* colonies growing on casamino acids strongly depends on pH. Large mycelia are only formed at pH 5 and 6. Under these conditions the development of the populations exhibits the behavior described in Section 5.2. It is characterized by the stable extension of the colony diameter on the cost of a decrease of local biomass density inside the mycelium. At a higher initial pH, colony extension collapses, i.e., it drops to extremely small rates at a diameter of approximately 10 mm (Fig. 5.33 and 5.34 A). 30 days after the end of the experiments, a visual inspection of the colonies showed an extremely sparse formation of filaments growing out from the growth front of the dense mycelium. This dense mycelium corresponds to the cell-density profiles shown in Fig. 5.33 (pH 7 and pH 8). It did not significantly expand compared to its state after 28 days of cultivation. However, the filaments reached a length of approximately 10 mm. Whether or not this behavior is reproducible and relevant for a general characterization of colony development under these conditions remains to be tested.
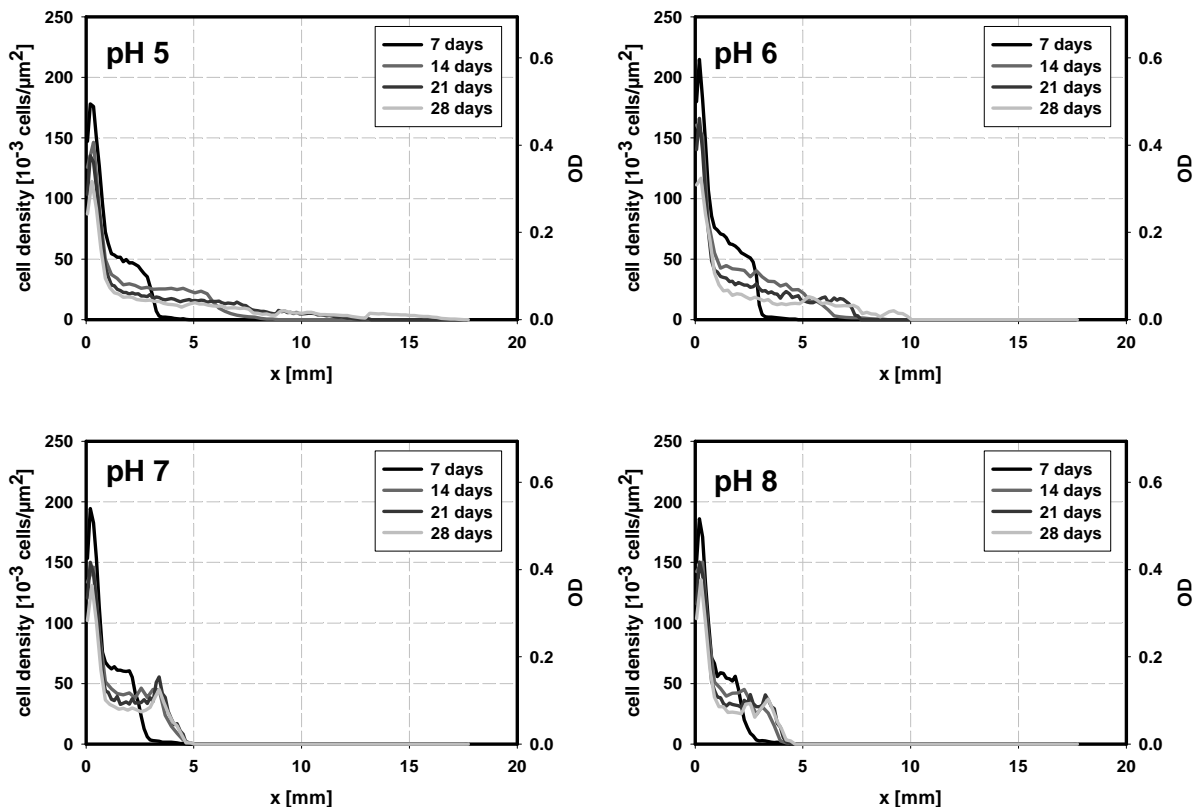
Figure 5.33: Spatio-temporal development of the colony-density profiles of carbon-limited *Y. lipolytica* colonies growing on casamino acids as the sole carbon source (medium C-CA-10). Influence of the initial pH in the growth substrate.
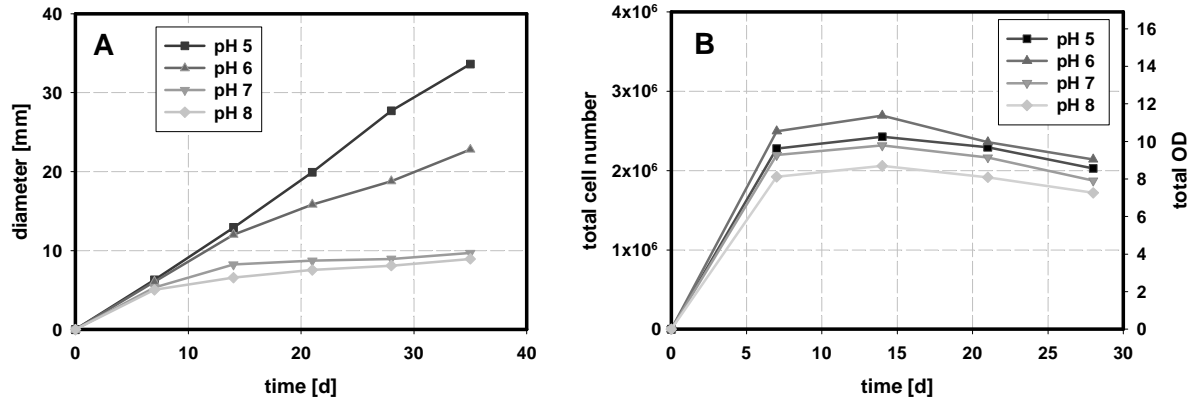
Figure 5.34: Extension of the colony diameters (A) and development of total cell numbers (B) of carbon-limited *Y. lipolytica* colonies growing on casamino acids as the sole carbon source (medium C-CA-10). Influence of the initial pH in the growth substrate.

Furthermore, the course of average pH in the substrate was monitored. Only at pH 8 an initial acidification is present (Fig. 5.35). At smaller initial pH, colonies continuously alkalize the substrate. In cultivations with an initial pH between 6 and 8, the substrate pH approaches similar values of approximately 7.0-7.5.
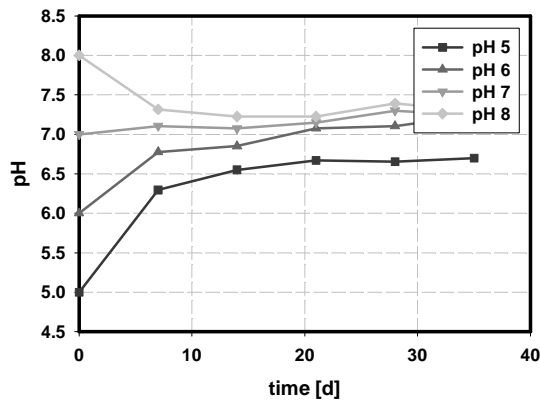
Figure 5.35: Changes of the average pH in the growth substrate during colony development of carbon-limited *Y. lipolytica* colonies growing on casamino acids as the only carbon source (medium C-CA-10). pH was estimated from the average of 5 sampling points along the longitudinal axis of the colonies.

6. MATHEMATICAL MODELS FOR YEAST COLONY DEVELOPMENT

In yeast colony development, the formation of complex morphologies results from the autonomous growth of individual cells. The growth of these individuals is controlled by interactions with their dynamically changing local environment. To abstract this process comprehensively, hybrid cellular automaton models describing discrete cells and continuous concentrations of nutrient sources and messengers (Dormann & Deutsch, 2002) were developed. The models were applied to simulate the spatio-temporal evolution of the cell-density profile in a growing yeast colony. In particular, the simulations are meant to reproduce the growth characteristics of yeast mycelia under carbon or nitrogen limitation which were elaborated in Section 5.2. Since growth of the colonies is symmetrical in the chosen experimental setup, calculations only account for one moiety of the colony, i.e., for the region between inoculation site and outer edge of the growth field. The simulations quantitatively predict a distribution of discrete cells, that can be easily compared to experimental results.

For the mathematical description of yeast colony development, strong simplifications of the actual microbial growth process are necessary. As described in Section 5, yeast colony development is biphasic. Immediately after the inoculation cells grow in the yeast-like morphology. After 2-4 days of cultivation, the differentiation into pseudohyphal cells can be observed. These pseudohyphal cells generate a mycelial structure that is covered by a considerable number of round cells. The transitions between the distinct morphotypes can be induced by several environmental factors and the knowledge about regulatory mechanisms is still limited. However, because of their phenotypic characteristics (elongated cell morphology, unipolar budding, polarized growth), pseudohyphal cells determine the behavior of developing yeast colonies. Therefore, the presence of different cell types is neglected in the mathematical description of the growth process. The development of yeast colonies is described based on the proliferation of unit cells that have the dimensions of pseudohyphal cells.

6.1. Diffusion-limited Growth (DLG)

The growth of microorganisms strongly depends on nutrient availability in their environment. In the absence of important nutrients, cells stop to proliferate and undergo a transition to a quiescent state (see Section 3.1.1). In order to account for this essential requirement, a numerical model was developed that describes the growth of yeast colonies based on the assumption of exclusively nutrient-controlled proliferation. This fundamental description of cellular growth also represents the basis of all further modeling approaches that simulate the potential influence of additional mechanisms.

The model incorporates proliferation of cells, consumption and diffusion of nutrient, and the transition of individual cells from an initially proliferating state to a stationary state. Proliferating cells ($n_{C,p}$) and stationary cells ($n_{C,s}$) reside on the same one-dimensional lattice $L(0,\ldots i,\ldots n)$, with $L(0)$ being the inoculation site and $L(n)$ representing the edge of the growth

field. The state s(i, t) of each lattice node is defined by the number of proliferating and stationary cells, and the concentration of nutrient (c_N), respectively.

$$s(i,t) = (n_{C,p}, n_{C,s}, c_N) \qquad\qquad (6.1)$$

$$c_N \in [0, \infty) \qquad\qquad (6.2)$$

$$n_{C,p}, n_{C,s} \in \{0,\ 1,\ 2, ...\} \qquad\qquad (6.3)$$

Growth Dynamics

Initially, inoculated or new born cells are in the proliferating state having the ability to give birth to a daughter cell. When cells divide, newborn cells grow in size at a constant rate. After they reach a critical cell size, mature cells enter a new replication cycle, now themselves giving birth to a new cell. In the automaton model cell divisions are assumed to occur at discrete intervals (Δt_p) (Equ. 5.1) representing the time span between birth and maturity of a cell.

For the distribution of newborn cells on the lattice, two different scenarios were tested for their influence on colony development. In a first approach, undirected growth of the cells was assumed. Daughter cells originating from proliferating cells at node (i) are placed randomly to the positions (i), (i-1), and (i+1). Accordingly, this scenario is referred to as random budding. Alternatively, the directed growth of the cells away from the inoculation site was implemented by placing cells born at node (i) exclusively to position (i+1). This behavior corresponds to the budding pattern of pseudohyphal cells which solely form new buds at the pole distal to the mother cells birth end. Therefore, the algorithm is referred to as distal budding.

Proliferating cells may change their state and become stationary. These cells are still viable but have lost their ability to form new cells. The change in the state (s_C) of the cells is controlled by different environmental factors. In the present model, the state transition is assumed to be controlled by nutrient availability (see Section 3.1.1). Proliferating cells cease growth and enter the stationary state when the local nutrient concentration drops to zero (Equ. 6.4). The state transition is assumed to be irreversible.

$$\text{DLG:} \quad s_C = \begin{cases} \text{proliferating} & \text{if} & c_N(i,t) > 0 \\ \text{stationary} & \text{else} \end{cases} \qquad (6.4)$$

A number of studies explains the formation of complex colony morphologies on the basis of a nutrient-controlled growth algorithm (Davidson *et al.*, 1996a; Kawasaki *et al.*, 1997; Matsushita *et al.*, 1998): According to this theory, cells in the periphery of a growing population take up all the nutrient that diffuses towards the colony. This causes truncation of growth in the inner colony regions while the colony edge continuously progresses away from the inoculation site, a phenomenon commonly named diffusion-limited growth (DLG).

Nutrient Balance

To maintain viability, all cells take up nutrient with rate ($r_{N, main}$),

$$r_{N, main} = m_C \cdot R \tag{6.5}$$

where (m_C) is the mass of a single cell, and (R) represents the mass-specific maintenance requirement. Additionally, proliferating cells take up nutrient with rate ($r_{N, prol}$) and transform it into new biomass, i.e. into a new daughter cell. ($r_{N, prol}$) is calculated from the cell mass (m_C) that is generated within the replication interval (Δt_p) (Equ. 6.6). The yield (Y) describes the efficiency with which a particular nutrient is transformed into biomass.

$$r_{N,prol} = \frac{m_C}{\Delta t_p \cdot Y} \tag{6.6}$$

Nutrient is balanced by solving the reaction-diffusion equation

$$\frac{\partial c_N(i,t)}{\partial t} = D \cdot \frac{\partial^2 c_N(i,t)}{\partial x^2} - r_{N,con}(i,t), \tag{6.7}$$

wherein

$$r_{N,con}(i,t) = min[r'_{N,con}(i,t), c_N(i,t) \cdot \Delta t_p^{-1}] \tag{6.8}$$

is the total nutrient consumption rate ($r_{N,con}$) at lattice node (i). Here

$$r'_{N,con}(i,t) = [r_{N,prol} \cdot n_{C,p}(i,t) + r_{N,main} \cdot (n_{C,p}(i,t) + n_{C,s}(i,t))] \cdot V_i^{-1}, \tag{6.9}$$

is the maximum uptake rate as derived from equations (6.5) and (6.6), and $c_N(i, t) \cdot \Delta t_p^{-1}$ represents the uptake rate as limited by the locally available nutrient. (V_i) denotes the volume that is assigned to each lattice node. In order to account for the limited nutrient reservoir in the agar substrate, boundary conditions are chosen according to

$$\left[\frac{\partial c_N(i,t)}{\partial x} \right]_{i=0,i=n} = 0 . \tag{6.10}$$

6.2.   Quorum Sensing (QS)

In order to test the effect of messenger-controlled growth on colony development, a model was developed that is based on the above described DLG model. *In addition* to the components described therein, the model incorporates the emission, diffusion, and decay of

a messenger. In accordance with the DLG model, the state definition of each lattice node is extended by the messenger concentration (c_M).

$$s(i,t) = (n_{C,p}, n_{C,s}, c_N, c_M) \qquad (6.11)$$

$$c_M \in [0, \infty] \qquad (6.12)$$

Growth Dynamics

As described by the DLG model, cells undergo a transition from the proliferating to the stationary state when the nutrient in the growth substrate is depleted. In the QS model, cells enter the quiescent state also, when local messenger concentration surpasses a critical concentration ($c_{M,crit}$).

$$\text{QS:} \quad s_C = \begin{cases} \text{proliferating} & \text{if} \quad c_N(i,t) > 0 \quad \text{and} \quad c_M(i,t) < c_{M,crit} \\ \text{stationary} & \text{else} \end{cases} \qquad (6.13)$$

Since all cells emit the messenger, its concentration is related to local cell number and serves as a mean to measure population density. Consequently, this mechanism is referred to as quorum sensing (QS). The state transitions in the model are assumed to be irreversible.

Nutrient and Messenger Balance

The messenger is emitted by all cells at a constant rate (Equ. 6.14), with (r_M) representing the total emission rate of the cells at node (i), and ($r_{M,\ spec}$) being the mass-specific messenger emission rate.

$$r_M(i,t) = [(n_{C,p}(i,t) + n_{C,s}(i,t)) \cdot m_C \cdot r_{M,spec}] \cdot V_i^{-1} \qquad (6.14)$$

The messenger decays with time constant (T_M). It is balanced by solving equation

$$\frac{\partial c_M(i,t)}{\partial t} = D \cdot \frac{\partial^2 c_M(i,t)}{\partial x^2} + r_M(i,t) - T_M^{-1} \cdot c_M(i,t). \qquad (6.15)$$

To account for the accumulation of messenger in the growth substrate, boundary conditions are chosen according to

$$\left[\frac{\partial c_M(i,t)}{\partial x} \right]_{i=0, i=n} = 0. \qquad (6.16)$$

Nutrient is balanced according to equations 6.5-6.10.

6.3. Nutrient-controlled Growth Incorporating Food Replenishment due to Cell Decay

From the experimental investigation of the carbon-limited growth of *Y. lipolytica* colonies, a hypothesis was derived that describes the development of characteristic colony-density profiles based on the interplay of cell decay and cannibalizing growth. According to this hypothesis, the decay products of dying cells in the colony interior diffuse outwards and serve as a secondary food resource in the progressing colony margin. Thus, colony expansion persists even in the absence of the primary nutrient. To test whether the observed growth characteristics can be reproduced by simulations, a mathematical model was developed that is based on the DLG model described in Section 6.1 and additionally incorporates the hypothesis of nutrient replenishment due to cell decay.

Since stationary cells decay continuously, their local concentration corresponds to an accumulation of organic matter rather then to a number of discrete individuals. Therefore, in contrast to the above described models, the quantity of stationary cells is described by real numbers (compare Equ. 6.3 and 6.19). The state of each lattice node is described by

$$s(i,t) = (n_{C,p}, n_{C,s}, c_N) \,, \tag{6.17}$$

with

$$n_{C,p} \in \{0,\ 1,\ 2,...\} \,, \tag{6.18}$$

and

$$c_N, n_{C,s} \in [0,\infty) \,. \tag{6.19}$$

Growth Dynamics

In order to simulate the influence of the described assumptions on yeast colony development, an exclusively nutrient-controlled proliferation of individual cells was assumed. Cells enter stationary phase when nutrient is depleted from the medium (Equ. 6.20). The state transition is defined to be irreversible.

$$\text{DLG:} \qquad s_C = \begin{cases} \text{proliferating} & \text{if} & c_N(i,t) > 0 \\ \text{stationary} & \text{else} \end{cases} \tag{6.20}$$

The influence of the budding pattern of individual cells on the morphology of the cell-density profile was tested for different budding patterns. Random budding was realized according to the algorithm described in Section 6.1 (see Growth Dynamics). Distal budding was implemented by placing the fraction

$$n_{C,p}{}^{*}(i,t_p) = \sigma \cdot n_{C,p}(i,t_p) \qquad\qquad (6.21)$$

$$\sigma = rand(0.7...1) \qquad\qquad (6.22)$$

of newborn cells originating from node (i) to the adjacent position (i+1). The remaining cells are distributed randomly between node (i) and (i-1).

Nutrient Balance

Stationary cells are assumed to decay exponentially with time constant (T_C) (see Section 5.2). The secondary nutrient resource released upon cell decay is lumped with glucose into a single nutrient pool denoted by (c_N). Thus, the rate of nutrient replenishment ($r_{N,rep}$) due to cell decay at lattice node (i) is described by

$$r_{N,rep} = T_C{}^{-1} \cdot n_{C,s}(i,t) \cdot m_C \cdot V_i{}^{-1}. \qquad\qquad (6.23)$$

Nutrient is balanced by solving equation

$$\frac{\partial c_N(i,t)}{\partial t} = D \cdot \frac{\partial^2 c_N(i,t)}{\partial x^2} - r_{N,con}(i,t) + r_{N,rep}(i,t). \qquad\qquad (6.24)$$

6.4.   Summary of Model Dynamics

In the automaton model, cell divisions are assumed to occur at discrete intervals (Δt_p) representing the time span between birth and maturity of a cell. Consequently, proliferation is modeled on the discrete time scale (t_p). In contrast, the state transition of the cells, diffusion of chemicals, messenger emission, decay of messenger, nutrient uptake as well as cell decay are assumed to occur on the continuous time scale (t). Model dynamics are summarized in Fig. 6.1.

$$t_p = t_p + \Delta t_p$$

proliferation*

$$n_{C,p}(i+1, t_p + \Delta t_p) = n_{C,p}(i+1, t_p) + n_{C,p}(i, t_p)$$

$$t = t + \Delta t$$

**

diffusion of nutrient and messenger

messenger emission

$$c_M(i, t + \Delta t)' = c_M(i, t) + r_M(i, t) \cdot \Delta t$$

messenger decay

$$c_M(i, t + \Delta t) = c_M(i, t + \Delta t)' \cdot \exp\left(-\frac{\Delta t}{T_M}\right)$$

cell decay

$$n_{C,s}(i, t + \Delta t)' = n_{C,s}(i, t) \cdot \exp\left(-\frac{\Delta t}{T_C}\right)$$

nutrient replenishment

$$c_N(i, t + \Delta t)' = c_N(i, t) + r_{N,rep}(i, t) \cdot \Delta t$$

nutrient uptake

if $(c_N(i, t + \Delta t)' \geq (r'_{N,con}(i, t) \cdot \Delta t))$ {
    $c_N(i, t + \Delta t) = c_N(i, t + \Delta t)' - r'_{N,con}(i, t) \cdot \Delta t$
    }
else $c_N(i, t + \Delta t) = 0$

set cell status

if $(c_N(i, t + \Delta t) = 0 \vee c_M(i, t + \Delta t) \geq c_{M,crit})$ {
    $n_{C,s}(i, t + \Delta t) = n_{C,s}(i, t + \Delta t)' + n_{C,p}(i, t)$
    $n_{C,p}(i, t + \Delta t) = 0$
    }
else {
    $n_{C,s}(i, t + \Delta t) = n_{C,s}(i, t + \Delta t)'$
    $n_{C,p}(i, t + \Delta t) = n_{C,p}(i, t)$
    }

Figure 6.1: Schematic illustration of the model dynamics. **Variables:** $n_{C,p}$ – number of proliferating cells, $n_{C,s}$ – number of stationary cells ($n_{C,s}'$ – intermediate number of stationary cells in time step Δt), c_N – nutrient concentration (c_N' – intermediate nutrient concentration in time step Δt), c_M – messenger concentration (c_M' – intermediate messenger concentration in time step Δt), t – time, t_p – discrete time scale for proliferation. **Parameters:** Δt_p – time step for growth dynamics, Δt – time step for diffusion of chemicals, T_M – time constant for messenger decay, T_C – time constant for cell decay. **Indices:** i - position of the lattice node. (*) Shows the implementation of proliferation according to the distal budding regime. (**) Indicates the start site of the algorithm. See text for further details.

6.5.   Parameterization of the Models

The model was scaled for space and time. Furthermore, the described processes were parameterized using estimates obtained in own experiments or derived from literature data.

Experimental Setup and Simulation Dynamics

The automaton models describe the growth of unit cells which correspond to pseudohyphal cells. Thus, the average length of the pseudohyphal cells determined in the experimental investigations (Table 5.1) was assigned to the length of a unit cell (l_C). The distance between two lattice nodes was chosen according to the unit-cell size. From the length of the growth-field moiety (l = 26 mm) and the cell length (l_C), the lattice size (n) was determined.

$$n = \left\lceil \frac{l}{l_C} \right\rceil \tag{6.25}$$

For the correct balancing of nutrient and messenger in the growth substrate, the agar height (h = 0.9 mm), calculated from the amount of agar filled into the petri dish (2 mL) and the tile width (w = 1 cm), were incorporated into the model by giving each lattice node a volume (V_i).

$$V_i = h \cdot w \cdot l_C \tag{6.26}$$

From the diffusion constant in agar (D) and the distance between two lattice nodes (l_C) the time step (Δt) for the discretization of the continuous time scale (t) was calculated (Fig. 6.1).

$$\Delta t = \frac{0.5 \cdot l_C^2}{D} \tag{6.27}$$

The replication time (Δt_p) was estimated from the extension rate (v) of the colony diameter and the unit-cell length (l_C).

$$\Delta t_p = \frac{2 \cdot l_C}{v} \tag{6.28}$$

Accordingly, the cell array was updated in intervals of (Δt_p) (see Fig. 6.1). Values estimated for (Δt_p) and (v) during growth of the yeasts on different nutrients are listed in Table 5.1.

Diffusion Constants of the Nutrients in Agar

According to Nicholson (2001), the diffusion constant (D_0) of a small molecule in water can be corrected for the diffusion in agar by

$$D = D_0 \cdot (1 - 0.023 \cdot \omega), \tag{6.29}$$

where (ω) is the weight percentage of agar. The influence of the temperature (T = [K]) is given by relation (Nicholson, 2001)

$$D_2 = D_1 \cdot \exp[0.02 \cdot (T_1 - T_2)], \tag{6.30}$$

wherein (T_1) represents the temperature at which the diffusion constant (D_1) is known, and (T_2) denotes the temperature for which the diffusion constant (D_2) is calculated. (For consistency the factor 0.02 in Equ. 6.30 should carry the unit $[K^{-1}]$.)

Longsworth (1953) reported a diffusion constant of $D_0 = 6.7 \cdot 10^{-10}$ $m^2 \cdot s^{-1}$ for glucose in water. In the same study, the diffusion constants of 20 amino acids and oligomers of amino acids were determined with values ranging from $D_0 = 10.6 \cdot 10^{-10}$ $m^2 \cdot s^{-1}$ (glycine) to $D_0 = 6.1 \cdot 10^{-10}$ $m^2 \cdot s^{-1}$ (leucylglycine). In the present study, the minimum value of $D_0 = 6.1 \cdot 10^{-10}$ $m^2 \cdot s^{-1}$ was chosen to calculate the diffusion speed of casamino acids in agar. Despite an extensive literature review no estimates of diffusion constants of ammonium ions in water were found. However, the diffusion constants of small molecules are mainly dependent on their molecular weight and charge. Thus, the diffusion constant of sodium ions ($M_{Na+} = 23$ $g \cdot mol^{-1}$ (Mortimer, 1987)) in water ($D_0 = 13 \cdot 10^{-10}$ $m^2 \cdot s^{-1}$ (D'Ans & Lax, 1998)) provides a realistic estimate for the diffusion rate of ammonium ions ($M_{NH4+} = 18$ $g \cdot mol^{-1}$ (Mortimer, 1987)). From the diffusion constants in water (D_0), the diffusion constants in 2 % (w/v) agar (D) were calculated according to Equ. 6.29 and used in the simulations (Table 6.1).

Table 6.1: Diffusion constants applied in the simulations. The diffusion constants in water (D_0) were corrected for diffusion in agar (D) using Equ. 6.29.

Nutrient	D_0 $[m^2 \cdot s^{-1}]$	D $[m^2 \cdot s^{-1}]$	Reference for D_0
glucose	$6.7 \cdot 10^{-10}$	$6.4 \cdot 10^{-10}$	(Longsworth, 1953)
casamino acids	$6.1 \cdot 10^{-10}$ *	$5.7 \cdot 10^{-10}$	(Longsworth, 1953)*
ammonium	$13.0 \cdot 10^{-10}$ **	$12.4 \cdot 10^{-10}$	(D'Ans & Lax, 1998)**

 * The diffusion constant for casamino acids in water were estimated from the diffusion constant of the amino acid dimer leucylglycine.

** The diffusion constant for ammonium ions in water was estimated from the diffusion constant of sodium ions in water.

Growth and Decay of the Cells

According to Tijhuis *et al.* (1993), the mass-specific nutrient-uptake rate to meet maintenance requirements (R) mainly depends on the cultivation temperature and only to a small extent on the particular nutrient resources. Therefore, for both applied carbon sources (glucose and casamino acids) the value of R = 0.01 $g \cdot g^{-1} \cdot h^{-1}$ (Tijhuis *et al.*, 1993) was used in the simulations. Considering the higher energy content of glucose when compared to amino acids, the application of an identical value for (R) on both nutrients appears questionable. However, in the absence of reliable information about the amino-acid uptake of microorganisms for maintenance requirements a constant value was applied in the simulations. In contrast, nitrogen sources do not serve as energy sources. Thus, under nitrogen-limiting conditions the maintenance term does not contribute to the balance of the limiting nutrient, i.e. R = 0 (Table 6.2).

The mass of a single cell (m_C) was estimated using equations

$$m_C = V_C \cdot \rho_C \cdot DW \qquad\qquad\qquad (6.31)$$

and

$$V_C = \pi/4 \cdot d_C^2 \cdot l_C, \qquad\qquad\qquad (6.32)$$

wherein (V_C) is the experimentally determined volume of a pseudohyphal cell, (ρ_C) is the density of the *wet* biomass and DW represents the dry weight fraction of the total cell mass. In separation studies, Datar & Rosen (1993) found a *wet* biomass density of $\rho_C = 1.1$ g·cm^{-3}. Large variations of fungal DW, reaching from 5 % (Barclay *et al.*, 1993) to 35 % (Birol *et al.*, 2002; Paul & Thomas, 1996), are known. They originate from a more or less strong vacuolization of the cells and the incorporation of storage materials (Paul & Thomas, 1996). The parameter (DW) was not determined experimentally but assigned to fit simulated results to data derived from the growth experiments. The sensitivity of simulated results to variations in the assumed DW was tested.

The yield (Y) describes the efficiency of the transformation of a particular substrate into cellular mass. In shake flask experiments, the yield coefficients of *Y. lipolytica* and *C. boidinii* on different nutrient sources were estimated (Table 6.2, see Section 4.4 for details). The influence of the pH, found for the glucose limited growth of *Y. lipolytica*, is not incorporated into the model. Simulations are carried out using a constant yield coefficient of Y = 0.33 g·g^{-1} determined at pH 5. According to a model of Heijnen *et al.* (1992), the yield of biomass on glucose is Y = 0.5 g·g^{-1}, a value that was confirmed in a number of studies using different yeasts. The reason for the deviations between this model and the experimentally determined yield for the glucose-limited growth of the yeasts was not further investigated.

Table 6.2: Biochemical and kinetic parameters for the growth *Y. lipolytica* and *C. boidinii* used in the simulations of the colony development. (Numbers in parentheses indicate parameters used in simulations for the growth of *C. boidinii*.)

Nutrient	Replication time Δt_p [h]	Yield Y [g · g^{-1}]	spec. maint. requirement* R [g · g^{-1} · h^{-1}]	cell length l_C [µm]	cell diameter d_C [µm]
carbon limitation					
glucose	1.4 (1.8)	0.33 (0.42)	0.01	30 (19)	2.3 (2.7)
casamino acids	1.3 (-)	0.14 (-)	0.01	27 (-)	3.0 (-)
nitrogen limitation					
ammonium	1.7 (2.1)	7.2 (5.2)	0	27 (24)	3.0 (2.7)
casamino acids	1.0 (1.6)	2.5 (2.3)	0	21 (21)	3.0 (2.7)

*Values were calculated according to (Tijhuis *et al.*, 1993)

The time constants for cell decay (T_C) were estimated from carbon-limited cultivations of *Y. lipolytica* on glucose as the only carbon source (Section 5.2, Table 5.2). In the simulations presented in Section 6.6.3, a value of $T_C = 329$ h was applied.

Parameters Describing Messenger-controlled Growth (QS)

In contrast to the model for DLG, the QS based model is only qualitative. A hypothetic messenger was introduced that mediates interaction between single cells based on the emission of chemical signals. In the model the messenger is emitted by all cells at a constant mass specific rate ($r_{M, spec}$). Cells cease growth when local messenger concentration surpasses the critical concentration ($c_{M, crit}$). Since the messenger is not further characterized, nutrient and messenger, for convenience, were assumed to have the same diffusion constant (D). The messenger decays exponentially with time constant (T_M).

Table 6.3: Selected parameters used in the simulations for messenger-controlled growth of the yeast *Y. lipolytica.*

Parameter	Definition	Value	Reference
$r_{M, spec}$	specific messenger emission rate	0.05 $g \cdot g^{-1} \cdot h^{-1}$	assigned
$c_{M, crit}$	critical messenger concentration	0.0004 $g \cdot L^{-1}$	assigned
T_M	time constant messenger decay	0.01 h	assigned

6.6.   Results of Mathematical Simulations

6.6.1.   Simulations of Diffusion-limited Colony Development

Fig. 6.2 illustrates the simulated development of the cell-density profile in a carbon-limited *Y. lipolytica* colony growing on glucose as the sole carbon source. Calculations were carried out under the assumption of nutrient-controlled proliferation. Furthermore, a random budding pattern of the individual cells was presumed. At early stages of the cultivation, rapid cell growth leads to an accumulation of high cell numbers and local depletion of nutrient close to the inoculation site (Fig 6.2). In the further course of the colony development, cells in areas depleted from nutrient cease growth. After 35 days nutrient is completely deprived from the substrate and the population cannot further extend (Fig 6.2). Please note that the drop in cell density at the left boundary of the growth field, i.e. at the inoculation site, is an artifact arising from the simulation routine. To save computation time, the model simulates the development of only one colony moiety. Thus, in contrast to the inner lattice nodes L(1, 2, ..., (n-1)), the position L(0) at x = 0 mm has only one neighbor from where it may receive newborn cells. The introduction of this asymmetry causes the drop in cell density at the left boundary but does not affect the overall behavior of the simulations.

In Fig. 6.3 (A) an overlay of simulated cell-density profiles at different cultivation times is shown. In this graph it becomes more obvious, that newborn cells are exclusively added at the outer edge of the colony. The amount of cells formed per time interval decreases over time and a monotonically declining profile evolves. Accordingly, the total cell number within the colony increases and saturates after approximately 20 days of cultivation (Fig. 6.3 B).
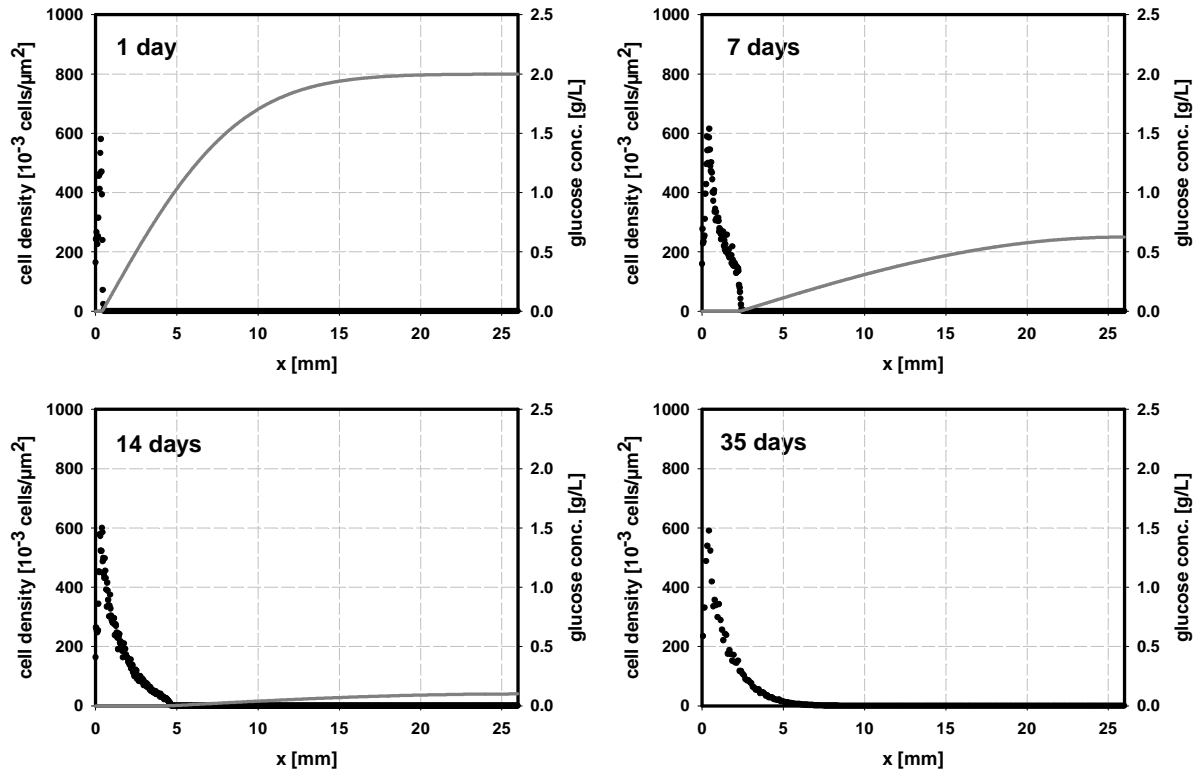
Figure 6.2: Simulated development of the cell-density profile under the assumption of DLG. Simulations describe the growth of a carbon-limited *Y. lipolytica* colony growing on glucose as the sole carbon source. (Initial glucose concentration: 2 g·L^{-1}, random budding, tile width 1 cm). Figures show the average of 10 replicate runs.
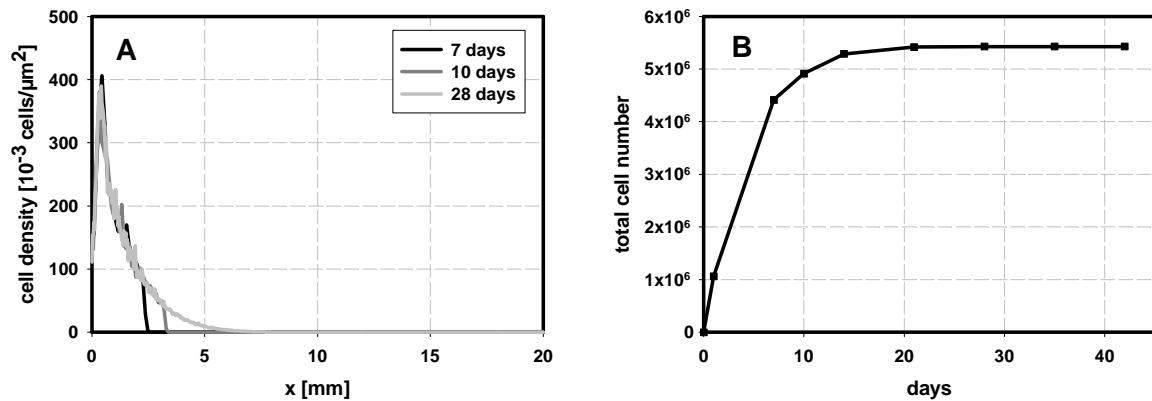
Figure 6.3: Simulated colony development under the assumption of DLG. (A) Overlay of cell-density profiles at different cultivation times. (B) Total cell number in one colony moiety. Simulations describe the growth of a carbon-limited *Y. lipolytica* colony growing on glucose. (Initial glucose concentration: 2 g·L^{-1}, random budding, tile width 1 cm). Figures show the average of 10 replicate runs.

Sensitivity of Model Predictions

To test the sensitivity of these predictions, simulations were carried out under variation of important simulation parameters and model assumptions. As expected, the total cell number accumulated in a colony increases with decreasing dry weight (DW) since the amount of

nutrient necessary to create a new cell declines with smaller cellular mass (Equ. 6.6, 6.31) (Fig. 6.4 A). Likewise, higher cell densities are created at higher initial glucose concentrations (Fig. 6.4 (B)).
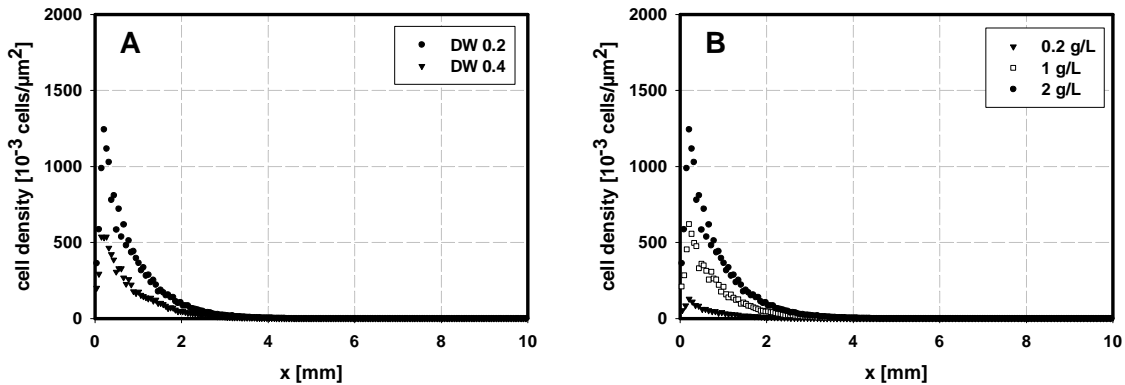
Figure 6.4: (A) Influence of variations of DW (initial glucose concentration: 2 g·L^{-1}), and (B) influence of initial glucose concentration (DW: 0.2) on the predicted final cell-density profiles for the diffusion-limited development of *C. boidinii* colonies growing on glucose. Simulated cultivation time was 3 weeks. (random budding, tile width 1cm). Figures show the average of 20 replicate runs.

Furthermore, the influence of the growth rate of the microorganism and the speed of diffusion was tested. When the replication interval falls below Δt_p = 0.01 h simulations show a constant cell density along the colony diameter (data not shown). Accordingly, with decreasing diffusion constant (D) the cell-density profile flattens and constant cell densities evolve when (D) significantly falls below 10^{-6} cm^2·s^{-1} (Fig. 6.5).
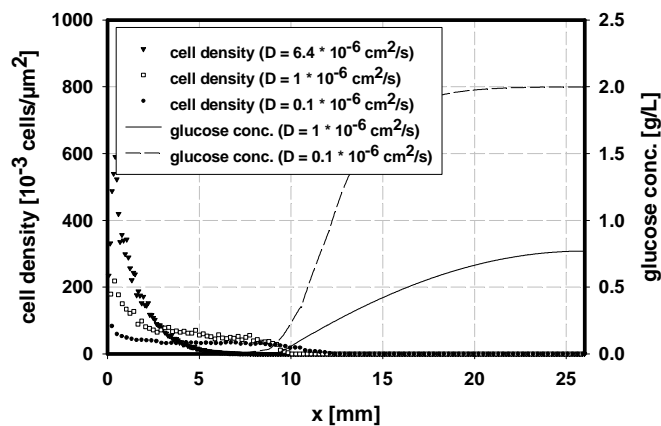
Figure 6.5: Influence of variations of the diffusion coefficient (D) on the predicted cell-density profile for the diffusion-limited development of a *Y. lipolytica* colony growing on glucose as the only carbon source. Simulated cultivation time was 28 days. Glucose in the simulation of D = 6.4·10^{-6} cm^2·s^{-1} is already depleted. (Initial glucose concentration: 2 g·L^{-1}, random budding, tile width 1cm). Figures show the average of 20 replicate runs.

In the above described simulations, a random budding pattern is assumed. Accordingly, newborn cells from position (i) are randomly placed to positions (i), (i+1) and (i-1). When

yeasts grow in the pseudohyphal morphology, unipolar budding is observed, i.e., new cells are exclusively formed at the distal pole of the mother cell. At the population scale, this behavior facilitates the directed growth of the colony boundary away from the inoculation site. It remains, however, unclear whether cells find the correct orientation due to the detection of nutrient gradients or due to the – most likely messenger-mediated – repulsion from high cell densities. Directed growth (distal budding) was implemented in the simulation routine by placing cells born at position (i) exclusively to node (i+1). Fig. 6.6 illustrates the influence of the budding pattern on the final cell-density profile and the accumulation of cells within the colony. The DLG model predicts a somewhat shallower cell-density profile for the distal budding regime (Fig 6.6 A). The total accumulation of cells is identical in both scenarios (Fig. 6.6 B). In contrast, the extension rate and the final colony diameter are significantly higher when distal budding is assumed (Fig. 6.7).
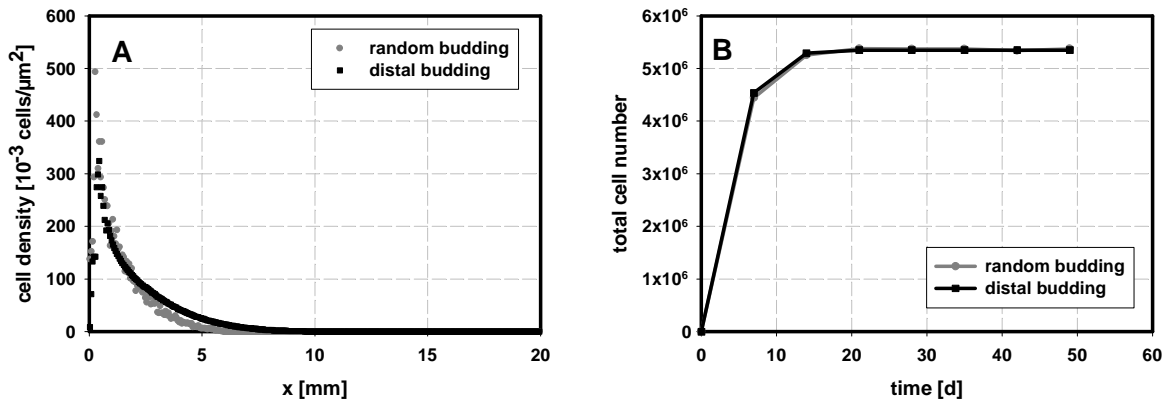
Figure 6.6: Influence of the assumed budding pattern on the simulated diffusion-limited development of *Y. lipolytica* colonies growing on glucose as the sole carbon source. (A) Cell-density profiles after 35 days of cultivation. (B) Total cell number within one colony moiety vs. time. (Initial glucose concentration: 2 g·L^{-1}, tile width 1 cm).
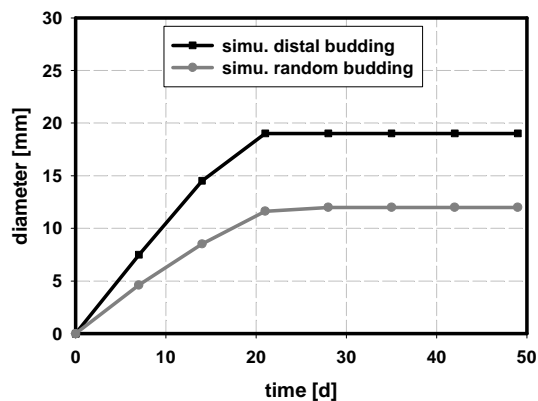
Figure 6.7: Influence of the assumed budding pattern on the simulated extension of the colony diameter during the diffusion-limited development of *Y. lipolytica* colonies growing on glucose as the sole carbon source. (Initial glucose concentration: 2 g·L^{-1}, tile width: 1 cm).

Scaling Effects

In cellular automaton models, scaling effects are commonly prevented by defining the distance between two lattice nodes according to the smallest unit in the system that is meant to be resolved. In the above described one-dimensional model, this smallest unit is represented by the size of an individual cell (l_C). However, since a volume is assigned to each lattice node, also the lateral extensions of a tile, i.e. its width (w) and height (h) (Equ. 6.26), are crucial parameters that influence the predictions of the model. In the one-dimensional model, the diffusion of nutrients in the plane perpendicular to the longitudual colony axis is neglected. This assumption, however, is only a good approximation when i) the cell number (n_C) per tile is high (i.e., the distances between the cells are small compared to their length), or ii) when the width of a tile (w) is defined similar to its length (l_C).

To investigate the effect of differently defined tile widths on the predictions of the model, simulations were carried out wherein (w) was chosen according to the cell size (30 μm) or equals the size of the growth field (1 cm) (Figs 6.8 and 6.9). In Fig. 6.8, the simulated final cell-density profiles and the accumulation of total cells in a diffusion-limited *Y. lipolytica* colony growing on glucose as the only carbon source are compared.
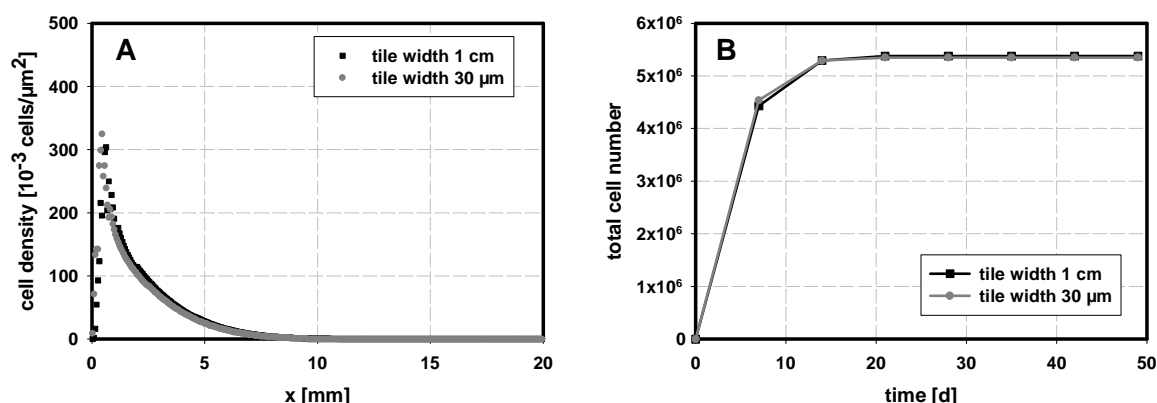
Figure 6.8: Influence of the tile width (w) on the simulated diffusion-limited development of *Y. lipolytica* colonies growing on glucose. (A) Cell-density profiles after 35 days of cultivation. (B) Total cell number within one colony moiety vs. time. (Initial glucose concentration: 2 g·L^{-1}, distal budding).

For both quantities, the predictions of the model are insensitive to the scaling of the tile width. Only a 0.55 % higher total cell number is calculated for a tile width of w = 1 cm when compared to a tile width of w = 30 μm. The cell-density profiles show an almost perfect overlay (Fig 6.8). In contrast, the simulated final colony diameters vary strongly depending on the scaling of the tiles (Fig 6.9). For a tile width of w = 1 cm, a 55 % larger final colony diameter is predicted when compared to simulations with w = 30 μm.
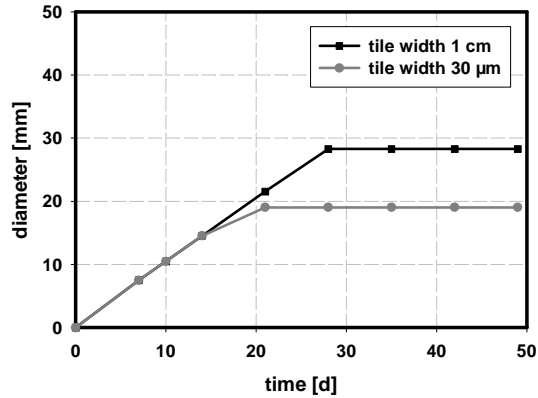
Figure 6.9: Influence of the tile width (w) on the simulated extension of diffusion-limited *Y. lipolytica* colonies growing on glucose. (Initial glucose concentration: 2 g·L^{-1}, distal budding).

6.6.2. Simulations of Quorum Sensing in Yeast Colonies

The mathematical simulations of colony development based on a QS mechanism are solely qualitative. They do not account for the effect of a particular chemical compound that serves as a messenger. Nevertheless, simulations can serve to elaborate important characteristics of a messenger-controlled colony development, thereby helping to identify the presence of such a mechanism in experimental studies and to test the plausibility of the described QS model.

In particular, the stability of the messenger can be shown to be a very crucial parameter: If the growth of the colony is assumed to be controlled by a volatile or extremely unstable messenger, a constant cell-density profile evolves from the beginning (Fig. 6.10).
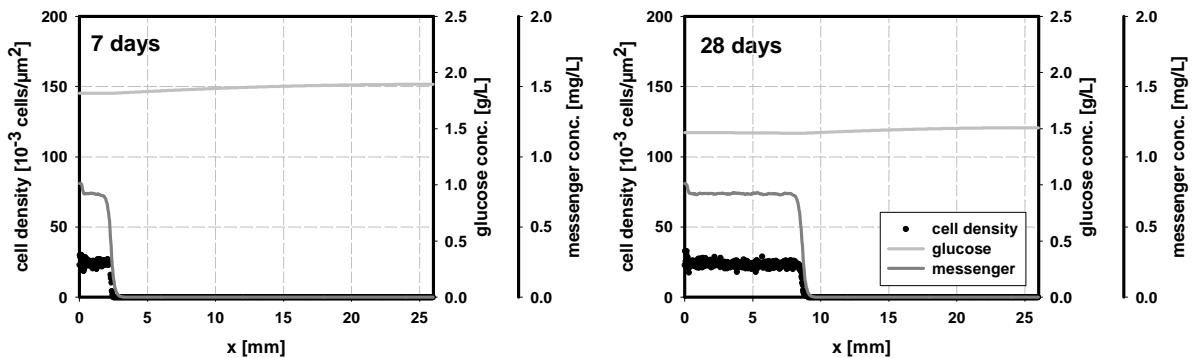
Figure 6.10: Simulations of yeast colony development under the assumption of quorum sensing for a glucose-limited *Y. lipolytica* colony. (Initial glucose concentration: 2 g·L^{-1}, critical messenger concentration: 0.4 mg·L^{-1}, distal budding, tile width: 1cm.) Figures show the average of 20 replicate runs.

In this parameter constellation, a linearly increasing total cell number can be expected (data not shown). Nutrient concentration declines gradually and uniformly throughout the agar substrate and no significant concentration gradient is established (Fig. 6.10) . Since the half-life time of the messenger is chosen very short, the messenger does not diffuse but rather

decays immediately after emission. Thus, critical messenger concentrations accumulate right behind the growing edge of the colony causing truncation of growth in these areas but permit proliferation at the colony boundary.

If proliferation is assumed to be controlled by a stable diffusible messenger, simulations predict the truncation of growth at early stages of colony development (data not shown). Since the diffusion of chemicals is much faster than the extension of the colony, the front of restrictive messenger concentrations passes the proliferating colony edge. As a consequence, cells in the colony margin become stationary and populations stop to extend.

6.6.3. Simulations of Nutrient-controlled Growth and Food Replenishment due to Cell Decay

The model was adopted to the carbon-limited growth of *Y. lipolytica* on glucose as the sole carbon source. Here, a distal budding pattern is assumed. In Fig. 6.11 the temporal development of several morphological quantities are shown. At the beginning of colony development high cell densities are accumulated close to the inoculation site (Fig. 6.11 A). In the further course of the cultivation, cells in the colony interior decay. Thereby, the nutrient reservoir in the growth substrate is replenished and proliferating cells utilize decay products as a secondary nutrient resource. The total cell number passes through a maximum and decreases at longer cultivation times (Fig. 6.11 B). Despite a continuous nutrient replenishment, the model predicts a final colony diameter of only approximately 26 mm (Fig. 6.11 C). The reason for the truncated colony extension becomes obvious in Fig. 6.11 D. Long after the colony stopped to extend, proliferating cells are still present in the colony. Secondary nutrients released upon cell decay are utilized by these proliferating cells before they can diffuse outwards to fuel growth in the colony margin. A qualitatively similar behavior is predicted under the assumption of random budding. The development of total cell numbers is identical in both scenarios but the colony extends at a smaller rate and reaches a smaller final diameter (approx. 20 mm) when growth is not directed (Appendix C).

The time constant for cell decay (T_C) was estimated from the decrease of local OD (see Section 5.2). In the experiments proliferating cells were not discriminated from stationary cells. Thus, the estimated rates may either correspond to the mere decay of stationary cells, or to the difference between cell decay and growth, respectively. In the latter case, time constants for cell decay can be assumed to be somewhat smaller than the estimated values. Therefore, simulations were repeated for smaller time constants. As shown in Fig. 6.12 A, simulations predict a drop in biomass accumulation for decreasing time constants. Higher colony diameters, however, are not reached (Fig. 6.12 B).
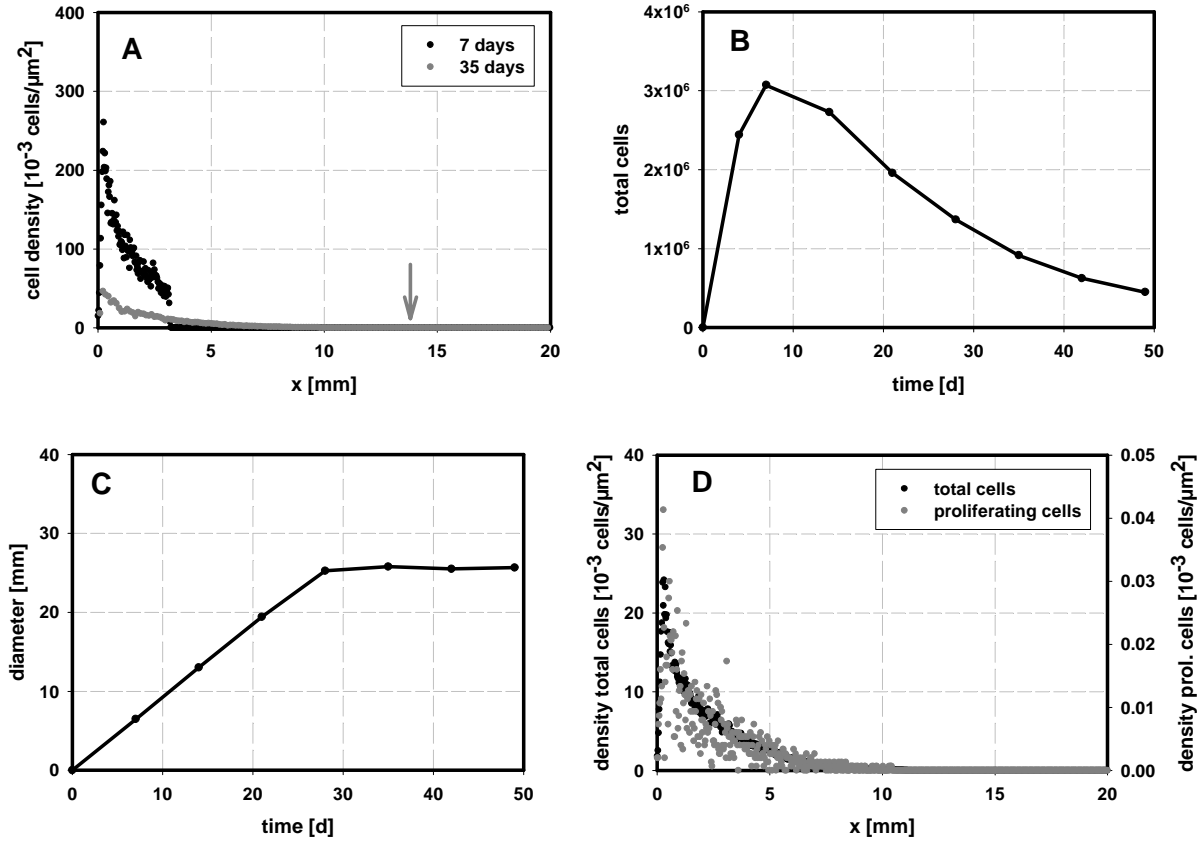
Figure 6.11: Simulations of glucose-limited growth of *Y. lipolytica* under the assumption of nutrient replenishment due to cell decay. (A) Cell-density profiles at 7 and 35 days of cultivation. (The arrow indicates the outer edge of the profile.) (B) Total cell number in one colony moiety vs. time. (C) Colony diameter vs. time. (D) Distribution of proliferating cells within the colony after 42 days of cultivation. (Initial glucose concentration: 2 g·L^{-1}, distal budding, tile width: 1cm.) Figures represent the average of 5 replicate runs.
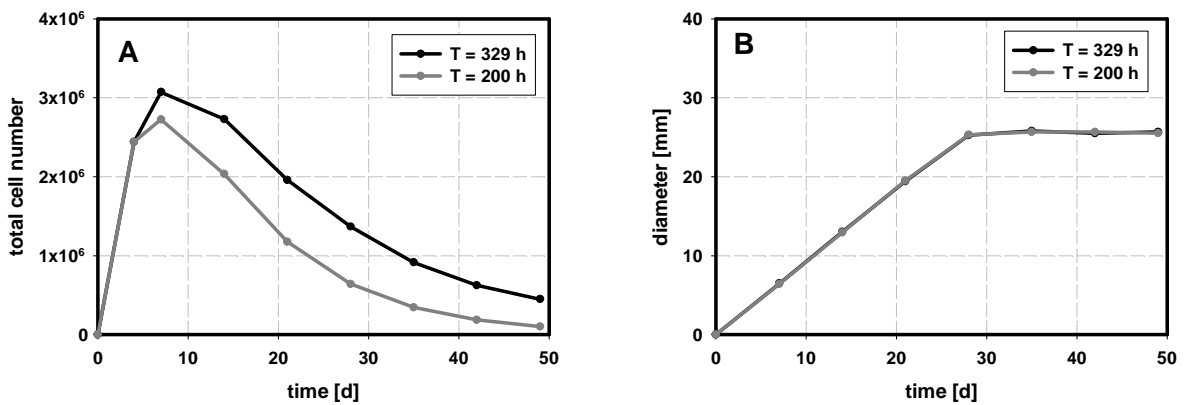
Figure 6.12: Influence of different time constants for cell decay on (A) the total cell number in one colony moiety and (B) colony extension during the glucose-limited growth of *Y. lipolytica* colonies. (Initial glucose concentration: 2 g·L^{-1}, distal budding, tile width: 1cm.) Figures represent the average of 5 replicate runs.

95

In the above described simulations of cannibalizing growth in yeast colonies, the transition of cells to a quiescent state is exclusively controlled by nutrient supply. As a consequence of cell decay and nutrient release, proliferating cells in the neighborhood of dying cells find sufficient food to continue their reproduction. Thus, growing cells are distributed over the whole colony and take up secondary nutrient. Thereby, cells in the colony boundary become starved and abort proliferation. In order to test whether the local nutrient utilization inside the colony is the only reason for the truncation of colony extension at small diameters, simulations were carried out wherein the proliferation of cells was restricted to a 1 mm wide zone behind the colony margin. Under this assumption, a continuous colony extension and the formation of large areas of fairly constant cell density is predicted. In contrast, no changes in the accumulation of total cell numbers are observed when the results are compared to simulations of unrestricted proliferation (compare Figs. 6.13 B and 6.11 B).
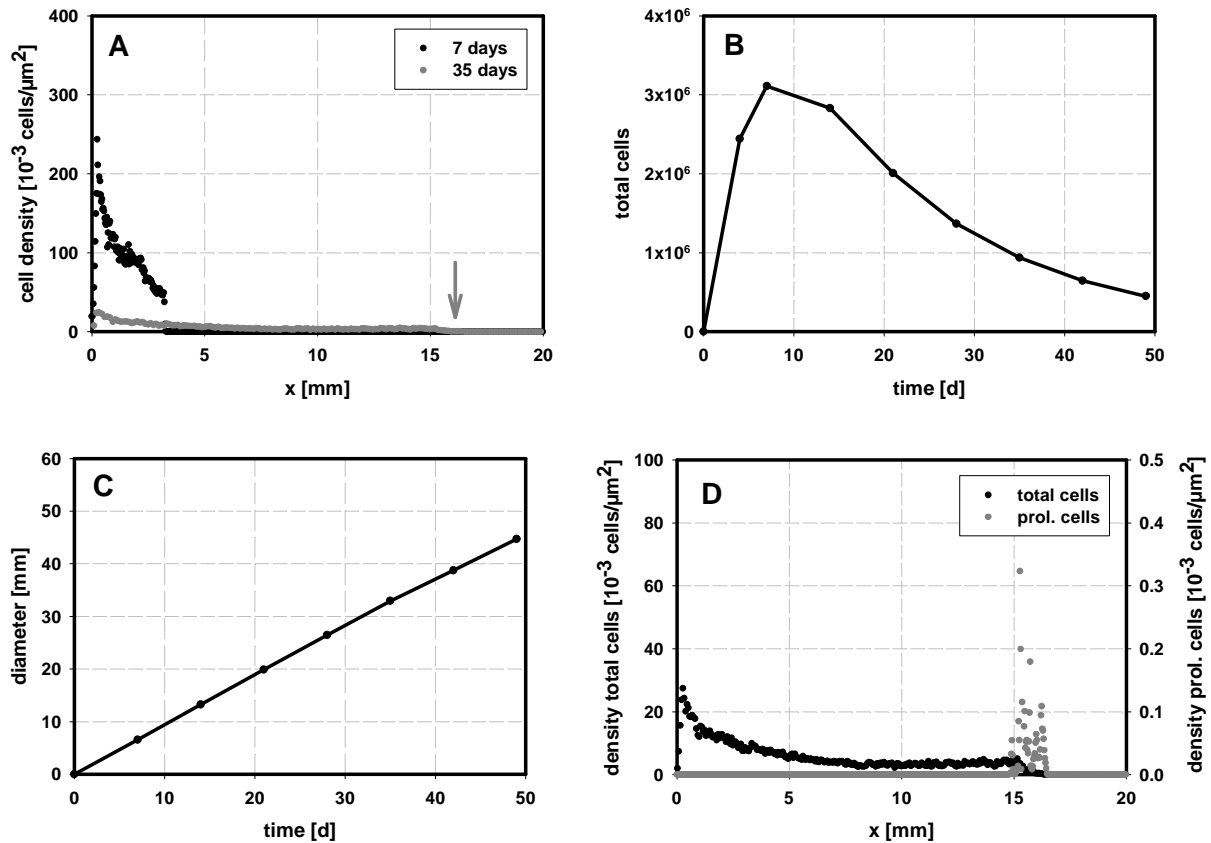
Figure 6.13: Simulations of glucose-limited growth of *Y. lipolytica* under the assumption of nutrient replenishment due to cell decay. Proliferation is restricted to a 1 mm wide zone at the colony boundary. (A) Cell-density profiles at 7 and 35 days of cultivation. (The arrow indicates the outer edge of the profile.) (B) Total cell number in one colony moiety vs. time. (C) Colony diameter vs. time. (D) Distribution of proliferating cells within the colony after 35 days of cultivation. (Initial glucose concentration: 2 $g \cdot L^{-1}$, distal budding, tile width: 1cm.) Figures represent the average of 5 replicate runs.

Since cell growth is restricted to the colony boundary, decay products released in the colony interior can diffuse outwards and ensure a stable extension of the colony. In contrast to the

exclusively nutrient-controlled mechanism, the formation of a monotonically declining nutrient concentration gradient over the colony is predicted.
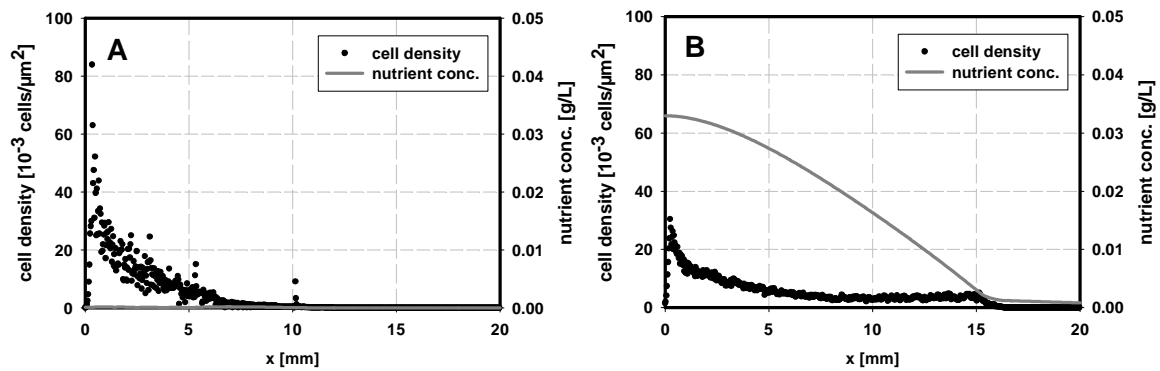
Figure 6.14: Comparison of simulated cell-density profiles and nutrient distributions in glucose-limited *Y. lipolytica* colonies after 35 days of cultivation. (A) Exclusively nutrient-controlled proliferation. (B) Proliferation restricted to the colony margin. (Initial glucose concentration: 2 g·L^{-1}, distal budding, tile width: 1cm.) Figures represent the average of 5 replicate runs.

7. DISCUSSION

7.1. Discussion of Experimental Results

7.1.1. Monitoring of Biomass Distributions by OD Measurements

In the present study, the colony development of yeasts was *quantitatively* analyzed to elaborate regulatory phenomena and to facilitate the balancing of limiting nutrient and biomass in the agar plate system. A new method for the monitoring of fungal colony growth was developed. This technique facilitates the estimation of cell-density profiles within the mycelia by OD measurements along the longitudinal colony axis. Local cell densities in the range of 0.005 cells·μm^{-2} can be resolved from the background noise (see Fig. 5.12). In contrast to the experimental study of Boswell *et al.* (2002), who cut out 1 cm square samples from the mycelium and dried these tiles to estimate biomass densities, the presented method allows for cell-density estimations with extremely high spatial resolutions (distance between two sampling points: 69 μm). Due to the small distance between the sampling points, the cell-density integral over the colony can be conveniently drawn yielding the total number of cells which is accumulated in the mycelium. Furthermore, OD measurements are non-invasive and facilitate the continuous observation of cell-density development in a single colony throughout the whole cultivation period.

The reliability of the method was evaluated by balancing the limiting nutrient and the *wet* biomass content of the colonies which was estimated by the integral of colony OD (see Section 5.3). Only for carbon-limited cells of the applied model yeasts, OD-measurements provide an accurate estimate of the biomass distribution inside a mycelium. Under these conditions, the vacuolization of cells, which is equivalent to a decreasing cellular mass, coincides with a drop of their OD. Thus, the biomass redistribution as found in carbon-limited *Y. lipolytica* colonies (Figs. 5.10 C and 5.14 A) can be precisely monitored. The carbon balances close for both model yeasts applying a realistic value of DW (Table 5.3). In contrast to carbon-limiting conditions, nitrogen-limited cells of the model yeasts show a very strong vacuolization right behind the proliferating colony margin. Furthermore, a pronounced formation of inclusion bodies that most-likely consist of incorporated storage carbohydrates is observed (Figs. 5.18 and 5.19). The storage of excess carbohydrates inside nitrogen-limited cells is a common phenomenon and was earlier reported for *Candida oleophila* in submers cultivations (Anastassiadis *et al.*, 2002), as well as for *S. cerevisiae* cells that enter stationary phase in the absence of nitrogen (Parrou *et al.*, 1999). However, this behavior of the yeasts hampers the quantification of cell densities by OD measurements. Due to the incorporation of storage material, vacuolated cells have an OD which may be even higher than the OD of exponentially growing cells that are filled with cytoplasm. Therefore, OD-measurements cannot discriminate between the local accumulation of cells or storage material, respectively. Thus, the results of the nitrogen balances (see Table 5.4) and the quantitative estimations of cell distributions inside nitrogen-limited colonies should be interpreted with extreme care.

7.1.2.   Growth of Model Yeasts on Different Nutrient Resources

Induction of Mycelial Colony Morphologies

Upon nutrient limitation, colonies of the model yeasts *Candida boidinii* and *Yarrowia lipolytica* switch to mycelial morphologies (Figs. 5.1-5.4). At small nutrient concentrations the extension rates of *Y. lipolytica* colonies tend to be higher then under optimum growth conditions, while the cell density within the colonies declines. This behavior can be interpreted as the switch from an exploitative to an explorative growth strategy. In search for new nutrient resources, the yeast mycelium covers a large area at a small expense of biomass and energy. In particular, carbon-limited *Y. lipolytica* colonies are able to form sparsely branched patterns under severe nutrient deficiency (Figs. 5.1 and 5.2). Due the similarities of the colony patterns to fungal mycelia, both yeasts can serve as model organisms for the investigation of fungal colony development.

The macroscopic transition to filamentous colony patterns is caused by a change in the morphology of individual cells on the microscopic scale. Both model yeasts exhibit a dimorphic switch and the transition to mycelial colony morphologies at small concentrations of *all* applied carbon and nitrogen sources (Figs. 5.1-5.4). These observations contradict the results of Dominguez *et al.* (2000) who found that in *Y. lipolytica* i) no filaments are induced in minimal medium, and ii) the starvation of the yeast for ammonium does not induce pseudohyphal development. Furthermore, the necessity of high ammonia concentrations for filament formation in *Y. lipolytica* (Ruiz-Herrera & Sentandreu, 2002; Szabo, 1999) was not confirmed by own experiments (see Fig. 5.1, ammonia-limited media). These partially contradictory results possibly originate from the application of different strains of the yeast *Y. lipolytica* and/or from different cultivation conditions applied in these investigations. While the above mentioned studies mainly investigate the effectors of dimorphism in liquid culture, here exclusively emers cultivations were carried out. The observations clearly suggest that cultivation conditions which induce differentiation should be characterized by studying the colony development of the yeasts rather than the filament formation in submers cultivations. Otherwise, possibly misleading results will be obtained.

Adaptation of Filamentous Colonies to Nutrient Availability

The adaptation of mycelial yeast colonies to nutrient limitation was investigated at two different initial concentrations of the limiting carbon or nitrogen source (see Section 5.1.2). While the macroscopic colony morphology was assessed only visually, quantitative measures such as the extension of the colony diameter (in particular, the final colony diameter), the morphology of colony-density profiles, and the total cell numbers of the colonies were used to characterize the adaptation of yeast mycelia to the availability of food resources.

Irrespective of the degree of nutrient limitation, *mycelial* colonies expand linearly at a constant rate (Fig. 5.7, Table 5.1). The observation of constant colony-extension rates at different initial nutrient concentrations is consistent with results reported for the growth of higher fungi (Gow, 1994). This behavior is apparently contradictory to the growth of yeast cells in liquid culture. Here, growth rates decline at small nutrient concentrations according to

the Monod relation. Thus, the observation of constant colony extension rates at extremely small nutrient concentrations either indicate that i) a different mechanism (e.g., a much higher substrate affinity) regulates growth of pseudohyphal cells, or ii) that this behavior is impressed by the system. I.e., cell growth and food limitation originating from slow diffusive transport may cause the nutrient concentration at the colony boundary to drop to a value that is fairly constant throughout the cultivation. At the present stage of investigation this question cannot be conclusively answered.

In contrast to the growth rates of the colony diameter, cell densities within the mycelium decline with decreasing food concentrations (Figs. 5.8 and 5.9). Thus, once growing in the mycelial morphology, yeast populations adapt to nutrient concentration by changing their cell density rather than by variations of their extension rates. In carbon-limited colonies, the total cell number in the populations is roughly proportional to the nutrient content of the growth substrate (Fig. 5.8). In nitrogen-limited populations, however, the drop in the total cell number does not correspond to the decrease in nutrient concentration (Fig. 5.9). This behavior most likely originates from the above discussed inaccurate quantification of nitrogen-limited cells by OD-measurements.

Spatio-temporal Development of Mycelial Yeast Colonies

A detailed investigation of the spatio-temporal development of mycelial yeast colonies was carried out for various nutrient resources at a single initial concentration. Growth conditions were chosen to induce mycelial colony morphologies in response to the limitation of food. On the other hand, applied initial nutrient concentrations were high enough to ensure an accumulation of local cell densities which could be resolved by OD measurements during cultivation times of at least 35 days.

Development of Carbon-limited Colonies

Growth under carbon-limiting conditions was investigated using glucose or casamino acids as the limiting nutrient source. Since growth of *C. boidinii* on casamino acid was extremely poor and heterogeneous, the development of the yeast was not investigated under these conditions.

When glucose serves as the limiting carbon source strong differences between the model yeasts are evident. The growth of *C. boidinii* colonies is characterized by the development of rapidly declining cell densities (Fig. 5.10 A). Local cell concentrations behind the progressing colony margin remain constant. The total cell number within the mycelium reaches a maximum value after 21 days of cultivation and exhibits only a slight decrease at later stages of colony development. The stop of colony extension at comparatively small colony diameters of approximately 12 mm (Fig. 5.7 A, Table 5.1) coincides with the depletion of glucose after 28-35 days (compare Figs. 5.10 A and 5.11). Thus, colony development of carbon-limited *C. boidinii* colonies is most-likely controlled by the availability of the primary nutrient resource.

In contrast to this behavior, glucose-limited *Y. lipolytica* colonies form mycelia that cover the whole growth substrate and exhibit regions of rather constant cell densities (Fig. 5.10 C). The populations continue to extend even after glucose is completely depleted from the substrate

(compare Figs. 5.10 A and 5.11). Thus, at late cultivation times the yeast uses an alternative carbon source to fuel proliferation at the colony boundary. In the inner parts of the colony, a continuously declining cell density was observed (Fig. 5.10 C). Furthermore, the removal of the colony interior after 14 days of cultivation resulted in an accumulation of smaller cell densities and an impaired extension of "cut-out" colonies when compared to their sound counterparts (Fig. 5.12). Therefore, it can be concluded that the secondary nutrient resource (which facilitates about 40 % of colony extension in the described experiments) is provided by compounds released during cell decay in the inner colony regions.

However, *the* crucial question about the nature of this cell decay cannot be answered at the current stage of investigation: The fundamental motivation for the application of yeast colonies as a model system for fungal growth was the assumption that yeast mycelia are built up of separate individual cells. Accordingly, the vacuolization of cells has to be viewed as an emission of cytoplasm into the agar substrate. The released compounds represent a secondary nutrient resource which freely diffuses and is eventually taken up by proliferating cells. On the other hand, microscopic images of the colony interior in glucose-limited *Y. lipolytica* colonies show remaining cell walls that appear to form a tube-like structure similar to hyphae (Fig. 5.18 D). Therefore, it cannot be precluded that the cytoplasm of vacuolated cells (or the decay products of this cytoplasm) is translocated *inside* the mycelium serving as a secondary and *internal* nutrient resource. Accordingly, the apparent cell decay inside expanding *Y. lipolytica* colonies results from the translocation of cytoplasm rather than from the decay of individual cells. This hypothesis would nicely explain the significantly higher time constants (T_C) estimated for the cell decay close to the colony origin (Table 5.2, see also Fig. 5.8 A): Since immediately after the inoculation cells grow in the yeast-like morphology, their cytoplasm cannot be transported from cell to cell. Consequently, the cytoplasm (i.e. biomass) remains localized and the local OD decreases at a much smaller rate.

The development of carbon-limited *Y. lipolytica* colonies utilizing casamino acids as the limiting nutrient source exhibits strong similarities to their growth on glucose. At the end of the cultivations colonies cover the whole growth field, large areas of constant cell densities are formed, and cells decay in the colony interior. However, neither the nutrient uptake was followed, nor the behavior of "cut-out" colonies was compared to sound colonies. Thus, although colony development appears to be ruled by identical processes, further experiments are necessary to ultimately confirm this conclusion.

The outlined hypothesis, obviously, contradicts the assumption of *Y. lipolytica* colonies being populations of autonomously replicating cells. In a personal consultation, Prof. Barth confirmed that *Y. lipolytica* colonies initially grow in a pseudohyphal morphology on minimal medium containing glucose as the only carbon source. Later in colony development, the yeast was observed to switch to the hyphal phenotype (Barth, 2004) which would enable internal translocation of cytoplasm. However, a pronounced vacuolization of cells is also evident in the inner parts of the colonies indicating a rapid transport or utilization of cytoplasm (Fig. 5.10 A). This observation implies that i) pseudohyphae of *Y. lipolytica* are able to *reopen* a connection at the poles between the cells, or that ii) this potential connection is never closed. Thus, the hypothesis about internal degradation of cytoplasm to serve as a nutrient resource puts up a number of questions that were not investigated in the

pseudohyphal development of *Y. lipolytica* so far. However, further research should be directed to verify external or internal translocation of decay products. To answer this question represents the key problem for the understanding of the colony development of *Y. lipolytica* under carbon-limiting conditions.

Development of Nitrogen-limited Colonies

The nitrogen-limited growth of yeast colonies was investigated applying ammonium sulfate or casamino acids as nutrient sources (Section 5.2.2). Because of the discussed difficulties in the quantification of biomass distributions inside nitrogen-limited mycelia, the development of colony-density profiles could be solely qualitatively monitored.

When *C. boidinii* and *Y. lipolytica* are cultivated on ammonium sulfate, colonies of both yeasts cover the whole substrate at the end of the cultivation. In the first 35 days of colony development no decrease in the local biomass density is observed and total cell number increases continuously (Figs. 5.15). Furthermore, no changes in colony growth are observed upon removal of the colony interior (Fig. 5.16.). Thus, strong similarities to the glucose-limited growth of *C. boidinii* are evident during this period. However, since ammonia-limited colonies proceed to expand until the edge of the growth field is reached, total cell number (total biomass) within the mycelium is likely to drop at longer cultivation times. The applied ammonia concentrations were extremely small (initial concentration 0.05 g·L^{-1}) and could not be determined experimentally. Therefore, an essential information for the characterization of ammonium-limited colony development is missing. A hypothesis about factors that control colony development when ammonium sulfate serves as the limiting nitrogen source cannot be drawn from these experimental results.

The nitrogen-limited development of *C. boidinii* and *Y. lipolytica* populations on ammonium sulfate showed the same qualitative pattern. Interestingly, growth of the model yeasts is clearly different when they use casamino acids as the sole nitrogen source. Populations of both yeasts grow linearly until the growth field is finally covered. However, while during the first 35 days of cultivation no drop in cell density and total cell number is observed in *C. boidinii* colonies (Fig. 5.17), the growth pattern of *Y. lipolytica* is similar to the carbon-limited development of the yeast. The cell density of *Y. lipolytica* colonies declines behind the propagating colony margin and total cell number passes through a maximum after 14 days (Fig. 5.17). The reason for this inconsistent behavior on different nitrogen sources was not identified. Differences possibly arise from the different degree of nitrogen limitation when ammonium sulfate or casamino acids served as the limiting nutrient. Experiments at a smaller initial casamino-acid concentrations will have to reveal whether growth of *Y. lipolytica* is regulated in a different manner when growing on organic nitrogen sources.

7.1.3. Influence of Environmental Factors on Colony Development

As summarized in the literature review, several chemical compounds were identified that influence the development of yeast colonies, and/or the morphology of individual cells when growing in liquid culture: Volatile ammonia serves as a long-range signal between adjacently growing yeast colonies and facilitates the directed growth of the colonies away from each

other (Palkova *et al.*, 1997; Palkova *et al.*, 2002). Fusel alcohols were shown to induce the morphological switch from round to pseudohyphal *S. cerevisiae* cells in liquid culture as well as on solid substrates (Lorenz *et al.*, 2000). An upshift of pH induces differentiation of *Y. lipolytica* cells in liquid culture while at low pH differentiation is prevented (Ruiz-Herrera & Sentandreu, 2002). Furthermore, the presence of citric acid in the growth medium was observed to induce differentiation in this yeast (Ruiz-Herrera & Sentandreu, 2002). In cultivations of *C. albicans*, farnesol was identified as a quorum-sensing molecule that inhibits the formation of hyphal cells (Hornby *et al.*, 2001). Thus, a considerable number of chemical compounds is produced by the microorganisms that have the potential to affect colony development at different system scales, i.e., at the microscopic level by influencing the morphology of individual cells, or at the population level by the creation of preferential growth directions. Until today, the effect of most compounds was only insufficiently discussed for their role in colony development and, mostly, only investigated for only few or one particular yeast species. Therefore, the question arises whether these or yet unknown compounds and environmental factors influence the growth behavior of *Y. lipolytica* and *C. boidinii* colonies or exert regulatory functions. It is, however, far beyond the scope of this study to identify particular chemical compounds that serve as potential messengers and to describe their effect in detail. Nevertheless, the described experiments may serve to elaborate growth conditions where the effect of metabolic by-products or messengers, respectively, cannot be neglected in the description of colony development. In particular, the response of colony morphology to the exposure of volatiles emitted by the yeasts, and the influence of pH in the growth substrate were investigated.

Influence of volatile compounds on colony morphology

Qualitative Effects of Volatile Compounds on Colony Development
In general, freshly inoculated colonies exhibit significant morphological changes when incubated in the headspace of a giant colony which grows on the same limiting nutrient. Interestingly, the presence of giant colonies did not prevent pseudohyphae formation under any conditions. Thus, quorum-sensing molecules such as farnesol or similarly acting compounds that prevent differentiation appear to be absent, or their effect is repressed by other regulatory mechanisms. All exposed colonies exhibit a less dense colony pattern when compared to undisturbed populations. Particularly in carbon-limited colonies of the model yeasts, a strong decrease of cell density can be observed (Figs. 5.20 and 5.21). Furthermore, the morphology of individual cells is shifted to the filamentous growth form. In contrast to undisturbed colonies, the mycelial network in exposed populations is not (or significantly less) covered by cells with a yeast-like morphology (Fig. 5.22). Thus, the drop of colony density is most-likely caused by the specific inhibition of a particular cell type, rather than by a generally impeded proliferation.
In giant colonies, cells grow in high densities under strong nutrient limitation. These populations emit volatiles that induce the development of sparse colony patterns in the small colonies although nutrient availability in these colonies is identical to their undisturbed

counterparts. Therefore, it can be concluded that a regulatory mechanism is present in yeast colonies which is mediated by the emission of chemical compounds and controls growth of individual cells with respect to the local cell density. Consequently, this mechanism can be regarded as quorum sensing.

However, from the above described observations it remains unclear whether this quorum-sensing mechanism regulates colony development *alone* or *in addition* to nutrient availability. To investigate this question, small colonies were exposed to the same concentrations of volatile compounds (one giant colony, inoculated with the same cell number, incubated at identical nutrient concentrations), but cultivated at different glucose concentrations. In Fig. 5.23 the morphology of glucose-limited *C. boidinii* colonies grown under different conditions is compared. Obviously, populations that are cultivated in the headspace of a giant colony accumulate smaller cell numbers. Comparing the morphology of exposed colonies it can be seen, that this effect is less pronounced at higher nutrient concentrations. (In cultivations of *C. boidinii* and *Y. lipolytica* on different nutrient resources the same tendency is found. Data not shown.) From this observation it becomes evident, that colony development (particularly the differentiation of cells) is not controlled by a single factor. The individual cells within exposed colonies appear to access the quality of a nutrient resource based on both, the nutrient concentration and the number of cells that is growing on this resource. According to this hypothesis, differentiation, as a prerequisite for explorative growth, is induced at comparatively high nutrient concentrations when local cell density in the habitat is large. The differentiation of *S. cerevisiae* cells in rich medium as a response to the presence of several alcohols was interpreted in a similar way (Lorenz *et al.*, 2000). These alcohols are formed in the amino-acid metabolism under nitrogen-limiting conditions. They may evaporate (or diffuse) from starved colony regions and signal the incoming shortage of nutrients to still unlimited remote parts of the population. Thereby, they induce differentiation and facilitate polarized growth away from regions depleted of nutrients.

Determination of pH Changes During Head-space Cultivations

The pH measurements serve to narrow down the list of possible candidates that induce morphological changes under different cultivation conditions, since several of the above mentioned morphogenic compounds influence the pH. The increasing pH in giant colonies growing on casamino acids as the limiting carbon source (Table 5.5) is consistent with findings of Palkova *et al.* (1997), who reported an alkalization of the medium under these cultivation conditions for a large number of yeasts. Since the upshift in pH in the giant colonies coincides with an elevated pH in the growth field of the small colonies, volatile ammonia may serve as a mediator of pH between the opposing populations. However, it is not clear, whether ammonia is actively emitted by the cells. Alternatively, the growth substrate of the giant colonies may be alkalinized due to the uptake of casamino acids via active proton-symport systems (Palkova *et al.*, 2002). As a consequence, ammonia is released from the medium because the ammonium-ammonia equilibrium is shifted towards higher concentrations of the volatile compound (Equ. 3.1 and 3.2).

In order to test whether ammonia is responsible for the observed changes, giant colonies were substituted by an artificial ammonia source. The incubation of small colonies under an

ammonia atmosphere induces morphological changes in exposed populations. However, the observed response is not as pronounced as in experiments with a second colony, although a higher pH in the growth substrate indicates the presence of higher ammonia concentrations. Thus, besides ammonia at least one additional compound is released by the giant colonies and affects growth in the small populations.

Exposed glucose-limited colonies exhibit morphological changes similar to colonies growing on casamino acids, but strongly acidify the medium. The shift towards smaller pH in exposed colonies indicates the transition of a volatile acidic compound. Alternatively, the pronounced acidification may be a response of exposed colonies to a neutral compound emitted by the giant colonies. Whatever the reason, pH itself was demonstrated not to be the inducing morphogen, since in Section 5.4.2 the cultivation of both yeasts at lower pH resulted in a delayed differentiation of individual cells and the accumulation of higher local cell densities. Thus, a yet unidentified – possibly acidic – volatile compound induces morphological changes in glucose-limited populations. Considering the observations of Ruiz-Herrera & Sentandreu (2002), citric acid certainly is a possible candidate that needs to be tested for its effect on colony morphology.

Nitrogen-limited *Y. lipolytica* colonies show a weak but still obvious response to the presence of the giant colony while *C. boidinii* colonies hardly exhibit morphological changes. Although giant colonies strongly acidify their growth substrate, pH in exposed colonies is somewhat higher than in undisturbed colonies. Thus, no acidic compound migrates between the colonies, or small populations actively control the pH of their growth medium.

The described experiments clearly prove the influence of volatile compounds on colony morphology. Since several morphogens that were investigated in earlier studies influence pH, simple measurements of this parameter indicate that additional morphogenic compounds must be emitted by yeast colonies. These compounds are not yet identified. In particular, carbon-limited *Y. lipolytica* and *C. boidinii* colonies emit chemicals that affect cell morphology and cell density within the mycelium. Although the interpretation of these experimental findings supports hypotheses about quorum-sensing in yeast colonies, it is solely based on the *qualitative* visual assessment of colony morphology. In particular, the identification of compounds responsible for these observations, the quantification of these chemicals in exposed colonies, and the detection of a specific molecular biological response are open problems that still have to be solved. Furthermore, it remains unclear to what extent volatile compounds affect the development of a single colony under the conditions described in Section 5.2. The cultivation conditions in both sets of experiments (Section 5.2 and Section 5.3) were clearly different: To increase the sensitivity of the bioassay for volatile compounds, exposed colonies were cultivated on small growth fields (dimensions: 2 cm x 2 cm) under severe nutrient limitation. In addition, the populations were incubated at very high concentrations of volatile compounds emitted by the giant colonies. Thus, the observed effects were obtained under comparatively extreme cultivation conditions. Whether or not such conditions occur during colony development in the experimental setup employed in Section 5.2 remains to be tested. Although the experimental basis is still very small and several questions about the nature and primary action of the volatile morphogens represent open problems, experiments clearly indicate the need for a further investigation of the

described phenomena since they appear to play a crucial role in the adaptation process of yeast colonies to nutrient availability and/or population density in their environment.

Influence of pH colony development

During the cultivation of the yeasts strong changes in pH are detected. Therefore, the influence of this factor on colony development was investigated. In particular, carbon-limited colonies of the model yeasts were cultivated under variation of the initial pH and otherwise identical conditions. The influence of pH on colony extension rates, development of cell-density profiles, and total biomass accumulation was investigated quantitatively. Furthermore, the average pH in the growth substrate was monitored.

In glucose-limited *Y. lipolytica* and *C. boidinii* colonies, a gradually declining local cell density and a smaller total biomass accumulation within the colonies can be observed with increasing initial pH (Figs. 5.27-5.31). While *Y. lipolytica* colonies tend to extend at smaller rates under acidic conditions, a reduced growth rate of *C. boidinii* colonies is observed at pH 8 (Figs. 5.28 and 5.30). Furthermore, both yeasts acidify the medium at early stages of colony development. In later phases of the cultivation, *Y. lipolytica* colonies elevate pH whereas pH remains fairly constant in *C. boidinii* populations (Figs. 5.29 and 5.32). Since *Y. lipolytica* utilizes cell decay products in the absence of glucose to facilitate colony extension, the upshift of pH is possibly caused by the utilization of peptides or amino acids as alternative carbon source (see Table 5.5 and Palkova *et al.* (1997)). The observation of significantly higher biomass accumulation in the colonies at pH 4 is not consistent with the pH-dependent biomass yields obtained in liquid culture (Fig. 5.1). Here, the yield of *C. boidinii* on glucose does not significantly vary at different pH-values and *Y. lipolytica* exhibits a maximum yield at pH 5 (Fig. 5.26). Furthermore, the final pH detected in submers cultivations is significantly lower when compared to pH in the growth substrate of the colonies (Table 5.7). This finding *appears* to indicate, that pH in yeast colonies is actively controlled rather than passively changed due to the emission of metabolic by-products. It was reported that yeast colonies growing on casamino acids as the sole carbon source alkalize and acidify the medium in a pulse-wise manner (Palkova & Forstova, 2000; Palkova *et al.*, 1997; Palkova *et al.*, 2002). Adjacently growing yeast colonies even synchronize periods of acidification and alkalization (Palkova & Forstova, 2000). Thus, the active control of pH in the growth medium of yeast colonies is not an unknown phenomenon. However, the differences between growth of the yeast in submers and emers cultivations under glucose-limiting conditions were not reported in literature so far. Since the pH of the substrate strongly affects colony development, and because several studies underline the importance of pH gradients for the orientation of mycelial growth (see Gow (1994) and references therein), this observation appears to be highly important in the search for regulatory phenomena in yeast colony development.

In contrast to glucose-limited colonies, *Y. lipolytica* populations growing on casamino acids as the limiting carbon source continuously alkalize the growth substrate. Only at pH 8 a slight acidification can be observed. However, since the first pH measurement was carried out after 7 days of incubation, an initial drop in pH at earlier cultivation times cannot be precluded. A stable extension of the colonies is only observed at pH 5 and 6. Under more alkaline

conditions, growth of the mycelia collapses at a diameter of 10 mm. At the time colony extension was aborted, an average pH of approximately 7.2 was detected in the substrate. The threshold pH for the truncation of growth in colonies exposed to an artificial ammonia source was estimated with 7.2-7.5 (Table 5.6). Both values are strikingly similar indicating that colony extension might collapse due to the surpass of a threshold pH, i.e., ammonia concentration in the substrate, restrictive for cell proliferation. On the other hand, colonies which are incubated at the initial pH 6 continue to extend although a similar pH is reached at later stages of cultivation (Fig. 5.35). These apparent discrepancies possibly arise from an insufficient spatial resolution of pH measurements. No pH gradients could be detected by the applied method although they are likely to be present. Furthermore, pH was monitored on a comparatively coarse scale which was impressed by the resolution of the test paper. Thus, although there is strong indication for the validity of the threshold hypothesis, only refined and locally resolved pH measurements can answer the open questions conclusively.

7.2. Discussion of Model Characteristics

In the mathematical section of this study, one-dimensional hybrid cellular automaton models were developed that describe the formation of yeast mycelia based on the growth of individual cells, and the interactions of these individuals with their dynamically changing environment. The models *quantitatively* predict the spatio-temporal development of several morphological measures and process variables, such as the colony diameter, the cell-density profile, the total cell number within the mycelium, as well as the nutrient and messenger concentration in the growth field. As shown in Section 6.6, the characteristic behavior of the models strongly depends on the regulatory mechanisms that are assumed to control the proliferation of individual cells. In the following section (7.2.1), these characteristics as well as the reliability of the model predictions are discussed.

7.2.1. Diffusion-limited Growth Model

The availability of nutrients represents the basis for microbial growth. This fundamental requirement was incorporated into a mathematical model which describes yeast colony development based on the exclusively nutrient-controlled proliferation of individual cells. The model was *scaled* for the growth of *C. boidinii* and *Y. lipolytica* on different nutrient resources (see also Section 7.3.1). All parameters are in the physiologically relevant range and the limiting nutrient is balanced for a defined reservoir. Simulations were carried out to elaborate patterns in colony development which are characteristic for a solely nutrient-controlled growth process.

Model Structure

In the presented DLG model, the replication interval (Δt_p) was defined to be independent from the local nutrient concentration. This definition was motivated by the observation of constant colony extension rates at nutrient concentrations that were changed over several orders of magnitude (see Figs. 5.1-5.4 and 5.7). As already discussed in Section 7.1.2, this behavior

may correspond to a constant extension rate which is inherent in filamentous cells. Alternatively, nutrient uptake by the cells and transport limitation due to slow diffusion of the nutrients may cause the food concentration at the colony boundary to drop to a value which is fairly constant throughout the cultivation period. Thus, the chosen definition of (Δt_p) represents an observation and does not explain its origin. However, the model correctly describes the consequences of such behavior by ensuring mass conservation.

An important discrepancy to published reaction-diffusion models is the definition of different nutrient-uptake kinetics. In a number of qualitative models nutrient uptake is assumed to be proportional to the square of local biomass concentration (Davidson, 1998; Davidson & Park, 1998; Davidson *et al.*, 1996a; Davidson *et al.*, 1996b; Davidson *et al.*, 1997), allowing for the complete uptake of nutrient even by a comparatively small cell number. In the present study, as well as in very recent quantitative models of fungal development (Boswell *et al.*, 2002; Boswell *et al.*, 2003), a correct linear relationship (Equ. 6.9) was chosen yielding a characteristically declining cell density as a result of simulations.

Furthermore, different budding regimes were incorporated into the model (see Growth Dynamics in Section 6.1). Distal budding was implemented by placing newborn cells originating from node (i) exclusively to the position (i+1), thereby giving the cells the tendency to grow faster away from the inoculation site. However, at the present stage of development, the model does not explain the potential origin of such behavior. Thus, as the distal budding scenario is defined, the growth towards higher nutrient concentrations, or the messenger-induced growth away from high cell densities (quorum-sensing) cannot be distinguished.

Model Parameterization

The model was scaled for the dimensions of the experimental setup. Furthermore, stoichiometric as well as kinetic parameters were either directly measured or derived from literature data (see Section 6.5). Thus, all biochemical parameters that describe the growth of the cells are in a realistic range. The parameters refer to measures commonly used in the quantitative description of biomass growth. Therefore, the quality of parameter estimations can be easily evaluated by their comparison to recognized data provided in the biochemical literature.

The correct parameterization of the diffusion process is crucial for the predictions of the model. From Equ. 6.29 the diffusion constant of small molecules in water can be corrected for the diffusion in an agar gel matrix. Interestingly, an agar concentration of 2 % (w/v) only causes a drop of approximately 5 % of the diffusion constant when compared to the free diffusion in water. This behavior was verified by a number of studies that investigated the diffusion of ions and carbohydrates in agar gel (see Nicholson (2001), Giannakopoulos & Guilbert (1986) and references therein). Beuling *et al.* (2000) estimated a diffusion constant of $D = 7.5 \cdot 10^{-10}$ $m^2 \cdot s^{-1}$ for glucose in 1.5 % (w/v) agar at a temperature of 30 °C. Correcting this value for temperature and agar content (Equs. 6.29 and 6.30) the obtained value is slightly higher but still in good agreement with the diffusion constant used in the simulations presented here. Since the gel-like matrix does not represent a strong resistance to the diffusion of nutrients when compared to free diffusion in water, the choice of diffusion

constants that are significantly smaller than those in water underestimates the speed of diffusion of nutrients and yields misleading results. As illustrated in Fig. 6.5, simulations only predict the generation of constant cell-density profiles when the diffusion constant (D) significantly falls below $1 \cdot 10^{-10}$ $m^2 \cdot s^{-1}$.

An important scaling effect was identified by variations of the tile with (w). While the predicted final cell-density profiles and the total accumulation of cells are insensitive to changes of this parameter, the final colony diameter varies markedly (Figs. 6.8 and 6.9). In simulations of the diffusion-limited growth of *Y. lipolytica* on glucose it was explicitly shown, that a 55 % higher colony diameter is calculated when compared to the predictions for a tile width of 30 µm. Thus, when the simulated final colony extension shall be compared to experimental results, simulations have to be carefully interpreted with respect to the parameter (w).

Characteristic Predictions

Contrary to qualitative models (Davidson *et al.*, 1996a; Davidson *et al.*, 1996b; Davidson *et al.*, 1997) but in agreement with a more recent quantitative approach (Boswell *et al.*, 2002), the presented simulations show the evolution of monotonically declining cell-density profiles. Furthermore, the predicted final colony diameter remains small when compared to the size of the growth field (Fig. 6.2). The budding pattern was shown to have a significant quantitative influence on the predictions of the model. When distal budding is assumed, the polarized growth of the cells away from the inoculation site results in a significantly higher rate of colony extension, a larger final diameter, and a somewhat shallower shape of the cell-density profile (Figs. 6.6 and 6.7). However, the general behavior of the model, i.e., the prediction of monotonically declining cell densities and comparatively small colony diameters, was found to be insensitive to parameter variations in the physiologically relevant range. Thus, these measures represent robust criteria to identify DLG as the major ruling mechanism in yeast colony development.

7.2.2.   Quorum-sensing Model

As described in Sections 5.3 and 3.1 of this study, messengers or metabolic by-products, respectively, have a strong influence on the morphology of individual cells, as well as on the development of preferential growth directions in the colonies. It therefore appears to be necessary to incorporate the effect of messenger-mediated cell-cell interactions into the mathematical description of yeast colony development.

In a first approach, the messenger is assumed to act directly on the proliferation of the cells, i.e., to stop cell growth at high concentrations. The model does not account for a particular compound which serves as a messenger. Thus, simulations only qualitatively describe the consequences of the QS assumption. However, due to the scaling of all the other growth processes, the model provides valuable information about the characteristics of a potential messenger and the expected colony development.

Simulations were carried out for different time constants of messenger decay (T_M). Under the assumption of volatile or unstable messengers, corresponding to short half life times of the messenger, they show the development of a constant cell-density profile (Fig. 6.10). Nutrient

concentration declines uniformly throughout the whole substrate and no considerable gradients are formed. Restrictive levels of messenger accumulate right behind the proliferating colony margin. This is the result of short residence times in the substrate, which cause the messenger to decay or to evaporate, rather than to diffuse. In the QS model, messenger emission and critical messenger concentration are not related to nutrient concentration. However, if e.g., an indirect proportionality between messenger emission and the concentration of limiting nutrient was assumed, the generation of declining cell density profiles is a trivial consequence (data not shown).

When half life time of the messenger significantly increases, the simulated colony development collapses at early stages of cultivation (data not shown). Since colony expansion is slow when compared to diffusion of nutrients in the agar, restrictive messenger concentrations accumulate in front of the proliferating colony margin and truncate growth. Thus, simulations clearly show that *if* the proliferation of cells is controlled by a messenger as suggested in Equ. 6.13, this messenger had to be *volatile* or *extremely unstable*.

7.2.3. Colony Development Comprising Nutrient Replenishment due to Cell Decay

During cultivations of *Y. lipolytica* on glucose, a growth mechanism was identified that ensures the stable expansion of colonies even in the absence of the primary nutrient resource. Food is replenished due to the continuous decay of cells in the colony interior thereby fueling proliferation of cells in the colony margin. To describe this behavior mathematically, the DLG model defined in Section 6.1 was extended by terms that account for the decay of stationary cells and nutrient replenishment (Equ. 6.23).

At the first glance, the incorporation of nutrient replenishment appears to be similar to an approach of Davidson *et al.* (1996b) and Davidson *et al.* (1997) (see also Appendix A). Here, the effect of different replenishment rates on the qualitative behavior of a diffusing activator front is investigated. However, the authors do neither discuss the origin of replenished nutrients, nor provide a balance for these compounds or for biomass, respectively (Davidson *et al.*, 1996b; Davidson *et al.*, 1997). The incorporation of nutrient replenishment in these models solely appears to serve to investigate the sensitivity of activator-wave progression to small and localized changes in nutrient concentration. In Boswell *et al.* (2002), the decay of inactive hyphae is considered in the initially discussed balance of hyphal elements. However, in their model the decay rate was set to zero since no decomposition of cells was observed during the comparatively short cultivation times applied in their experimental study. Furthermore, the replenishment of the nutrient reservoir due to the release of decay products was neither discussed nor explicitly modeled.

Model Structure

Experimental investigations of growth of *Y. lipolytica* indicate that the process of cell decay plays a crucial role in colony development. However, the exact nature of the cell decay is not known. As explicitly discussed in Section 7.1.2, the decrease in biomass density might be caused by i) an actual decay of individual cells, i.e., by the emission of cytoplasm into the agar substrate. Alternatively, it might be ii) the consequence of a translocation of cytoplasm *inside* the mycelium. In the present study, a model was developed which facilitates the

investigation of effects arising from the first hypothesis. Consequently, the model describes the decay of individual cells and the emission of the decay products into the agar.

The exact composition of the nutrient that is released upon cell decay is not known. In studies of carbon-limited growth of *S. cerevisiae*, a protein content of 45 % - 60 %, and a (storage)carbohydrate fraction of up to 40 % of the total cellular mass were detected (Nissen *et al.*, 1997). Therefore, it appears to be reasonable to assume that the secondary nutrient resource has a similar composition. However, neither the yield on this complex nutrient mixture, nor the diffusion rates of the individual compounds are known. Because of these uncertainties, the model does not distinguish between primary and secondary nutrient and both resources are pooled into a single reservoir (Equs. 6.23 and 6.24).

Similar to the simulations of DLG, the effect of different budding patterns on colony extension and cell-density development inside the mycelium was investigated. In addition, a random component was introduced into the mathematical description of the distal budding regime (Equs. 6.21 and 6.22). The introduction of these terms serves to average out artifacts, i.e., unusual high local fluctuations in cell density (data not shown), which arise in simulations that apply the deterministic distal budding regime of the DLG model (see Growth Dynamics in Section 6.1).

Characteristic Predictions

The simulations of exclusively nutrient-controlled proliferation and nutrient replenishment due to cell decay yield monotonically declining cell-density profiles and final colony diameters that are comparable to the DLG regime (Fig. 6.11, compare to Fig. 6.8). Consistently with the behavior found in simulations of DLG, higher final colony diameters and a somewhat shallower cell-density profile is predicted under the assumption of distal budding (see Appendix C). However, despite the continuous replenishment of the nutrient reservoir, colonies fail to extend at longer cultivation times. This behavior was shown to be insensitive to variations in the time constant for cell decay (T_C) (Fig. 6.12). In contrast to resting diffusion-limited colonies, proliferating cells are still present long after the colony stopped to enlarge (Fig. 6.11). Thus, the truncation of colony growth is the result of sustained proliferation of cells behind the colony margin. Nutrients released upon cell decay are utilized by replicating cells before they diffuse to the colony boundary to facilitate proliferation.

"Islands" of proliferating cells initially form when the concentration profiles of primary and secondary nutrient overlap at the colony margin. Since active cells are supplied from both sides, the proliferating boundary splits up into a subpopulation that utilizes the primary nutrient resource and a fraction that takes up the nutrient originating from cell decay. This *qualitative* behavior is insensitive to changes in the diffusion constant of the secondary nutrient: As a prerequisite for a continuous colony expansion, the front of secondary nutrient has to reach the proliferating margin before cells stop to proliferate in the absence of glucose. Thus, irrespective of differences in the diffusion constants, concentration profiles of primary and secondary nutrient will overlap at some point in the cultivation causing the characteristic split of the proliferating boundary.

From these conclusions the question arises, what cell-density profiles develop when growth is restricted to the colony boundary. Therefore, the simulation routine was changed setting all

cells to the stationary state when they are further than 1 mm behind the outer edge of the colony. Under this assumption, the model predicts sustained colony expansion and the formation of constant cell-density profiles at long cultivation times (Fig. 6.13). Since proliferating cells are only present in the colony margin (Fig 6.13 D), the secondary nutrient is not taken up inside the colony but diffuses outwards along a concentration gradient which spans from the colony center to the boundary (Fig. 6.14). These results are insensitive to small variations in the width of the proliferating zone (data not shown).

The restriction of proliferation to the colony margin clearly contradicts the objective of this study to describe the evolution of macroscopic patterns solely based on microscopic interaction rules. Here, the incorporation of a global information into the numerical routine influences the local behavior of cells. Therefore, the outlined simulations, clearly, do not explain why such a growth front can be expected to form. Nevertheless the simulations provide valuable information about the consequences of such a potential mechanism (see Section 7.3.3).

7.3.   Comparison of Experiments and Simulations

As described in Section 5, the development of yeast colonies strongly depends on the particular environmental conditions and on the applied yeast species. These observations appear to indicate, that colony growth under different cultivation conditions is controlled by distinct regulatory mechanisms. Based on the above described experiments, several hypotheses about the nature of these regulatory mechanisms were established. To test these hypotheses for their relevance in colony growth, mathematical models were developed that predict the influence of distinct fundamental assumptions on pattern formation. The models are scaled facilitating the quantitative comparison of the simulations with experimental results.

Considering the still small and incomplete basis of understanding of the colony growth process, as well as the considerable number of estimated parameters, this modeling philosophy does not aim to yield absolute agreement between experimental and simulated results. Simulations rather serve to elaborate morphological measures that are characteristic for a particular regulatory mechanism within the physiological parameter range. Accordingly, significant discrepancies of the simulations from experimental results can lead to a rejection of a fundamental assumption. In turn, the reproduction of the correct experimental trend by the simulations may serve as an indicator for the validity of a hypothesis.

7.3.1.   Diffusion-limited Growth in Yeast Colonies

In Section 6.1 a DLG model for the development of yeast colonies is described that predicts monotonically declining cell-density profiles and small colony diameters when compared to the size of the growth field (see Section 6.6.1 and the discussion in Section 7.2.1). This qualitative behavior was shown to be insensitive to variations of several parameters in the physiologically relevant range. Thus, comparisons of simulated cell-density profiles and final

colony diameters with experimentally derived data can serve to identify DLG as the ruling mechanism in colony development.

In Figs. 7.1-7.4, cell-density profiles estimated after 35 days of cultivation and the colony diameter extension of nitrogen-limited *Y. lipolytica* and *C. boidinii* colonies, as well as of carbon-limited *Y. lipolytica* colonies are compared to DLG simulations. Under all conditions, simulations and experimental results show large discrepancies. Even when the maximum final colony diameter is estimated by scaling the model to the width of the growth field (w = 1 cm), the predicted colony diameters by far underestimate the experimentally determined colony expansion. When casamino acids serve as the limiting nutrient source, the description of the diffusion process by a single diffusion constant appears to be questionable. However, in the simulations the smallest reported diffusion constant of an amino acid dimer was applied. Even then, the model predicts a final diameter considerably smaller than found in the experiments. Therefore, the hypothesis of DLG can be clearly rejected for the nitrogen-limited growth of both model yeasts on casamino acids and ammonium sulfate, as well as for the carbon-limited growth of *Y. lipolytica*.
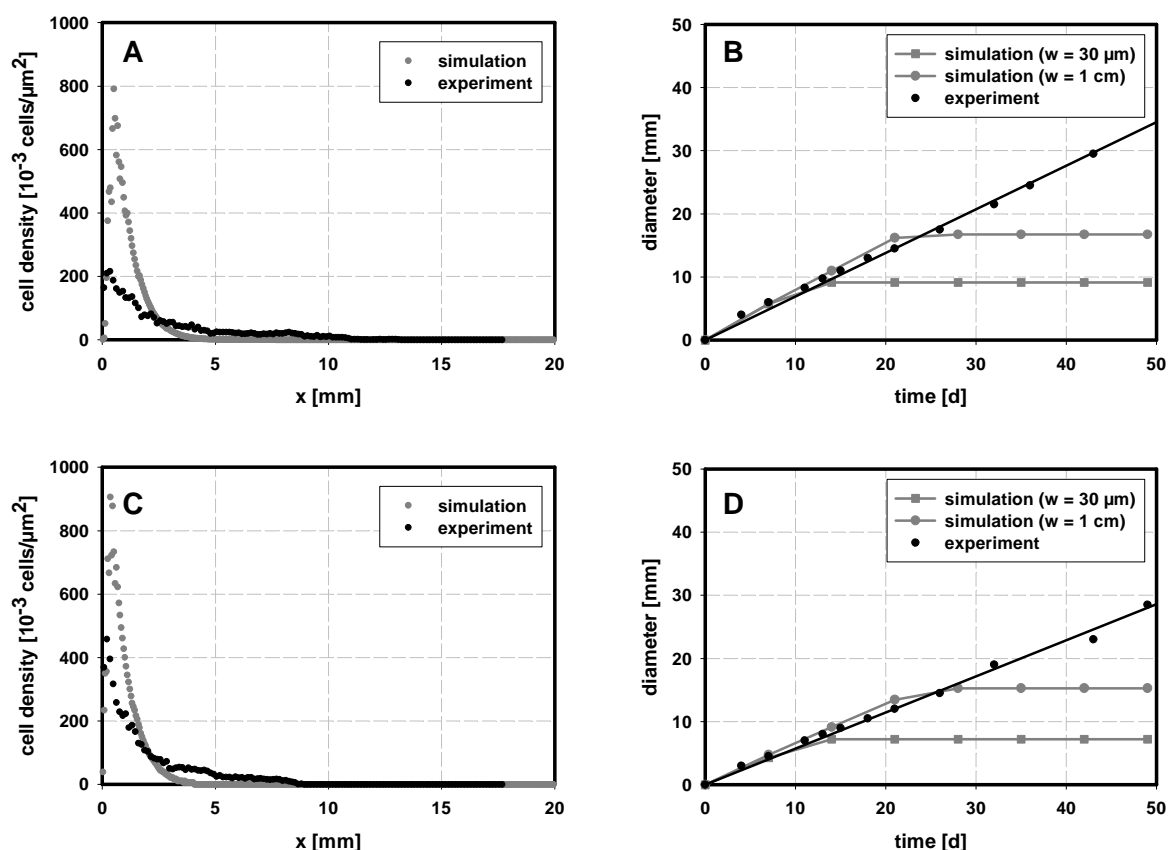
Figure 7.1: Comparison of experimentally determined and simulated (A, C) cell-density profiles after 35 days of cultivation, and (B, D) colony diameter extension of nitrogen-limited *Y. lipolytica* (A, B) and *C. boidinii* (C, D) colonies growing on ammonium sulfate as the sole nitrogen source. Experiments were carried out on N-A-0.05 medium. Simulations are based on the assumption of DLG and show the results for a distal budding regime (DW = 0.05). For further details of the parameterization see Section 6.5.
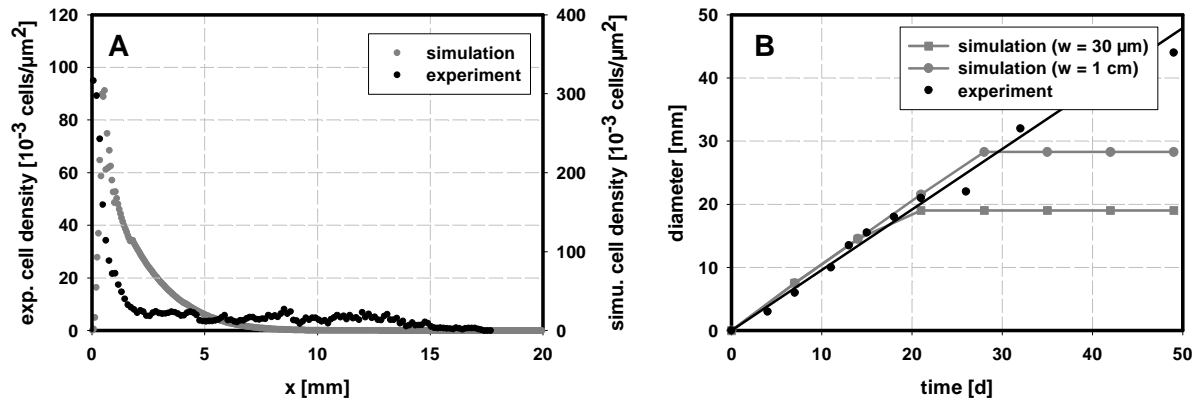
Figure 7.2: Comparison of experimentally determined and simulated (A) cell-density profiles after 35 days of cultivation, and (B) colony diameter extension of carbon-limited *Y. lipolytica* colonies growing on glucose as the sole carbon source. Experiments were carried out on C-G-2 medium. Simulations are based on the assumption of DLG and show the results for a distal budding regime (DW = 0.2). For further details of the parameterization see Section 6.5.
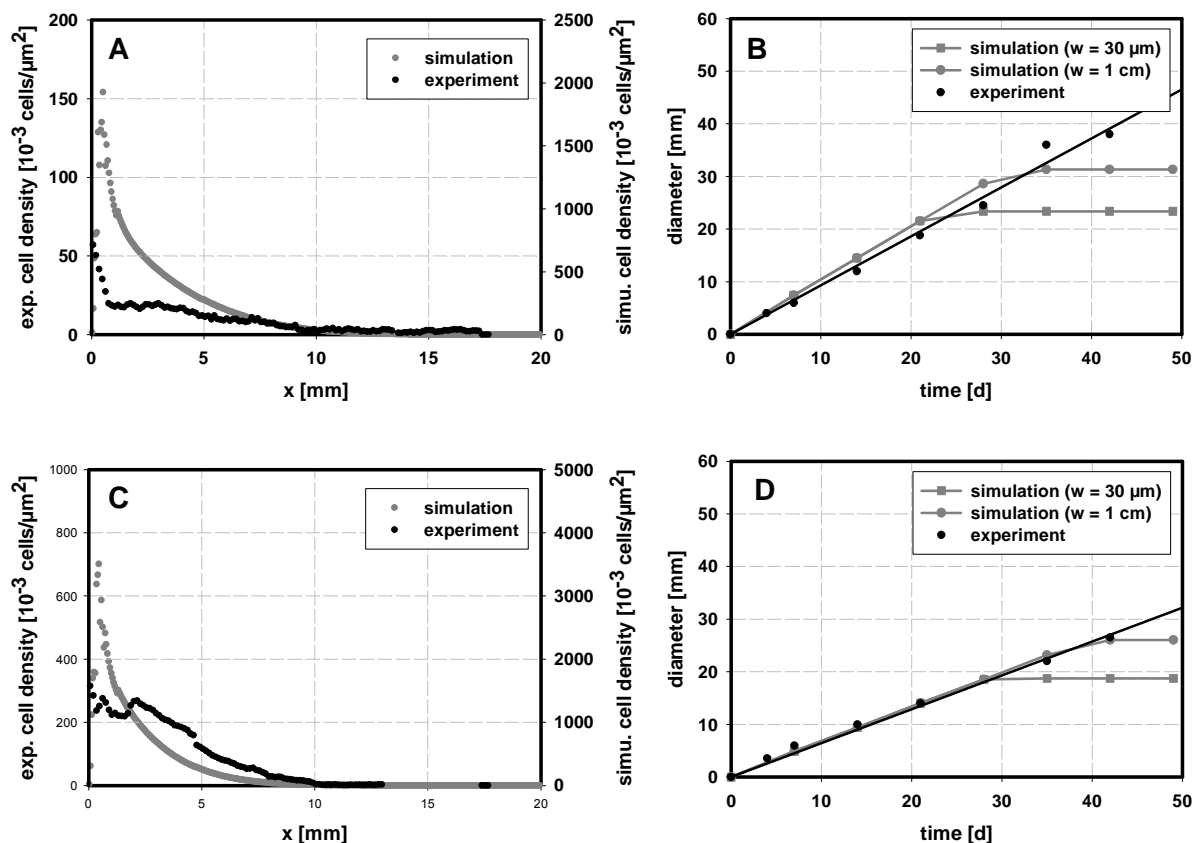
Figure 7.3: Comparison of experimentally determined and simulated (A, C) cell-density profiles after 35 days of cultivation, and (B, D) colony diameter extension of nitrogen-limited *Y. lipolytica* (A, B) and *C. boidinii* (C, D) colonies growing on casamino acids as the sole nitrogen source. Experiments were carried out on N-CA-2 medium. Simulations are based on the assumption of DLG and show the results for a distal budding regime (DW = 0.2). For further details of the parameterization see Section 6.5.
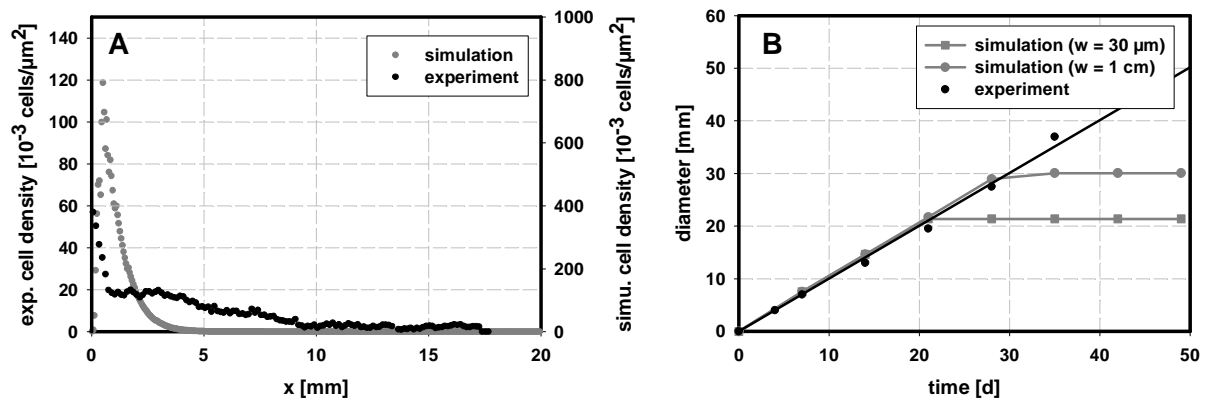
Figure 7.4: Comparison of experimentally determined and simulated (A) cell-density profiles after 35 days of cultivation, and (B) colony diameter extension of carbon-limited *Y. lipolytica* colonies growing on casamino acids as the sole carbon source. Experiments were carried out on C-CA-10 medium. Simulations are based on the assumption of DLG and show the results for a distal budding regime (DW = 0.2). For further details of the parameterization see Section 6.5.

Under all experimentally tested growth conditions, only the glucose-limited development of *C. boidinii* colonies exhibits DLG-like characteristics. In Fig. 7.5 experimental results are compared to simulations. Considering the strong abstraction of the growth process, the model predictions for the final cell-density profile, the total biomass (cell) accumulation and the final colony diameter are in excellent agreement with the experimental findings. In contrast to the experiments, the simulation predicts a pronounced cell-density peak close to the inoculation site (Fig. 7.5 A). This behavior arises from implementation of distal budding into the simulation routine. Contrary to the experiment, where cells are initially round exhibiting a random budding pattern, in the simulation newborn cells - from the beginning - are exclusively placed distal to the inoculation site. Since cells grow exponentially in the early stages of the cultivation, this small change causes a very steep ascent in cell density and a significantly higher peak than in the experimental profile.

The estimated glucose content of the growth field considerably differs from the simulations. In particular at early stages of the cultivation, a smaller glucose content is calculated than found in the experiments. The reasons for these deviations are not clear and possibly require a further refinement of the glucose assay rather than changes in the simulation routine.

However, measurements show that the stop of colony expansion coincides with the depletion of glucose from the growth substrate (see Section 5.2). Furthermore, the DLG model is able to reproduce the spatio-temporal development of several morphological characteristics *quantitatively*. Combining these findings, DLG can be identified as the ruling construction principle in glucose-limited *C. boidinii* colonies.
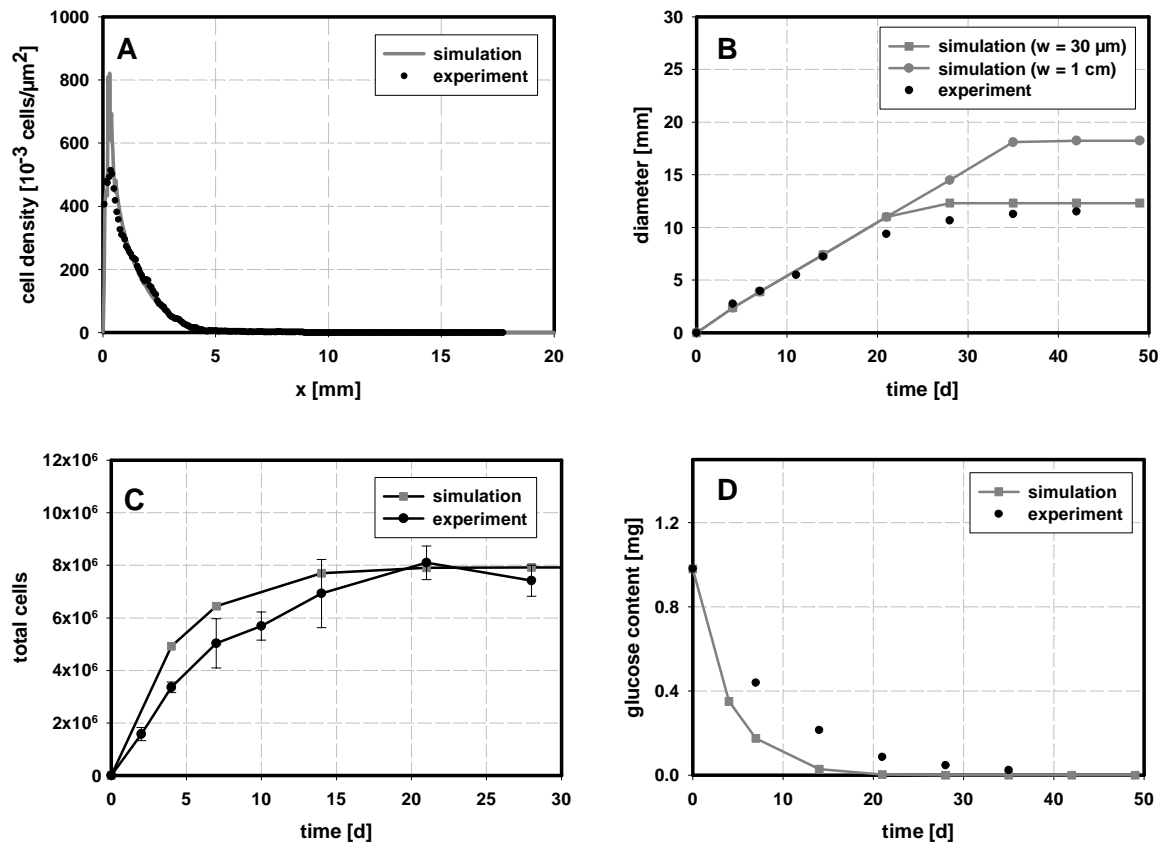
Figure 7.5: Comparison of characteristic morphological parameters of glucose-limited *C. boidinii* colonies with simulated results based on the assumption of DLG (distal budding, DW 0.2). (A) cell-density profile after 35 days of cultivation. (B) Colony diameter vs. time. (C) Total cell number vs. time. (D) Glucose content of the growth field vs. time.

As discussed in Section 7.2.1, the extension rate of the colony diameter is influenced by the budding pattern of individual cells. For the distal budding regime, a faster colony extension and a higher final colony diameter are predicted (Fig. 6.7). Hence, if the replication time (Δt_P) of the cells is known (e.g., through the observation of individual cells by time lapse photography), a comparison of simulated extension rates with experimental measurements could provide indication about the presence of mechanisms that induce polarized growth of the cells. Using this method, Cohen *et al.* (1996) demonstrated in an analysis of bacterial population development that colony-extension rates observed in experiments cannot be reached assuming a solely random movement of bacterial cells. Thus, they concluded a chemotactic mechanism has to be present which gives bacterial movement a bias towards higher nutrient concentrations or away from high cell densities, respectively. In the present study, the replication interval (Δt_P) of the cells was estimated from the extension rate of the colony diameter and the average length of the pseudohyphae (Equ. 5.1). Direct measurements of the generation time using time lapse photography were not carried out. Since in the experiments the orientation of individual pseudohyphae only little deviates from the longitudual axis of the colony, the estimations of (Δt_P) are only slightly biased towards smaller values. On the other hand, this approximation implicitly incorporates the assumption of distal budding into the model. Thus, the agreement between colony extension rates

simulated under the postulation of distal budding and experimentally observed colony extension rates (Figs. 7.1 – 7.5) is a consequence of the parameterization of the model. In contrast to studies of Cohen *et al.* (1996) on bacterial colony development, predictions of the model for different budding regimes cannot be used as an indicator for the presence of chemotactic signals. On the background of a large number of uncertainties and open questions, this loss of information appears to be acceptable for the benefit of a convenient approximation of replication intervals.

7.3.2. Quorum Sensing in Yeast Colonies

In the present study, the ability of yeast colonies to adopt their cell density to nutrient availability in the environment is investigated. Upon nutrient-controlled growth this adaptation is facilitated passively. Due to the diffusive limitation, colonies with different densities are formed at changing nutrient concentrations in the environment (see Fig. 6.4). Alternatively, the regulation of colony density may be facilitated by an active mechanism which is mediated by a messenger (metabolic by-product). This phenomenon is commonly referred to as quorum sensing. However, in the case of yeast colony development different aspects of QS have to be distinguished. In particular, the *hypothetic* messenger-controlled proliferation of individual cells (see Section 6.2), as well as the differentiation of cells into distinct morphotypes, and the directed growth of cells away from high population densities represent QS phenomena that are referred to differently.

As extensively discussed, the differentiation of yeast cells, i.e., the transition from the yeast-like morphology to the pseudohyphal growth form, is *also* controlled by QS. In addition to nutrient limitation, pseudohyphal cells are induced by the presence of metabolic by-products or messengers. Because of their phenotypic characteristics, pseudohyphal cells enable a directed and accelerated extension of the colony. Thereby, the accumulation of high cell densities is prevented or at least alleviated. These QS effects were not explicitly modeled. The differentiation of cells was neglected and colony development was described based on the growth of one cell type, namely the pseudohyphal morphotype. The potentially growth-directing effect of messengers was implemented by the distinct placement of newborn cells (see Growth Dynamics in Section 6.1). Here, the emission, the transport, and the action of the messenger was not incorporated into the model.

In the QS model developed in Section 6.2, colony development is described on the fundament of messenger-controlled proliferation of individual cells. According to this model, cells emit a messenger and stop to proliferate once the local amount of messenger surpasses a threshold concentration. In a number of simulations it was elaborated, that this messenger has to be volatile or extremely unstable to ensure a stable colony extension (see Sections 6.6.2 and 7.2.2). Investigations of the effect of volatile metabolic by-products on colony morphology showed that in particular under carbon-limited conditions compounds are emitted which strongly decrease the cell density in exposed colonies (Section 5.4.1). However, in comparison to the environmental conditions present during the development of single colonies (Section 5.2), rather extreme cultivation conditions were applied: The growth fields and the nutrient concentrations for the test colonies were very small. Furthermore,

colonies were exposed to comparatively high amounts of volatile compounds. Thus, if QS in yeast colonies was based on volatile compounds and the threshold mechanism described by Equ. 6.13, under these extreme cultivation conditions a truncated or at least impaired colony extension, respectively, of exposed colonies had to be observed. However, both effects could not be detected. Furthermore, during the experimental investigation of colony development no growth pattern was identified that meets the characteristics elaborated for the messenger-controlled colony growth (compare to Section 6.6.2). Therefore it is concluded, that in yeast colonies no mechanism is present which controls proliferation based on the above described threshold mechanism. The presence of a more subtle QS mechanism, e.g., which inhibits the formation of a particular cell type, or prevents the formation of secondary buds (i.e., which acts on branching frequency rather than on proliferation in general) shall not be precluded by the outlined investigations.

7.3.3. Nutrient Replenishment and Cell Decay in Yeast Colonies

When *Y. lipolytica* is cultivated under carbon limitation, or when casamino acids serve as the only nitrogen source, the continuous colony extension coincides with a strong cell decay in the colony interior. Since for the DLG on these nutrients a comparably small colony diameter is predicted by the simulations (Section 7.1.3), the hypothesis can be derived that colonies extend in the absence of the primary nutrient source utilizing decay products of cells that were formed in the beginning of the cultivation. In case of glucose-limited growth of *Y. lipolytica* colonies, this hypothesis was experimentally verified. The estimation of the glucose content in the growth field showed that colonies continue to extend even when glucose is completely depleted from the medium (compare Figs. 5.7 and 5.11). Since an impaired colony extension was observed upon the removal of the colony interior, the utilization of cell material as the alternative carbon source was confirmed (Fig. 5.12). On the other hand, the mechanism of the cell decay is still under question (see Section 7.1.1). Whether the decrease of local biomass concentration is caused by an emission of cytoplasm into the growth substrate, or results from the translocation of cytoplasm inside the mycelium cannot be conclusively answered based on the presented experiments.

Decreasing Biomass Densities as a Consequence of the Autonomous Decay of Individual Cells

In a first approach the assumption of an autonomous decay of individual cells was transferred into a mathematical model. The model describes I) nutrient-controlled growth of individual cells and incorporates II) cell decay, III) nutrient replenishment, and IV) diffusion of the secondary nutrient through the agar substrate *in addition* to V) the above described DLG model. Basic characteristics of the model are discussed in Section 7.2.3.

In the present section, simulations are adopted to the colony development of *Y. lipolytica* on glucose as the limiting carbon source. The model is parameterized according to Section 6.5. As the only difference to the simulations shown in Section 6.6.3, a second time constant for cell decay (T_C) is introduced to account for the significantly different decay rates at the inoculation site when compared to other parts of the mycelium (Tab. 5.2). These differences

may arise from the presence of different cell types in the colonies. In the colony center, round yeast-like cells are formed in the beginning of the cultivations while the filamentous parts of the colonies mainly consist of pseudohyphal cells. Alternatively, cells born in the beginning of the cultivation may have accumulated more storage carbohydrates since initially they grow in the presence of excess glucose. Consequently they may survive longer on stored nutrients. Whatever the reason, the observation was incorporated into the model assuming that cells within a radius of 1.5 mm around the inoculation site decay with time constant T_{C1} = 615 h, whereas all other cells decay with T_{C2} = 342 h, a value representing the average of time constants at distances of 2-6 mm from the colony center (Tab. 5.2).

In Fig. 7.6 the simulated and experimentally monitored development of glucose-limited *Y. lipolytica* colonies are compared. Predicted and measured cell-density profiles after one week of cultivation are in excellent agreement (Fig. 7.6 A). However, neither the colony-density profile after 35 days (Fig. 7.6 B) nor the sustained colony extension at longer cultivation times can be reproduced by the model (Fig. 7.6 C). In the simulations, colonies stop to extend at comparatively small diameters because proliferating cells are distributed across the colony and take up secondary nutrient before it can reach the colony boundary (see Sections 6.5.3 and 7.2.3).
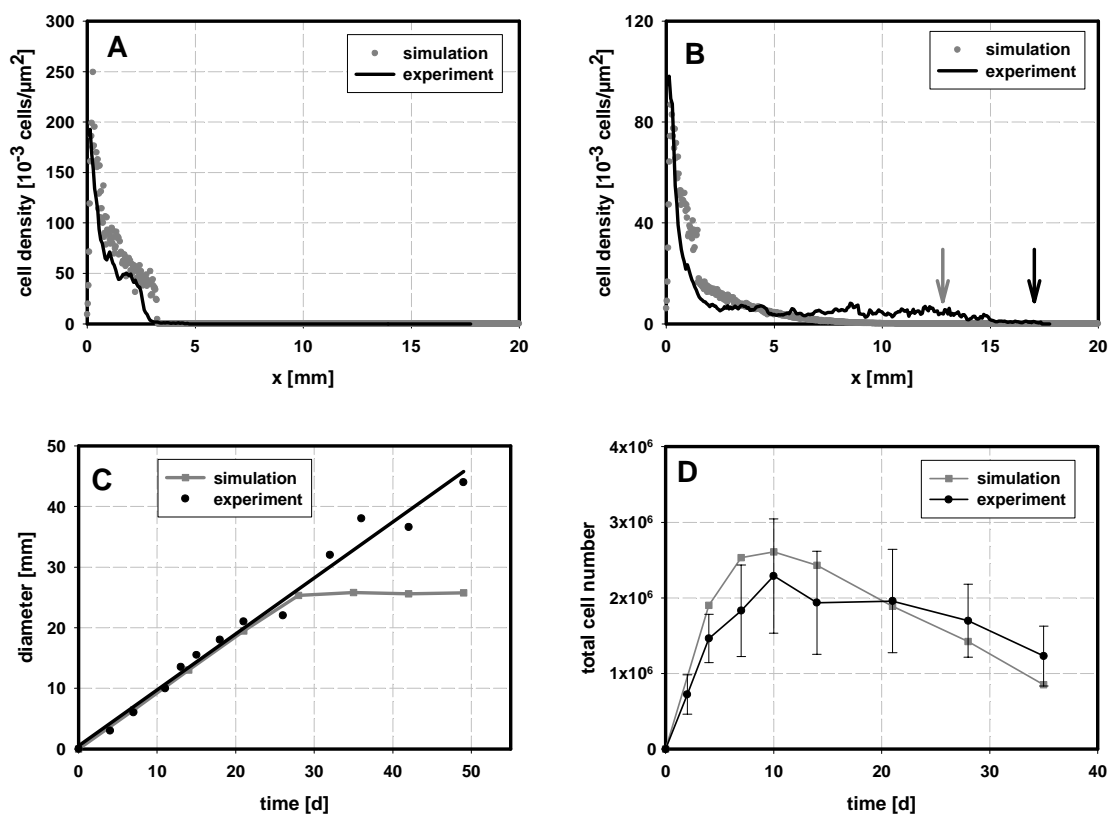
Figure 7.6: Comparison of simulated and experimentally derived morphological characteristics for the glucose-limited growth of *Y. lipolytica* colonies. Cell-density profiles after (A) 7 days (B) 35 days. (C) Colony diameter vs. time. (D) Total cell number vs. time. Colonies were cultivated on C-G-2 medium. (DW = 0.27, distal budding, w = 1 cm). For further details of the parameterization see Section 6.5. Figures show the average of 5 replicate runs.

Since the significant lack-of-fit is insensitive to parameter variations (Section 7.2.3), results indicate the presence of additional regulatory mechanisms or a wrong set of model assumptions, respectively. In any case, colony development of *Y. lipolytica* on glucose is *not* adequately explained by the processes (I – V) described above – a result which could be only elaborated on the basis of mathematical simulations.

Although the model cannot reproduce sustained colony extension, the course of total biomass accumulation is in good agreement with the experiment (Fig. 7.4 D). Thus, differences between measurements and simulations are very unlikely to originate from inaccurate nutrient or biomass balances. Colony expansion is rather truncated due to the distribution of proliferating cells over the whole colony. From this observation the question can be derived, whether the restriction of proliferation to the colony boundary is sufficient to yield agreement between simulated and estimated data. Accordingly, the simulation routine was changed by assigning all cells to the stationary state when they are further than 1 mm behind the colony margin. (Results of the simulations are not sensitive to small changes in the width of this margin. Data not shown.) In Fig. 7.7 results obtained with the modified simulation routine are compared to experimental data.
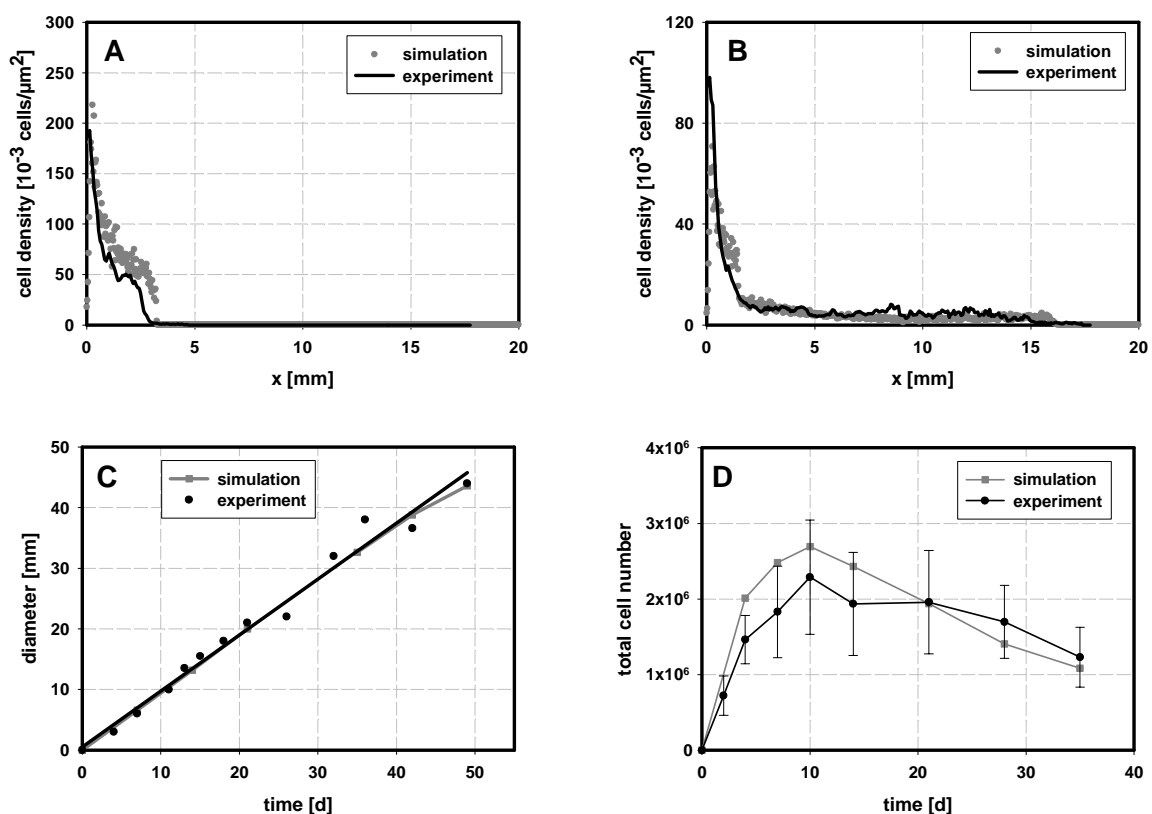
Figure 7.7: Comparison of simulated and experimentally derived morphological characteristics for the glucose-limited growth of *Y. lipolytica* colonies. In the simulations, proliferation was restricted to a 1 mm wide zone at the colony boundary. Cell-density profiles after (A) 7 days (B) 35 days. (C) Colony diameter vs. time. (D) Total cell number vs. time. Colonies were cultivated on C-G-2 medium. (DW = 0.27, distal budding, w = 1 cm). For further details of the parameterization see Section 6.5. Figures show the average of 5 replicate runs.

The model quantitatively reproduces the characteristic behavior of glucose-limited *Y. lipolytica* colonies which comprises rapid accumulation of cells at the inoculation site (Fig. 7.7 A), the formation of large areas with constant cell density in the course of the cultivation (Fig. 7.7 B), sustained colony extension (Fig. 7.7 C), and biomass accumulation that peaks after 10 days of colony development (Fig 7.7 D). Please note that the good fit of experimental results to simulated data for a DW of 0.27 also supports the plausibility of biomass estimations by the OD measurements (see Sections 5.3 and 7.1.1).

Due to the described change in the simulation routine, a global information was implemented into the cellular automaton model. As explicitly discussed in Section 7.2.3, this manipulation clearly contradicts the fundamental idea of cellular automaton models. It does neither prove the presence of such mechanism nor provides information about biological interactions that potentially repress proliferation inside the colony. However, despite this very crude - and certainly questionable - approach, simulations show that the presence of a mechanism which represses proliferation inside the colony is sufficient to mimic the dynamic development of the colonies quantitatively. Furthermore, in the model the transition to stationary phase was defined to be irreversible (Equ. 6.20). This, however, stands in contrast to experimental studies that report the reentry of resting cells into the cell cycle in the presence of elevated carbon-source concentrations (Granot & Snyder, 1993). Since in the colony interior comparatively high concentrations of secondary nutrient accumulate when proliferation is restricted to the colony boundary (Fig. 6.14), this mechanism also ensures that stationary cells do not start to proliferate as a consequence of increasing nutrient availability. Thus, when yeast populations extend utilizing decay products released upon decay of autonomous cells in their interior, a mechanism is necessary that drastically slows down or completely restricts proliferation behind the growing colony margin.

Decreasing Biomass Densities as a Consequence of the Translocation of Cytoplasm inside the Mycelium

The stable colony extension of carbon-limited *Y. lipolytica* colonies is hard to explain on the basis of an autonomous decay of individual cells. Only when a regulatory mechanism (i.e., the restriction of proliferation to the colony boundary) is postulated which is lacking any experimental evidence so far, simulations can reproduce the experimentally determined growth pattern. Not only because of these obvious discrepancies, the hypothesis of internal translocation of cytoplasm should be favored. Another important indicator for the internal transport hypothesis is the morphology of vacuolated cell walls that is strikingly similar to tube-like *hyphal* structures. Furthermore, it does not appear plausible that an essential nutrient (cytoplasm) is emitted into the agar, although this resource is already held by the fungus: The diffusive translocation of this secondary nutrient resource via the external growth substrate bears a number of risks and cannot be controlled by the yeast. Other microorganisms in the habitat may compete for the released nutrients. Furthermore, in their natural environment yeasts settle on a large variety of growth substrates with changing diffusive properties. Thus, a stable and reproducible transport of nutrients across comparatively long distances in the environment appears to be impossible. It is, therefore, hard to believe that such a mechanism would succeed in evolution.

The description of the colony development of *Y. lipolytica* on the basis of internal translocation of cytoplasm requires a number of significant changes in the model structure. In the following section a hypothetic mechanism shall be discussed which already provides a sketch of the new model:

Clearly, when cytoplasm can be translocated inside the microorganism, the colony has to be viewed as a fungal mycelium which is built up of hyphae. The extension of a hyphal element is restricted to its tip. According to the nomenclature used by (Nielsen, 1993), the hyphal compartment which is located closest to these growing tips is called the *apical compartment*. This compartment may comprise several cells and synthesizes building blocks for the extension of the cell wall. The part of the mycelium which is filled with cytoplasm but which is not directly involved in branching or tip extension is called the *subapical compartment*. Finally, the *hyphal compartment* comprises hyphal sections that are vacuolized and metabolically inactive.

In own experimental studies, the extension rate of the hyphae was found to be constant and independent from the nutrient concentration in the environment (see Section 5.1). This behavior is consistent with observations reported for experimental characterizations of hyphal growth in liquid culture, i.e., in homogeneous systems. In these studies the extension rate of fungal hyphae was found to be widely independent from the nutrient concentration in the medium (Spohr *et al.*, 1998). Such a behavior can be explained by assuming that the internal nutrient resource, i.e., cytoplasm, is utilized compensating the lack of external nutrients. Considering that the survival of a fungal colony is guaranteed when the outermost apical cell reaches the next localized nutrient patch, it appears reasonable that the cytoplasm of subapical hyphal cells is utilized to fuel the propagation of the mycelium. In this approach, the extension rate of the hyphae is not determined by nutrient supply but represents an inherent *constant* that generates a *demand* for nutrients. This demand is satisfied using the available nutrient resources (cytoplasm, external nutrient), whereby the external nutrient is preferentially utilized. Please note that the suggested mechanism stands in contrast to the nutrient-controlled extension rate of the hyphae postulated by Boswell *et al.* (2002 and 2003). Furthermore, it is suggested that apical cells utilize the cytoplasm of the subapical compartment which is closest to the tips. I.e., the cytoplasm is degraded near the tips, whereas vacuoles are formed at the opposite side of the subapical compartment. By the proposed mechanism, the translocation of intracellular nutrient resources (released upon the degradation of cytoplasm) across long distances can be prevented. Vacuole formation is commonly believed to create an intracellular pressure to facilitate the transport of cytoplasm towards the propagating tip region (Nielsen, 1993). The translocation of cytoplasm has to be regarded as a convective rather than a diffusive flux, respectively.

As shown by the experimental and mathematical investigation of the colony development of *Y. lipolytica*, the nutrients released upon the degradation of cytoplasm are essential for the extension of the fungal mycelium (Section 5.2.1). Since in the Boswell model (Boswell *et al.*, 2002) for fungal growth the cytoplasm present in hyphal cells prior to vacuolization does not contribute to the nutrient balance, an important factor in colony development is neglected. Furthermore, this observation also points to the need for drastic changes in the description of fungal growth in submers cultivations. In structured models for the growth of fungi in liquid

culture, the vacuolization of hyphae is described as a nutrient-dependent phenomenon. I.e., at low external nutrient concentration hyphae are assumed to vacuolize at a higher rate (Nielsen, 1993; Paul & Thomas, 1996). Interestingly, most authors do not comment on the reason for the observed behavior. Only Paul & Thomas, (1996) cite the hypothesis formulated earlier by Righelato *et al.* (1968), that cytoplasm is used to support growth in the apical cells. However, the design of their model does not account for this growth-supporting effect (Paul & Thomas, 1996). The here presented theoretical approach provides a mechanistic explanation for the observed behavior. In this scenario, the vacuolization of hyphae is the logical consequence of the utilization of cytoplasm to compensate the lack of external nutrients.

In the DLG model, the proliferation of the yeast cells is assumed to be controlled by nutrient supply. Accordingly, yeast enter the stationary state when local nutrient concentration drops to zero (Equ. 6.4). Since in the here discussed model, apical yeast cells are always supplied by nutrients, i.e., external or internal resources, the entry into the stationary phase cannot be explained based on the complete depletion of the local nutrient resources. Therefore, the branching frequency, in particular the formation of secondary branches, is suggested to be a function of the external nutrient concentration (see also Paul & Thomas (1996)). However, since the fungal mycelium extends even in the absence of external nutrients, the branching frequency is likely to be controlled by at least one additional factor. In a number of experiments, the medium pH was shown to strongly influence the local accumulation of cells (see Sections 5.4.2 and 7.1.3). When glucose-limited yeast colonies are cultivated at identical nutrient concentrations, a decreasing initial pH results in the accumulation of higher local cell densities (e.g. Fig. 5.27). With increasing initial pH, the local cell densities gradually decline. Thus, branching frequency is likely to be *also* controlled by the local pH. Yeasts alkalinize their growth substrate when they utilize nitrogen-containing carbon sources such as amino acids or proteins (Table 5.5, (Palkova *et al.*, 1997; Zikanova *et al.*, 2002)). Thus, the increasing pH in the medium may signal the fungus the enhanced utilization of its own cytoplasm and the depletion of energy-rich carbon sources in its environment (Palkova *et al.*, 1997; Zikanova *et al.*, 2002). Accordingly, a decreasing branching frequency induced by an elevated pH may serve to explore the environment at an economical expense of internal nutrients. Indeed, the increase of pH in glucose-limited *Y. lipolytica* colonies was observed at later stages of the cultivation (Fig. 5.29).

Clearly, the suggested mechanism is speculative and requires a number of experimental and mathematical investigations to support the outlined assumptions. However, it combines several phenomena observed in the present study, and opens a way to extend the mechanisms identified in yeast colony development to the growth of higher fungi.

8. SUMMARY

In the present study, the dimorphic yeasts *Candida boidinii* and *Yarrowia lipolytica* were applied as model organisms to study regulatory mechanisms in the colony development of simple fungi. The macroscopic colony patterns formed by the yeasts exhibit strong similarities to mycelia formed by higher fungi. However, under most cultivation conditions mycelial yeast colonies are built up of individual pseudohyphal cells. Thus, nutrient translocation inside the mycelium can be neglected which significantly simplifies the experimental characterization and mathematical description of the colony development.

The yeasts were cultivated on solid agar substrates under the limitation of different carbon (glucose, casamino acids) and nitrogen sources (ammonium sulfate, casamino acids). It was shown that both yeasts form filamentous colony patterns in response to the limitation of all tested nutrient sources. The transition from compact colony morphologies to filamentous patterns is the prerequisite for an effective nutrient search at a minimum expense of nutrients and biomass. In the case of *Y. lipolytica* colonies, the change in colony morphology coincides with an increase of the colony-diameter-extension rate. This behavior corresponds to a change from an exploitive to an explorative growth mode.

To study the spatio-temporal development of yeast colonies a new method for the estimation of biomass distributions was developed. The method is based on the spatially-resolved determination of the colony OD by transmitted light microscopy. Applying this technique it is possible to *non-invasively* and *quantitatively* monitor the development of cell-density profiles, and the total accumulation of biomass inside carbon-limited yeast colonies. Under nitrogen limitation the yeasts *Y. lipolytica* and *C. boidinii* strongly incorporate storage carbohydrates which hampers the quantification of cells by OD measurements, i.e., the method does not allow for the distinction between the accumulation of cells or storage carbohydrates, respectively. Furthermore, an experimental setup was chosen which enforces a one-dimensional colony growth as the prerequisite for the comparison of experimental data with simulations derived from the one-dimensional models developed in this study.

The spatio-temporal development of mycelial colonies was characterized using several morphological measures, such as the growth rate of the diameter, the development of the cell-density profile, and the total accumulation of cells. Yeast *mycelia* adapt to declining nutrient concentrations by a decrease of their cell density, whereas the extension rate of the colonies remains constant. Strong qualitative differences in the growth behavior between the yeasts were observed. Carbon-limited colonies of *C. boidinii* growing on glucose stop to extend at a small colony diameter when compared to the dimensions of the growth field. The cell-density profile declines monotonically from the inoculation site to the edge of the colony. The cell density behind the propagating colony margin remains constant once established. Since the stop of colony extension coincides with the depletion of the limiting carbon source glucose, it is concluded that colony development of *C. boidinii* under these conditions is controlled by the availability of the primary nutrient resource.

In contrast to this behavior, carbon-limited *Y. lipolytica* colonies finally cover the whole growth field. In the course of the cultivation, the cell density in the inner colony regions declines and the total biomass accumulated in the mycelium declines continuously after it

reaches a maximum after approximately 10 days of incubation. As explicitly shown for glucose limitation, colonies proceed to extend in the absence of the primary nutrient resource. Since an impaired colony growth and the formation of mycelia with smaller cell densities was observed upon the removal of inner parts of the colony, it is concluded that *Y. lipolytica* colonies utilize their own cellular material to fuel the extension of the population. Although it was not experimentally verified whether the decrease in biomass density behind the progressing colony margin is caused by an autonomous decay of individual cells, or by the translocation and degradation of cytoplasm inside the mycelium, the latter hypothesis is clearly favored by the author. In any case, the necessity to incorporate cell decay and nutrient replenishment processes into the biomass and nutrient balances for the description of fungal growth in heterogeneous systems was clearly shown.

The development of nitrogen-limited colonies of the model yeasts was only monitored qualitatively. When ammonium sulfate serves as the limiting nitrogen source, the growth field was covered by both yeasts at the end of the cultivation. Throughout the observed time span of 35 days, no drop of the biomass density was evident in the inner colony areas. The nitrogen-limited growth of *C. boidinii* on casamino acids as the sole nitrogen source also exhibits these characteristics. In contrast, under these conditions *Y. lipolytica* colonies show a growth pattern that is similar to the behavior of the yeast under carbon limitation. It was speculated that these differences arise from the different degree of nitrogen limitation when ammonium sulfate or casamino acids served as the limiting nutrient resources.

In addition to the influence of the nutrient concentration, the effect of environmental factors on colony development was investigated. Motivated by literature data, the qualitative influence of volatile compounds (metabolic by-products, messengers), emitted by the yeasts under nutrient limitation, on the morphology of exposed colonies was tested. In particular, under carbon-limiting conditions a strong decrease of the cell density was observed in exposed populations. The drop in cell density is mainly caused by the suppression of the yeast-like cell type. Furthermore, the sensitivity of the colonies to the volatile compounds appears to depend on both, the amount of volatile compounds and the nutrient concentration in the growth field. These results indicate that volatile compounds may play an important role as long-range starvation or quorum-sensing signals, respectively. It is suggested that these compounds coordinate colony development by signaling remote parts of the population an incoming nutrient limitation before it actually takes effect. As a response, differentiation to pseudohyphal cells can be induced in these colony areas facilitating the directed growth away from regions of high cells densities and/or from regions where nutrients are deprived.

The experimental conditions applied in the bioassay were chosen very stringent to amplify the response of exposed colonies to the volatile compounds. This was the prerequisite for a convenient illustration of the volatile-induced effects by the mere comparison of photographs of exposed colonies and undisturbed populations. However, due to the application of extreme cultivation conditions no conclusions can be drawn about the actual influence that volatile compounds exert in the development of a single colony, e.g., under the conditions imposed in Sections 5.1 and 5.2. Before the role of volatile compounds in a colony can be exactly described, these substances have to be identified, and their concentration as well as the sensitivity of the yeast cells to the presence of these compounds has to be determined

under different cultivation conditions. Both requirements are not fulfilled by this study but should be subject to further investigations.

Furthermore, the influence of the medium pH on colony development was investigated. Carbon-limited *Y. lipolytica* and *C. boidinii* colonies were cultivated at identical initial nutrient concentrations but under variations of the initial pH of the growth substrate. Under all cultivation conditions a strong effect of the pH was determined. When the yeasts are cultivated on glucose as the sole carbon source, the cell density of the mycelia declines gradually with increasing pH. While *Y. lipolytica* colonies extend faster at high pH, the extension rate of *C. boidinii* colonies declines. When *Y. lipolytica* utilizes casamino acids as the only carbon source, colony growth collapses after few days of cultivation when the initial pH of the growth substrate is equal or higher than 7. Furthermore, the time course of the average pH in the medium was monitored. During glucose-limited growth, both yeasts initially acidify the medium. In the further course of the cultivation, the pH in the growth substrates of *Y. lipolytica* colonies increases slightly. Since alkalization of the medium is only observed when yeasts utilize nitrogen-containing carbon sources (such as cytoplasm), this finding is consistent with the observation of cannibalizing growth of *Y. lipolytica* colonies under limitation of the external nutrient resource. The stop of colony extension observed in *Y. lipolytica* colonies growing on casamino acids at a high initial pH is most-likely caused by the surpass of a threshold pH which is restrictive for growth. This threshold pH was estimated in parallel experiments and is strikingly similar to the pH reached when colony extension collapsed. By the outlined experiments it was elaborated that the pH in the growth medium plays a crucial role in the regulation of cell density within yeast colonies. In addition, observed differences between pH values reached in submers and emers cultivations point to the possibility that pH is actively controlled during colony development. Because of its crucial importance in yeast colony development, the role of pH should be carefully investigated in further studies. In particular, a refined spatial resolution and an improved accuracy of the pH measurements are likely to provide further insight into adaptation mechanisms that are induced or mediated by this factor.

In the second part of the study, cellular automaton models for the growth of yeast colonies were developed to investigate the influence of potential regulatory mechanisms on the predicted colony patterns. In these models colony development is described on the basis of the proliferation of discrete cells and continuous concentrations of nutrients and messengers. The presence of different cell types, i.e., round yeast-like cells and pseudohyphal cells, is neglected. The dimensions of the unit cells are assigned to the average size of the elongated pseudohyphal cell type. The models are scaled for space and time, and all physical and biochemical parameters are in the physiologically relevant range. Therefore, simulations can be quantitatively compared to experimental results.

As the fundament for the mathematical description of yeast colony development, a DLG model was developed which incorporates the nutrient-controlled growth of cells, the transition of cells from an initially proliferating state to the stationary state upon nutrient deficiency, as well as the uptake and the diffusion of the nutrient. When an exclusively nutrient-controlled proliferation of the cells is assumed, simulations show that the nutrient which diffuses towards the colony is taken up by proliferating cells in the colony boundary. The cells in the

colony interior pass to the stationary state as a consequence of nutrient limitation. When the DLG model is parameterized for the growth of the yeasts on agar substrates, for all applied nutrient resources a monotonically declining cell-density profile and a small final colony diameter is predicted. This qualitative behavior is insensitive to parameter variations in the physiologically relevant range. Thus, these characteristics can serve as robust criteria to identify DLG mechanisms in yeast colony development. In case of the carbon-limited growth of *C. boidinii* on glucose, simulations are in excellent agreement with experimental results. Thus, under these conditions DLG is the ruling construction principle in *C. boidinii* colonies. For all other combinations of yeast species and cultivation conditions, large discrepancies between experimental results and DLG simulations are evident. Therefore, the DLG mechanism is rejected under these conditions.

In a further modeling approach, the hypothesis of messenger-controlled growth was tested for its influence on the predicted growth patterns. It was postulated, that all cells emit a messenger which is restrictive to growth once its concentration surpasses a certain threshold. When the messenger is assumed to be a stable compound, restrictive messenger concentrations accumulate in front of the colony margin causing the truncation of proliferation. Thus, simulations show that only an extremely unstable or volatile messenger can ensure a continuous colony extension. When this messenger is emitted at a constant rate and the microorganisms exhibit a constant sensitivity to this messenger, the generation of even cell-density profiles is predicted by the model. In the experimental characterization of colony development no similarities to this characteristic behavior were found. Furthermore, despite the application of rather extreme cultivation conditions in investigations on the influence of volatile compounds on colony development, no truncated or impaired extension of exposed colonies was observed. Hence, it appears more than unlikely that colony development is controlled on the basis of the postulated threshold mechanism. However, this line of arguments does not preclude that QS in yeast colonies is mediated by more subtle mechanisms. In particular, the induction of pseudohyphal cells, the polarization of growth away from high cell densities, as well as the repressed formation of secondary buds, i.e., the regulation of branching frequency, are phenomena that are potentially messenger-mediated.

Carbon-limited *Y. lipolytica* colonies proceed to extend in the absence of the primary nutrient resource utilizing cellular material to fuel proliferation. This behavior is reflected by the continuously decreasing biomass density in the inner colony regions and a net decrease of the total biomass which is accumulated in the colonies. As outlined in the experimental section, it still remains unclear whether the decreasing biomass density is the result of an actual decay of individual cells, or caused by the translocation of cytoplasm through a hyphal network. In a first modeling approach, an autonomous decay of individual cells and a diffusive distribution of the decay products through the agar was assumed. Despite strong simplifications (single pool for primary and secondary nutrient, identical diffusion coefficients for glucose and cell decay products) it was elaborated, that under these conditions a stable colony expansion is impossible although the nutrient reservoir is continuously replenished. Only if an additional mechanism is active which represses the proliferation of cells behind the colony margin, the simulations quantitatively reproduce the growth patterns of *Y. lipolytica* colonies observed under glucose-limited conditions. However, this mechanism is lacking any

experimental evidence so far. Furthermore, it could be only incorporated by implementing a *global* information into the simulation routine by setting all cell to the stationary state once they are further than 1 mm behind the colony margin. Thus, the strong discrepancies between the experimental results and simulations arising from the assumption of autonomous cell decay and external nutrient transport add further indications which support the hypothesis of *internal* translocation of cytoplasm in carbon-limited *Y. lipolytica* colonies.

The here presented models have a simple structure and are free from bias arising from not explicitly discussed assumptions. They provide quantitative predictions for the influence of different regulatory mechanisms on the growth patterns of yeast colonies. Therefore, the comparison of simulations with experimental results allows to identify a particular regulatory mechanism, or may serve to reject a model assumption. In the eyes of the author, this recognition of an inadequate fit as a valuable information, and the complete renunciation for the "tuning" of the models is a vital requirement to support the experimental investigation of fungal colony development effectively by mathematical analysis.

9. REFERENCES

Anastassiadis, S., Aivasidis, A. & Wandrey, C. (2002). Citric acid production by *Candida* strains under intracellular nitrogen limitation. *Appl. Microbiol. Biotechnol.* **60**, 81-87.

Atlas, R. M. (1996). *Handbook of Microbiological Media*, 2 edn. Bocaraton: CRC Press.

Barclay, C. D., Legge, R. L. & Farquhar, G. F. (1993). Modelling the growth kinetics of *Phanerochaete chrysosporium* in submerged static culture. *Appl. Environ. Microbiol.* **59**, 1887-1892.

Barnett, J. A. (1990). *Yeasts: Characteristics and identification*, 2 edn. Cambridge: Cambridge University Press.

Barth, G. (2004). Institute of General Microbiology, TU Dresden, Dresden, Germany, Personal communication.

Barth, G. & Gaillardin, C. (1997). Physiology and genetics of the dimorphic fungus *Yarrowia lipolytica. FEMS Microbiol. Rev.* **19**, 219-237.

Ben-Jacob, E., Schochet, O., Tenenbaum, A., Cohen, I., Czirok, A. & Vicsek, T. (1994). Generic modelling of cooperative growth patterns in bacterial colonies. *Nature* **368**, 46-49.

Beuling, E. E., van Den Heuvel, J. C. & Ottengraf, S. P. (2000). Diffusion coefficients of metabolites in active biofilms. *Biotechnol. Bioeng.* **67**, 53-60.

Birol, G., Undey, C., Parulekar, S. J. & Cinar, A. (2002). A morphologically structured model for penicillin production. *Biotechnol. Bioeng.* **77**, 538-552.

Boddy, L. & Abdalla, S. H. M. (1998). Development of *Phanerochaete velutina* mycelial cord systems: effect of encounter of multiple colonised wood resources. *FEMS Microbiol. Ecol.* **25**, 257-269.

Boschke, E. & Bley, T. (1998). Growth patterns of yeast colonies depending on nutrient supply. *Acta Biotechnol.* **18**, 17-27.

Boswell, G. P., Jacobs, H., Davidson, F. A., Gadd, G. M. & Ritz, K. (2002). Functional consequences of nutrient translocation in mycelial fungi. *J. Theor. Biol.* **217**, 459-477.

Boswell, G. P., Jacobs, H., Davidson, F. A., Gadd, G. M. & Ritz, K. (2003). Growth and function of fungal mycelia in heterogeneous environments. *Bull. Math. Biol.* **65**, 447-477.

Cohen, I., Czirok, A. & Ben-Jacob, E. (1996). Chemotactic-based adaptive self-organization during colonial development. *Physica A.* **233**, 678 - 698.

D'Ans, J. & Lax, E. (1998). *Taschenbuch für Chemiker und Physiker*, 4 edn. Heidelberg: Springer.

Datar, R. V. & Rosen, C.-G. (1993). Cell and cell debris removal: centrifugation and crossflow filtration. In *Bioprocessing*, pp. 472-503. Edited by G. Stephanopoulos. Weinheim: VCH.

Davidson, F. A. (1998). Modelling the qualitative response of fungal mycelia to heterogeneous environments. *J. Theor. Biol.* **195**, 281-292.

Davidson, F. A. & Park, A. W. (1998). A mathematical model for fungal development in heterogeneous environments. *Appl. Math. Lett.* **11**, 51-56.

Davidson, F. A., Sleeman, B. D., Rayner, A. D. M., Crawford, J. W. & Ritz, K. (1996a). Context-dependent macroscopic patterns in growing and interacting mycelial networks. *Proc. R. Soc. Lond. B* **263**, 873-880.

Davidson, F. A., Sleeman, B. D., Rayner, A. D. M., Crawford, J. W. & Ritz, K. (1996b). Large-scale behavior of fungal mycelia. *Math. Comput. Modelling* **24**, 81-87.

Davidson, F. A., Sleeman, B. D., Rayner, A. D. M., Crawford, J. W. & Ritz, K. (1997). Travelling waves and pattern formation in a model for fungal development. *J. Math. Biol.* **35**, 589-608.

Dominguez, A., Ferminan, E. & Gaillardin, C. (2000). *Yarrowia lipolytica*: An organism amenable to genetic manipulation as a model for analyzing dimorphism in fungi. In *Dimorphism in human pathogenic and apathogenic yeasts*, pp. 151-172. Edited by H. Ernst & S. A. Basel: Karger.

Donnelly, D. P. & Boddy, L. (1997). Resource acquisition by the mycelial-cord-former *Stropharia caerulea*: effect of resource quantity and quality. *FEMS Microbiol. Ecol.* **23**, 195-205.

Dormann, S. & Deutsch, A. (2002). Modeling of self-organized avascular tumor growth with a hybrid cellular automaton. *In Silico Biol.* **2**, 393-406.

Ernst, J. F. (2000). Regulation of dimorphism in *Candida albicans*. In *Dimorphism in human pathogenic and apathogenic yeasts*, pp. 98-111. Edited by J. F. Ernst & A. Schmidt. Basel: Karger.

Fujikawa, H. (1994). Diversity of the growth patterns of *Bacillus subtilis* colonies. *FEMS Microbiol. Ecol.* **13**, 159 - 167.

Gellissen, G. (2000). Heterologous protein production in methylotrophic yeasts. *Appl. Microbiol. Biotechnol.* **54**, 741-750.

Giannakopoulus, A. & Guilbert, S. (1986). Determination of sorbic acid diffusivity in model food gels. *J. Food Technol.* **21**, 339-353.

Gimeno, C. J., Ljungdahl, P. O., Styles, C. A. & Fink, G. R. (1992). Unipolar cell divisions lead to filamentous growth: Regulation by starvation and RAS. *Cell* **68**, 1077-1090.

Gow, N. A. R. (1994). Growth and guidance of the fungal hypha. *Microbiology* **140**, 3193-3205.

Gow, N. A. R., Robbins, P. W., Lester, J. W., Brown, A. J. P., Fonzi, W. A., Chapman, T. & Kinsman, O. S. (1994). A hyphal-specific chitin synthase gene (*CHS2*) is not essential for growth, dimorphism, or virulence of *Candida albicans.* Proc. Natl. Acad. Sci. USA **91**, 6216-6220.

Granot, D. & Snyder, M. (1993). Carbon source induces growth of stationary phase yeast cells, independent of carbon source metabolism. *Yeast* **9**, 465-479.

Heijnen, J. J., van Loosdrecht, M. C. M. & Tijhuis, L. (1992). A black box mathematical model to calculated auto- and heterotrophic biomass yields based on Gibbs energy dissipation. *Biotechnol. Bioeng.* **40**, 1139-1154.

Hornby, J. M., Jensen, E. C., Lisec, A. D., Tasto, J. J., Jahnke, B., Shoemaker, R., Dussault, P. & Nickerson, K. W. (2001). Quorum sensing in the dimorphic fungus *Candida albicans* is mediated by farnesol. *Appl. Environ. Microbiol.* **67**, 2982-2992.

Hughes, C. L. & Boddy, L. (1994). Translocation of ^{32}P between wood resources recently colonised by mycelial cord systems of *Phanerochaete velutina. FEMS Microbiol. Ecol.* **14**, 201-212.

Kawasaki, K., Mochizuki, A., Matsushita, M., Umeda, T. & Shigesada, N. (1997). Modeling spatio-temporal patterns generated by *Bacillus subtilis. J. Theor. Biol.* **188**, 177-185.

Komeda, T., Tazumi, K., Shimada, H., Kano, K., Hayashi, T., Saito, H., Tsumura, H., Kato, N., Sakai, Y. & Kondo, K. (2002). Production of active bovine cathepsin C (dipeptidyl aminopeptidase I) in the methylotrophic yeast *Candida boidinii. Appl. Microbiol. Biotechnol.* **59**, 252-258.

Kron, S. J., Styles, C. A. & Fink, G. R. (1994). Symmetric cell division in pseudohyphae of the yeast *Saccharomyces cerevisiae. Mol. Biol. Cell* **5**, 1003-1022.

Kurtzman, C. P. & Robnett, C. J. (1998). Identification and phylogeny of ascomycetous yeasts from analysis of nuclear large subunit (26S) ribosomal DNA partial sequences. *Antonie Van Leeuwenhoek* **73**, 331-371.

Longsworth, L. G. (1953). Diffusion measurements at 25 °C, of aqueous solutions of amino acids, peptides and sugars. *J. Am. Chem. Soc.* **75**, 5705-5709.

Lorenz, M. C., Cutler, N. S. & Heitmann, J. (2000). Characterization of alcohol-induced filamentous growth in *Saccharomyces cerevisiae. Mol. Biol. Cell* **11**, 183-199.

Lucas, C. & van Uden, N. (1986). Transport of hemicellulose monomers in the xylose-fermenting yeast *Candida shehatae. Appl. Microbiol. Biotechnol.* **23**, 491-495.

Matsushita, M., Wakita, J., Itoh, H., Rafols, I., Matsuyama, T., Sakaguchi, H. & Mimura, M. (1998). Interface growth and pattern formation in bacterial colonies. *Physica A.* **249**, 517-524.

Middelhoven, W. J. & Kurtzman, C. P. (2003). Relation between phylogeny and physiology in some ascomycetous yeasts. *Antonie Van Leeuwenhoek* **83**, 69-74.

Miled, C., Mann, C. & Faye, G. (2001). Xbp1-mediated repression of CLB gene expression contributes to the modifications of yeast cell morphology and cell cycle seen during nitrogen-limited growth. *Mol. Cell Biol.* **21**, 3714-3724.

Mortimer, C. E. (1987). *Chemie. Das Basiswissen der Chemie.*, 5 edn. Stuttgart: Thieme.

Mösch, H.-U. (2000). Pseudohyphal development in *Saccharomyces cerevisiae.* In *Dimorphism in human pathogenic and apathogenic yeasts,* pp. 185-200. Edited by H. Ernst & A. Schmidt. Basel: Karger.

Nicholson, C. (2001). Diffusion and related transport mechanisms in brain tissue. *Rep. Prog. Phys.* **64**, 815-884.

Nielsen, J. (1993). A simple morphologically structured model describing the growth of filamentous microorganisms. *Biotechn. Bioeng.* **41**, 715-727.

Nissen, T. L., Schulze, U., Nielsen, J. & Villadsen, J. (1997). Flux distributions in anaerobic, glucose-limited continuous cultures of *Saccharomyces cerevisiae. Microbiology* **143**, 203-218.

Nobre, A., Lucas, C. & Leao, C. (1999). Transport and utilization of hexoses and pentoses in the halotolerant yeast *Debaryomyces hansenii. Appl. Environm. Microbiol.* **65**, 3594-3598.

Olsson, S. & Gray, S. N. (1998). Patterns and dynamics of ^{32}P-phosphate and labelled 2-aminobutyric acid (^{14}C-AIB) translocation in intact basidiomycete mycelia. *FEMS Microbiol. Ecol.* **26**, 109-120.

Palecek, S. P., Parikh, A. S. & Kron, S. J. (2002). Sensing, signalling and integrating physical processes during *Saccharomyces cerevisiae* invasive and filamentous growth. *Microbiol.* **148**, 893-907.

Palkova, Z. & Forstova, J. (2000). Yeast colonies synchronise their growth and development. *J. Cell Sci.* **113**, 1923-1928.

Palkova, Z., Janderova, B., Gabriel, J., Zikanova, B., Pospisek, M. & Forstova, J. (1997). Ammonia mediates communication between yeast colonies. *Nature* **390**, 532-536.

Palkova, Z., Devaux, F., Icicova, M., Minarikova, L., Le Crom, S. & Jacq, C. (2002). Ammonia pulses and metabolic oscillations guide yeast colony development. *Mol. Biol. Cell* **13**, 3901-3914.

Parrou, J. L., Enjalbert, B., Plourde, L., Bauche, A., Gonzalez, B. & Francois, J. (1999). Dynamic responses of reserve carbohydrate metabolism under carbon and nitrogen limitations in *Saccharomyces cerevisiae. Yeast* **15**, 191-203.

Paul, G. C. & Thomas, C. R. (1996). A structured model for hyphal differentiation and penicillin production using *Penicillium chrysogenum. Biotechnol. Bioeng.* **51**, 558-572.

Righelato, R. C., Trinci, A. P. J., Pirt, S. J. & Peat, A. (1968). The influence of maintenance energy and growth rate on metabolic activity, morphology and conidiation in *Penicillium chrysogenum. J. Gen. Microbiol.* **50**, 399-412.

Ritz, K. (1993). Fungal growth in heterogeneous environments. In *SCRI annual report for 1993*, pp. 54-57: SCRI.

Ritz, K. (1995). Growth response of some soil fungi to spatially heterogeneous nutrients. *FEMS Microbiol. Ecol.* **16**, 269-280.

Ritz, K., Millar, S. M. & Crawford, J. W. (1996). Detailed visualisation of hyphal distribution in fungal mycelia growing in heterogeneous nutritional environments. *J. Microbiol. Methods* **25**, 23-28.

Rizzi, M., Baltes, M., Theobald, U. & M., R. (1997). *In vivo* analysis of metabolic dynamics in *Saccharomyces cerevisiae.* Mathematical model. *Biotechnol. Bioeng.* **55**, 592-608.

Ruiz-Herrera, J. & Sentandreu, R. (2002). Different effectors of dimorphism in *Yarrowia lipolytica. Arch. Microbiol.* **178**, 477-483.

Schlegel, H. G. (1992). *Allgemeine Mikrobiologie*, 7 edn. Stuttgart: Thieme.

Spohr, A. B., Dam-Mikkelsen, C., Carlsen, M., Nielsen, J. & Villadsen, J. (1998). On-line study of fungal morphology during submerged growth in a small flow-through cell. *Biotechnol. Bioeng.* **58**, 541-553.

Suzuki, M. & Nakase, T. (2002). A phylogenetic study of ubiquinone-7 species of the genus *Candida* based on 18S ribosomal DNA sequence divergence. *J. Gen. Appl. Microbiol.* **48**, 55-65.

Szabo, R. (1999). Dimorphism in *Yarrowia lipolytica*: filament formation is suppressed by nitrogen starvation and inhibition of respiration. *Folia Microbiol. (Praha)* **44**, 19-24.

Szabo, R. & Stofanikova, V. (2002). Presence of organic sources of nitrogen is critical for filament formation and pH-dependent morphogenesis in *Yarrowia lipolytica. FEMS Microbiol. Lett.* **206**, 45-50.

Teusnik, B., Diderich, J. A., Westerhoff, H., Dam, K. & Walsh, M. C. (1998). Intracellular glucose concentrations in derepressed yeast cells consuming glucose is high enough to reduce the glucose transport rate by 50 %. *J. Bacteriol.* **180**, 556-562.

Tijhuis, L., van Loosdrecht, M. C. M. & Heijnen, J. J. (1993). A thermodynamically based correlation for maintenance Gibbs energy requirements in aerobic and anaerobic chemotrophic growth. *Biotechnol. Bioeng.* **42**, 509-519.

Werner-Washburne, M., Braun, E., Johnston, G. C. & Singer, R. A. (1993). Stationary phase in the yeast *Saccharomyces cerevisisae. Microbiol. Rev.* **57**, 383-401.

Zikanova, B., Kuthan, M., Ricicova, M., Forstova, J. & Palkova, Z. (2002). Amino acids control ammonia pulses in yeast colonies. *Biochem. Biophys. Res. Commun.* **294**, 962-967.

INDEX OF FIGURES

INDEX OF TABLES

APPENDIX A

REACTION-DIFFUSION MODELS FOR THE GROWTH OF FUNGAL MYCELIA

A.1 Models that neglect nutrient translocation within the mycelium

Model Structure:

In a number of papers reaction-diffusion models were presented that abstract fungal growth by the autocatalytical production of an activator (a) from a nutrient (energy) source (s) (Davidson *et al.*, 1996a; Davidson *et al.*, 1996b; Davidson *et al.*, 1997). In these models nutrient and activator are freely diffusible and the presence of hyphal boundaries is neglected. The proliferation of cells is not explicitly modeled, but biomass is assumed to be produced by the action of activator (a) and supposed to be laid down closed to, but in front of any diffusion front of the activator. Furthermore, the activator is assumed to decay exponentially and nutrient is replenished when the local concentration drops below the initial concentration (s_0). Based on these basic assumptions the reaction-diffusion model was defined according to equations (A.1) and (A.2) (Davidson *et al.*, 1996b; Davidson *et al.*, 1997)

$$\frac{\partial a}{\partial t} = \Delta a + a^2 \cdot s - \mu \cdot a \tag{A.1}$$

$$\frac{\partial s}{\partial t} = D \cdot \Delta s - a^2 \cdot s + g \cdot (s_0 - s) \tag{A.2}$$

wherein (D) represents the ratio of the diffusion constants of activator (a) and nutrient (s), and (μ) and (g) are positive constants that determine the rate of activator decay and substrate replenishment, respectively.

Focus of the Models:

Numerical simulations for various parameter constellations and initial conditions were carried out that exhibit macroscopic patterns similar to experimental observations (Davidson *et al.*, 1996b; Davidson *et al.*, 1997): In the absence of nutrient replenishment (g = 0), the activator front progresses as a traveling wave of constant amplitude. The peak in activator concentration qualitatively corresponds to the proliferating margin of a fungal colony that expands outward from the inoculation site. Since this margin always contains the same activator concentration, such behavior can be interpreted as the formation of constant cell-density profiles in a growing mycelium. In replenished systems (g ≠ 0) sustained localized activator peaks arise behind the traveling wave front showing striking similarities to the inhomogeneous biomass distribution that is occasionally observed within fungal mycelia. Furthermore, simulations of the growth of adjacent colonies yield collapsing activator fronts for non-replenished systems, and the formation of demarcation zones coinciding with the reflection of the activator waves in case of nutrient replenishment. These results of

mathematical simulations reflect experimental observations of mutual repulsion, or merging behavior of fungal mycelia.

Points of Criticism:

Despite qualitative similarities between simulations and experimental results, the model structure is highly questionable. The introduction of a replenishment term (Equ. A.2, term3) appears to be unmotivated, since in experiments the uptake of nutrient by the cells is not compensated by an external source. Areas depleted from nutrient may be supplied with new resources by translocation of nutrients through the mycelial network. Alternatively, the decay of existing biomass into utilizable compounds may provide a secondary nutrient resource. However, the definition of the replenishment term does not account for the described natural processes.

Furthermore, nutrient uptake is assumed to be proportional to the square of a local activator concentration (Equ. A.2, term 2), i.e. biomass concentration. This definition of the reaction term is obviously wrong but allows for the complete conversion of nutrient by comparatively small local activator concentrations. Thus, the model appears to predict diffusion-limited growth coinciding with the formation of a constant cell-density profile even when growth of the fungal colony is slow when compared to diffusion.

Considering the above mentioned shortcomings of the model structure in addition to the test of solely qualitative parameter constellations, the presented simulations do not correspond to mechanisms that regulate fungal colony development, nor provide any additional insight into process dynamics that influence the outcome of growth experiments.

A.2 Models that incorporate nutrient translocation within the mycelium

Model Structure:

The mathematical description of fungal colony development was further developed by the same group of authors (Davidson, 1998; Davidson & Park, 1998). The model accounts in its most recent form for the uptake of external nutrient (s_e) into the mycelium, the translocation of internal nutrient (s_i), and the conversion of internal nutrient into biomass (m). The outlined interactions are mathematically described by the following set of equations (Davidson, 1998; Davidson & Park, 1998),

$$\frac{\partial m}{\partial t} = -\nabla \mathbf{J}_m + f_m(m, s_i, s_e, \mathbf{x}, t) \tag{A.3}$$

$$\frac{\partial s_i}{\partial t} = -\nabla \mathbf{J}_i + f_i(m, s_i, s_e, \mathbf{x}, t) \tag{A.4}$$

$$\frac{\partial s_e}{\partial t} = -\nabla \mathbf{J}_e + f_e(m, s_i, s_e, \mathbf{x}, t) \tag{A.5}$$

with $\mathbf{x} \in R^2$ and $(\mathbf{J_x})$ and (f_x) representing the corresponding flux and reaction terms. According to the Michaelis-Menten-like relation (A.6)

$$f_m = c_1 \cdot m^2 \cdot \left(\frac{s_i}{k_1 + s_i} - m \right) \tag{A.6}$$

biomass (m) is produced autocatalytically from the *internal* nutrient (s_i). (c_1) and (k_1) are positive constants. Here, (c_1) can be interpreted as a parameter that describes the efficiency of the substrate-into-biomass conversion, and (k_1) represents the substrate affinity of the microorganism. Again, a quadratic proportionality was chosen to describe substrate utilization by the local biomass concentration (Equ. A.6). The contribution ($-c_1 \cdot m^3$) (Equ. A.6) is meant to account for the assumption that "biomass density is self-limiting due to space restrictions" (Davidson, 1998).

The model aims to describe the uptake of external nutrient (s_e) in excess of the local needs and its intracellular translocation to areas depleted for resources. Since the *active* uptake of nutrients requires metabolic energy, this process is assumed to depend on the intracellular nutrient concentration (Equ. A.7, term 2). In contrast, leakage of nutrient across the hyphal boundary is defined as a process exclusively driven by diffusion (Equ. A.7, term 3). The positively defined parameters (c_2), (c_3), (c_4) and (k_2) provide the possibility to scale the described processes.

$$f_i = -c_2 \cdot m^2 \cdot \frac{s_i}{k_1 + s_i} + c_3 \cdot s_i \cdot \frac{s_e}{k_2 + s_e} - c_4 \cdot m \cdot (s_i - s_e) \tag{A.7}$$

Accordingly,

$$f_e = c_5 \cdot \left(-c_6 \cdot m \cdot \frac{s_e}{k_2 + s_e} + c_4 \cdot m \cdot (s_i - s_e) \right) \tag{A.8}$$

accounts for the uptake and replenishment of external nutrient, wherein (c_5) and (c_6) are positive constants. (c_5) is chosen smaller than 1 since the removal of a definite amount of nutrient from the comparatively large extracellular nutrient reservoir contributes less to concentration changes in the external nutrient concentration than the addition of the same amount to the small biomass volume (Davidson, 1998).

Equ. (A.9) accounts for higher extension rates of fungal colonies in the presence of higher internal nutrient concentrations, with ($\mathbf{J_m}$) being the biomass flux and (D_m) representing the corresponding diffusion constant.

$$J_m = -D_m \cdot s_i \cdot \nabla m \tag{A.9}$$

Since internal nutrient is not translocated in the absence of cells and high concentrations of hyphae are assumed to increase the total flux through the mycelium, the flux of intracellular nutrient ($\mathbf{J_i}$) is defined to be proportional to the local biomass concentration (m) and the intracellular diffusion constant (D_i) (A.10).

$$J_i = -D_i \cdot m \cdot \nabla s_i \tag{A.10}$$

External nutrient diffuses according to Fick's law with (D_e) representing the diffusion constant of nutrient in the substrate.

$$J_e = -D_e \cdot \nabla s_e \qquad\qquad\qquad\qquad (A.11)$$

Focus of the Model:

The model was meant to describe the growth of fungal mycelia in heterogeneous environments. In particular, simulations were qualitatively compared to experimental results obtained for the growth of a fungus on chessboard arrays consisting of tiles with different nutrient concentrations. Simulations show that the fungus takes up nutrients in excess of local needs at high-nutrient tiles, and translocates these nutrients through the mycelium to support the growth on low-nutrient tiles.

Points of Criticism:

In contrast to the above described activator models, the authors waived for the incorporation of nutrient replenishment terms which represents a significant improvement compared to previous studies. However, to define a quadratic relationship between nutrient utilization and biomass concentration still represents a significant shortcoming (Equ. A.6 and A.7).

More important, the authors assume the biomass density to be self-limiting due to space restrictions (Davidson, 1998). This *verbal formulation* implies that the *generation* of new hyphae is restricted due to the limited volume of the growth substrate. However, the *mathematical definition* of this process (Equ. A.6) implies that hyphae which already exist *decay* at a rate which is proportional to the 3rd power (!!!) of their local concentration. Thus, the definition of (f_m) is highly dubious.

In Equ. A.7 the uptake of external nutrient (s_e) was defined to be proportional to the internal nutrient concentration (s_i). As explicitly discussed in Section 3.3.1, this formulation of the nutrient uptake completely neglects the inhibiting effect which high internal nutrient concentrations exert on the uptake of additional external nutrient resources. Furthermore, the gain of internal nutrient is assumed to be proportional to the internal nutrient concentration (Equ. A.7, term 2) whereas the removal of external nutrient is proportional to the local biomass concentration (Equ. A.8, term 2). The authors did not discuss the reasons for the introduction of this asymmetry. In the light of the outlined weaknesses, the proposed mechanism for the uptake of external nutrients in excess of local needs should be carefully reviewed.

Please note further, that the biomass flux ($\mathbf{J}_m$) increases for higher biomass gradients (Equ. A.9). However, this definition of mycelial extension is certainly questionable considering the fact that fungal hyphae are immobile, i.e., do not diffuse but extend by linear apical growth.

The model was only qualitatively parameterized, i.e., the origin of parameter estimations was not discussed. Adding this shortcoming to the highly questionable model structure, the results of the simulations are very unlikely to reproduce the behavior of fungal mycelia in a mechanistic manner.
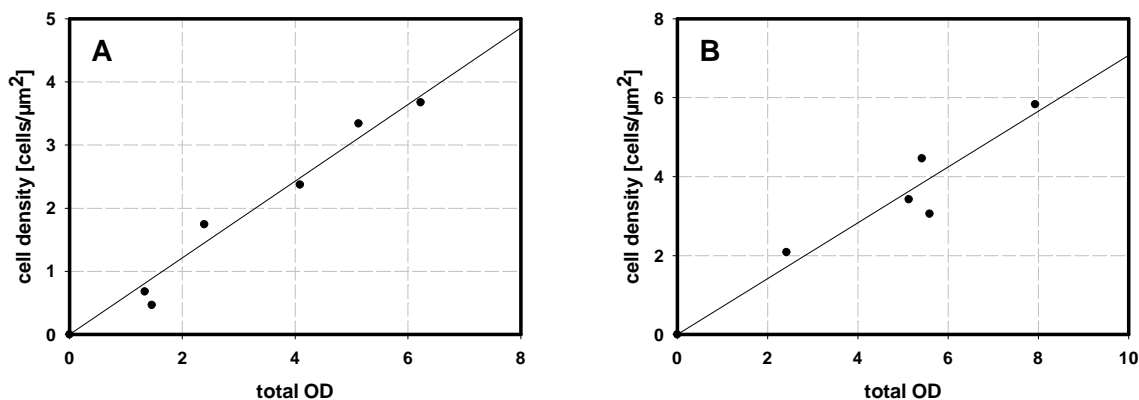
APPENDIX B

CALIBRATION CURVES: BIOMASS vs. OD
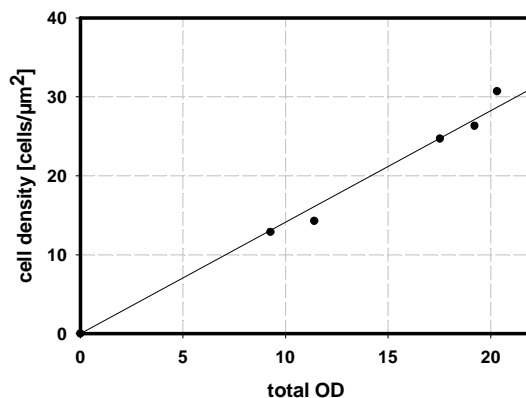

Figure B.1: Cell density vs. "total OD" plot for the determination of the calibration factor (K) of carbon-limited *C. boidinii* colonies. Cells were cultivated on C-G-2 medium. The "total OD" of young colonies was estimated at different points of time within the first 36 h of cultivation. See text for details.

**Figure B.2:** Cell density vs. "total OD" plot for the determination of the calibration factor (K) of nitrogen-limited (A) *Y. lipolytica* and (B) *C. boidinii* colonies. Cells were cultivated on N-A-0.05 medium. The "total OD" was estimated after 21 days of cultivation for different parts of the colonies. The cell number estimated for these colony parts was plotted vs. the OD integral. See text for details.

APPENDIX C

SIMULATIONS OF THE GLUCOSE-LIMITED COLONY DEVELOPMENT OF *Y. LIPOLYTICA* UNDER THE ASSUMPTION OF NUTRIENT REPLENISHMENT DUE TO CELL DECAY - RANDOM BUDDING VS. DISTAL BUDDING.
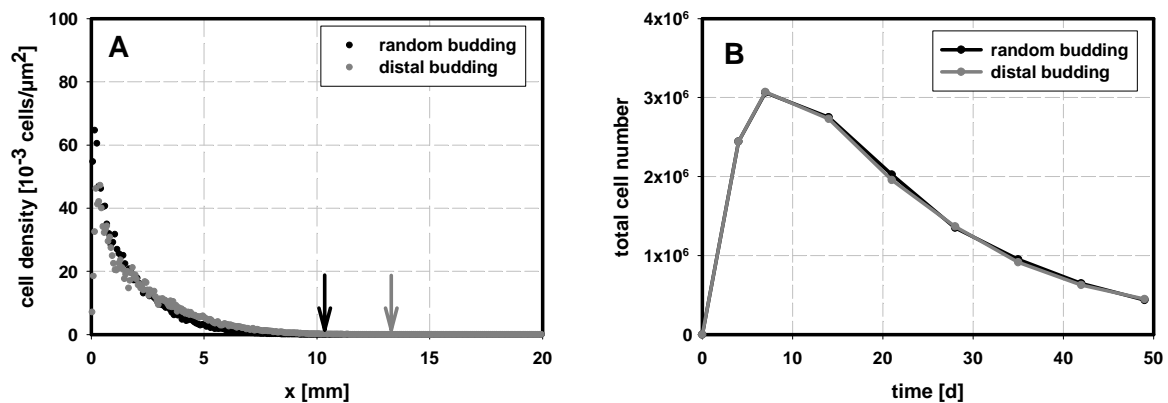
Figure C.1: Influence of the postulated budding pattern (distal budding vs. random budding) on simulations of the glucose-limited growth of *Y. lipolytica* under the assumption of nutrient replenishment due to cell decay. (A) Cell-density profiles at 35 days of cultivation. (The arrows indicate the outer edge of the profile.) (B) Total cell number in one colony moiety vs. time. (Initial glucose concentration: 2 g·L^{-1}, tile width: 1cm.) Figures represent the average of 5 replicate runs.
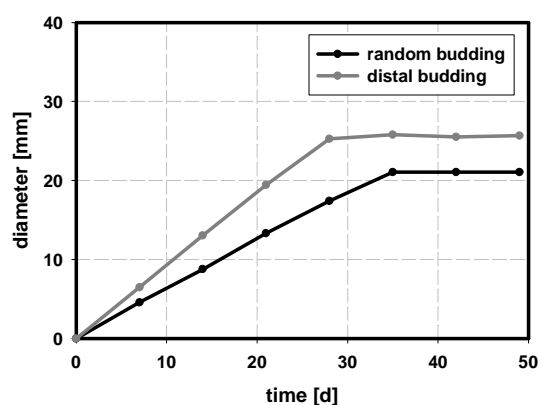
Figure C.2: Influence of the postulated budding pattern (distal budding vs. random budding) on the simulated extension of the colony diameter during the glucose-limited growth of *Y. lipolytica* under the assumption of nutrient replenishment due to cell decay. (Initial glucose concentration: 2 g·L^{-1}, tile width: 1cm.) Figures represent the average of 5 replicate runs.

THESES

Theses Derived from Experimental Investigations

1. The yeasts *Yarrowia lipolytica* and *Candida boidinii* form mycelial colony patterns similar to higher fungi when starved for nitrogen or carbon sources.

2. Measurements of the colony OD at carbon-limited *Y. lipolytica* and *C. boidinii* colonies facilitate the monitoring of the carbon distribution inside the growing mycelia as a prerequisite for the accurate balancing of the limiting nutrient resource.

3. Nitrogen-limited cells of the yeasts *Y. lipolytica* and *C. boidinii* strongly incorporate storage carbohydrates which makes the quantitative monitoring of the nitrogen distribution by OD measurements impossible under these growth conditions.

4. Mycelial colonies of *Y. lipolytica* and *C. boidinii* adapt to nutrient limitation by decreasing the biomass density within the mycelium while the extension rate of the colony diameter remains constant.

5. Carbon-limited *C. boidinii* colonies form monotonically declining cell-density profiles and extend linearly until a final colony diameter is reached which is small when compared to the size of the growth field.

6. The stop of colony extension in carbon-limited *C. boidinii* populations growing on glucose as the sole carbon source coincides with the depletion of glucose from the growth substrate.

7. Carbon-limited *Y. lipolytica* colonies form constant cell-density profiles and extend linearly until the populations cover the whole growth field. The formation of constant cell-density profiles is the result of a continuous decay of cells behind the progressing colony margin which coincides with the extension of the populations.

8. Carbon-limited *Y. lipolytica* colonies growing on glucose as the sole carbon-source proceed to extend after the depletion of the primary carbon source utilizing a secondary carbon source which is released upon cell decay.

9. During the first five weeks of cultivation, nitrogen-limited *Y. lipolytica* and *C. boidinii* colonies form monotonically declining cell-density profiles. In the course of the cultivation they extend linearly until the edge of the growth field is reached.

10. Volatile metabolic by-products or messengers released during the carbon-limited growth of *Y. lipolytica* and *C. boidinii* populations strongly influence the morphology of colonies that are exposed to these compounds.

11. Volatile compounds released upon the starvation for carbon sources repress the formation of yeast-like cells in *Y. lipolytica* and *C. boidinii* colonies.

12. The pH of the growth substrate strongly influences the development of carbon-limited *Y. lipolytica* and *C. boidinii* colonies.

13. The extension rate of carbon-limited *Y. lipolytica* colonies growing on glucose as the only carbon source increases with higher initial pH of the growth substrate while the cell density inside the mycelium declines.

14. In carbon-limited *C. boidinii* colonies growing on glucose as the only carbon source the cell density within the mycelium, and the extension rate of the populations decrease with higher initial pH of the growth substrate.

15. When *Y. lipolytica* colonies grow under carbon limitation with casamino acids as the only carbon source, colony extension is truncated at comparatively small diameters when the initial pH of the growth substrate is 7 or higher. The collapse of colony development is most-likely caused by the surpass of a threshold pH in the substrate which is restrictive to proliferation.

16. Yeasts change the pH of their growth medium during the cultivation. During glucose-limited growth, the final pH reached in submers or emers cultivations markedly differs under otherwise identical growth conditions. This points to a potential active regulation of the medium pH during yeast colony development.

Theses Derived from Mathematical Simulations

17. Yeast colony development can be comprehensively and quantitatively modeled applying cellular automaton models.

18. Exclusively nutrient-controlled proliferation of individual cells results in the diffusion-limited growth of the yeast population.

19. Simulations of the diffusion-limited growth of *Y. lipolytica* and *C. boidinii* colonies on various nutrient sources predict monotonically declining cell-density profiles and final colony diameters which are small when compared to the size of the growth field. These characteristics are insensitive to parameter variations in the physiologically relevant range and may, therefore, serve as robust criteria to identify diffusion-limited growth mechanisms in yeast colony development.

20. If in yeast colonies a quorum-sensing mechanism is present which truncates proliferation of individual cells when a critical messenger concentration is surpassed, the mediating messenger has to be volatile or extremely unstable to ensure a continuous colony extension.

21. If the nutrient reservoir in the growth substrate is replenished by a secondary resource released upon the decay of individual cells, colonies do not reach final diameters which are significantly higher than in the absence of nutrient replenishment.

22. If the nutrient reservoir is replenished due to cell decay, proliferating cells in the neighborhood of decaying cells take up the released nutrients before they can diffuse outwards to fuel the proliferation of cells in the progressing colony margin. As a consequence, proliferating cells are present across the whole colony long after the primary nutrient resource is depleted.

Theses Derived from the Comparison of Experimental Results and Mathematical Simulations

23. Carbon-limited colonies of *C. boidinii* grow diffusion-limited.

24. Nitrogen-limited colonies of *Y. lipolytica* and *C. boidinii*, as well as carbon-limited colonies of *Y. lipolytica* do not grow diffusion-limited.

25. The sustained colony extension of carbon-limited *Y. lipolytica* colonies in the absence of the primary nutrient resource is facilitated by the translocation of cytoplasm inside the mycelium and the utilization of this cytoplasm in apical cells as a secondary nutrient resource.

26. The branching rate in carbon-limited *Y. lipolytica* colonies is controlled by the external nutrient concentration and at least one additional factor.

27. *Y. lipolytica* cells that exhibit a pseudohyphal morphology are able to exchange cytoplasm.

Danksagung

Mein Dank gilt Herrn Prof. Thomas Bley für seine Anregung zu diesem interessanten Thema, für die Freiheit und die Unterstützung, welche mir bei allen meinen Arbeiten gewährt wurde, und für sein Vertrauen in mich und den erfolgreichen Abschluss dieser Dissertation.

Besonders möchte ich mich bei Herrn Dr. Andreas Deutsch für die intensive und freundschaftliche Betreuung, sowie die außerordentlich fruchtvollen und offenen Diskussionen bedanken.

Ich möchte mich bei Herrn Prof. Rudibert King für sein Interesse an dieser Dissertation und seine Bereitschaft, als Gutachter aufzutreten, bedanken.

Mein Dank geht an die eigentlichen „Erstgutachter" dieser Arbeit, Christian Löser, Kai Ostermann und Jost Weber, die mir als Freunde und Kollegen viele wertvolle und kritische Hinweise während der experimentellen und mathematischen Studien, sowie bei der Erstellung der schriftlichen Arbeit gegeben haben. Insbesondere möchte ich mich bei Kai für seine geduldige Einführung in die „Kunst" des gentechnischen Arbeitens bedanken.

Holger Reinsch trug erheblich zum Gelingen dieser Arbeit bei, indem er während seiner Diplomarbeit eine unglaubliche Menge an (harten!) Daten erzeugte. Danke Holger!!!

Mein ausdrücklicher Dank geht an Arend Große, der als studentische Hilfskraft alle anfänglichen Irrtümer und Enttäuschungen mit durchschritten hat und durch sein exaktes und zuverlässiges Arbeiten eine große Hilfe war.

Ganz besonders herzlich möchte ich mich bei allen meinen aktuellen und ehemaligen Kollegen am ILB für ihre Unterstützung bedanken. Insbesondere möchte ich Heike Pfennig und Annegret Lenk nennen, die mir durch das Abnehmen unendlich vieler Kleinigkeiten das Arbeiten deutlich erleichtert haben.

Meiner Familie möchte ich für die moralische und materielle Unterstützung danken, die mir während der gesamten letzten Jahre, über Studium und Promotionsphase hinweg, zuteil wurde.

Mein Dank geht an all meine Freunde, insbesondere an die beste WG meines Lebens mit Karsten, msü, und Steffen (in alphabetical order), deren Verdienst vor allem darin bestand, mich nach der Uni nicht mehr an diese Dissertation denken zu lassen.

Ich bin dankbar für die Geduld und vor allem die Liebe meiner Freundin Romy Rothe, die ich auch in den schwierigen Phasen der letzten Jahre genießen durfte.